

# OxyFuel combustion of Coal and Biomass

**Toftegaard, Maja Bøg**

*Publication date:*
2011

# OxyFuel Combustion of Coal and Biomass

**Ph.D. Thesis**

**Maja Bøg Toftegaard**

**CHEC Research Centre**
**Department of Chemical Engineering**
**Technical University of Denmark**

**DONG Energy Power**
**Power Technology**
**Chemical Engineering**

**March 31, 2011**

# Preface and Acknowledgements

The work presented in this thesis has been conducted under the Industrial PhD programme supported by the Ministry of Science, Technology, and Innovation. The dissertation is submitted in accordance with the partial requirements for the Ph.D. degree at the Department of Chemical and Biochemical Engineering, Technical University of Denmark. The Ph.D. study was carried out in the period April 2007 to March 2011 in collaboration between DONG Energy Power, Chemical Engineering and the CHEC (Combustion and Harmful Emission Control) research centre at the Department of Chemical and Biochemical Engineering at the Technical University of Denmark. The work has been funded by DONG Energy and the Ministry of Science, Technology, and Innovation. The experimental work has likewise been partly funded by Energinet.dk through the PSO projects "PSO 7171 – Oxyfuel combustion for below zero $CO_2$ emissions" and "PSO 010069 – Advanced diagnostics on Oxy-fuel combustion processes". The project has been supervised by Professor Anker Degn Jensen, Professor Peter Glarborg, Associate Professor Peter Arendt Jensen, and Senior Engineer, Lic.Tech. Bo Sander (DONG Energy Power).

I wish to thank all my supervisors for their invaluable support and guidance throughout the project and for continuously challenging my ideas and results in order to improve the project. I am grateful to M.Sc. student Bjørn Maribo-Mogensen and Research Associate Professor Weigang Lin for their involvement in the experimental work. I would also like to thank the technical staff and the workshop at Department of Chemical and Biochemical Engineering, especially Thomas Wolfe, for helping me conquer a stubborn experimental setup.

My former and present colleagues at both the Technical University of Denmark and DONG energy all deserve my gratitude. Special thanks go to Rudolph Blum, Alice Jochumsen, and Ole Hede Larsen for believing in me, even at times when I did not, and to Ulrik Borg, the best office mate one could imagine.

Maja Bøg Toftegaard
Fredericia, March 2011

# Summary

The power and heat producing sector is facing a continuously increasing demand to reduce its emissions of $CO_2$. Oxyfuel combustion combined with $CO_2$ storage is suggested as one of the possible, promising technologies which will enable the continuous use of the existing fleet of suspension-fired power plants burning coal or other fuels during the period of transition to renewable energy sources.

The oxyfuel combustion process introduces several changes to the power plant configuration. Most important, the main part of the flue gas is recirculated to the boiler and mixed with pure oxygen. The oxidant thus contains little or no nitrogen and a near-pure $CO_2$ stream can be produced by cooling the flue gas to remove water. The change to the oxidant composition compared to combustion in air will induce significant changes to the combustion process.

This Ph.D. thesis presents experimental investigations on the combustion of coal, biomass (straw), and blends of coal and straw in air and $O_2/CO_2$ mixtures. The experiments have been performed in semi-technical scale in a once-through 30 $kW_{th}$ swirl-stabilized flame. The work has focused on improving the fundamental knowledge on oxyfuel combustion of coal and straw at conditions relevant to suspension-fired boilers by clarifying the effect of the change in combustion atmosphere on fuel burnout, flame temperatures, emissions of polluting species (NO, $SO_2$, and CO), fly ash quality, and deposit formation. This work is one of the first to investigate the important aspects of ash and deposit formation during co-firing of coal and biomass and combustion of pure biomass in oxyfuel atmospheres in semi-technical scale.

The presented work has lead to the identification of reference operating conditions which enables a direct comparison of combustion in air and oxyfuel atmospheres. Apart from slightly improved burnout and reduced emissions of NO during oxyfuel combustion these operating conditions yield similar combustion characteristics in both environments.

Co-firing coal and biomass or combustion of pure biomass in an oxyfuel power plant could yield a significant, additional $CO_2$ reduction, or even lead to below-zero emissions of $CO_2$ from power production. This work has shown that no significant changes occur to the fundamental combustion characteristics for straw when burned in the $O_2/CO_2$ atmosphere. Additionally, the combustion of a coal/straw blend with a straw share of 50 wt% has added valuable understan-

ding to the trends in ash and deposits chemistry for coal/straw co-firing.

Recirculation of untreated flue gas in oxyfuel plants will increase the in-boiler levels of NO and $SO_2$ significantly. Experiments with simulated recirculation of NO and $SO_2$ have provided insight into the mechanisms of the significant reduction in NO emission rates from the boiler and the increased uptake of sulphur in fly ash and deposits which were observed.

The single-largest penalty to the electrical efficiency and operating expenses of an oxyfuel power plant is the production of near-pure oxygen by cryogenic distillation. This thesis presents a possible strategy for reducing the oxygen demand and hence the penalty to the process. The strategy exploits the fact that the oxygen excess level during oxyfuel combustion is not directly linked to the flow of oxidant but can be adjusted independently. By increasing the concentration of oxygen in the oxidant, *i.e.* by reducing the flue gas recirculation ratio, it is possible to achieve similar burnout at lower oxygen excess levels. Further work on implications of this strategy are necessary in order to fully clarify its potential for improving the process economics of oxyfuel combustion.

Generally, no characteristics of the oxyfuel combustion process have been identified in this work which would be detrimental to its implementation as a carbon capture technology in full-scale power plants.

# Resumé (Summary in Danish)

Kraftværkssektoren står overfor stadigt stigende krav til reduktion af dens $CO_2$-udledning. Oxyfuel forbrænding kombineret med $CO_2$-lagring er en af de mulige og lovende teknologier, som vil muliggøre en fortsat anvendelse af kul og andre brændsler i den eksisterende porteføljе af suspensionsfyrede kraftværker i overgangsperioden til vedvarende energi.

Ombygning af eksisterende kraftværker til oxyfuel forbrænding vil medføre adskillige ændringer i proceskonfigurationen. Vigtigst af disse er, at hovedparten af røggassen recirkuleres til kedlen hvor den blandes med ren ilt. Forbrændingsgassen indeholder derfor kun lidt eller intet nitrogen og en $CO_2$-strøm af høj renhed kan derfor produceres ved tørring af røggassen. Ændringen af forbrændingsgassens sammensætning i forhold til sammensætningen af luft vil medføre betydelige ændringer i forbrændingsprocessen.

Denne ph.d.-afhandling fremlægger eksperimentelle undersøgelser af forbrændingen af kul, biomasse (halm), og blandinger af kul og halm i luft og $O_2/CO_2$ blandinger. Forsøgene er udført i semi-teknisk skala i en 30 $kW_{th}$ swirl-stabiliseret flamme. Arbejdet har fokuseret på at forøge den grundlæggende forståelse af oxyfuel forbrænding af kul og halm ved betingelser, som er relevante i forhold til suspensionsfyrede kedler, ved at klarlægge effekten af ændringen i forbrændingsatmosfæren på udbrænding, flammetemperaturer, emissioner af forurenende komponenter (NO, $SO_2$ og CO), flyveaskekvalitet og belægningsdannelse. Dette arbejde er et af de første til at undersøge de vigtige problemstillinger omkring aske- og belægningsdannelse under samfyring af kul og biomasse og ved forbrænding af ren biomasse i oxyfuel atmosfærer i semi-teknisk skala.

Det præsenterede arbejde har ført til identificeringen af reference driftsbetingelser som muliggør en direkte sammenligning af forbrænding i luft og oxyfuel atmosfærer. Bortset fra en fordelagtig, let forøget udbrænding og en reduceret NO-udledning ved oxyfuel forbrænding medfører disse driftsbetingelser ens karakteristika for forbrændingsprocessen i begge miljøer.

Samfyring af kul og biomasse eller forbrænding af ren biomasse i et oxyfuel kraftværk kan give en betydelig, ekstra reduktion af $CO_2$-udledningen eller endda føre til en negativ $CO_2$-udledning fra elproduktionen. Dette arbejde har vist at der ikke opstår nogen betydelige ændringer i de grundlæggende forbrændingsprocesser når halm afbrændes i $O_2/CO_2$-atmosfæren. Derudover har anvendelsen af

en kul/halm blanding med en halmandel på 50 wt% tilført værdifuld forståelse af tendenser i aske- og belægningskemi for samfyring af kul og halm.

Recirkulering af ubehandlet røggas i oxyfuel kraftværker vil øge niveauerne af NO og $SO_2$ i kedlen markant. Forsøg med simuleret recirkulering af NO og $SO_2$ har tilvejebragt indsigt i mekanismerne bag det observerede, betydelige fald i NO-emissionen fra kedlen og den forøgede indbinding af svovl i flyveaske og belægninger.

Den største, enkeltstående reduktion af elvirkningsgraden i et oxyfuel kraftværk i forhold til et konventionelt værk stammer fra produktionen af ilt ved kryogen destillation. Denne afhandling præsenterer en mulig strategi til reduktion af iltforbruget og dermed en forøgelse af den samlede elvirkningsgrad for processen. Strategien udnytter det faktum, at iltoverskuddet i oxyfuel forbrænding, i modsætning til forbrænding i luft, ikke længere er direkte knyttet til mængden af forbrændingsluft, men kan varieres uafhængigt. Ved at forøge koncentrationen af ilt i oxidanten, dvs. ved at mindske recirkulationsforholdet, er det muligt at opnå en sammenlignelig udbrændingsgrad ved lavere iltoverskud. For at klarlægge denne strategis potentiale i forhold til en forbedring af procesøkonomien for oxyfuel kraftværker er videre undersøgelser dog nødvendige.

Overordnet set har dette arbejde ikke identificeret nogle karakteristika ved oxyfuel forbrændingsprocessen, som vil gøre den uegnet til storskala implementering.

# Contents

# Chapter 1

# Introduction

The world, and especially the developing countries such as China and India, is facing an increasing growth in the demand for electrical power [1, 2]. New power plants are thus being constructed at a considerable rate in order to keep up with this demand [1–3]. The majority of the recently constructed and planned power plants, on a world-wide basis, are coal fired [1, 2]. Coal is a cheaper and more abundant resource than other fossil fuels such as oil and natural gas while at the same time being a very safe and reliable fuel for power production [4, 5].

In the developed countries an increasing part of the energy consumption is being produced from renewable sources of energy; wind, biomass, solar, hydro power, etc. [1] The main purpose of the shift from a fossil fuel based production to renewable energy is to decrease the emission of greenhouse gases, primarily $CO_2$. Especially the emission of $CO_2$ from the combustion of fossil fuels has gained great focus in recent years in connection with the discussions of global warming. Since the beginning of the industrialization in the late part of the $18^{\text{th}}$ century the amount of $CO_2$ in the atmosphere has increased sharply from about 280 to 380 ppm, [6], see Figure 1.1 on the following page.

Table 1.1 lists the current and projected $CO_2$ emissions, in Gton carbon per year, from power generation (both electricity and heat) [1]. Both the emissions and the coal share of the emissions are seen to increase toward 2030 for the world as a whole. Even though the $CO_2$ emissions are seen to increase within Europe the percentage increase is much less pronounced than for the rest of the world and the coal share of the emissions is expected to decrease. Despite the fact

Table 1.1: Estimated $CO_2$ emissions from power generation (Gton C/year). The numbers in parenthesis indicate the percentage coal share of the emissions. Data taken from [1].

| Region | 2005 | 2015 | 2030 |
|---|---|---|---|
| World | 3.0 (72) | 4.0 (74) | 5.1 (74) |
| European Union | 0.38 (70) | 0.39 (66) | 0.42 (61) |

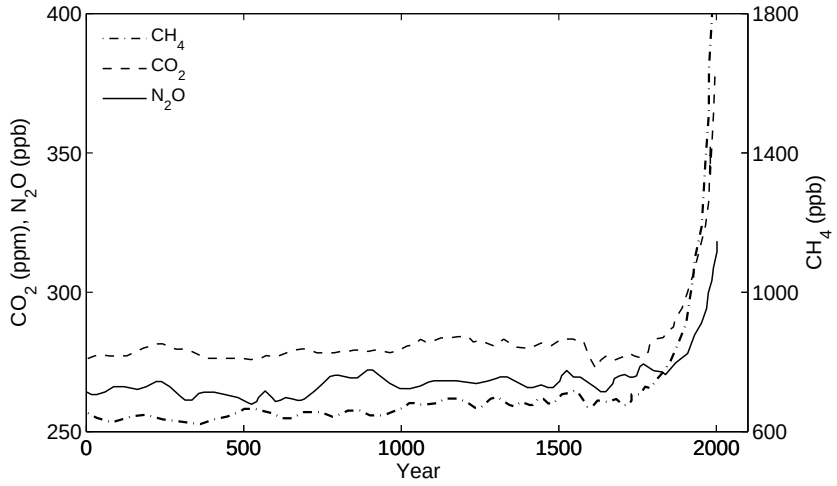


Figure 1.1: Development in the concentrations of important long-lived greenhouse gases in the atmosphere over the last 2,000 years. The increases in concentrations since about year 1750 are attributed to human activities in the industrial era. Reprinted from [6].

that the ultimate goal for most countries is to phase out all fossil fuels in heat and power production as well as in the transport sector, the share of renewable energy sources increases only slowly and the world will depend on fossil fuels for many years to come. A rapid move away from fossil fuels could result in great conflicts concerning water and land use between biomass for energy production, food production, and forestation [7] as well as in serious disruption to the global economy [8]. The latter is mainly caused by the long lifetime of the energy supply infrastructure. In the transitional period, technologies are sought which will enable the continuous usage of fossil fuels and at the same time eliminate the emission of $CO_2$.

## 1.1 Carbon Capture and Storage

Since power plants constitute large point sources of $CO_2$ emission the main focus is related to their operation. Currently, several possible technologies are being investigated which will enable the so called Carbon Capture and Storage (CCS) from power plants [5, 8–14]. Both researchers in universities and other research institutions, most manufacturers of boilers and other power plant related equipment, and many power companies are active. CCS will act as a complimentary technology to the ongoing work related to increasing fuel efficiency and the change toward fuels with lower fossil carbon content, *e.g.* natural gas and/or biomass. As indicated by the term CCS, the elimination of $CO_2$ emissions include two consecutive operations:

1. Capture of $CO_2$ from the power plant flue gas

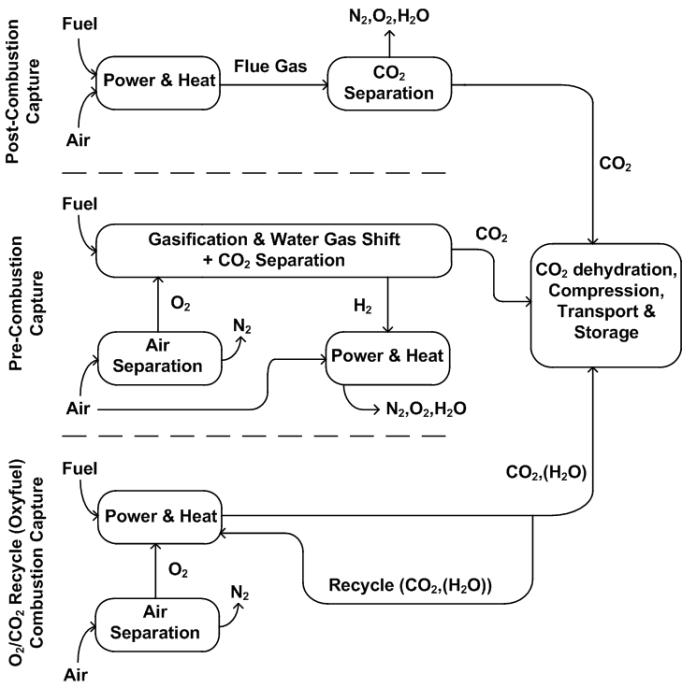


Figure 1.2: Possible, overall plant configurations for the three main categories of carbon capture technologies. Adopted from [10].

2. Storage of the $CO_2$ (incl. transport to storage site)

The identified technologies for carbon capture can be divided into four main categories [5, 11, 12, 15–19], described briefly below. Figure 1.2 shows the main operations concerned with the post-, pre-, and oxyfuel combustion technologies.

**Post-combustion capture** $CO_2$ is separated from the flue gas of conventional coal-fired power plants. The separation is typically performed via chemical absorption with monoethanolamine (MEA) [18, 20–24]. The demonstrated scale of operation is, however, significantly smaller than the typical size of power plants [23] and serious penalties to the plant efficiency, about 10-14 percent points, exist at the current state of development [5, 8, 12, 23, 25–31]. Retrofit to existing plants is considered relatively simple since the capture unit can be added downstream of the boiler and flue gas cleaning systems without significant changes to the original plant [8, 32]. There are, however, strict requirements for removal of $SO_2$ and $NO_2$ from the flue gas prior to the $CO_2$ capture since these compounds react irreversibly with the absorbent leading to its degradation. The chilled ammonia process also belongs in the category.

**Pre-combustion capture** Pre-combustion capture is typically used synonymously with Integrated Gasification Combined Cycle power plants with

$CO_2$ capture and termed IGCC-CCS. Coal gasification is applied to obtain syngas containing CO, $CO_2$, and $H_2$. The CO is transformed into $CO_2$ by the water-gas shift reaction and can then be separated from the remaining hydrogen-containing gas before the latter is combusted in a gas turbine. Some techno-economic calculations [11, 19, 33–35] show that IGCC has promising process economics and plant efficiency characteristics. However, high capital costs are associated with plant construction and IGCC plants are generally much more complicated systems than suspension fired boilers [36, 37] and retrofit is not a viable option for the latter [19, 36, 38, 39]. Only few electricity producing IGCC units exist [17, 34, 40–42], none of which are equipped with CCS. Only few IGCC plants exist and the demonstrated availability is significantly smaller than for the more matured, conventional pulverized coal-fired power plants (80-85 % vs. $\sim$96 %, respectively) [5, 19, 34, 37, 40, 43]. This is a consequence of the limited operating experience along with the highly integrated nature of the IGCC plants.

**Oxyfuel combustion** By near elimination of molecular nitrogen from the combustion medium the flue gas will consist mainly of $CO_2$ and water. The plant configuration typically suggested involves flue gas recirculation to the burners to control the flame temperature to within the acceptable limits of the boiler materials. Implementation of the oxyfuel combustion technology in existing pulverized coal-fired power plants will induce a larger change in the plant configuration when comparing to the post-combustion absorption process mentioned above. This is due to an introduction of several, new auxiliary processes. Several of the earlier techno-economic assessment studies indicate that oxyfuel combustion should be the most energy and cost efficient of the carbon capture technologies [9, 25, 27, 44–49]. The main disadvantage of the oxyfuel combustion technology is the need for almost pure oxygen. The available large-scale technology for air separation is based on cryogenic distillation which will impose a very large energy penalty on the plant [50]. The expected efficiency drop is about 7–11 percent points, or about 15–30 % of the generated electricity (net power output), depending on the initial plant efficiency [5, 8, 12, 15, 17, 27, 31, 44, 45, 51–54].

**Emerging technologies** Technologies such as membrane separation, chemical looping combustion, carbonation-calcination cycles, enzyme-based systems, ionic liquids, mineralization, etc. impose the possibility to drastically reduce the cost of electricity and the energy penalty concerned with carbon capture from power plants [14, 16, 55, 56]. However, these technologies have not been demonstrated at sufficient scales for industrialization.

The choice of technology will depend on several factors. First and foremost, the economy and the expected development in plant efficiency is of importance. The maturity, expected availability, operating flexibility, retrofit or green-plant built,

local circumstances, utilities preferences, etc. will likewise have to be taken into account. No general acceptance of superiority of one of the presented technologies over the others exist. Several techno-economic studies also indicate that with the current knowledge on the technologies no significant difference in cost within the limits of precision of the applied cost estimates can be determined between amine absorption capture, coal-based IGCC type capture, and oxyfuel combustion capture [5, 8, 39, 51, 52, 57, 58].

Because of the large changes induced in the power plant by the implementation of oxyfuel combustion, more research is needed to fully clarify the impacts of the introduction of this technology. Many laboratory scale investigations of the technology have been performed within the last two decades and it is generally accepted that it is possible to burn coal and natural gas in an $O_2/CO_2$ atmosphere. On the other hand, it is likewise recognized that much work still remains in obtaining sufficient insight into the effects on *e.g.* emissions, residual products such as fly ash, flue gas cleaning, heat transfer, etc.

## 1.2 Retrofitting Conventional Suspension-fired Power Plants for OxyFuel Combustion Carbon Capture

In open literature, oxyfuel combustion with recirculation of flue gas was proposed almost simultaneously by Horn and Steinberg [44] and Abraham et al. [46] in the early eighties. Abraham et al. proposed the process as a possible mean to produce large amounts of $CO_2$ for Enhanced Oil Recovery (EOR) whereas Horn and Steinberg had in mind the reduction of environmental impacts from the use of fossil fuels in energy generation. As such, the technology received renewed interest in the mid-90ties in connection with the re-emerging discussions of global warming caused by increased $CO_2$ levels in the atmosphere [12].

Oxy-combustion can in principle be applied to any type of fuel utilized for thermal power production. The research interests have mainly been focused on coal and natural gas since these are the most abundant fuels. Application of CCS through oxy-combustion of biomass or blends of coal and biomass will result in a possible mean of extracting $CO_2$ from the atmosphere and thereby possibly inverting the presumed anthropogenic caused changes to the climate [11, 18, 19].

Figure 1.3 on the next page provides a sketch of a coal-fired oxyfuel plant with indications of the major process steps and the necessary energy inputs and low-temperature-heat outputs new to the plant when retrofitting an existing coal-fired unit. The sketch covers the original state-of-the-art plant with boiler, coal mills, and flue gas cleaning equipment. The final processing of the $CO_2$ stream, *i.e.* the

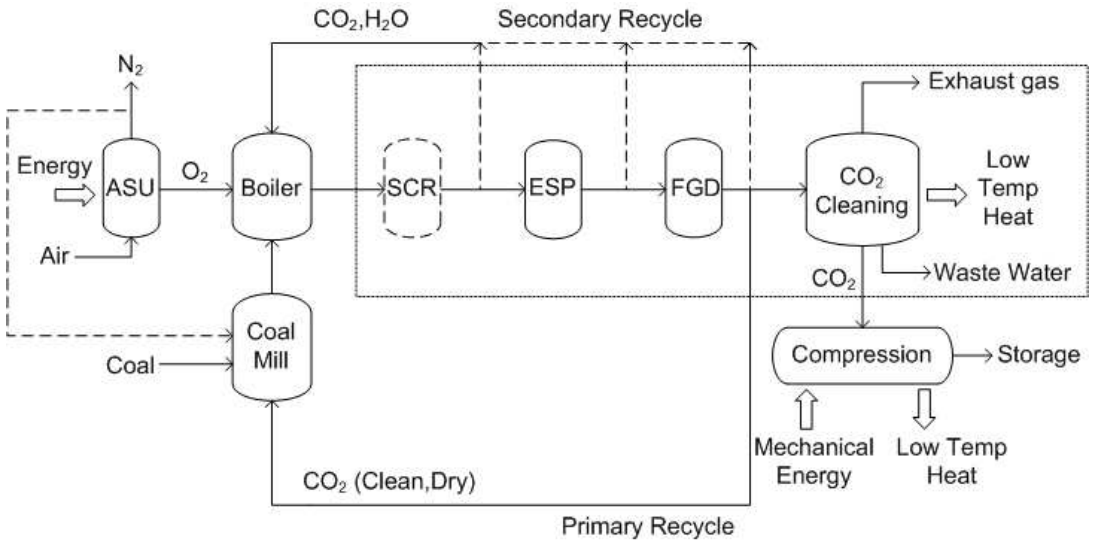


Figure 1.3: Possible configuration of an oxyfuel power plant. ASU: Air Separation Unit, SCR: Selective Catalytic Reduction reactor ($DeNO_x$), ESP: Electrostatic Precipitator, FGD: Flue Gas Desulphurization. Energy inputs and low-temperature heat outputs new to the plant in case of a retrofit are indicated.

removal of water and the non-condensible gases like $O_2$, $N_2$, Ar, etc. to meet the requirements regarding purity of the $CO_2$ stream, as well as the air separation unit (ASU) to provide the combustion process with almost pure oxygen, ducts and fans for external recirculation of flue gas to the burners in order to control flame temperatures, and the compression step for the $CO_2$ stream before it is transported to the storage site are new to the plant.

The review of the literature performed by this author [59] (Appendix A) has discussed the effects of retrofitting a suspension-fired power plant to oxyfuel operation and has shown that oxyfuel combustion of pulverized coal is technically and economically feasible for retrofitting of existing power plants. At the same time, oxyfuel combustion for $CO_2$ recovery and sequestration is a competitive power generation technology in relation to post-combustion capture with amines. However, a number of critical aspects regarding the technology have been identified, as listed below. These are the issues which should be investigated experimentally to ensure that the technology is in fact a useful alternative to post-combustion capture for retrofit of suspension-fired boilers.

- The cost and efficiency penalties associated with the technology are significant and should preferably be reduced. However, this is a common issue for the currently most developed CCS technologies.
- The significant risk of lowering the availability of the plant due to the introduction of the additional auxiliary equipment.

- The relatively low, permissible gradients for load change in the air separation unit compared to those for the thermal cycle could provide a problem with respect to operation of the plant in a system with a large amount of decentralized, non-constant electricity sources, *e.g.* wind mills. In Denmark, all central power plants are run with frequent changes in the load to adjust to the demand for electricity.
- The missing capability of current air separation units to run at low load without major penalties to the efficiency will require several oxygen plants running in parallel, as well as some sort of storage/buffer capacity. A storage capacity could partly solve some of the issues related to load changes, see above.
- The application of two purification steps, *i.e.* both the air separation unit and the pre-compression purification due to leakage of air into the flue gas ducts is one of the major disadvantages to the process. Post-combustion, in comparison, only needs the amine absorption step. The exact requirements for the final $CO_2$ quality are still to be determined and they will dictate the plant configuration with respect to the different purification units.
- The significant changes to the combustion process, including the potential effects on boiler heat uptake, fly ash quality, and fire-side corrosion likewise provide challenges.

Several of the above aspects are difficult to examine either theoretically or during small-scale tests. Only the operation of a larger-scale demonstration plant will provide the necessary information and experience.

The majority of issues regarding the combustion process are, on the other hand, possible to clarify in smaller scale experiments. Much work has already been done in this area including heat uptake and burner stability measurements as well as aspects regarding coal particle ignition, burnout, flame propagation, radiating properties of the flame, boiler efficiency, and changes in emission levels, see Section 1.3. However, several issues still require more insight in order to lay the ground for determining whether or not to apply oxyfuel combustion for carbon capture and storage in the future portfolio of power and heat producing plants.

## 1.3 OxyFuel vs Air-Firing – The Combustion Process

This section summarizes the knowledge found in open literature regarding oxyfuel combustion fundamentals and the relative variations when compared to conventional combustion in air. The chapter is build on the review paper "OxyFuel Combustion of Solid Fuels" [59] written by the author, see Appendix A.

### 1.3.1 Flame and Gas-Phase Temperatures

One of the key concerns when retrofitting conventional air-fired boilers to oxyfuel combustion is achieving similar temperature and heat uptake profiles in the radiative and convective sections of the boiler. The differences in thermo-chemical properties between $CO_2$ and $N_2$ causes changes in the heat and mass transfer rates within a boiler if $CO_2$ is substituted directly for $N_2$ in the oxidizer.

Data from pilot-scale experimental setups have shown that it is possible to match the temperature and heat uptake by increasing the inlet oxygen concentration during oxyfuel combustion to about 27-35 vol% compared to the 21 % found in air. The span covers the impact from fuel type and applied operating conditions, primarily the oxygen excess. High-rank fuels generally require an inlet concentration of oxygen in the upper end of the suggested interval while fuels of lower rank yield comparable tempeature profiles with lower oxygen inlet concentrations.

$CO_2$ and $H_2O$ are radiating gases whereas $N_2$ is not. The radiative heat transfer in oxyfuel combustion is thus higher than in air combustion at the same flame temperature. In order to match the heat uptake profile in a retrofitted boiler the flame temperature should thus be kept lower than during air operation.

### 1.3.2 Ignition and Burnout

Devolatilization and ignition of coal particles are affected by the change in oxidizer composition from air to oxyfuel combustion. The rate of devolatilization is primarily determined by the surrounding gas temperature as the difference in thermal conductivity of $N_2$ and $CO_2$ is relatively small. Particle ignition, on the other hand, is a strong function of both the transport properties of the gas phase surrounding the particles as well as the combustion heat release rate and the reactivity of the local fuel-oxidizer mixture. Ignition times comparable to those observed during air combustion can be obtained by increasing the oxidizer oxygen concentration to 27-35 vol%, *i.e.* by achieving similar flame temperature to air-firing. Burnout of volatiles and char are likewise affected by the high $CO_2$ and $H_2O$ concentrations in the flame. Especially the lower diffusivity of both oxygen and small hydrocarbons in $CO_2$ compared to $N_2$ is an important factor. Generally, an improvement in char burnout is reported in the literature when the oxyfuel combustion flame temperature matches that of air combustion. This improvement is assumed to be caused primarily by the higher oxygen partial pressure in the vicinity of the burning particles. Increased residence time of particles within the furnace due to a smaller flue gas volume would likewise contribute to an increase in the burnout efficiency for oxyfuel combustion compared to air-firing. Even though contribution of gasification by $CO_2$ and/or $H_2O$ to the increased burnout is suggested several times in literature, it is questionable if this effect is of significant importance for the conversion of the fuel on the time scales relevant

to suspension-fired boilers.

CO levels in the flame zone are generally reported to increase significantly in oxyfuel combustion compared to air-firing. Even though the high $CO_2$ levels limits CO oxidation at high temperatures complete conversion is expected when excess oxygen is present during cool-down of the flue gas. CO emission rates similar to air combustion have been reported in literature for the larger of the test furnaces.

### 1.3.3 Formation of Gaseous Pollutants

The general conclusion in published literature is that the amount of $NO_x$ emitted from an oxyfuel power plant can be reduced to somewhere between one-third and half of that from combustion in air. Sulphur oxides is the other major pollutant from coal-fired combustion. The emission of these oxides is, however, not reduced to the same degree as $NO_x$.

#### 1.3.3.1 NO

The potential for reducing the $NO_x$ emissions from a power plant considerably compared to air-firing has been one of the key drivers in oxyfuel combustion research, particularly in USA and thus, $NO_x$ emissions from oxyfuel combustion is probably the single most investigated area of this technology.

Due to the very low levels of molecular nitrogen in the oxyfuel oxidant a potential exists to reduce the emissions rate considerably compared to combustion in air through near elimination of both thermal and prompt $NO_x$ formation. The results reported in the literature generally show that combustion in air yields the highest $NO_x$ emissions, oxyfuel combustion based on synthetic gas mixtures ($CO_2$ + $O_2$) yields lower emission rates at comparable conditions, whereas oxyfuel combustion with recirculation of flue gas yields the lowest emission rates. Reductions of up to 70–80 % have been reported for the latter. Different suggestions to the specific mechanisms responsible for the reduction have been proposed. However, it is generally accepted that reburning reactions play a major role. Experiments indicate that increasing the oxygen concentration and the oxygen excess yield higher emission rates. On the other hand, the use of oxidant staging, recycling of wet flue gas, increasing the partial pressure of $NO_x$ in the oxidant, increasing the oxygen purity, and limiting the air ingress into the boiler works to decrease the emission rate.

Most of the reported experiments yield a decrease in the $NO_x$ emission rate during oxyfuel combustion. However, some experiments show an increase which is suggested to be caused by the fact that the mechanism of Fuel-$NO_x$ formation is very sensitive to the method with which oxygen and fuel is mixed in the flame. As oxyfuel burners are typically adopted from air-firing principles the resulting

fluid dynamics of the flame can be disadvantageous with respect to $NO_x$ emissions even though the flames are stable.

#### 1.3.3.2 $SO_2$

The substitution of $N_2$ by $CO_2$ in oxyfuel combustion does not affect the release of sulphur from the coal during combustion. However, the increased oxygen partial pressure necessary to maintain an appropriate flame temperature increases the formation rate of $SO_3$. During operation with a flue gas recycle without $SO_2$ removal the $SO_2$ and thus the $SO_3$ levels in the boiler and flue gas ducts increases significantly which will enhance the risk of sulphur-induced corrosion at both high and low temperatures. Increased risk of low-temperature corrosion by sulphuric acid condensation and a higher acid dew point are some of the major concerns regarding sulphur in oxyfuel combustion. High in-boiler concentrations of sulphur oxides can likewise increase retention of S in the fly ash. Increased retention will reduce the $SO_2$ emission rate but could at the same time yield problems with further utilization of the fly ash in cement and concrete production.

### 1.3.4 Ash and Deposit Formation

The transformations of coal mineral matter during combustion are affected by the temperature and the gas phase composition surrounding the coal particles. At low combustion temperature (for below 30 % $O_2$ in $CO_2$) a shift in the size distribution of the sub-mircometer sized fly ash towards smaller particles can be observed. Increasing the $O_2$ partial pressure to match the flame temperature of air combustion provides a size distribution similar to that found during air combustion. The ash quality is crucial to its application in cement and concrete production. Significantly increased sulphur retention could cause problems in this respect. The propensity for slagging and fouling in oxyfuel combustion is likewise subject to research. At this point, the reported results suggest that only minor changes compared to air-firing will result from the change in the combustion environment.

### 1.3.5 Co-Firing Coal and Biomass

Utilization of renewable biomass fuels such as wood, straw, and other energy crops in thermal power plants with carbon capture and storage is attracting increased attention. The combination of $CO_2$ neutral fuels with CCS opens up a possibility of extracting $CO_2$ from the atmosphere. Until now, only few experiments on oxyfuel combustion of biomasses have been reported in open literature. It is expected that further work on co-firing of biomass and coal in oxyfuel atmospheres will reveal comparable changes to the combustion fundamentals as is the case when biomass is introduced during combustion of coal in air. However, this area

of research is still relatively young when considering suspension-fired boilers and research on oxyfuel combustion of pulverized biomass could thus also be beneficial to the research within the conventional air-firing area.

## 1.4 Project Objectives

This PhD is aimed at improving the fundamental knowledge on oxyfuel combustion of coal and biomass (straw) at conditions relevant to suspension-fired boilers. The subjects specifically investigated cover:

- The general combustion characteristics of coal, straw and their blends (with 20 and 50 wt% straw) in an atmosphere of $O_2/CO_2$ with focus on the influence of excess oxygen and high $CO_2$ levels on burn-out
- Formation and emission of pollutants (CO, NO, and $SO_2$) as a function of excess oxygen, oxidant composition, and fuel
- The fate of N and S during simulation of flue gas recirculation without removal of NO and $SO_2$
- Ash and deposits characteristics – with emphasis on the chemical composition and the fate of potassium, sulphur, and chlorine during co-firing of biomass with coal
- The potential for reducing oxygen excess while maintaining high burnout

Comparison to representative reference data for combustion of coal, straw and their blends in air is performed. The objectives have been addressed by theoretical considerations and experiments in semi-technical scale. The following chapters contain the results of the work. The applied experimental setup and the methods used in the data treatment are presented in Chapter 2. Chapter 3 describes the observed differences in combustion fundamentals when changing the combustion atmosphere from $N_2$-based (air) to $CO_2$-based (oxyfuel) using pure coal as fuel. The impact on the combustion characteristics and the fly ash and deposit formation when pure biomass (straw) and blends of coal and biomass are combusted in air and oxyfuel atmospheres are discussed in Chapter 4. Chapter 5 is devoted the special topics related to the more specific process implications associated with oxyfuel combustion. The chapter is in two parts with the first part addressing the fate of N and S during simulation of flue gas recirculation without removal of NO and $SO_2$ for oxycoal combustion. The second part of Chapter 5 concerns potential improvements to the process economy for retrofitted power plants by means of reducing the oxygen demand. Chapters 6 and 7 summarize the work and point to more areas within the oxyfuel combustion technology which require further research.

# Chapter 2

# Experimental Methods

In the first part of this chapter, a short description of the experimental setup is given. A more thorough description is available in the design report for the setup [60]. The second part of this chapter provides overviews of the most important parts of the considerations regarding the operation of the experimental setup and the pre-treatment of the experimental data. The full description of the experimental considerations and calculation procedures is given in [61].

## 2.1 Description of the Experimental Setup

The 30 kW down-fired solid fuel combustor, shown in Figure 2.1 on the following page, has an inner diameter of 315 mm and a height of about 1.9 m. Table 2.1 on page 18 shows the design data for the setup. The combustion chamber is insulated with 80 mm two-layer refractory lining and cooled with room-temperature cooling air drawn through a void between the reactor shell and an outer insulation shell.

There are 8 measuring ports along the combustion chamber which can be used for *e.g.* thermocouples, gas sampling lines, deposit probe insertion, and other measuring probes. The ports are numbered 1 to 8, starting with 1 from the top. Fly ash is collected in the ash sampling system, see Figure 2.2 on page 15, which withdraws a portion of the flue gas through the bottom of the reactor. The sampling rate is between 60 and 150 L/min depending on the specific operating condition of the setup. Three fractions of ash are collected from the system designated "bottom", "cyclone", and "filter" ash. The results on fly ash composition, etc. will be from a mixture of those three fraction unless otherwise stated.

A loss-in-weight controlled twin-screw feeder (K-Tron K-ML-KT20-H-110L) feeds the pulverized solid fuel particles onto a vibrating table (Scan-Vibro) which acts as both a conveyor and for levelling out instabilities in the fuel flow from the feeder. From the vibrating table the fuel particles fall into the central, primary

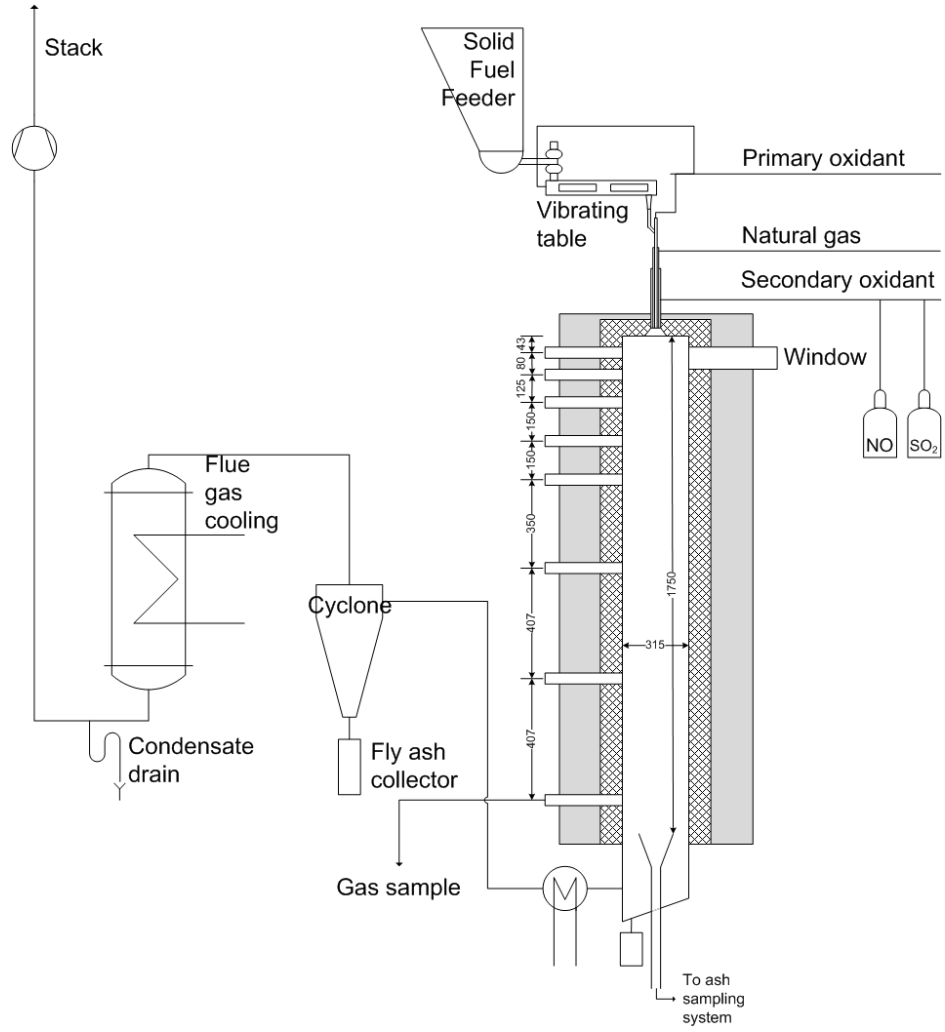


Figure 2.1: Schematic of the 30 kW swirl burner setup. All measures are in mm.

burner tube. A fraction of the primary oxidant is introduced in the back-end of the vibrating table to assist the feeding of fuel. The remaining, primary oxidant flow is fed directly into the central burner tube. The split between the two primary oxidant flows is adjusted during start-up of an experiment in order to achieve the best stability of the solid fuel feeding.

The burner is mounted on top of the combustion chamber as seen in Figure 2.3 on page 16. It consists of three tubes, two for primary and secondary oxidant and a separate natural gas inlet which is used during reactor heat-up and during the transition to the solid fuel flame. The secondary oxidant is introduced in the burner in two separate streams, an axial flow and a tangential flow. The latter is responsible for creating a swirling motion and the swirl number is adjusted by choosing the ratio between the axial and tangential flow. A detailed diagram of the burner is seen in Figure 2.4 on page 17.

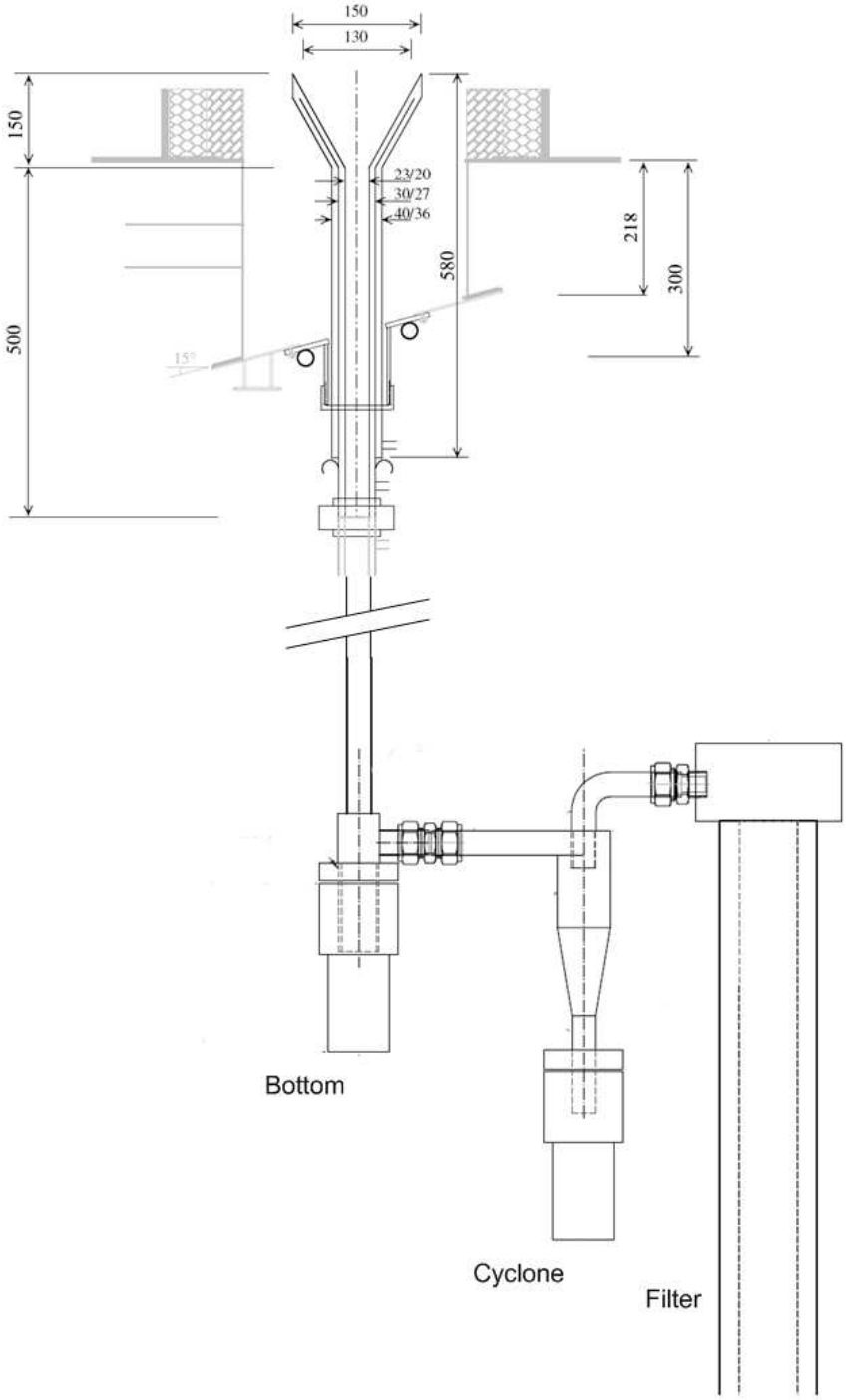


Figure 2.2: Sketch of the ash sampling system. The system consists of an about 2.5 m long vertical tube with a funnel, which is inserted through the bottom of the reactor. The vertical tube ends in a heated cup which collects the ash particles too big to follow the flue gas stream drawn through the cyclone and the filter. The cut-size of the fly ash sampling filter is 1 $\mu$m.

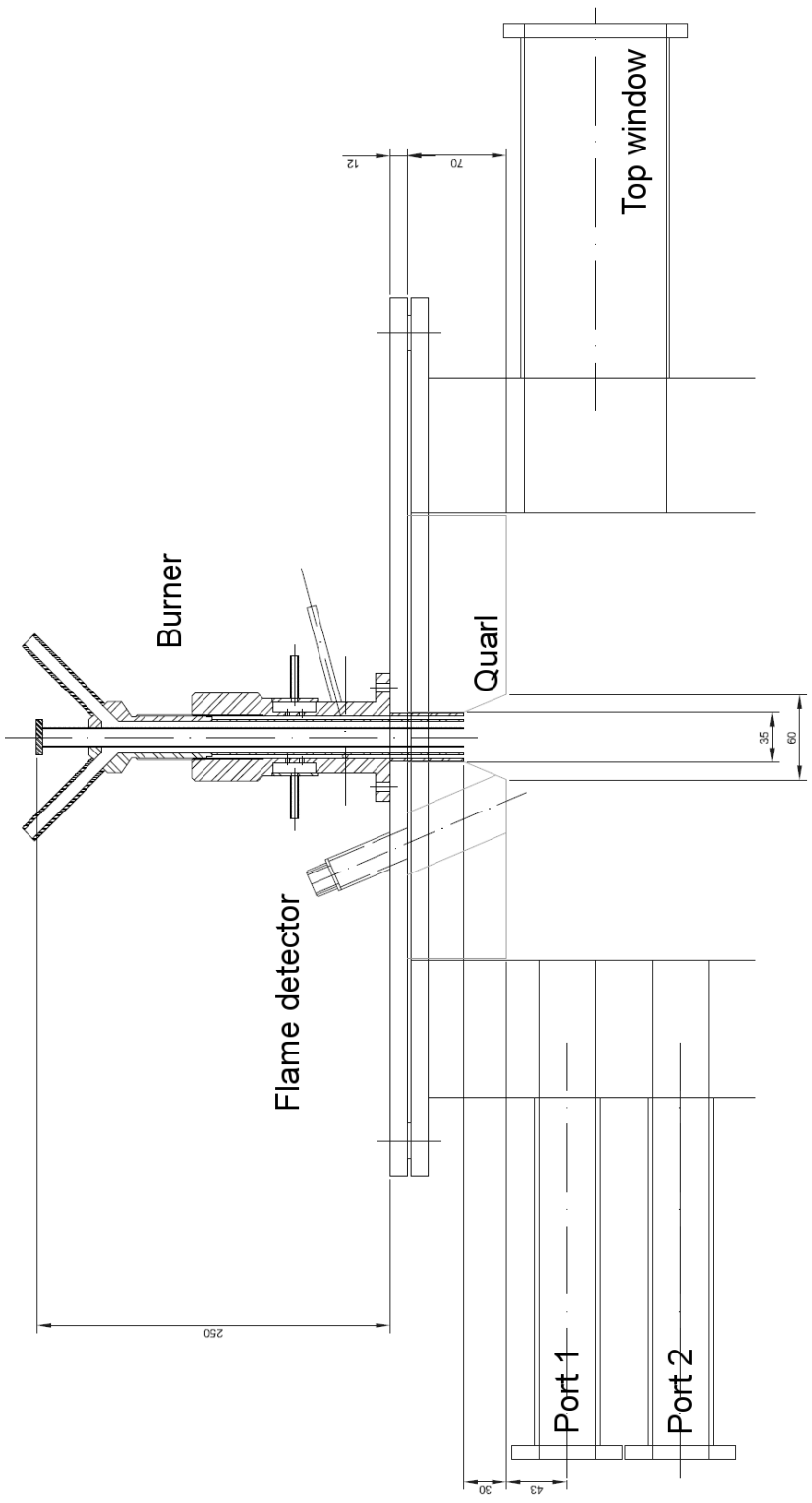


Figure 2.3: Detailed sketch of burner mounted in the top of the reactor chamber.

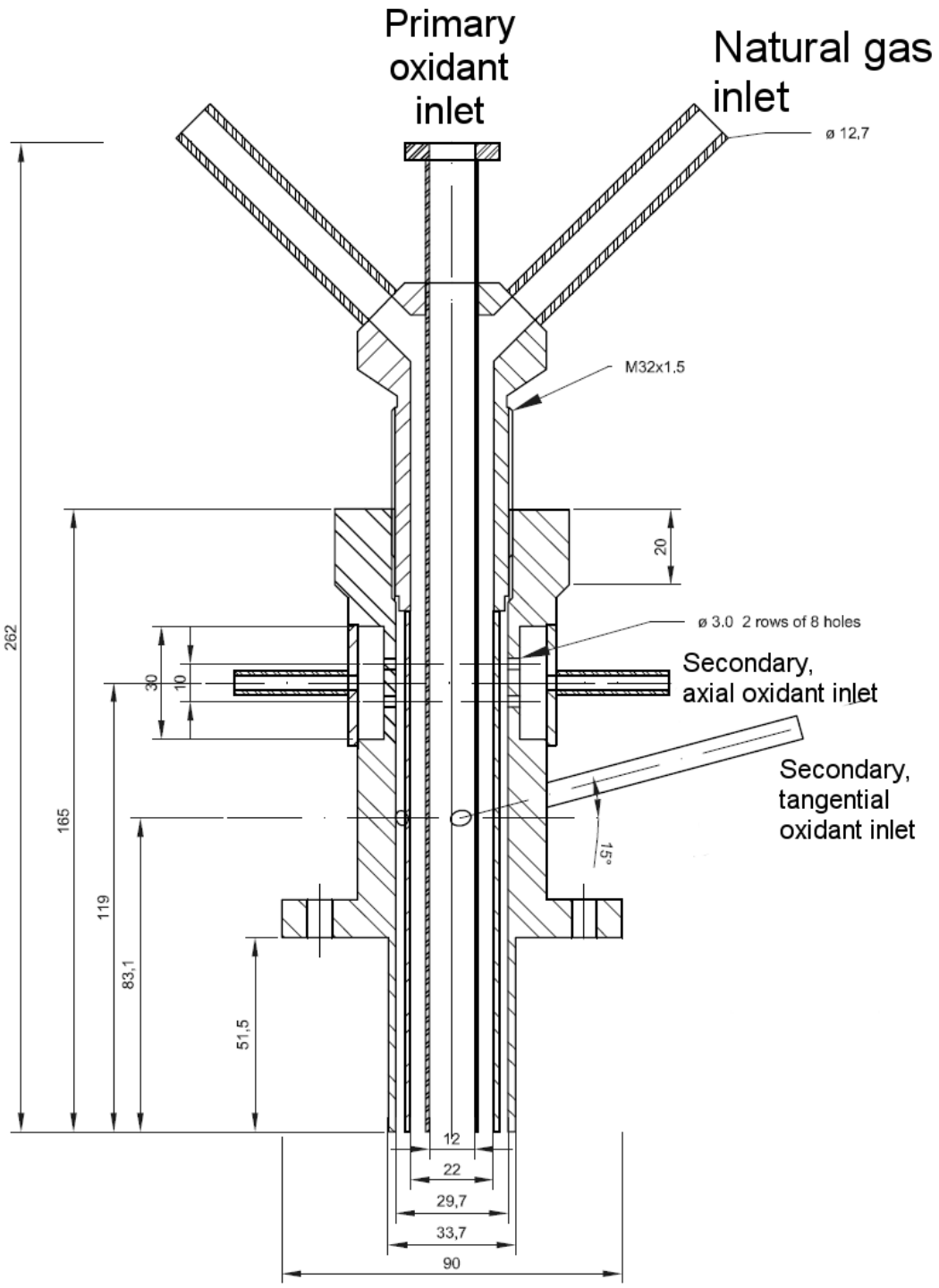


Figure 2.4: Detailed sketch of burner.

Table 2.1: Design data for experimental setup

| Parameter | Value |
|---|---|
| Reactor inner diameter | 315 mm |
| Reactor height, total | 1.9 m |
| Port 1, distance from burner | 43 mm |
| Port 2, distance from burner | 123 mm |
| Port 3, distance from burner | 248 mm |
| Port 4, distance from burner | 398 mm |
| Port 5, distance from burner | 548 mm |
| Port 6, distance from burner | 898 mm |
| Port 7, distance from burner | 1305 mm |
| Port 8, distance from burner | 1712 mm |
| Ash sampling system, distance from burner | 1.75 m |
| Sampling rate, ash sampling system | 60–150 L/min |
| Flue gas sampling position | Port 8 |
| Flue gas sampling rate | 3 L/min |
| Deposit sampling position | Port 7 |
| Temperature mapping, ports: | 1-5, 7 |

For both air and oxyfuel experiments the primary oxidant flow is set at 20 vol% of the total oxidant flow at the reference conditions. This implies that the linear velocity of the primary oxidant leaving the burner will differ when the combustion atmosphere and/or the stoichiometry is changed. However, the swirl number is kept constant to obtain similar conditions for air and oxyfuel experiments.

The flow of oxidant is controlled by manual valves and adjusted according to readings from rotameters. A more accurate monitoring is performed by mass flow controllers in the oxidant mixing panel. The mass flow controllers are likewise responsible for correctly mixing the oxidant for oxyfuel experiments according to settings which are controlled in LABVIEW.

The combustor is heated by natural gas combustion over-night or for at least 14 hours before an experiment starts in order to achieve stable temperatures of the reactor lining. For oxyfuel combustion experiments the oxidant is switched to an $O_2/CO_2$ mixture before the solid fuel feeding is started. After a minimum of 1 hour with pure solid fuel combustion the combustion chamber temperature profile as well as the flue gas composition have stabilized and the measurements and sampling can be initiated. Depending on the scope of the test the measurements will proceed for about 2-6 hrs.

The reactor is a once-through type reactor and thus has no ducts for recirculating flue gas in oxyfuel operation. $O_2/CO_2$ mixtures are produced at chosen

molar ratios from gas bottles in the oxidant mixing panel. The primary and secondary oxidant flows are of the same composition. When adding NO and/or $SO_2$ to the oxidant in order to simulate recirculation of flue gas without prior gas cleaning (oxyfuel), these components are solely added to the secondary, tangential fraction of the oxidant. For air combustion the oxidant is supplied as pressurized air.

Flue gas samples are continuously drawn from the lowest measuring port (#8). The gas sample is filtered and dried before entering on-line gas analysers. Two analysers (Rosemount NGA 2000) are available, one which measures $O_2$, CO, and $CO_2$, and one which measures NO and $SO_2$. $NO_2$ has not been measured as it has been assumed that only negligible amounts leaves the reactor at the relatively low oxygen excess ratios and temperatures utilized [62]. For oxyfuel experiments with high oxygen concentration in the oxidizer ($> 40$ %), a measurable amount of $NO_2$ may be formed in the flame. However, it will most likely be destroyed before reaching the flue gas sampling position [62]. Different ranges are available for the individual gases on each analyser and the calibration is performed according to the expected flue gas composition. For oxyfuel experiments, $CO_2$, $N_2$, and $O_2$ are simultaneously measured on a MicroGC (Varian CP-4900) about every 2 minutes. The radial variation of the flue gas composition at port 8 was found to be relatively small during a test on a natural gas/air flame. Unless otherwise specifically noted, the flue gas sample is thus retrieved from within port 8 and not from the centre of the reactor in order to limit the dust loading on the flue gas particle filter.

## 2.2 Solid Fuel

### 2.2.1 Fuel Characterization

During the experiments two different fuels have been utilized, a bituminous coal from El Cerrejon, Colombia (COCERR), and pulverized straw pellets made from cereal straw (wheat and barley in a non-specified ratio). Fuel analysis have been performed by the laboratory at Ensted Power Station and the results are seen in Table 2.2 on the next page. The coal was delivered in 2007 from the OxyCoal-UK project in which DONG Energy participated and was ground at delivery. The straw was delivered as pellets from Køge Biopillefabrik in March 2010. The pellets were pulverized by Teknologisk Institut with a specification of 100 % being below 700 $\mu$m. The measured particle size distribution for the two fuels is shown in Figure 2.5 on page 21. The median particle sizes for the two fuels are given in Table 2.2.

The mean particle size of the straw is generally much smaller than usually utilized when co-firing straw at low weight fractions in suspension-fired boilers. However, when biomass constitute the major fraction of the fuel in suspension-

Table 2.2: Properties of El Cerrejon bituminous coal (Colombian) and Danish, pulverized, cereal straw pellets.

| **Fuel** | **Coal** | **Straw** |
|---|---|---|
| KT Journal number | 228-66 | 228-77 |
| **Heating value** (MJ/kg, as received) | | |
| LHV | 27.09 | 16.40 |
| **Proximate analysis** (wt%, as received) | | |
| Moisture | 5.03 | 5.10 |
| Ash | 9.62 | 4.40 |
| Volatile | 34.86 | 72.40 |
| Fixed carbon (by difference) | 50.49 | 18.10 |
| **Ultimate analysis** (wt%, daf) | | |
| C | 80.70 | 48.62 |
| H | 5.41 | 6.41 |
| N | 1.69 | 0.49 |
| S | 0.726 | 0.094 |
| Cl | 0.016 | 0.419 |
| O (by difference) | 11.46 | 43.97 |
| **Ash forming elements composition** (wt%, dry) | | |
| Al | 1.1 | 0.011 |
| Ca | 0.16 | 0.44 |
| Fe | 0.51 | 0.0076 |
| K | 0.18 | 1.00 |
| Mg | 0.14 | 0.054 |
| Na | 0.060 | 0.050 |
| P | 0.0078 | 0.062 |
| Si | 2.7 | 0.91 |
| Ti | 0.054 | 0.008 |
| Bulk density (kg/m$^3$) | 1000 | 450 |
| Particle diameter, median/$d_{50}$ ($\mu$m) | 47 | 330 |

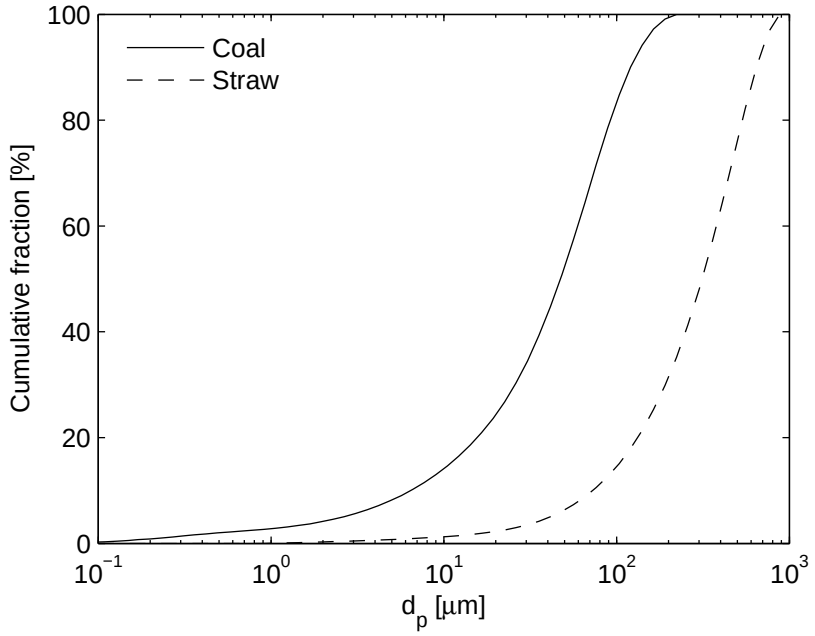


Figure 2.5: Cumulative particle size distributions for coal and straw. The distribution type is volumetric and is obtained from a Malvern laser diffraction particle size measurement.

fired boilers the particle size distribution is closer to the one used in the present experiments. The main reason is the need for the biomass to aid in flame stabilization. When co-firing straw up to about 20 wt%, coal acts to stabilize the flame and less strict demands regarding the particle size of the straw particles are necessary.

For experiments simulating co-firing of coal and straw two mixtures have been made by Teknologisk Institut. The mixtures have a 20 and 50 wt% content of straw. This corresponds to approximately 13 and 38 % straw on a thermal basis, respectively. The 20 wt% mixing ratio has been chosen based on the fact that it constitutes the maximum limit for the case where the fly ash is used for concrete [63]. The 50 wt% ratio is designed to give a relatively even distribution between datapoints and to aid in investigating the ability of coal to capture large amounts of potassium from biomass, which is important from a corrosion and $DeNO_x$ catalyst deactivation perspective.

The ratios of coal to straw in the blends were checked with TGA after arrival [61]. The average straw shares in each blend are seen in Table 2.3 on the next page. Note that the 50 wt% blend was delivered in two batches. The deviation from the specified straw share for the 50 wt% blends is taken into account in the data treatment.

Table 2.3: Overview of measured straw shares for fuel blends

| Specified straw share | 20 wt% | 50 wt%, B1[a] | 50 wt%, B2 |
|---|---|---|---|
| Measured | 20 | 52 | 46 |

[a] B1 = Batch 1, B2 = Batch 2

Table 2.4: Solid fuel feeder set points for applied fuels

| Fuel | Feeding rate, SP [kg/hr] |
|---|---|
| Coal | 3.99 |
| 20 wt% straw blend | 4.33 |
| 50 wt% straw blend | 5.0 |
| Straw | 6.6 |

### 2.2.2 Fuel Feeding Rates

For all experiments reported the solid fuel feeding system has been operated at a set point corresponding to a thermal load of 30 kW. Table 2.4 shows the set points of the feeding system for the different fuels which have been investigated.

The solid fuel feeding rate is logged as the feeder net weight signal in each data sampling point (usually each second). The actual feeding rate can thus theoretically be determined from the slope of the weight signal in each data point. Figure 2.6 on the next page shows an example of the net weight signal during straw combustion and illustrates the limited number of bits in the data sampling system causing the data points to be stair shaped with a step height corresponding to approximately 55 g.

Due to the nature of the data, one of two options for determining the fuel feeding rate can be chosen; (1) calculating an average feeding rate based on the data for the entire experiment, or (2) make an estimation based on a given number of data points before and after the data point (time) of interest.

The solid fuel feeding rate has been observed to yield both fast and slow fluctuations due to perturbations caused by *e.g.* step changes of the sub-pressure in the reactor and occasionally insufficient PID parameters in the control system of the feeder. A feeding rate based on (2) is thus likely to yield a better estimate of the instantaneous value provided the averaging time interval around the data point is of an appropriate size.

Figure 2.7 on the facing page shows the calculated fuel feeding rate during a limited time interval for an experiment with combustion of pure straw. The figure likewise shows the feeder set point, the average feeding rate for the entire period with solid fuel feeding, and the average feeding rate during the time interval

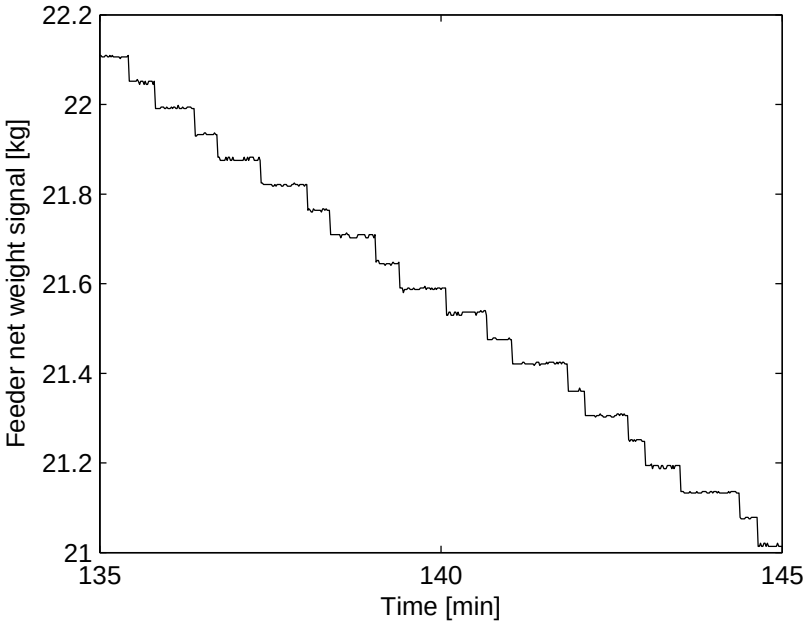


Figure 2.6: Example of weight signal from solid fuel feeder as a function of time for combustion of pure straw.

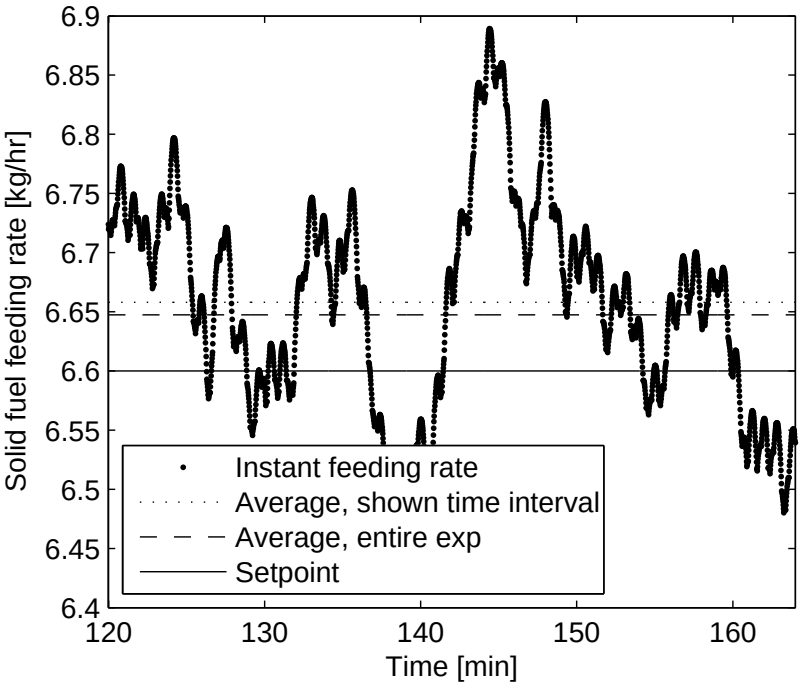


Figure 2.7: Calculated instantaneous and averaged solid fuel feeding rates for an experiment with combustion of pure straw.

shown in the figure. It is seen that the instantaneous feeding rate fluctuates on both a short and long time scale. A small deviation in feeding rate ($\sim 1$ %) from the feeder set point is likewise observed, both for the selected time interval and for the entire experimental run.

In general, the average feeding rate is satisfactorily close to the set point. However, fluctuations occur which will have an impact on the combustion process. The instantaneous fuel feeding rate is thus used during the data treatment.

## 2.3 Experimental Considerations and Calculation Procedures

This section describes calculation procedures related to the evaluation of the collected experimental data and the considerations and assumptions made in that respect. The section also includes analysis procedures for the samples collected during the experiments. Additionally, examples of the determination of operating conditions based on the available measurements from the setup are given.

### 2.3.1 Data Structure

52 of the experimental runs performed on the swirl burner setup have been selected for data treatment. The sections below provide an introduction to the data collected during the individual experiments.

#### 2.3.1.1 Numbering of Experiments

The experiments are numbered according to the following principle:

$$\text{Exp no.} = \text{XY\#\_E} \tag{2.1}$$

where X designates the fuel (S = straw, C = coal, M20 = 20% straw/coal blend, M50 = 50 % straw/coal blend), Y is the oxidant (A = air, O = oxyfuel), # is a running number for the specific combination of fuel and oxidant, and E indicates any additional data besides measurements of the exit flue gas composition (A = ash sampling, D = deposit sampling, T = temperature mapping with S-type thermocouple, M = Mapping with FTIR probe, L = oxygen excess different from the reference value of 5 vol% $O_2$ in dry flue gas, B = burner settings variation tests, S = $SO_2$ addition to oxidant, N = NO addition to oxidant). An example:

$$\text{Exp no.} = \text{SO05\_ADLT}$$

In the given example pure straw (S) has been combusted in $O_2/CO_2$ (O). The experiment is the fifth for that fuel/oxidant combination (05) and the stoichiometry was different from the reference conditions chosen (L). During the experiment fly ash (A) and a deposit sample (D) has been collected and a temperature profile was measured with a thermocouple (T).

#### 2.3.1.2 Operating Parameters Overview

Table 2.5 on the next page provides an overview of the settings and variations of the key operating parameters applied during the experimental campaign. The table is divided according to the oxidant type and the four different fuels investigated. A further sub-division is made for oxyfuel combustion experiments with respect to the oxidant composition. More specific settings regarding individual oxidant flows and sampling rates can be seen in [61].

#### 2.3.1.3 Raw Data

During experiments numerous data are logged. Most data are sampled automatically with LABVIEW; pressures, temperatures, gas concentrations, flows of NG and oxidizer, etc. For each experiment a data file is thus produced which contains the necessary data to characterize and analyse the experiment. The data have typically been logged with an interval of one second. Other data are logged manually or semi-automatically; flow rates of oxidizer to the individual registers of the burner, ash sampling velocity, as well as gas analysis results from the MicroGC.

Figure 2.8 on page 27 shows an example of the most important online data logged for an experiment with air as oxidant (M20A01_ADT). The specific experiment is for the 20 wt% straw/coal blend as fuel. During the experiment both fly ash and a deposit sample has been collected, and a temperature mapping has been performed. Time 0 corresponds to the initiation of the change from a NG flame to solid fuel feeding.

The flue gas composition is observed to fluctuate with a relatively high frequency. This is caused by formation of fuel agglomerates on the vibrating table which leads to instabilities in the fuel supply to the burner. From the $CO_2$ and $O_2$ data variations in the average fuel flow to the burner can likewise be observed as fluctuations with a significantly lower frequency. Deviations in the fuel flow from the set point are typically caused by disturbances of the reactor pressure which again influences the solid fuel feeding system.

From the NO and $SO_2$ data the approach to steady state for the solid fuel flame can be observed as a decrease and increase, respectively, in the concentrations over a period of approximately 90 minutes. Typically, this stabilization period is also associated with a change in the temperature at port 5. The reason is mainly that the NG flame is significantly shorter than the solid fuel flame and hence the temperature profile of the reactor will change, even though it was attempted to match the adiabatic temperature of the NG flame to the solid fuel flame. The approach to steady state has been observed to occur at different velocity for each experiment, depending primarily on the setting for the NG flame run prior to the experiment and the solid fuel, with coal stabilizing faster than pure straw, the coal flame being significantly shorter.

Table 2.5: Overview of operating parameter set points and their variations during the experimental campaign

| | Load | Fuel flow | Inlet $O_2$ | $\lambda$ | Flue gas exit $O_2$ | Oxidant flow | Swirl number | Inlet NO | Inlet $SO_2$ |
|---|---|---|---|---|---|---|---|---|---|
| **Air** | [$kW_{th}$] | [kg/hr] | [vol%] | [-] | [vol%, dry] | [Nl/min] | [-] | [ppmv] | [ppmv] |
| Coal | 30 | 3.99 | - | 1.1, 1.15, 1.25, 1.3 | 2, 2.8, 4.3, 5 | 525, 550, 595, 620 | 1.7, 1.8, 1.9, 2 | - | - |
| Straw | 30 | 6.6 | - | 1.3 | 5 | 600 | 1.8 | - | - |
| 20 wt% blend | 30 | 4.33 | - | 1.3 | 5 | 620 | 1.8 | - | - |
| 50 wt% blend | 30 | 5.0 | - | 1.3 | 5 | 615 | 1.8 | - | - |
| **Oxyfuel** | | | | | | | | | |
| Coal | 30 | 3.99 | 25 | 1.24 | 5 | 490 | 1.8 | - | - |
| Coal | 30 | 3.99 | 30 | 1.13 | 3.5 | 370 | 1.8 | - | - |
| Coal | 30 | 3.99 | 30 | 1.19 | 5 | 390 | 1.8 | 0, 500, 1300, 2000 | 0, 500, 1500, 3500 |
| Coal | 30 | 3.99 | 33.3 | 1.16 | 5 | 345 | 1.8 | - | - |
| Coal | 30 | 3.99 | 35 | 1.15 | 5 | 325 | 1.8 | - | - |
| Straw | 30 | 6.6 | 30 | 1.22 | 5 | 390 | 1.8 | - | - |
| Straw | 30 | 6.6 | 40 | 1.09 | 3 | 260 | 1.8 | - | - |
| Straw | 30 | 6.6 | 50 | 1.025, 1.05, 1.075, 1.09 | 1, 2, 3, 3.6 | 195, 200, 205, 208 | 1.7, 1.8, 1.9, 2 | - | - |
| 20 wt% blend | 30 | 4.33 | 30 | 1.19 | 5 | 390 | 1.8 | - | - |
| 50 wt% blend | 30 | 5.0 | 30 | 1.2 | 5 | 390 | 1.8 | - | - |

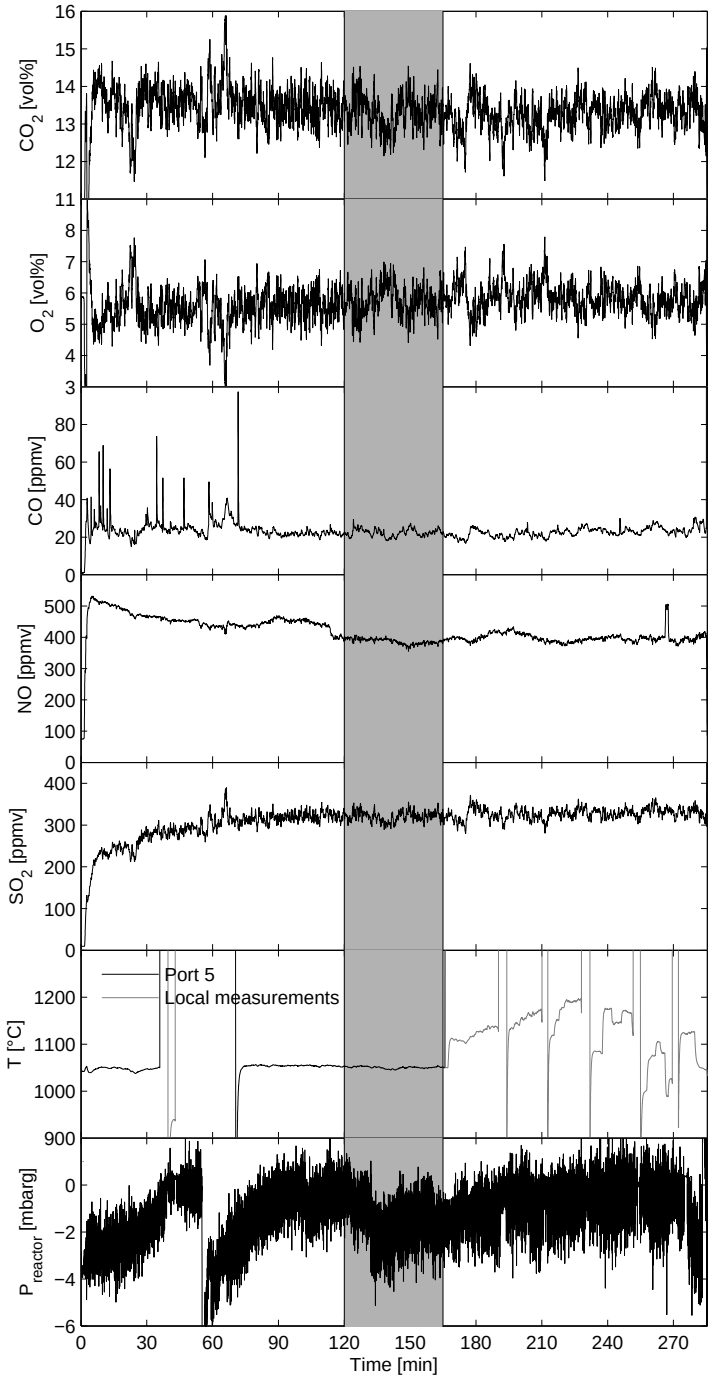


Figure 2.8: Concentrations of major flue gas components ($CO_2$, $O_2$, CO, NO, and $SO_2$) as function of time for experiment M20A01_ADT, as well as the pressure at the top of the reaction chamber, the reference temperature measured at the reactor wall at a vertical position about 55 cm from the burner (port 5), and the local temperature measurements conducted with the S-type thermocouple probe. The shaded area indicates the part of the data which are used during further data analysis.

The data within the time interval patched in grey are used for calculating mass balances, determining emission rates, conversion ratios of fuel-N and -S, etc. The time interval is preferably situated in a period where the reactor has reached steady state, has run stably, and without any measurement ports being opened to the surroundings in order to limit false air ingress.

Figure 2.9 on the next page shows the corresponding data for coal combustion at oxyfuel conditions (CO16_AL). Since the online gas analyser cannot measure $CO_2$ concentrations above 25 vol% it cannot be used for oxyfuel flue gas. Instead, the microGC is used to collect $CO_2$ data. The microGC measures $O_2$ and $N_2$ in addition to the $CO_2$ and these data are likewise shown. The sampling interval for the microGC measurements is significantly longer than the one second obtainable for the online analysers. Typically, the microGC provides data with a 1.5 to 2 minute interval.

Good correlation between the online and GC measurements of $O_2$ is observed. The $N_2$ measurements are seen to follow the trend of the reactor pressure. The $N_2$ present is a consequence of air leaking into the reactor system, with the ingress being a direct function of the sub-pressure in the reactor. The level of false air ingress is typically below 5 % of the total oxidant flow. Frequent CO peaks are registered compared to the example in Figure 2.8. This is caused by the fact that the stoichiometry for the oxyfuel example is lower and the sensitivity of the combustion process to fuel feeding instabilities thus has increased. The CO peaks in the time interval patched in grey are directly correlated to peaks in $SO_2$ which indicates feeding of excess fuel compared to the set point at distinct times.

An overview of all experiments can be found in the data collection [64]. For each experiment the objective is stated together with the basic operating parameters and a list of comments to the course of the experiment. For all experiments the flue gas, temperature, and pressure data are shown.

## 2.3.2 Sampling

In order to characterize the combustion process at the investigated operating conditions three types of samples are drawn from the setup; Flue gas, fly ash, and deposits. The following sections describe the sampling methods.

### 2.3.2.1 Flue Gas

Flue gas is continuously drawn from measurement port #8 (at a vertical position 1.7 m downstream of the burner within the furnace chamber) by the aid of a gas pump situated in a gas conditioning system. The flow rate is about 3 L/min. The gas conditioning system removes particles and moisture from the gas sample.

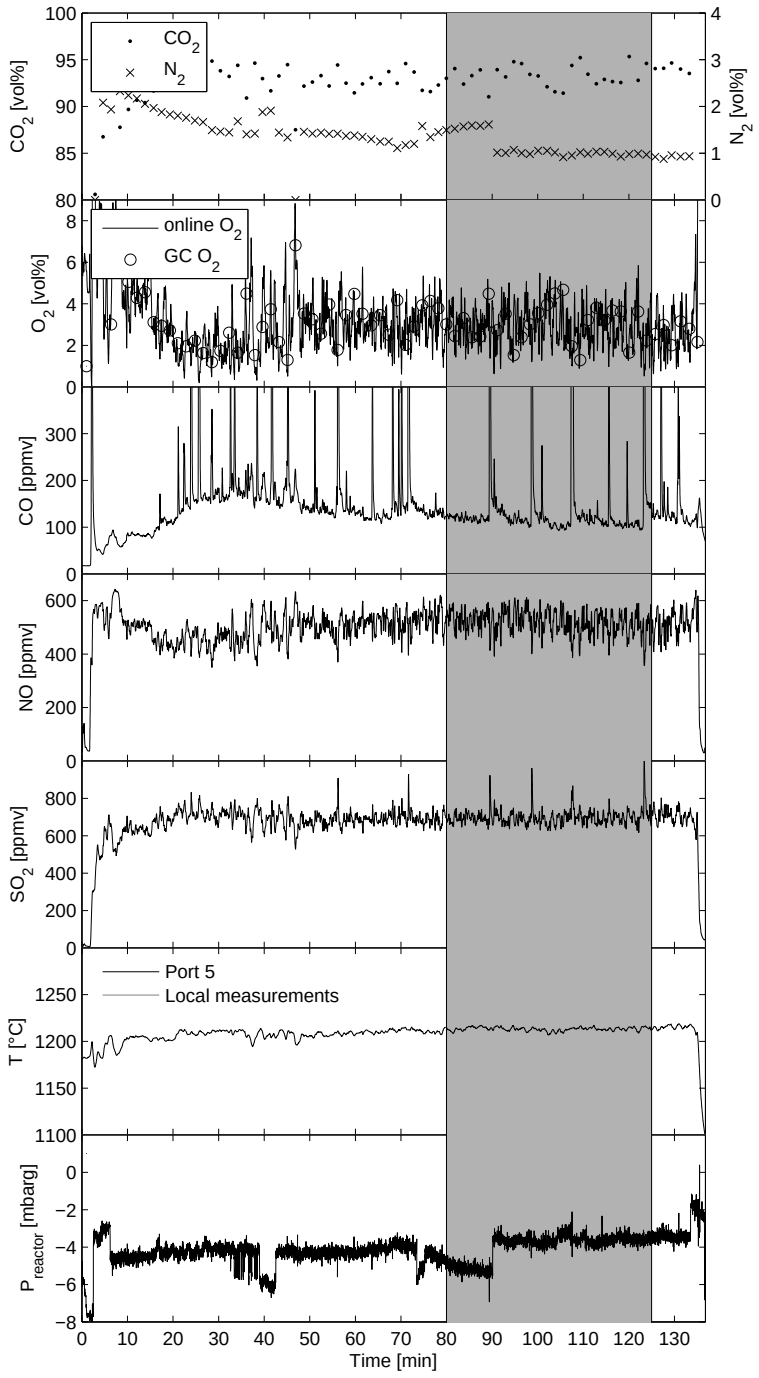


Figure 2.9: Concentrations of major flue gas components ($CO_2$, $N_2$, $O_2$, CO, NO, and $SO_2$) as function of time for experiment CO16_AL as well as the pressure at the top of the reaction chamber, and the reference temperature measured at the reactor wall at a vertical position about 55 cm from the burner (port 5). No local temperature measurements have been performed. The shaded area indicates the part of the data which are used during further data analysis.

Table 2.6: Uncertainties on flue gas species measurements dependent on measuring range and calibration gas

| Gas species | Range UL[a] | Cal. gas | Uncertainty[b] |
|---|---|---|---|
| $O_2$ | 10 % | 9.52 % | 0.2 % |
| $O_2$ | 5 % | 4.5–5.0 % | 0.1 % |
| $CO_2$ | 25 % | 18.8–19.3 % | 0.5 % |
| CO | 4000 ppm | 3800 ppm | 90 ppm |
| CO | 1000 ppm[c] | 100 ppm | 10 ppm |
| NO | 1500 ppm | 900 ppm | 20 ppm |
| $SO_2$ | 2500 ppm | 2500 ppm | 60 ppm |
| $SO_2$ | 1500 ppm | 950 ppm | 20 ppm |
| $SO_2$ | 500 ppm | 460 ppm | 10 ppm |
| $O_2$, $\mu$GC | 10 % | 0–9.52 % | $< 0.2$ % |
| $N_2$, $\mu$GC | 100 % | 0–99.95 % | $< 0.2$ %[d] |
| $CO_2$, $\mu$GC | 100 % | 0–99.95 % | $< 1$ % |

[a] UL = upper limit

[b] Total uncertainty on measurement

[c] Lowest UL available for CO

[d] For measurements below 10 % $N_2$

**Uncertainty on Flue Gas Composition from Continuous Gas Analysers** The online gas analysers are calibrated prior to each experiment and adjusted if necessary. The gas species concentrations determined by the analysers are associated with an uncertainty. The uncertainty is the sum of the instrument uncertainty which is 1 % of the chosen measurement range and the uncertainty on the calibration gas composition (2 % on each species in the gas for all applied calibration gases). Table 2.6 provides an overview of the generel uncertainties on the flue gas measurements.

**Evaluation of Flue Gas Data** The raw flue gas measurements are used to determine several quantities with which the individual experiments are compared. It is difficult to compare experiments performed at different operating conditions based directly on the measured concentration of flue gas species. Instead, a parameter such as the emission rate (also denoted the specific emission) of NO, $SO_2$, and CO can be used. The emission rate corrects the NO, $SO_2$, and CO data for variations in stoichiometry, etc., and can be determined from Eq. (2.2).

$$\mathrm{E}_i = \frac{y_i \cdot F_{FG,\,dry} \cdot M_i}{\dot{m}_{SF} \cdot LHV} \qquad [\mathrm{mg/MJ}] \tag{2.2}$$

where $y_i$ is the mole fraction of species $i$ in the dry flue gas, $F_{FG,\,dry}$ is the dry flue gas flow [mole/s], $M_i$ is the molar mass of species $i$ [mg/mole], $\dot{m}_{SF}$ is the

mass flow rate of solid fuel [kg/s], and $LHV$ is the lower heating vale of the fuel [MJ/kg].

With respect to NO and $SO_2$ another parameter used in the data analysis is the Fuel-N to NO or Fuel-S to $SO_2$ conversion ratio (CR). The conversion ratio is calculated from Eq. (2.3).

$$\mathrm{CR}_i = \frac{y_i \cdot F_{FG,\,dry} \cdot M_i}{x_{i,\,fuel} \cdot \dot{m}_{SF}} \qquad [\%] \tag{2.3}$$

$x_{i,\,fuel}$ is the mass fraction of N or S in the fuel.

#### 2.3.2.2 Fly Ash

Fly ash is sampled through the bottom of the reactor. The sample probe is funnel shaped and the inlet to the probe has a diameter of 150 mm. The probe centreline is aligned with the reactor centre. The probe covers approximately 23 % of the cross sectional area of the reactor.

In order to sample fly ash with a size distribution comparative to the overall distribution in the flue gas, isokinetic sampling should be performed. During ash sampling the flow rate through the ash sampling system has been adjusted in order to reach near-isokinetic conditions under the assumption of a flat velocity profile. The assumption of a flat velocity profile is rather crude since the flow at the reactor outlet is laminar (Re $\approx$ 1000). However, due to the position of the sampling probe in the reactor bottom it has been assumed that the ash particle size distribution in the sample will not differ significantly from the overall distribution, even though ideal sampling is not performed. The construction of the ash sampling system, see [60], makes it very difficult to accurately control the flow rate through the probe as it is adjusted with a ball valve and according to readings of the sub-pressure at the sampling pump. The flow rate is calculated based on readings from a gas meter.

Ideally, the ash sampling system should collect 23 % of the ash species fed with the solid fuel. However, part of the ash is deposited within the reactor and the ash yield will thus be below 100 %. Ideal conditions also include a perfectly even distribution of the ash across the reactor cross-sectional area. Visual observation of the flames showed a tencency for larger particles to be concentrated around the burner/reactor centreline. This could lead to a biased size distribution with a relatively higher number of large particles. The yield of ash, $Y_{\mathrm{ash}}$, is determined from (2.4).

$$Y_{\mathrm{ash}} = \frac{m_{\mathrm{ash,\,sampled}}}{m_{\mathrm{ash,\,sampled,\,theoretical}}} \tag{2.4}$$

Where $m_{\mathrm{ash,\,sampled,\,theoretical}}$ is determined according to (2.5):

$$m_{\mathrm{ash,\,sampled,\,theoretical}} = \dot{m}_{ash,\,SF} \cdot \Delta t_{ash} \cdot \frac{F_{ash\,sampling}}{F_{FG,\,dry}} \tag{2.5}$$

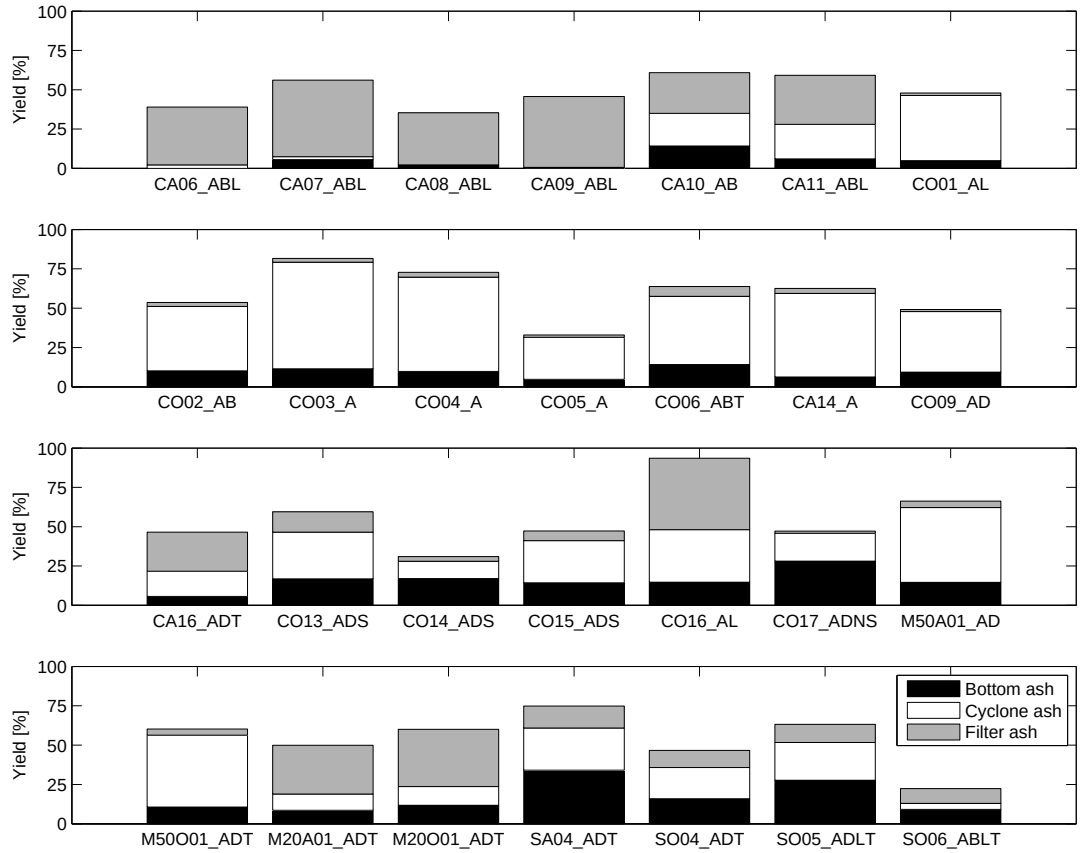


Figure 2.10: Ash yields for all experiments with ash sampling listed in chronological order. The yield is determined from the sampling flow-based method. The distribution of the total ash sample on the three fractions; bottom, cyclone, and filter ash, is given.

$\dot{m}_{ash,\,SF}$ is the mass flow of ash fed in with the solid fuel (SF), $\Delta t_{ash}$ is the time with ash sampling, $F_{ash\,sampling}$ is the average flow rate through the ash sampling system and $F_{FG,\,dry}$ is the dry flue gas flow. $F_{FG,\,dry}$ is determined at ideal conditions, *i.e.* without false air ingress, see Appendix B, Eq. (B.7). The dry flue gas flow is used since the flow rate through the ash sampling system likewise has been measured when dry.

Figure 2.10 shows the obtained ash yields for all experiments with ash sampling. The total yield is divided on the three ash fractions collected from the sampling system. From the data it is seen that the ash yield for the majority of experiments is about 50 %. However, both significantly higher and lower yields have been obtained. The very low yields could have been caused by partly blockage of the ash sampling system, *e.g.* by deposits that have fallen into the probe. For experiments with very high yields there may be a risk that ash from a prior experiment has been transfered. However, this risk is small as the sampling system was cleaned after each run.

The distribution of ash between the three positions in the sampling system is seen to vary. There is a tendency for filter ash to be the primary fraction during coal/air experiments and for cyclone ash to be the primary fraction during coal/oxyfuel experiments. A possible explanation could be the lower flow rate through the sampling system (90 Nl/min versus 150 Nl/min, typically) for oxyfuel experiments. The lower flow rate provides a longer residence time in the cooled section of the probe. Combined with the higher concentration of $H_2O$ in the oxyfuel flue gas (9 % versus 6 %) the ash particles may be more moist when reaching the cyclone leading to a higher collection efficiency. The split between the three fractions does not have an effect on the final results for the individual experiments. The same trend is not seen for the latter experiments with the other fuels. The relatively high bottom ash yields for straw experiments is caused by large char particles ($d_p = 0.5 - 1$ mm).

#### 2.3.2.3 Deposits

A deposit probe, see Figure 2.11 on the following page, was used to collect samples from a fixed position in the reactor (port #7, 1.3 m from the burner). The probe has an outer diameter of 16 mm and an inserted length of 275 mm. The probe is inserted perpendicular to the flue gas flow. The deposit probe is cooled by pressurized air and the metal surface temperature is kept at an average about 500 ℃ by adjustment of the cooling air flow.

In connection with inserting the deposit probe the flue gas temperature at the reactor centre was measured with an S-type thermocouple. The measured temperature was generally in the range 900-950 ℃.

The deposit samples were collected by scraping off the deposit from the probe. The deposit was removed separately from the downstream and upstream parts of the probe in order to determine the mass of each fraction.

Based on the collected masses of deposit, $m_{dep}$, the deposit flux, $N_{dep}$, can be determined, see Eq. (2.6).

$$N_{dep} = \frac{m_{dep}}{A_{probe} \cdot \Delta t} \quad [\mathrm{g/m^2 \cdot hr}] \tag{2.6}$$

$A_{probe}$ is the upstream or downstream area of the probe (half the surface area of the probe) and $\Delta t$ is the time during which the deposit has been collected, typically 2 hr.

#### 2.3.2.4 Analysis of Fly Ash and Deposit Samples

All fly ash samples have been analysed for their loss-on-ignition (LOI). LOI is used as a measure of the burnout efficiency of the fuel. LOI is determined from

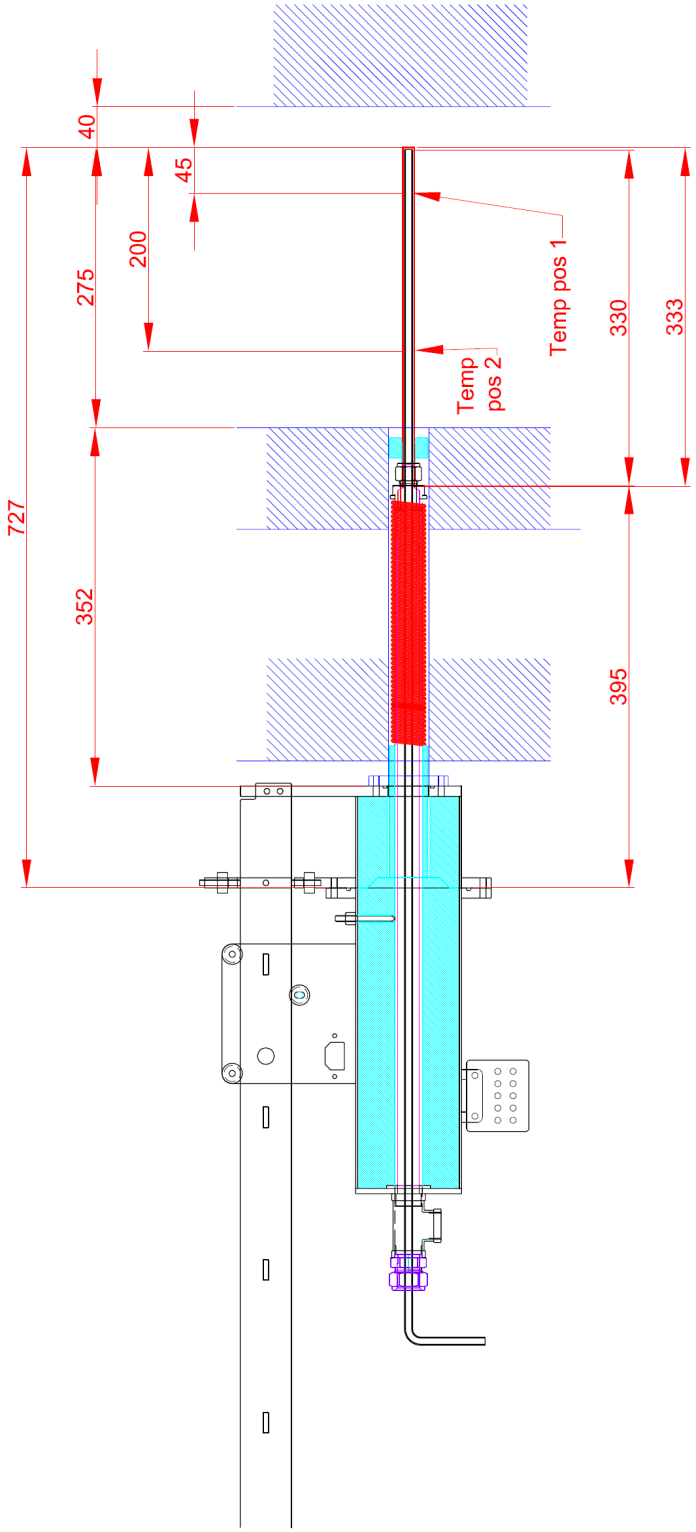


Figure 2.11: Sketch of deposit probe inserted in reactor

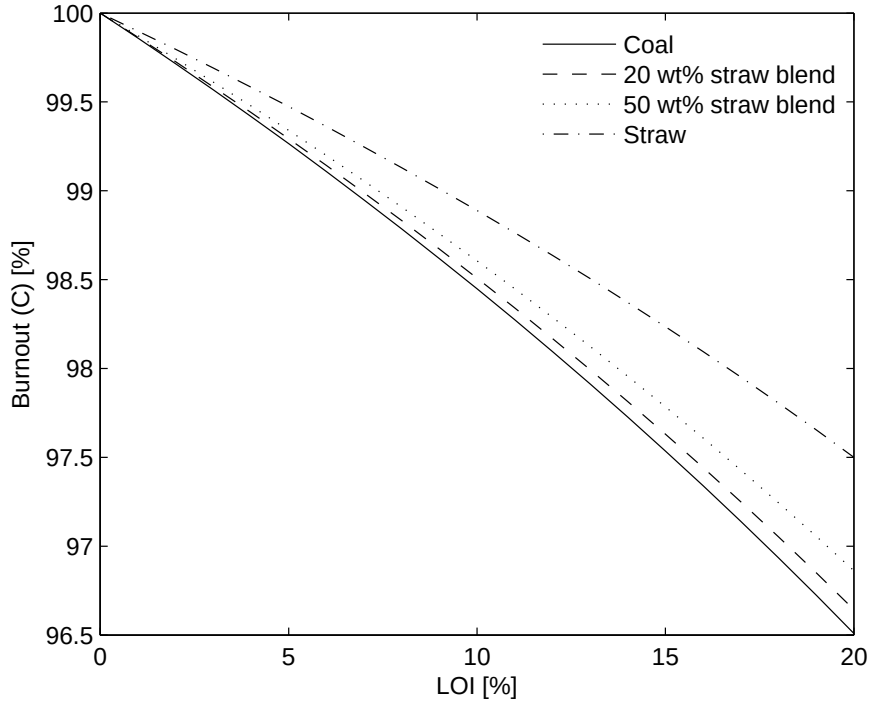


Figure 2.12: Correlation between measured LOI and carbon burnout for the four fuels investigated.

the mass loss observed when heating 1 g of dry ash sample to 550 ℃ in air for 2 hr or until constant mass, see (2.7).

$$\mathrm{LOI} = \frac{m_{dry} - m_{heated}}{m_{dry}} \tag{2.7}$$

Figure 2.12 shows the correlation between fuel burnout (on a carbon basis) and the LOI measured in fly ash. The data are produced under the assumption that all LOI consist of carbon. It is seen that an LOI of 5 % which is the maximum allowable value for fly ash used in concrete production [63] corresponds to about 99.5 % burnout. The increasing carbon burnout efficiency with increasing straw share of the fuel is caused by the relatively lower ash content in straw compared to coal.

Selected samples have been analysed for the carbon content of the ash at the laboratory at the DONG Energy Ensted Power Plant (ENV). A comparison of the carbon content and the measured LOI showed a significant deviation when the fuel contained straw, see Figure 2.13 on the following page. The difference between LOI and carbon content is believed to be caused by the presence of primarily H and O in straw char particles.

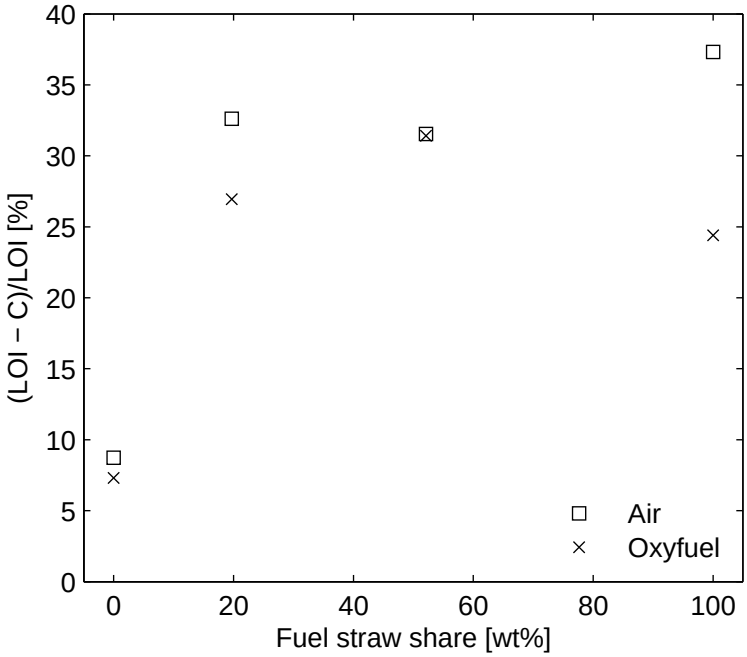


Figure 2.13: Difference between LOI and carbon content of fly ash as function of fuel straw share. Comparison of air and oxyfuel environments at the reference operating conditions.

In addition to analysis of the carbon content selected ash samples have been analysed with respect to their total S, Cl, and ash forming species content (Al, Si, Fe, K, Ca, Mg, Na, Ti, P). The content of water soluble K, Na, Mg, Ca, P, S, and Cl has likewise been determined. These analysis were also performed at ENV.

Deposit sampling was generally performed during a period of 2 hours in order to have sufficient sample for analysis. All collected deposits have been analysed with respect to their total content of S. Selected samples have likewise been analysed for the total Cl and ash forming species content (Al, Si, Fe, K, Ca, Mg, Na, Ti, P). The content of water soluble species (K, Na, Mg, Ca, P, S, and Cl) have been determined for all of the upstream samples. In some cases the sample mass collected from the downstream part of the probe was to small for an analysis of water soluble species to be performed.

#### 2.3.2.5 Temperature Mapping

Temperature mappings with an S-type thermocouple have been performed for most fuel/oxidizer combinations. The measured temperature profiles for each experiment marked with a "T" are included in the data collection [64]. For some fuel/oxidizer combinations, especially coal experiments, several of the experimental runs include temperature measurements. An averaged data set is thus made

from the different experimental runs at similar operating conditions. For some of the earlier experiments, the temperature profile measurements were performed prior to the reactor reaching steady state temperature. This is especially relevant for ports 1 and 2 were the change from the NG flame to the solid fuel flame induces the greatest change to the fuel ignition and thus the temperature and radiation intensity. The averaged data sets are thus made without measurements performed less than 1.5 hour after the shift from the natural gas flame to the solid fuel flame.

Figure 2.14 on the next page shows the average, radial temperature profiles in the top five measurement ports in the reactor for combustion of the four different fuel blends in air. For experiments with no repetition of measurements, *i.e.* no error bars in the plot, it can be considered safe to assume that the uncertainty is of comparable size to the uncertainty for other fuel/oxidizer combinations in the same measurement point. The profiles are seen to be almost constant across the reactor in ports 3-5. A small temperature decrease is observed close to the reactor walls ($\pm$15.75 cm). In ports 1 and 2 a rather steep temperature gradient can be observed close to the reactor centre due to the flame front. The absence of the gradient for some fuels is due to insufficient resolution of the measurements.

The profiles in port 1 are only shown for one half of the reactor. The measurements performed at positive values of $R$ are generally seen to be significantly higher than for the corresponding position at negative values of $R$. Figure 2.15 on page 39 shows the temperature measurements together with the concentrations of NO and CO in the exit flue gas during the time of temperature measurements. The increase in temperature is associated with a sharp increase in NO formation and a decrease in CO formation. The measured decrease in CO is less sharp due to a delayed effect in the online CO analyser making it unable to reproduce step changes in concentration from high to low values. The changes in temperature and emissions indicate a shift in flame properties from a low-$NO_x$ flame to a high-$NO_x$ flame. Figure 2.16 on page 39 shows pictures of the flame taken from the reactor bottom for each position of the thermocouple. A significant difference in flame shape can be observed. When inserted in front of the burner ($R > 0$) the thermocouple acts as a flame holder drawing the flame base closer to the burner creating a shorter and more intense flame producing more NO. Due to this phenomenon, all temperature measurements taken at positive values of $R$ in port 1 have been omitted from the averaged temperature profiles.

It should be noted that the temperature profiles have been measured with shielded thermocouples (S-type shielded with ceramics). Hence, the temperature measurements are significantly influenced by the radiative heat flux within the reactor, primarily from the walls.

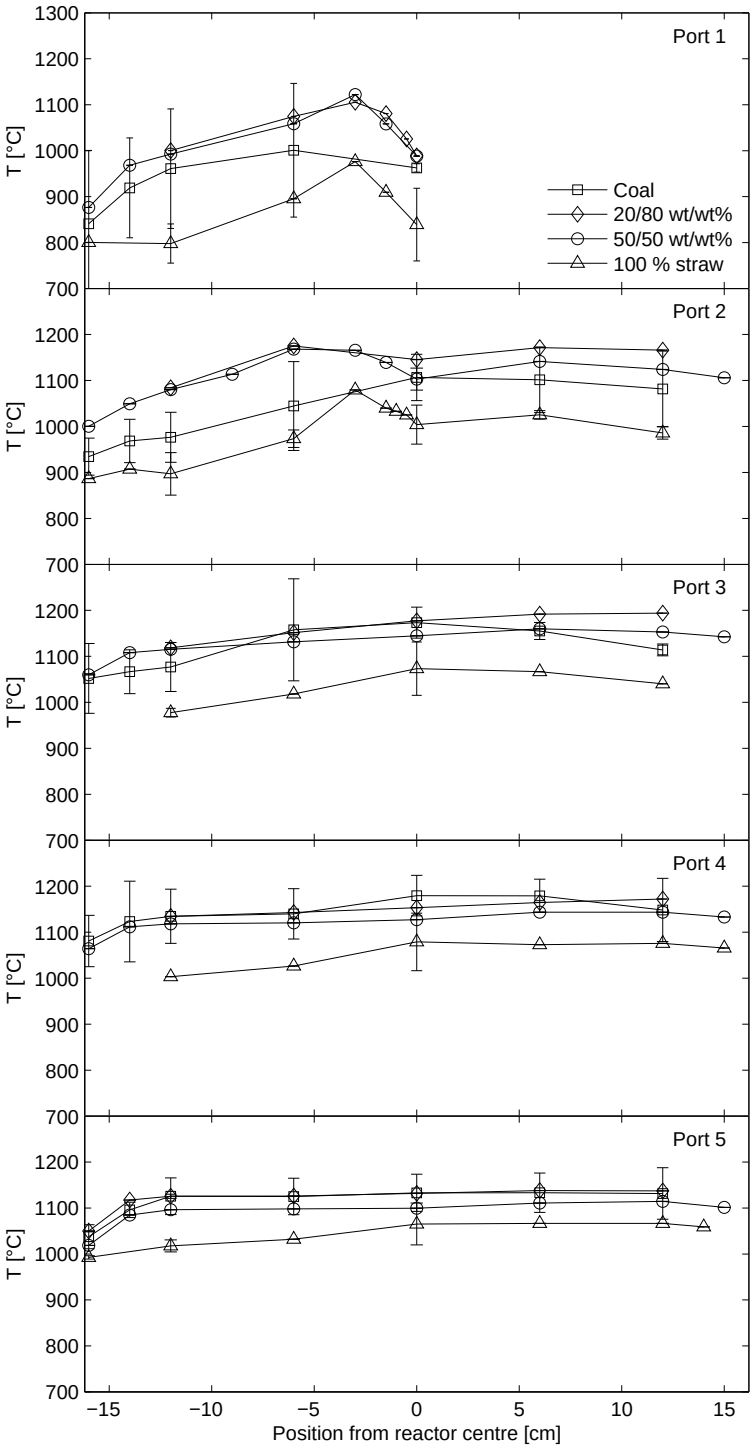


Figure 2.14: Temperature profiles measured with S-type thermocouple for the four different solid fuel mixtures combusted in air. Errorbars correspond to two times the standard deviation for repeated measurements.

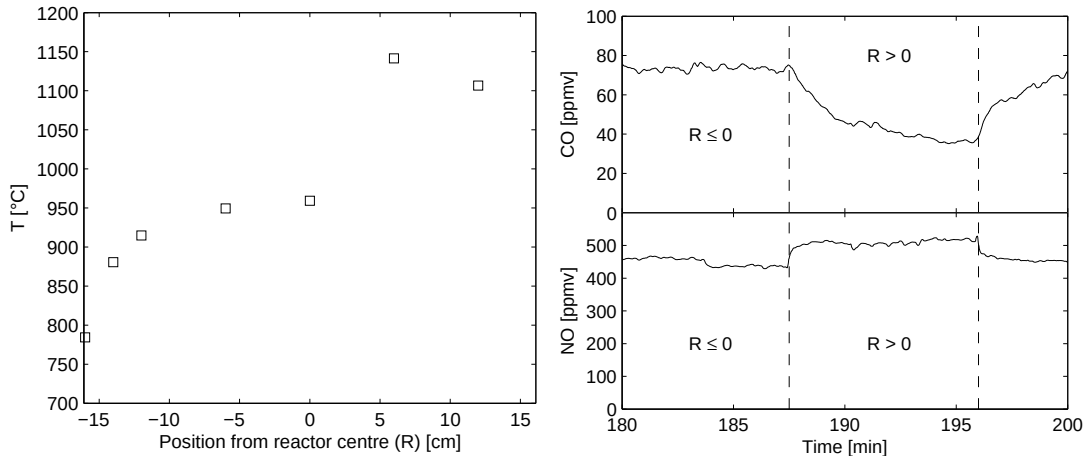


Figure 2.15: Left: Radial temperature profile in measurement port 1 for experiment CA15_T. Right: Shifts in NO and CO emissions depending on the radial position of the thermocouple tip during temperature measurements in measurement port 1. The thermocouple is moved across the reactor from negative to positive values of $R$.

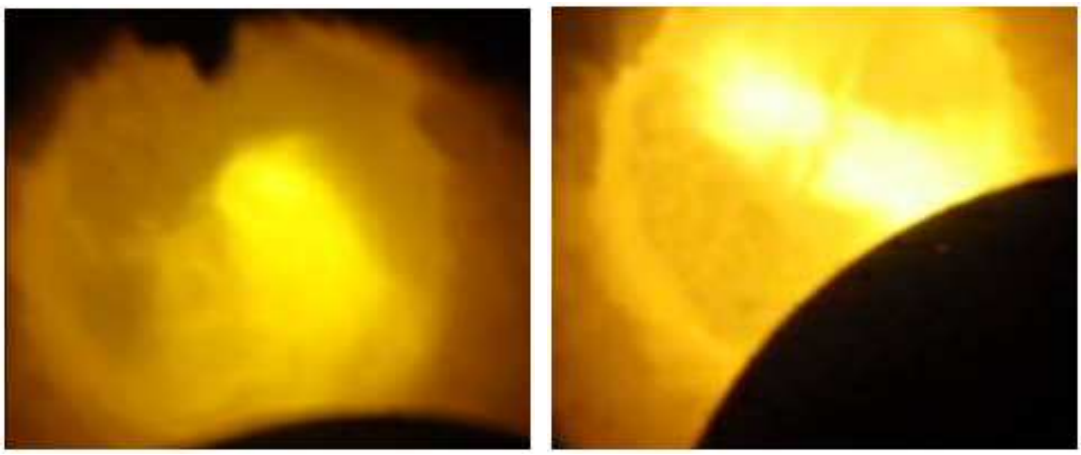

Figure 2.16: Left: Coal/air flame, thermocouple at $R < 0$. Right: Coal/air flame with thermocouple inserted across burner mouth, $R > 0$.

#### 2.3.2.6 Advanced Diagnostics – Gas-Phase Temperature and Composition

In addition to the temperature mapping with shielded thermocouples and the analysis of the flue gas withdrawn from the bottom of the reactor, mapping of the reactor chamber through the top five measurement ports has been performed with a special, miniature fibre-optic FTIR (Fourier Transform Infra Red) probe. The probe was specially designed for this work and was applied for 5 reference experiments (coal/air, coal/oxyfuel, straw/oxyfuel, M50/air, and M50/oxyfuel). The probe enables measurements of local gas phase temperature and composition ($CO_2$, $H_2O$, and CO) in oxyfuel combustion whereas it is applicable for temperature measurements during air-firing. The principle of the gas temperature measurements is described in [65] and principles of the gas concentration measurements in [66], but a short outline of the FTIR system is provided in the following. A more detailed description of the system and the method of data treatment is provided in [67].

Visualization of the probe and its dimensions is given in Figure 2.17 on the facing page. When the FTIR probe is operated with the purpose of gas-phase concentration measurements the probe needs to operate with a beam stop as seen in Fig. 2.17. The beam stop is cooled by two 4 mm stainless steel tubes placed beside the probe with optics. The optical path length (field of view in Fig. 2.17) is 30 mm and the diameter of the probe with optics is only 10 mm. The small probe diameter ensures minimal disturbance of the flue gas within the setup and the relatively short path length ensures very localized measurements. A purged ceramic tube is mounted at the probe tip to reduce disturbances from particles in the flue gas and the cooled probe tip. Thermal light from the hot slab of gas between the ceramic tip and the beam stop is collected by a small 4 mm ZnSe lens focused on an IR-fibre connected to the FTIR-spectrometer. Gas-phase temperature measurements can be performed both with and without the presence of the beam stop. It is the emission signal from $CO_2$ that is used to determine the gas temperature and the signal needs to be strong enough for a temperature interpretation to take place. As the signal strength relates to the number of $CO_2$ molecules in the optic path, measurements in air are carried out without beam stop to ensure a longer path length, and therefore an increased number of $CO_2$ molecules. Determination of the gas-phase temperature is a necessary step in the determination of the gas-phase composition. Hence, it was not possible to use the probe for mapping the gas-phase composition during air combustion. Another consequence is that measurements in air are averages over a longer, however undetermined, distance than in oxyfuel flames.

The FTIR-spectrometer was mounted with a sensitive liquid nitrogen cooled InSb-detector sensitive in the range 1800 - 7000 $cm^{-1}$. Approximately 60 double-sided single scan spectra per minute could be obtained with a spectral resolution of 2 $cm^{-1}$. These spectra yielded time dependent concentration and gas-phase

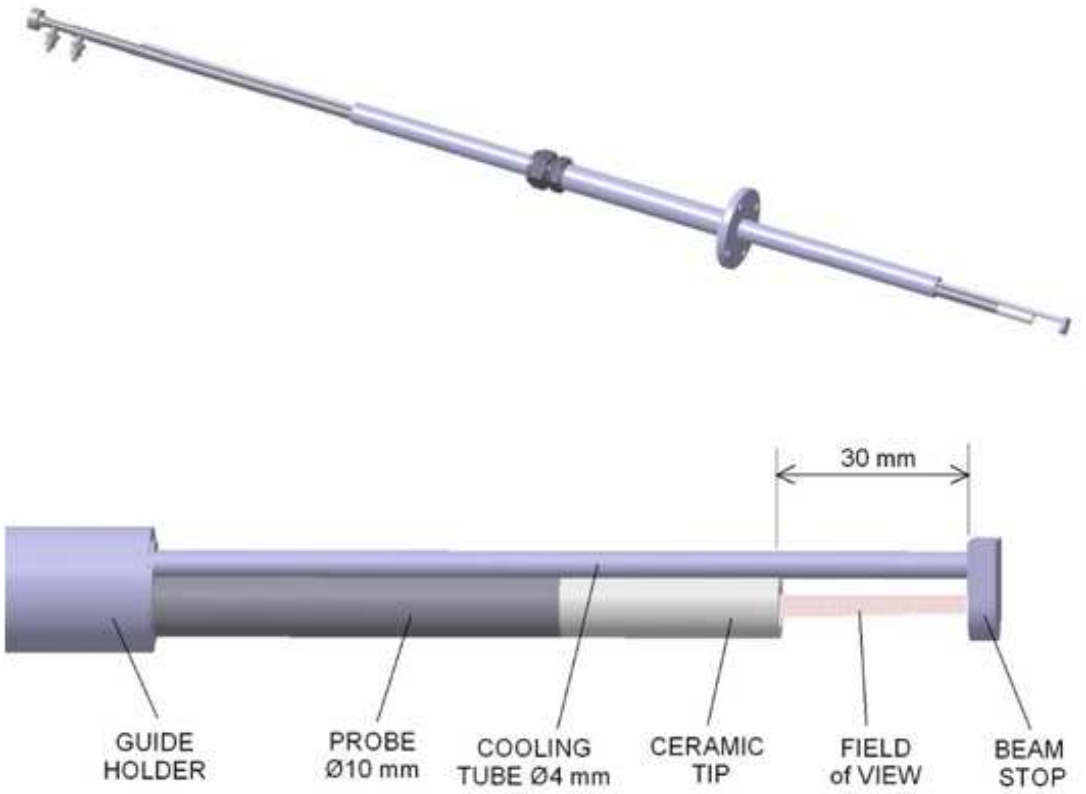


Figure 2.17: Top: The water-cooled fibre-optic probe for measurements of gas temperature and gas composition in the experimental setup. The FTIR-probe is inserted into a port holder with flange for leak tightness and easy handling during experiments. Bottom: Tip of the fibre-optic probe. Gas temperature and gas composition is measured along a 30 mm path between the beam stop and the front of the ceramic tip. Thermal light is collected with a 4 mm diameter ZnSe lens and focused on the end of a 550 $\mu$m IR-fibre placed in the 10 mm water-cooled probe.

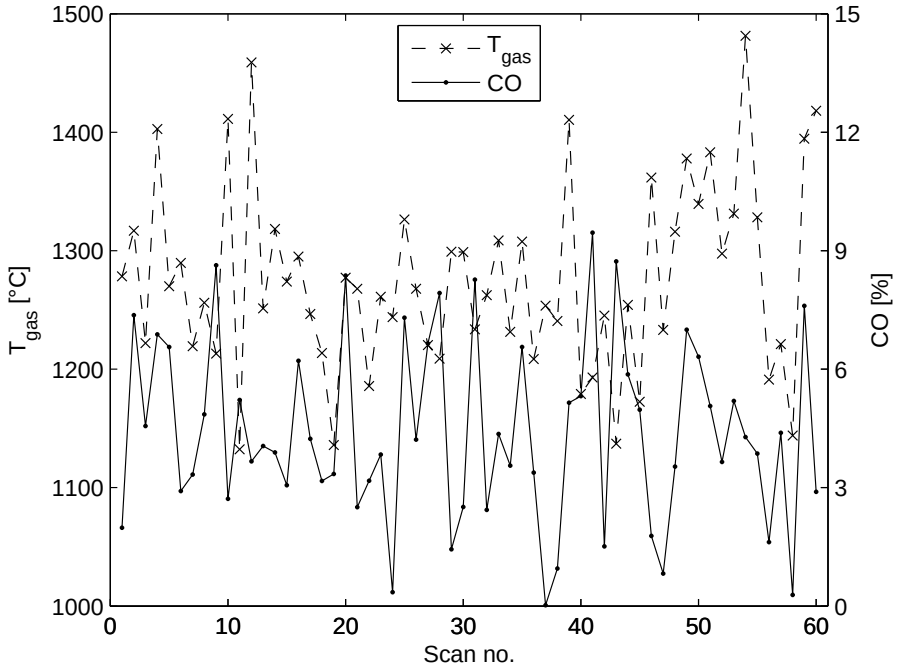


Figure 2.18: Time dependent gas-phase temperature and CO concentration data for the reactor centre position ($R = 0$) at port 3 for M50/oxyfuel combustion.

temperature profiles, from which average and standard deviation values of concentrations and temperatures could be determined. Figure 2.18 shows an example of the collected data. The high spectral resolution provides sufficiently well defined absorption peaks in the spectra allowing for determination of the gas species concentrations. A notebook PC has been used to control data acquisition and store data during experiments. The system was calibrated before and after experiments with a portable black body source with an uncertainty of $\pm 3\,^{\circ}\mathrm{C}$.

The FTIR technique is reliable though it cannot be stated as accurate for estimation of gas phase concentrations of $H_2O$, $CO_2$, and CO. The accuracy of the method is dependent on the similarity between the reference emission spectra of the gases and those obtained in the experiments as the transmittance intensity is not a linear function of concentration. Especially for $H_2O$ a deviation existed. The unsteady flow phenomena encountered primarily in the upper two measurement ports induced large uncertainties on the measured gas species concentrations. Close to the fuel jet some of the measurements failed to yield physically sound results. The $CO_2$ and $H_2O$ data are not shown in this thesis.

An investigation of the influence of the presence of the beam stop on the measured gas-phase temperatures showed a significant effect. Figure 2.19 on page 44 shows a comparison of the radial temperature profiles in ports 1-5 for the combustion of the 50 wt% straw blend for FTIR measurements both with and without the beam

stop and the measurements performed with the thermocouple. The figure illustrates the significant cooling effect of the beam stop. The difference is on average about 100-200 ℃. The cooling effect from the beam stop yields measurements comparable to the use of a traditional thermocouple. When operated without the beam stop the resolution of the temperature gradient observed in port 1 was weakened. This, on the other hand, illustrate the superiority of the fixed path length obtained during operation with the beam stop. On an overall level, it is concluded that the most accurate determination of the gas-phase temperature during oxyfuel combustion is obtained while the probe is operated without the beam stop. In this case the FTIR probe showed superior to traditional temperature measurements using a thermocouple in determining the gas-phase temperatures and providing a measure for the level of fluctuations due to mixing of fuel, oxidant, and hot flue gases. Generally, the fluctuations are observed to increase when the probe approaches the flame front which is located within the interval $R = [-6; 0]$ cm.

### 2.3.3 Combustion Conditions

The experiments have been operated at several different combustion conditions as shown in Table 2.5 on page 26. The investigated parameters for the four fuel types include:

**Combustion oxidant type** Air and $O_2/CO_2$ mixtures

**Stoichiometry** The theoretical oxygen concentration in the dry flue gas has been varied within the interval from 1 to 5 vol%. The applied stoichiometric oxygen excess ratios have accordingly been in the interval 1.025 to 1.3.

**Oxidant $O_2$ concentration** Only relevant for oxyfuel experiments. The values applied are: 25, 30, 33, 35, 40, and 50 %. Not all values have been used for all fuels.

**Residence time** This parameter has not been controlled but is a function of the oxidant type and stoichiometry due to the fixed length of the experimental setup. The calculated average residence times are ranging from 2.6 to 5.3 seconds.

**Burner settings** The influence of varying the burner swirl number, the linear velocity of the primary oxidant leaving the burner, etc. have been investigated in order to find operating conditions with a stable flame. The investigations were performed for coal/air combustion. No clear correlation between burner settings and flame properties were found for the range of investigated parameters [61].

The characterization of the combustion oxidant is described in Section 2.3.3.1 whereas considerations regarding residence time are provided in Section 2.3.3.2.

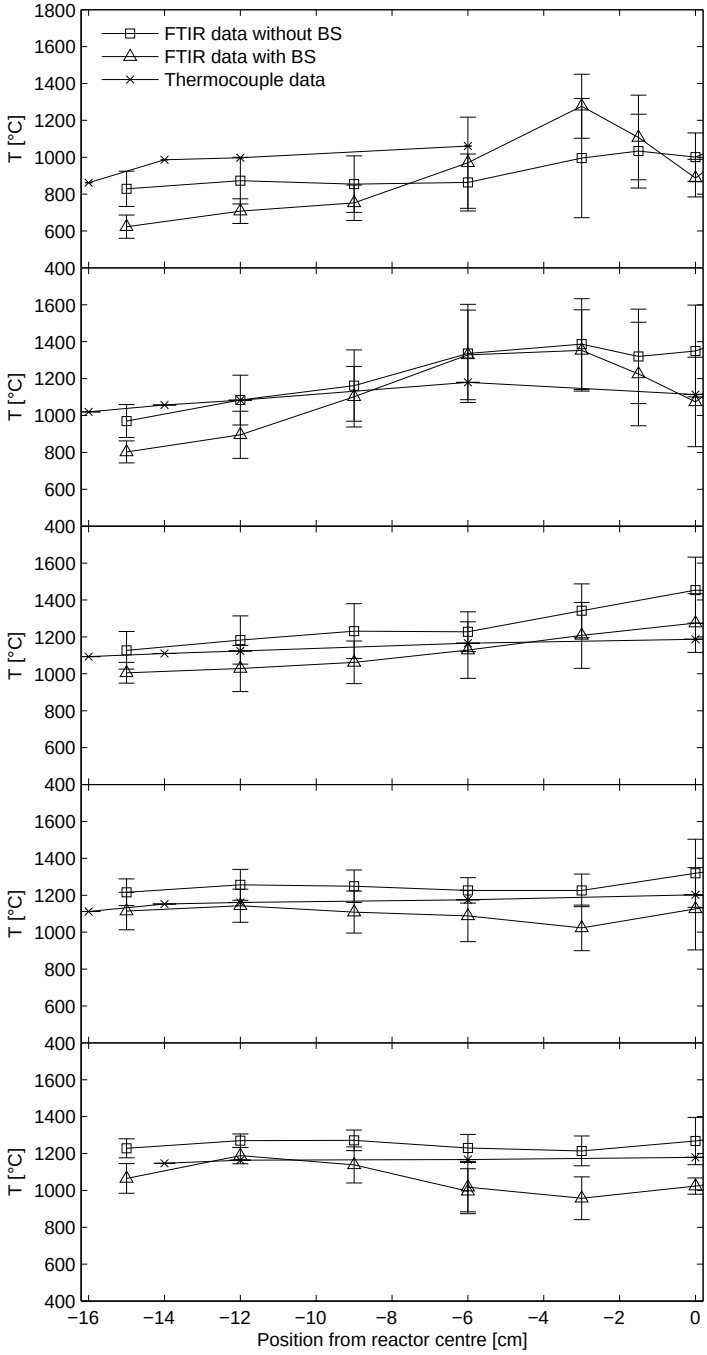


Figure 2.19: Comparison of temperature measurements in ports 1-5 for M50/oxyfuel combustion. FTIR data are taken with and without the beam stop (BS) mounted on the probe. Only measurements at negative radii are shown. Error bars on thermocouple data correspond to two times the standard deviation on repeated measurements. Error bars on FTIR data correspond to two times the standard deviation for the 60 scans and provide a measure of the level of fluctuations in the given measurement position.

#### 2.3.3.1 Combustion Oxidant and Stoichiometry

When comparing air and oxyfuel combustion experiments it is important to consider which stoichiometric measure to use in order to match the combustion conditions. Three different measures for the combustion stoichiometry can be applied; the stoichiometric oxygen excess ratio, $\lambda$, the dry flue gas oxygen concentration, $y_{O_2}^{dry}$, and the wet flue gas oxygen concentration, $y_{O_2}^{wet}$ see Eqs. (B.5) and (B.9) in Appendix B.

It should be noted that the three stoichiometric parameters impacts the combustion process in different ways. The stoichiometric excess oxygen ratio provides information on the oxygen to fuel ratio within the flame whereas the flue gas $O_2$ concentration determines the conditions during fuel/char burnout. The wet flue gas oxygen concentration is the actual condition which the char particles experience during burnout, whereas the dry concentration is the parameter easiest to determine and thus would typically be the parameter from which a power plant is controlled. The distinction between the wet and dry oxygen concentration is relevant due to an about 50 % higher concentration of $H_2O$ in the oxyfuel atmosphere compared to air in the case of a dry flue gas recycle. For a wet recycle, the difference will be larger. The difference is caused by the decreased flue gas flow leading to a higher relative difference between wet and dry $O_2$ for oxyfuel combustion than combustion in air.

Figure 2.20 on the following page shows a comparison of the stoichiometric oxygen excess ratio and the dry flue gas oxygen concentration for air and $O_2/CO_2$ atmospheres with different oxygen concentrations at the inlet. From the figure it is seen that a fuel particle burning at a given stoichiometric oxygen excess ratio in an oxyfuel atmosphere with higher than 21 % $O_2$ in the oxidant will experience a higher partial pressure of $O_2$ in the burnout stages of the combustion than for combustion in air.

Figure 2.21 on page 47 shows a comparison of the development in fly ash loss-on-ignition as function of the three different measures for the combustion stoichiometry for air and oxyfuel combustion experiments using coal as fuel. Only oxyfuel experiments performed with 30 % $O_2$ in the oxidant are shown. Due to the differences in the composition of the combustion atmosphere between air and oxyfuel combustion the data points for the two atmospheres are seen to move relative to each other when the independent variable is changed.

It is the partial pressure of $O_2$ rather than $\lambda$ that influences the rate of combustion. For that reason it has been chosen to use the flue gas oxygen concentration as parameter when comparing air and oxyfuel combustion experiments and matching reference conditions. For simplicity, the concentration in the dry flue gas is chosen.

**False Air Ingress** Due to a safety demand of operating the experimental setup at sub-pressure ($P_{reac} \leq -2$ mbarg) a risk of false air entering the combustion

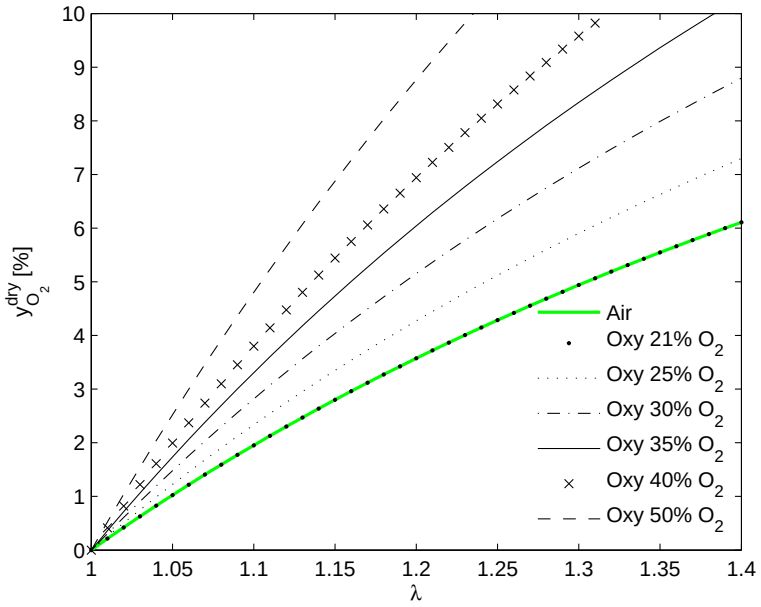


Figure 2.20: Comparison of the stoichiometric oxygen excess ratio, $\lambda$, and the concentration of $O_2$ in the dry flue gas for complete combustion of coal in air and $O_2/CO_2$ atmospheres with different oxygen concentrations at the inlet.

process is present. False air can enter the experimental setup in two ways:

- Into the gas sampling system – this amount of false air enters the gas sample at low temperature and can thus be considered a pure diluting agent without any effect on the combustion process. A test of the false air ingress into the gas conditioning system showed that the dilution factor for the gas sample is about 0.05–0.1 % of the sample flow of 3 L/min.

- Into the reactor – whether false air entering the reactor should be taken into account when determining stoichiometric values, etc., depends on its entering point and mixing with the remaining flue gas within the reactor. Two scenarios are relevant:

  - Near the burner – false air entering the reactor near the flame zone should be included in the calculations with the same significance as the oxidizing agent introduced through the burner. This will yield higher oxygen excess than can be determined theoretically from the fuel and oxidant flows.
  - Downstream of burner – false air entering very close to the sampling position can be regarded a pure diluting agent, since the residence time and temperature is low enough for the influence on the combustion process to be assumed insignificant. Additionally, it is unknown whether full mixing with the entire flue gas flow has been obtained.

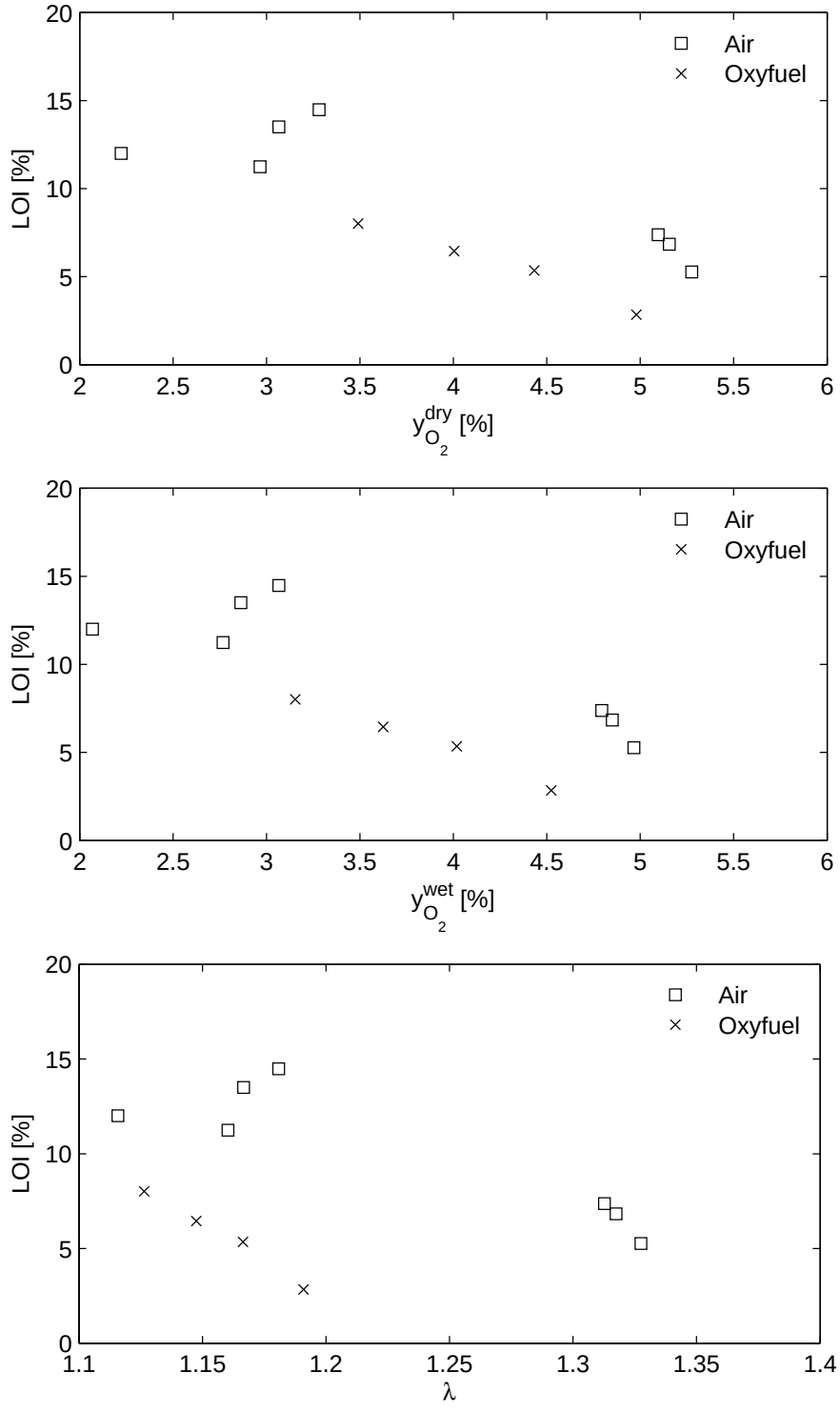


Figure 2.21: Comparison of loss-on-ignition (LOI) for coal combustion in air and 30% $O_2/CO_2$ at different stoichiometries with three different stoichiometric parameters acting as independent variable.

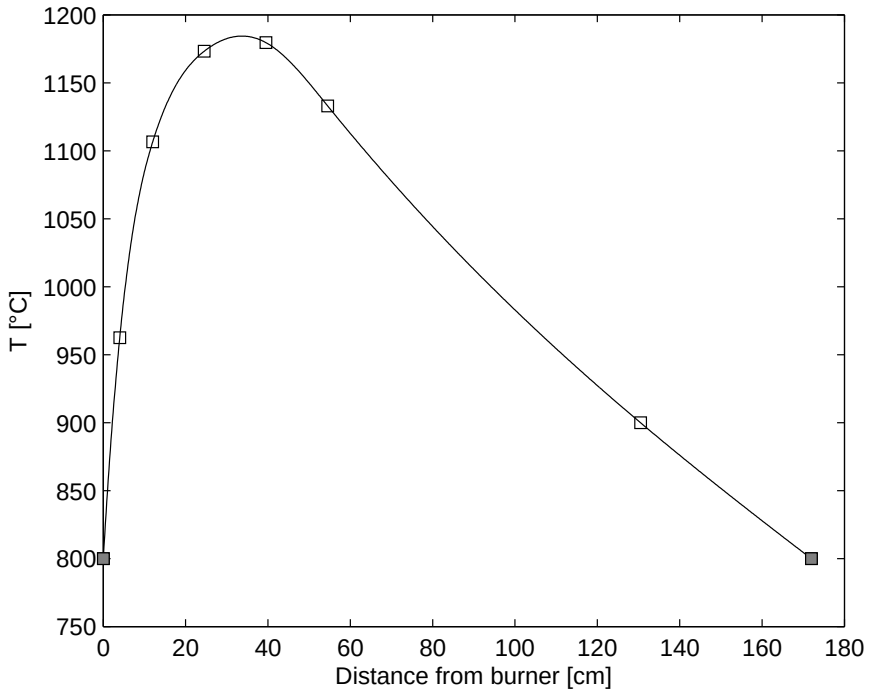


Figure 2.22: Temperature profile along reactor estimated from a cubic spline interpolation of the measured average temperatures in ports 1-5 and 7 and temperature estimates at the burner exit (L = 0) and ash sampling probe (L = 175 cm), closed symbols. Data are for coal/air combustion at the reference operating conditions and are measured with a thermocouple.

Different leak tests showed that the majority of the false air entering the reactor can be treated as a pure diluting agent [61]. The combustion stoichiometry is thus determined solely from the fuel and oxidant inlet flows.

#### 2.3.3.2 Residence Time

An estimate of the average residence time of fuel particles in the reactor can be determined from a temperature profile and the theoretical total flue gas flow. The temperature in each position along the reactor is determined from a cubic spline interpolation of the average temperature profiles (reactor centre values) determined for each fuel/oxidizer combination with a thermocouple. Figure 2.22 shows an example of one of the estimated temperature profiles. The temperature immediately above the ash sampling probe has been assumed to be 100 ℃ below the value measured in port 7. The burner exit temperature has been selected in the range 700-850 ℃ depending on the fuel/oxidizer combination and the operating conditions. The value has generally been chosen in order to yield a smooth profile. The exact value has only a small effect on the calculated residence time.

Table 2.7: Average residence time for different oxidizers at selected flue gas oxygen levels.

| Oxidizer | $y_{O_2}^{dry}$ | $\tau$ [s] |
|---|---|---|
| Air | 5 | 2.6-2.7 |
| 25 % $O_2/CO_2$ | 5 | 3.6 |
| 30 % $O_2/CO_2$ | 5 | 3.7-3.9 |
| 35 % $O_2/CO_2$ | 5 | 4.5 |
| 40 % $O_2/CO_2$ | 3 | 4.8 |
| 50 % $O_2/CO_2$ | 2 | 5.3 |

The residence time is calculated from Eq. (2.8).

$$\tau = \int \frac{dL}{u(L)} = \sum_i \frac{\Delta L_i}{u(L_i)} \tag{2.8}$$

where $L$ is the total reactor length and $u(L)$ is the average linear velocity of the flue gas at a given position, $L$, in the reactor. The velocity profile and recirculation zones are not included in the calculation. In order to estimate the residence time, the reactor length is split into a number of volume elements within which the average temperature and linear gas velocity is determined, see (2.9).

$$u(L) = \frac{V_{FG}}{A_{reactor}} \cdot \frac{T(L)}{T_0} \tag{2.9}$$

$V_{FG}$ is the volumetric flue gas flow [$Nm^3/s$], $A_{reactor}$ is the cross-sectional area of the reactor (constant), $T(L)$ is the flue gas temperature in position $L$, and $T_0$ is the reference temperature, 273.15 K. The flue gas is assumed to behave as an ideal gas.

Table 2.7 shows the residence times determined for each of the oxidizer compositions applied in the experiments. An increase of about 40-50 % in the average residence time of gas and particles in the reactor occurs when changing from air to oxyfuel combustion (30 % $O_2$) due to the lower flue gas flow. This will have an impact on the combustion process and the burnout efficiency in the two different combustion atmospheres.

## 2.4 Molar Balances

Molar balances for the elements C and S of the form

$$MB = \frac{X_{out}}{X_{in}} \tag{2.10}$$

have been set up. $X_i$ are in units of [kmole/s]. Several levels of detail have been made for the balances with respect to the "out" term. Each new level build on the previous.

**Level 1** Only flue gas measurements are taken into account, full burnout of the fuel is assumed. Calculated for both C and S.

**Level 2** For experiments with ash sampling. It is assumed that all ash fed to the reactor end up as fly ash with the measured average carbon or sulphur content (if the C analysis does not exist the LOI value is used in determining the degree of burnout on a carbon basis and from that the C content of ash). C and S.

**Level 3** For experiments with ash sampling. The amount of fly ash sampled compared to the theoretical amount is used to determine the split between ash ending up as fly ash and ash retained in the reactor as deposits. It is assumed that the fraction of ash retained in the reactor yields complete burnout. Only C.

**Level 4** For experiments with ash and deposit sampling. The sulphur analysis on deposits is used to correct for the split between fly ash S and deposits S. Only S.

Level 1 can be calculated for each experiment performed, whereas levels 2-4 are only applicable to experiments with fly ash (and deposits) sampling. The equations for each individual level can be seen in Appendix C.

Balances for the remaining major elements in the combustion process; O, N, and H could likewise be set up. However, due to the design of the experimental setup and the analysis/data available these balances would be of a more theoretical interest. For instance, the N balance, which is highly relevant for oxyfuel experiments, would be heavily influenced by false air ingress into the reactor and would thus act more as a measure of this ingress than as a mass balance. For O and H, assumptions on the amount of water in the flue gas would be necessary and introduce a significant uncertainty on the results.

### 2.4.1 Carbon

The carbon balance is determined in each data point (time) and Figure 2.23 on the facing page shows an example of the development of the balance during the selected time interval for data analysis for an experiment with fly ash sampling. The balance is seen to fluctuate which is believed to be caused by the uncertainty on the fuel flow determination, see Section 2.2.2. Due to a high degree of burnout, no visual difference exist between the three levels. For the shown example, the data does not yield a 100 % fulfilment of the carbon balance. However, the

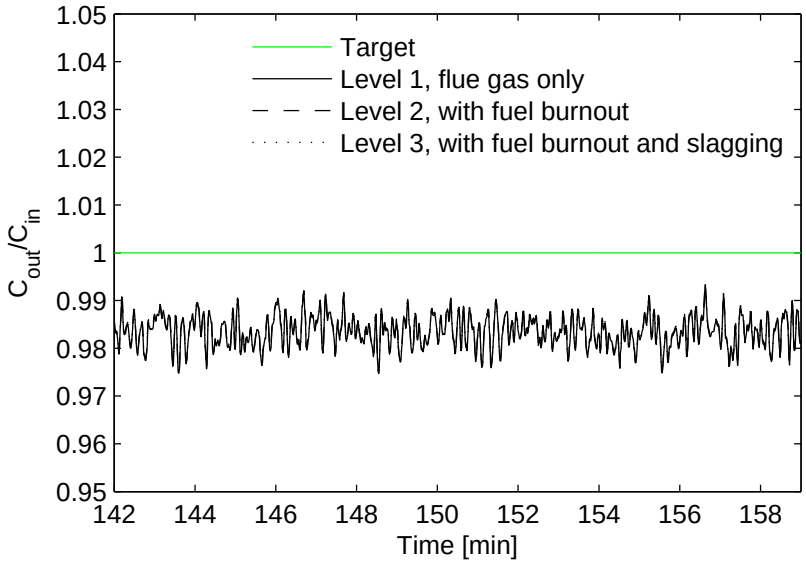


Figure 2.23: Carbon balance fulfilment as function of time for combustion of the fuel blend with 50 % straw in air (M50A01_AD).

error on the balance for the shown example is within 2 % and is considered very satisfactory.

Figure 2.24 on the next page shows the averaged carbon balance fulfilment for all air and oxyfuel experiments as function of the fuel composition. Only the highest level value is plotted for each individual experiment. For all air experiments the balance is seen to be satisfied to within an error of 3 %. This does not give cause to any remarks when taking the complexity of the experimental setup into account. However, the oxyfuel carbon balances show significantly larger errors, up to 15 %. As seen in Figure 2.25 on page 53 this is primarily a consequence of narrow time intervals chosen for data analysis. It is seen that the largest deviations occur for experiments with time intervals less than 10 minutes of length. Within these time intervals only few $CO_2$ measurements are available. In order to determine the carbon balance at each time, a linear interpolation is made between the data points from the GC. This approach is of course associated with a large degree of uncertainty the fewer the GC measurements within the time interval, as peak measurements will influence the results relatively much. In relation to the remaining data analysis the deviation seen here does not have an effect, as the GC measurements of $CO_2$ are not used to determine other parameters. It is thus considered safe to use all the experiments.

### 2.4.2 Sulphur

The sulphur balance is determined in each data point (time) and Figure 2.26 on page 54 shows an example of the development of the balance during the selected

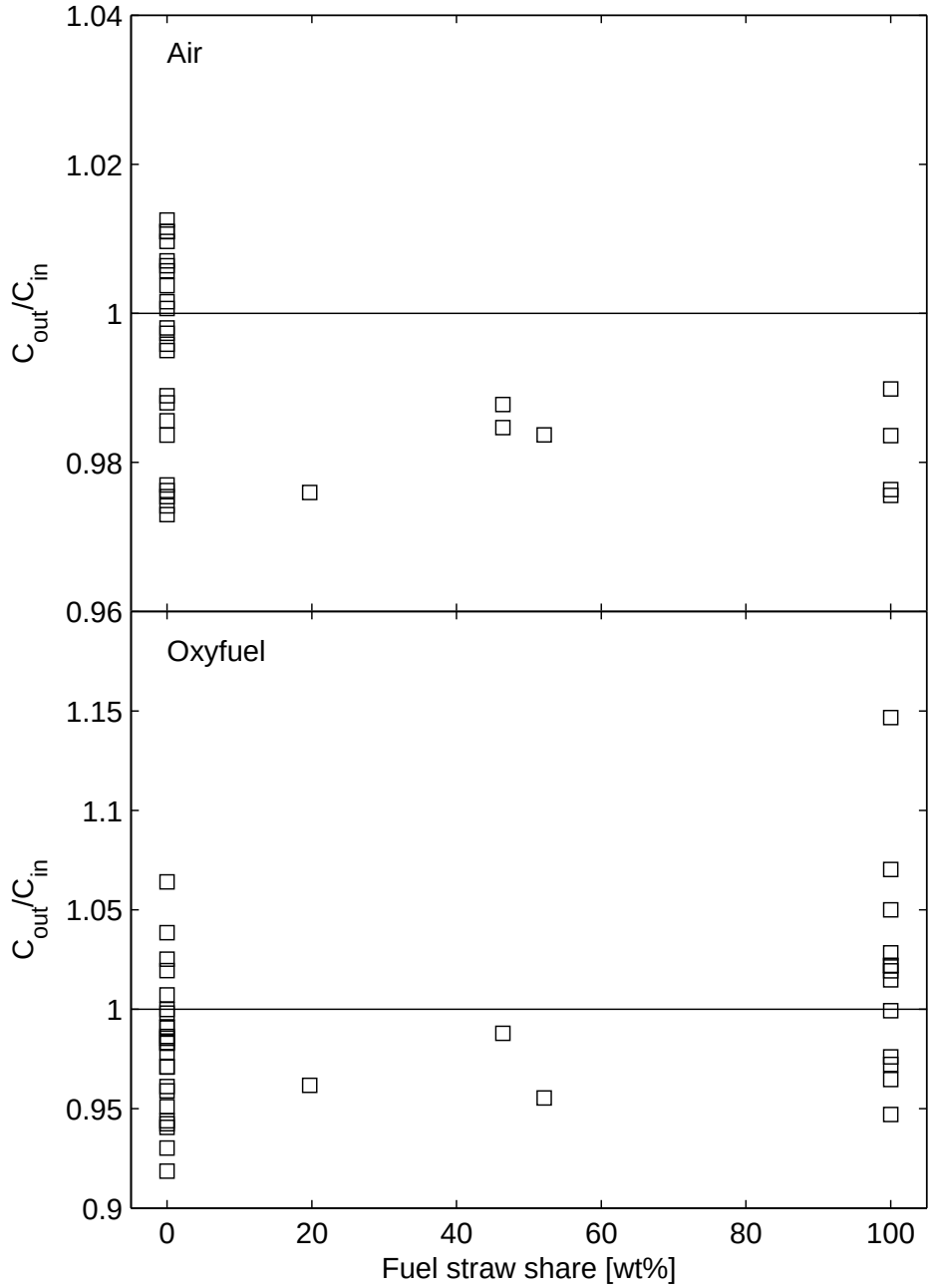


Figure 2.24: Carbon molar balance for air and oxyfuel experiments as function of the straw share of the fuel. Note that the scaling on the y-axis is different.

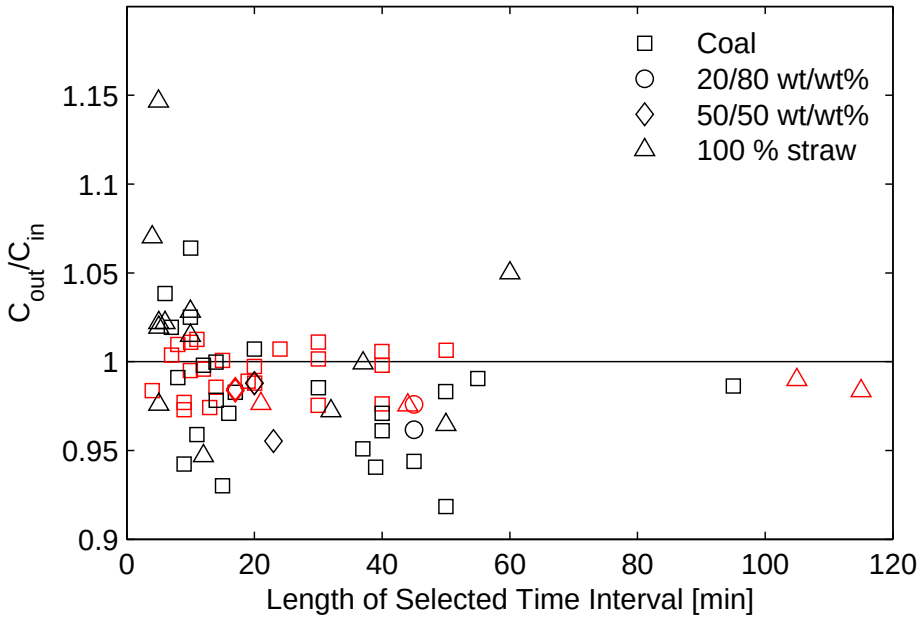


Figure 2.25: Carbon balance fulfilment (air: red symbols, oxyfuel: black symbols) as function of the length of the selected time interval for data treatment.

time interval for data analysis for the same experiment as discussed above. A similar fluctuating behaviour as for the carbon balances is seen. Still, the amplitude of the fluctuations is within reasonable levels. Advancing from the pure flue gas data approach (level 1) to accounting for sulphur in the fly ash (level 2) improves the overall balance with about 20 % points for the shown example. Taking the split between sulphur in fly ash and deposits into account (level 4) improves the fulfilment even further and the resulting overall error is less than 10 %. For the shown experiment the sulphur content in the fly ash is 0.8 wt% whereas it is 4.4 wt% in the deposit sample (upstream part). The relatively low error on the balance at level 4 indicates that the sulphur concentration in the upstream part of the deposit sample taken through port 7 is close to representative for all the deposits in the reactor chamber for the shown example. Taking sulphur retention in deposits into account has thus shown of considerable importance when determining sulphur balances.

Figure 2.27 on page 55 shows the averaged sulphur balance fulfilment for all air and oxyfuel experiments as function of the fuel composition. At level 1, a significant deviation exist between incoming and outgoing sulphur from the setup for all fuels. The deviation increases with increasing straw share of the fuel indicating the presence of increased amounts of alkali and alkali-earth species during combustion leading to sulphur retention in solid phases. As was shown for the example in Figure 2.26 on the next page, taking sulphur in the fly ash into account

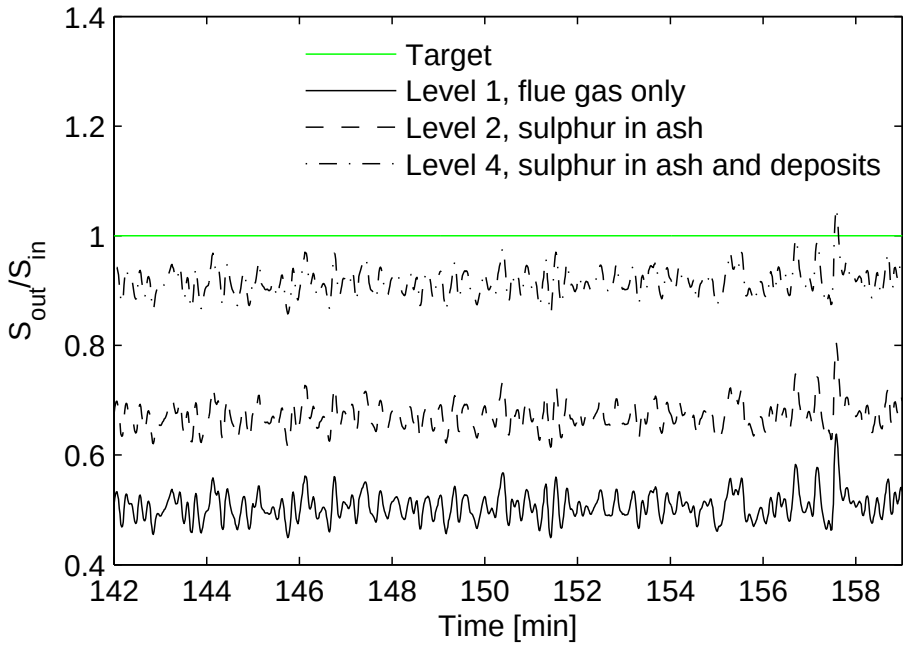


Figure 2.26: Sulphur balance fulfilment as function of time for combustion of the fuel blend with 50 % straw in air (M50A01_AD).

(level 2) improves the closure of the balance for all fuels. However, for the blends a significant error is still present, most pronounced for the high straw share. For pure straw combustion sulphur retention in ash can explain most of the sulphur missing at level 1. For all fuel/oxidizer combinations (except coal/air where the data are not available) accounting for sulphur in deposits (level 4) yields closures to within 10 %. Except for 100 % straw/oxyfuel the sulphur content of the deposit sample is higher than in the fly ash sample. For that particular experiment, level 2 overshoots and the inclusion of sulphur in the deposit thus improves the balance even though the trend in the data points is opposite to the remaining experiments. Based on the shown balances, the deposit samples can be considered representative for all the deposits within the reactor for all fuel/oxidizer combinations.

The significant retention of sulphur in deposits could explain the general problems which are encountered when performing sulphur mass balances on full-scale boilers [68]. The transient nature of sulphur retention in deposits (depends on fuel and operating conditions) induces great uncertainties on those investigations.

Besides sulphur in ash and deposits, the flue gas will contain minor amounts of $SO_3$. The $SO_3$ has not been measured and it is assumed that ignoring it only introduces a minor error on the sulphur balance. Furthermore, since the flue gas sample is dried by condensation before analysis a small amount of sulphur could be lost with the condensate due to dissolution of $SO_2$ and $SO_3$ and/or reaction

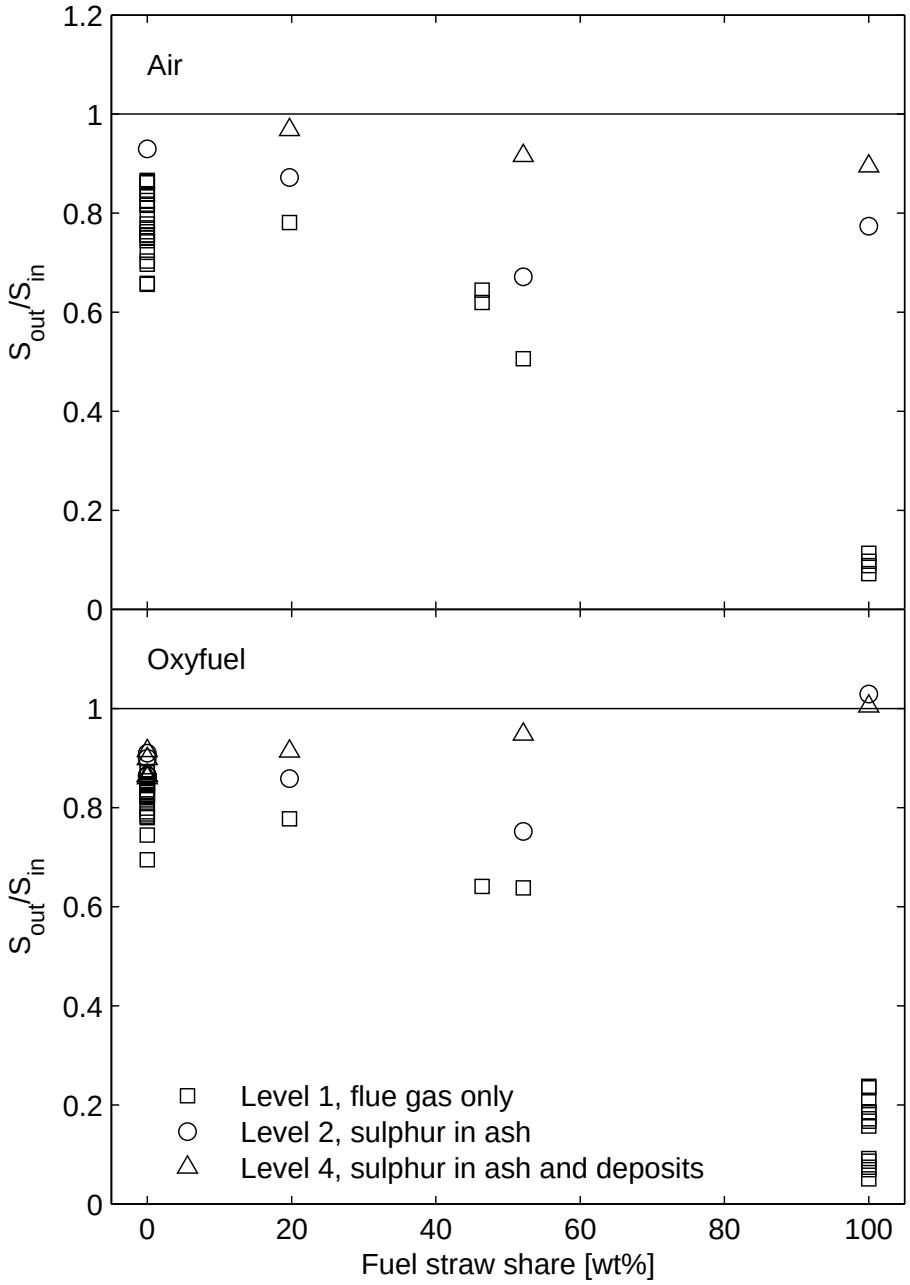


Figure 2.27: Sulphur molar balances for air and oxyfuel experiments as function of the straw share of the fuel.

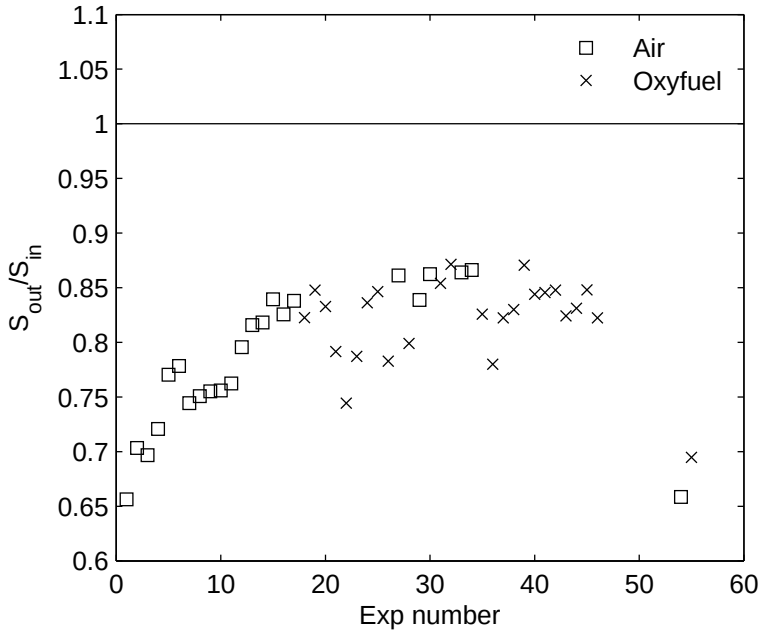


Figure 2.28: Sulphur balances at level 1 for coal combustion in air and $O_2/CO_2$ atmospheres as function of the experiment number (chronological order).

with ash. No quantification of the loss has been made. However, according to results reported by Fleig et al. [69] the sulphur lost with the condensate constitute no more than 0.5 % of the fuel-S forflue gas $SO_2$ concentrations comparable to this work.

For the pure coal a relatively large difference exists between the individual experiments. Figure 2.28 shows the sulphur balance fulfilment at level 1 in chronological order for the coal experiments. An increasing trend is seen during the first part of the first series of experiments (Exp number $< 50$). During this period several problems were encountered with the flue gas conditioning system and the poor degree of fulfilment is most likely due to reaction between moist ash in the sampling line and the $SO_2$ in the flue gas. The $SO_2$ data from these experiments are used with caution during the further data treatment. Additionally, a significant drop in the degree of fulfilment can be observed between the first experimental campaign (Exp number $< 50$) and the following campaign (Exp number $> 50$). During the execution of the latter two experiments problems with low suction capacity of the gas sampling pump were observed. This may have provided enough residence time for $SO_2$ from the flue gas to react with ash in the gas conditioning system. The $SO_2$ data for these experiments (CA17_M and CO18_M) are likewise used with caution during further data treatment.

# Chapter 3

# Air and OxyCoal Combustion Reference Cases

This chapter describes the experimental work related to the investigation of the differences in combustion fundamentals when changing the combustion atmosphere from $N_2$-based (air) to $CO_2$-based (oxyfuel). The analysis focuses on emissions, burnout, temperature profiles, deposit formation, and ash quality when using coal as fuel. Based on the investigations reference operating conditions are chosen for each type of combustion oxidant which allows a direct comparison of the oxidant types and yield combustion conditions which are relevant with respect to a comparison to full-scale power plants.

## 3.1 Determining Reference Conditions for Air Firing – Controlling Stoichiometry

The purpose of applying the swirl burner in the current experimental investigations is to simulate combustion in full-scale power plants. However, this is a challenge when performing experiments in down-scaled experimental setups.

The determination of the reference operating conditions for coal combustion in air, when the thermal load is fixed (30 kW), is thus limited to determining an appropriate oxygen excess level. In full-scale power plants an oxygen excess of about 15 %, corresponding to 3 % $O_2$ in the dry exit flue gas, is typically applied in order to achieve satisfying burnout of the fuel. The work related to choosing the reference operating conditions for coal combustion in air in the swirl burner has taken its starting point in these conditions.

### 3.1.1 Obtaining Burnout Comparable to Full-Scale Boilers

It can be difficult to obtain high burnout (low loss-on-ignition (LOI)) for solid fuels burned in small-scale experimental setups. However, in order for the results

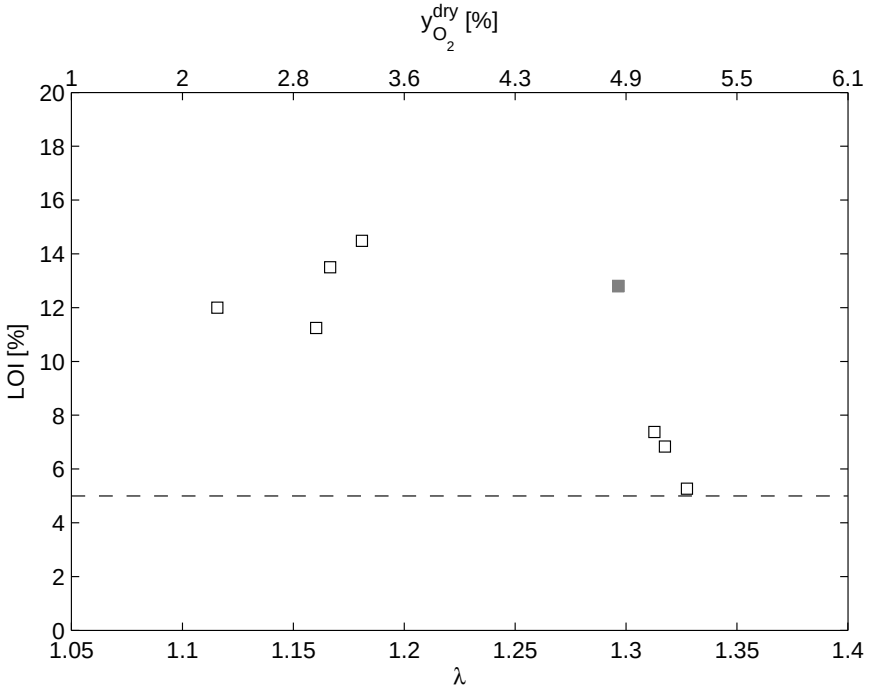


Figure 3.1: Loss-On-Ignition (LOI) for fly ash from coal/air combustion as function of the combustion stoichiometry given both as the stoichiometric oxygen excess ratio, $\lambda$, and the theoretical oxygen concentration in the dry flue gas, $y_{O_2}^{dry}$. The dashed line indicate the target LOI value of 5 % according to the maximum allowable LOI for fly ash used in concrete. Note that the two x-axes are not linearly dependent.

from small-scale experiments to be as applicable as possible to operation of full-scale plants a demand is that the burnout is comparable. In this project a target LOI value of 5 % for the ash fraction is therefore put up. This target value corresponds to the maximum allovable LOI for fly ash sold for concrete production [63].

Figure 3.1 shows the development in coal burnout for increasing oxygen excess. It is observed that due to the small scale of the experimental setup it is not possible to yield satisfying burnout at 15 % oxygen excess ($\lambda = 1.15$). Instead, between 30 and 35 % excess oxygen should be applied. The fixed length of the swirl burner setup causes the residence time to decrease with increasing oxygen excess, a factor which counteracts the improvement from increasing oxygen partial pressure in the burnout phase of combustion. For high oxygen excess ratios one might thus observe a decrease in burnout for the applied setup. It should be noted that the fact that an LOI of 5 % has been achieved is very satisfying and not something to take for granted for a setup of the current size.

The data point marked in grey is most probably an outlier as is discussed in Section 3.1.2.

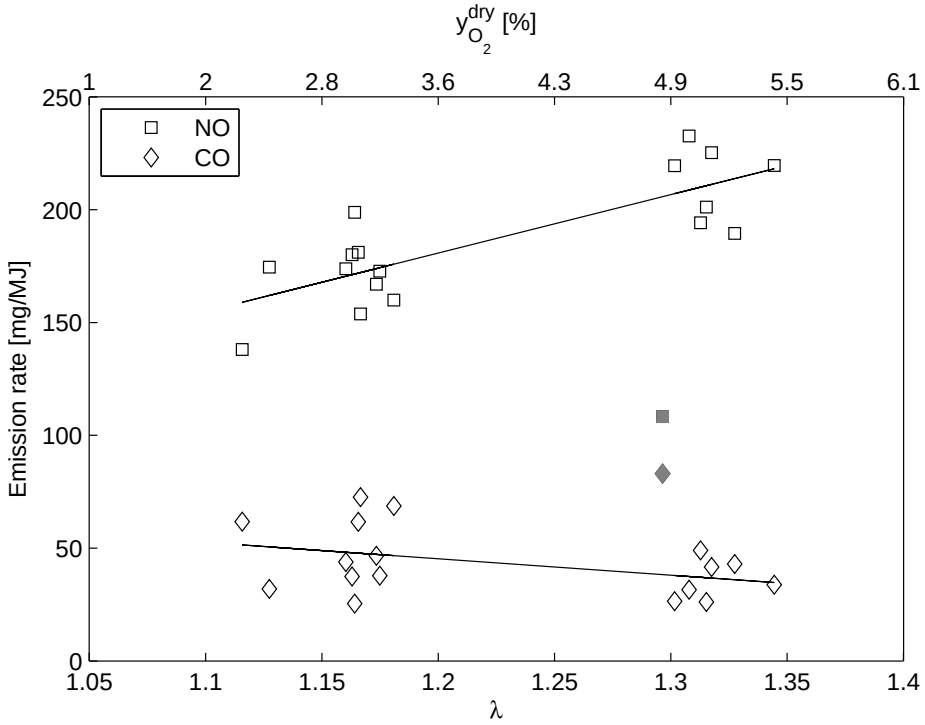


Figure 3.2: Emission rates of NO and CO for coal/air combustion as function of the combustion stoichiometry given both as the stoichiometric oxygen excess ratio, $\lambda$, and the theoretical oxygen concentration in the dry flue gas, $y_{O_2}^{dry}$. The full lines show the trends for the two data sets (open symbol data). Note that the two x-axes are not linearly dependent.

### 3.1.2 Effect of Excess Air on Pollutant Emission Rates

The NO and CO concentrations in the flue gas are typically a function of the oxygen excess. CO is related to the burnout and should thus decrease with increasing oxygen excess. NO formation is typically promoted by increasing oxygen excess [70] as is also seen in Figure 3.2. The observed NO emission rate is at the same level as in full-scale suspension-fired boilers.

$SO_2$ emissions (not shown) are independent of oxygen excess within the experimental uncertainty as long as the combustion is performed with excess oxygen. Almost all fuel bound sulphur is released to the gas phase as $SO_2$ when pure coal is combusted and the retention of S in ash and deposits is not strongly influenced by the oxygen excess.

The experiment at $\lambda = 1.29$ (grey points) falls outside the trend observed for the remaining experiments, as was also seen in Figure 3.1. Compared to the remaining data sets, this particular experiment is characterized by a significantly lower NO emission and a decreased burnout (high LOI and high CO) which are characteristic features of a low-$NO_x$ flame. The most probable reason for this

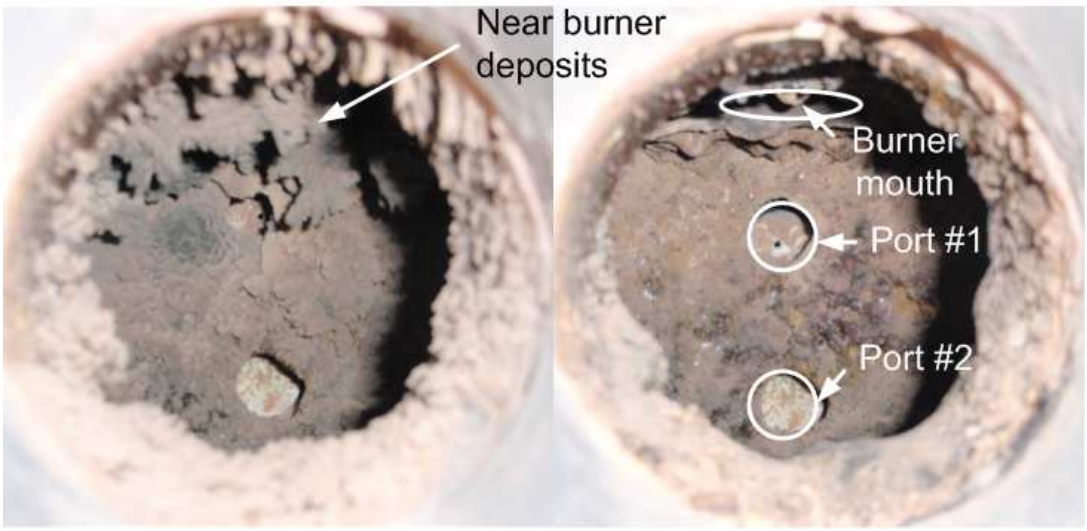


Figure 3.3: Left: Build-up of deposits around burner quarl (top centre) and on furnace walls observed through the top window of the experimental setup. Right: Inside of furnace after removal of deposits near burner.

shift in flame properties is build-up of deposits around the burner quarl during the experiment. This may lead to changes in the near burner fluid dynamics pattern at the flame base causing less $O_2$ to mix into the fuel. Generally, significant slagging was observed during the coal combustion experiments as seen in Figure 3.3. The deposits were removed between experiments.

Figures 3.4 and 3.5 show that the outlier (grey point) match the linear correlation between NO and CO emission rates as well as the linear correlation between the loss-on-ignition and the NO emission rate. This strongly indicates that it is solely the flame properties that have changed.

### 3.1.3 Reference Operating Conditions Chosen

In order to have a combustion process which best matches full-scale, a stoichiometric oxygen excess ratio of $\lambda = 1.3$ has been chosen as reference condition for combustion of coal in air. This excess oxygen ratio yields a theoretical concentration of $O_2$ in the dry exit flue gas of about 5 vol% and a loss-on-ignition for the fly ash which approaches the limit of 5 % set up for fly ash used for cement and concrete production. The reference operating conditions are summarized in Table 3.1.

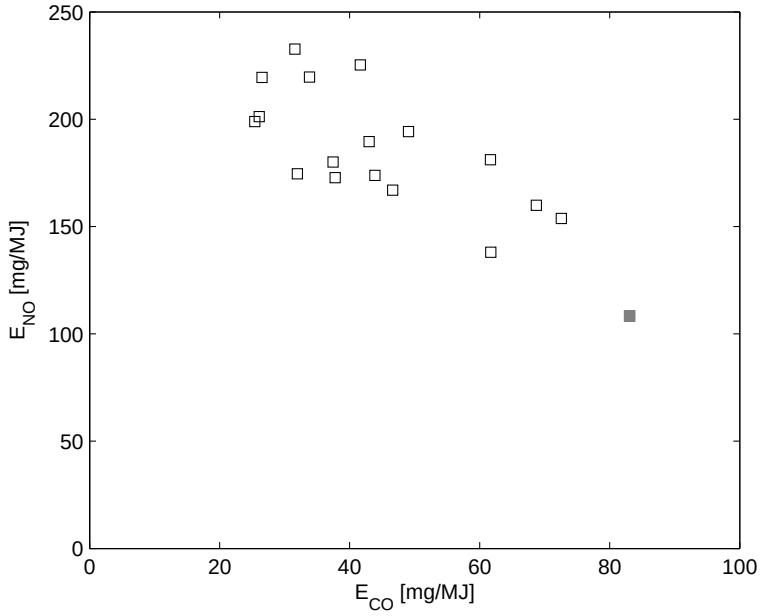


Figure 3.4: Correlation between NO and CO emission rates for coal combustion in air at a range of operating conditions (oxygen excess ratios).

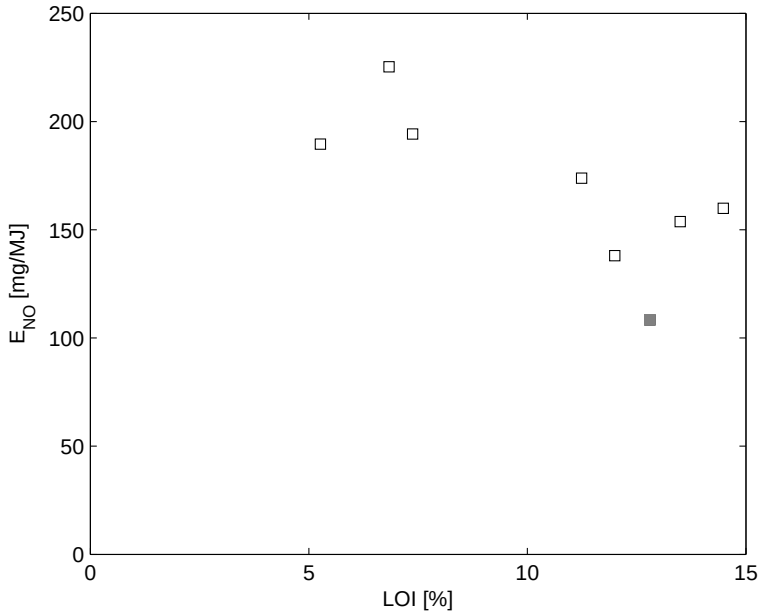


Figure 3.5: Correlation between obtained burnout of fuel, measured by the LOI of the fly ash, and the specific NO emission for coal/air combustion over a range of operating conditions (oxygen excess ratios)

Table 3.1: Operating parameters for coal combustion in air at the reference condition

| Operating parameter | Unit | Value |
|---|---|---|
| Load | $kW_{th}$ | 30 |
| Fuel flow | kg/hr | 3.99 |
| $\lambda$ | | 1.3 |
| Flue gas exit $O_2$ | vol% | 5 |
| Oxidant flow | Nl/min | 620 |
| Swirl number | | 1.8 |

## 3.2 Determining Reference Conditions for Oxy-Coal Combustion

Four parameters can be applied as reference in the attempt of choosing the operating conditions for oxyfuel combustion which provides a match to air combustion; the three stoichiometric parameters, $\lambda$, $y_{O_2}^{wet}$, and $y_{O_2}^{dry}$, and the burnout of the fuel. As described in Section 2.3.3.1, the change from air to oxyfuel atmospheres induces a new correlation between the stoichiometric parameters. In the current work it has been chosen to use the oxygen excess during burnout measured in the dry exit flue gas, $y_{O_2}^{dry} = 5$ %, as a fix point between air and oxyfuel combustion. The results below thus focus on observing the effect on burnout and emissions when varying the oxygen concentration in the inlet gas and achieving comparable temperature profiles (measured with an S-type thermocouple).

### 3.2.1 Effect of Inlet Oxygen Concentration on Burnout and Emissions

Figures 3.6 and 3.7 show the effect of varying the inlet oxygen concentration on burnout and emissions. No significant difference in the LOI can be observed when maintaining constant $O_2$ concentration in the dry flue gas while changing the inlet oxygen concentration. The increased residence time associated with the increase in inlet oxygen concentration does not take effect either. The absence of an improved burnout could be caused by the fact that fuel feeding instabilities were present during these experiments possibly leading to periods with poor burnout regardless of the combined effect of the initially increased partial pressure of oxygen and the longer residence time.

From the emissions results the effect of the increasing availability of oxygen in the flame is observable. The average NO emission rate increases nearly 100 % when increasing the inlet oxygen concentration from 25 to 35 %. Due to the small variations in the stoichiometry between the individual experiments it is not possible to observe a significant trend in the CO emission. The data point marked

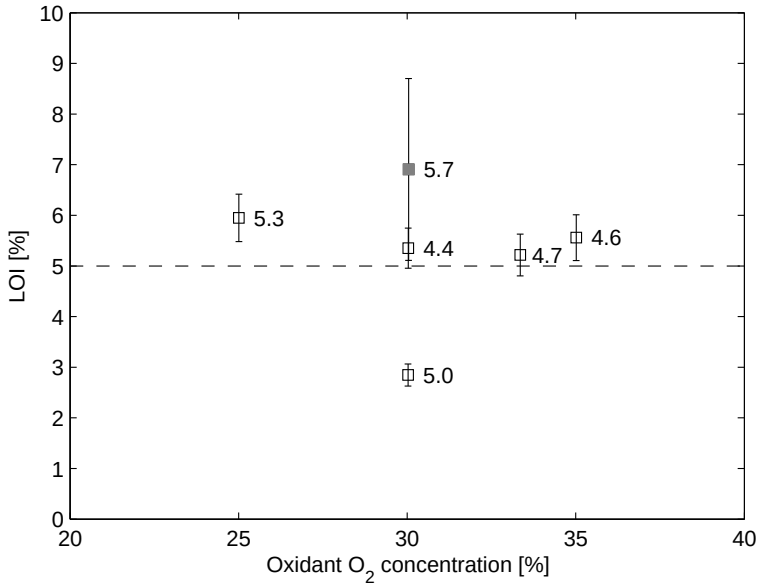


Figure 3.6: Loss-On-Ignition (LOI) for fly ash from coal/oxyfuel combustion as function of the concentration of $O_2$ in the $O_2/CO_2$ oxidant mixture. The numbers associated with each data point specifies the average oxygen concentration in the dry exit flue gas, $y_{O_2}^{dry}$ [%], as it was not possible to match the stoichiometry exactly for all experiments. Error bars correspond to two times the standard deviation on the LOI analysis.

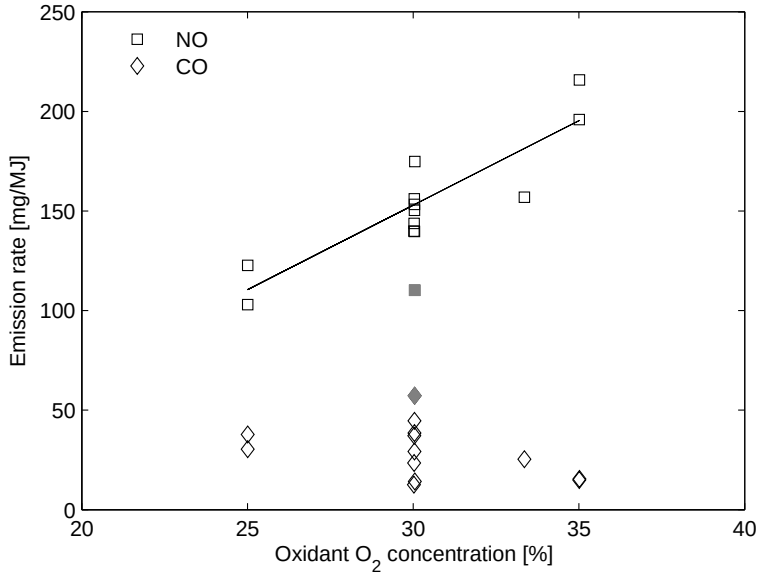


Figure 3.7: Emission rates of NO and CO from coal/oxyfuel combustion as function of the concentration of $O_2$ in the $O_2/CO_2$ oxidant mixture. The experiments have been carried out at flue gas oxygen concentrations in the interval $y_{O_2}^{dry} \in [4.2; 5.7]$ %. The line indicates the trend in the NO data (open symbols).

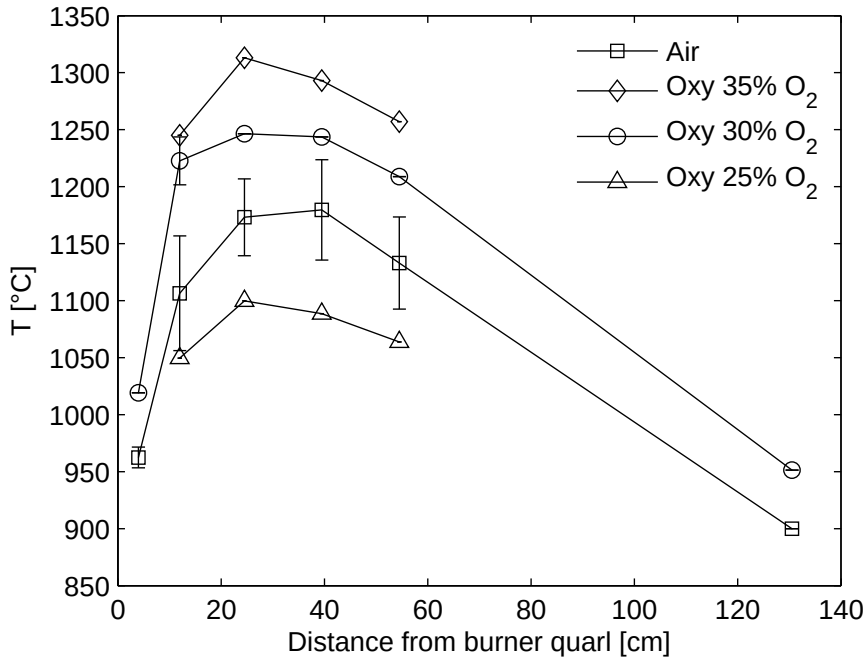


Figure 3.8: Reactor centre temperature profiles measured with S-type thermocouple for pure coal combustion in air and oxyfuel atmospheres with different inlet oxygen concentrations. The $O_2$ concentration in the exit flue gas has been kept at 5 % for all experiments. Error bars correspond to two times the standard deviation for repeated measurements.

in grey shows the same characteristics as the low-$NO_x$ experiments described in relation to the air reference experiments. From the raw data a clear shift in NO emission was observed prior to ash sampling due to a change in the burner settings. For the remaining data treatment this experiment is considered an outlier.

### 3.2.2 Matching Air and OxyCoal Combustion Flame Temperatures

Centreline temperature profiles were measured for coal combustion in air and three different $O_2/CO_2$ atmospheres as seen in Figure 3.8. The temperature is observed to increase with increasing concentration of $O_2$ at the inlet. However, the peak temperature for the oxyfuel flames, observed at measurement port #3 (24.8 cm from the burner quarl), does not shift its vertical position as a consequence of the change in oxidant composition. For all oxidants a relatively high temperature is observed in the top of the reactor (close to the burner).

A comparison of the air reference temperature profile and the oxyfuel profiles indicates that an inlet oxygen concentration of 27-28 % would yield a match.

Table 3.2: Operating parameters for coal combustion in $O_2/CO_2$ at the reference condition

| Operating parameter | Unit | Value |
|---|---|---|
| Load | $kW_{th}$ | 30 |
| Fuel flow | kg/hr | 3.99 |
| Inlet $O_2$ | vol% | 30 |
| $\lambda$ | | 1.19 |
| Flue gas exit $O_2$ | vol% | 5 |
| Oxidant flow | Nl/min | 390 |
| Swirl number | | 1.8 |

### 3.2.3 OxyCoal Reference Operating Conditions Chosen

Based on the measured temperature profiles and fly ash quality it has been chosen to use 30 % $O_2$ as the reference inlet oxygen concentration. The higher temperatures observed at 30 % $O_2$ compared to 25 % $O_2$ at the inlet yields slightly improved burnout on average. Table 3.2 summarises the reference operating conditions.

## 3.3 Comparing Air and OxyCoal Reference Experiments

This section will investigate the differences in the combustion process between air and oxyfuel reference experiments. Due to the fact that it proved difficult to match the stoichiometry exactly to the defined reference condition, it has been chosen to consider experiments which have been run at an oxygen concentration in the dry exit flue gas between 4.5 and 5.5 % as reference cases.[1]

### 3.3.1 Changing Combustion Atmosphere – Effect on Combustion Fundamentals

FTIR mapping of the gas phase temperatures at the chosen reference conditions were performed in order to achieve a more accurate comparison than possible from the simple temperature measurements. Figure 3.9 on the following page shows the radial profiles determined with both the FTIR probe and the thermocouple in ports 2 and 4 (12.3 and 39.8 cm from the burner). Near the burner, only a small difference exist between the average temperatures measured for combustion

[1]The relevant experiments are named CA10_AB, CA12_T, CA13_T, CA14_A, CA15_T, CA16_ADT, CA17_M, CO09_AD, CO10_T, CO12, and CO18_M.

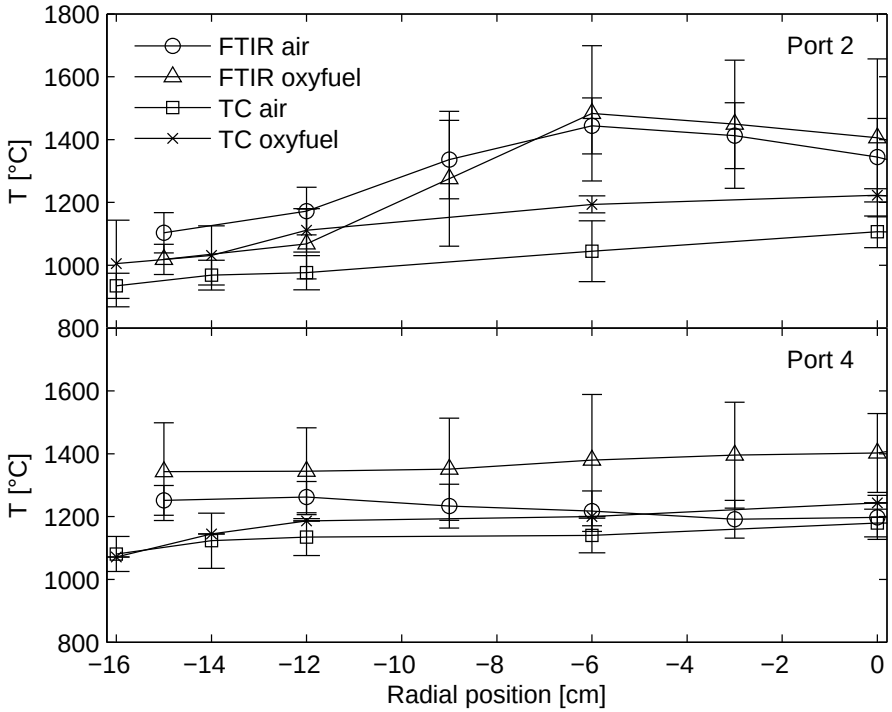


Figure 3.9: Comparison of radial FTIR gas-phase temperature profiles and profiles determined with an S-type thermocouple in selected measurement ports (2 and 4). Error bars on thermocouple data correspond to two times the standard deviation on repeated measurements. Error bars on FTIR data correspond to two times the standard deviation for the 60 scans and provide a measure of the level of fluctuations in the given measurement position.

Table 3.3: Average Loss-on-ignition (LOI [%]), emission rates for NO, $SO_2$, and CO (in [mg/MJ]), and the Fuel-N $\rightarrow$ NO ($CR_N$) and Fuel-S $\rightarrow$ $SO_2$ ($CR_S$) conversion ratios [%] at the air and oxyfuel reference conditions. The uncertainties correspond to two times the standard deviation on repeated experiments.

| | LOI | NO | $SO_2$ [a] | CO | $CR_N$ | $CR_S$ |
|---|---|---|---|---|---|---|
| Air | $6.5 \pm 2.2$ | $212 \pm 33$ | $389 \pm 15$ | $36 \pm 18$ | $19 \pm 3$ | $85 \pm 3$ |
| Oxyfuel | 2.8 [b] | $152 \pm 32$ | $382 \pm 44$ | $20 \pm 16$ | $13 \pm 3$ | $84 \pm 10$ |

[a] The two experiments with advanced diagnostics mapping (CA17_M, CO18_M) have been omitted due to inconsistencies in $SO_2$ mass balances.

[b] Only one experiment is available, uncertainty is unknown.

in air and the reference oxyfuel atmosphere with the FTIR probe. Further down the reactor, the oxyfuel flue gas maintains a higher average temperature. This is most likely due to a combination of the higher heat capacity of $CO_2$ and the fixed amount of cooling air passing the outer surface of the reactor. Compared to the thermocouple data, significantly higher temperatures are observed near the burner when the true gas-phase temperature is measured (FTIR).

Table 3.3 provides a direct comparison of the air and oxyfuel reference experiments regarding burnout and emissions. For the burnout, only one oxyfuel experiment is available within the selected stoichiometric interval. The available experiment shows significantly better burnout than the air references. However, if the observed uncertainty for the air experiments is transferred to the oxyfuel data the difference can no longer be considered significant. It should be noted that the observed uncertainties (95 % confidence levels) become large when only few data points are available as is the case for the present investigation. Liu et al. [71] showed in their 20 kW once-through setup that the carbon-in-ash decreases from about 12.4 to 5.1 % for a UK bituminous coal when changing from air to 30% $O_2/CO_2$ as oxidant. They kept the stoichiometric oxygen excess ratio, $\lambda = 1.2$, constant for the two combustion atmospheres. This stoichiometric excess ratio corresponds to 3.6 and 5.2 % $O_2$ in the dry exit flue gas, respectively. Due to the lower level of $O_2$ during burnout in air compared to the oxyfuel atmosphere, the relative difference in burnout efficiency is larger for the experiments reported by Liu et al. [71] than for this work where the burnout conditions have been kept similar. However, their results are in godd agreement with the comparison shown in Figure 2.21 on page 47 for this work using $\lambda$ as the independent variable.

Considering the emissions of CO and $SO_2$, no difference between the two combustion atmospheres can be determined. This is in agreement with observations from other once-through setups as reported by Liu et al. [71] and Croiset and coworkers [72, 73]. The conversion of Coal-S to $SO_2$ is slightly higher, 86-90 % for both atmospheres, in [71] than observed in this work. This could be a result of

the different Fuel-S contents (UK bit: 2.06 % compared to 0.62 % (COCERR)). With a lower sulphur content of the parent coal a comparably larger capacity for capture of sulphur exist in the fly ash if the amount of the different ash-forming species is similar. The Fuel-S to $SO_2$ conversion would thus be lower for the low-sulphur coal.

With respect to NO there is a tendency for decreasing emission rate when changing from air to oxyfuel combustion. On average, the NO formation during oxyfuel combustion of coal is reduced about 28 % compared to air-firing. Croiset and coworkers [72, 73] and Liu et al. [71] likewise reported a reduction in the NO emission compared to combustion in air in their once-through experiments. Liu et al. [71] showed that the Coal-N to NO conversion ratio was 27.6 % for air combustion and was reduced to about 80 % of that (22.6 %) for combustion in 30 % $O_2/CO_2$. The Fuel-N conversion ratio determined in this work is slightly lower for both air and oxyfuel combustion. This is most likely due to differences in the burner design and operating conditions. Four aspects regarding the combustion process could contribute to the reduced NO emission during oxyfuel combustion of the applied coal.

**Reduced thermal NO formation** The near elimination of $N_2$ from the oxyfuel oxidant will limit the formation of NO to Fuel-NO. In pulverized coal flames Fuel-NO typically accounts for about 80 % of the NO emission [70]. However, due to the high levels of NO formed from Fuel-N, temperatures in excess of 1900 °C should be obtained in order for thermal NO to contribute significantly to the NO emission from coal flames [70]. In this work flue gas temperatures up to 1700 °C were observed (Fig. 3.9). The difference in NO emission rates between air and oxyfuel combustion is thus not expected to be caused by reduced formation of thermal NO.

**Smaller flue gas volume** The smaller flue gas volume during oxyfuel combustion compared to combustion in air at comparable oxygen levels in the flue gas will reduce the dilution of the NO concentration within the furnace. A higher level of NO in the flue gas will increase the reaction rate for the 2. order reduction of NO with other nitrogen-containing species [70] thus leading to reduced NO emission.

**Increased formation of CO in flame** CO is known to promote the reduction of NO over char [70]. In-flame CO levels are reported to increase significantly during oxyfuel combustion compared to air-blown flames [59] and there is thus an increased potential for reduction of NO over char. CO levels of 5 % on average for oxyfuel combustion were measured about 12 cm from the burner (port 2) in this work, see Figure 4.8 on page 86.

**Near burner fluid dynamics** Depending on the obtained stoichiometry at the point of mixing of fuel and oxidant, NO emission rates can both increase

and decrease when changing from air to oxyfuel combustion. Mixing at reducing conditions will lead to an increase in the formation of NO whereas NO formation is inhibited at both stoichiometric and fuel-lean conditions. The presence of high $CO_2$ concentrations acts to increase the concentration of OH radicals under fuel-rich conditions thus promoting NO formation from volatile-N. When mixing occurs at conditions with oxygen excess, the reduced formation of NO is caused by a limitation of the O/H radical pool, particularly O, from the increased level of $CO_2$ [74, 75]. Since the burner applied in this work has been operated in high-$NO_x$ mode, *i.e.* mixing of fuel and oxidant takes place at fuel-lean conditions, a decrease in NO formation compared to the air reference case should be expected.

The observed difference in the emission rate of NO from combustion in air and the reference oxyfuel atmosphere is most likely a consequence of a combination of the latter three effects. The relative importance of each mechanism is unknown.

### 3.3.2 Changing Combustion Atmosphere – Effect on Ash Quality and Deposit Formation

The particle size distribution for the fly ashes from air and oxyfuel combustion are shown in Figure 3.10 on the following page. Both distributions have the general, bimodal appearance with a peak between 0.1 and 1 $\mu$m and another around 10 $\mu$m. The small particles typically originate from aerosols and approximately 10-20 % (volume basis) of the fly ash particles have diameters below 1 $\mu$m. The larger particles stems from the residual ash particles formed during combustion. The reduced burnout during air combustion can explain the shoulder at 100 $\mu$m as the presence of residual carbon will increase the particle size of residual ash particles, see Figure 3.11 on the next page.

A full analysis with respect to the composition of the fly ash samples from experiments CA14_A and CO09_AD and the deposits from experiments CA16_ADT and CO09_AD have been obtained. Figure 3.12 on page 71 shows a comparison of the bulk composition of the fuel ash, fly ash, and deposits for the coal references. Except for S and Cl, the bulk composition of the fuel and fly ashes are similar. The main part of S and Cl is released to the flue gas as $SO_2$ and HCl. There is a slight tendency for the Si and Fe levels to increase in the deposits and the Al level to decrease. However, the difference to the ash fractions is small.

Even though the bulk composition of the fuel and fly ashes is similar, it is unknown whether there could be a difference in the types of minerals present in the two combustion atmospheres. An obvious question is if the significantly increased concentration of $CO_2$ in the furnace could lead to increased carbonate formation. Table 3.4 on page 71 shows the results from an analysis of the total carbon (organic and inorganic) and the total organic carbon (TOC) content of

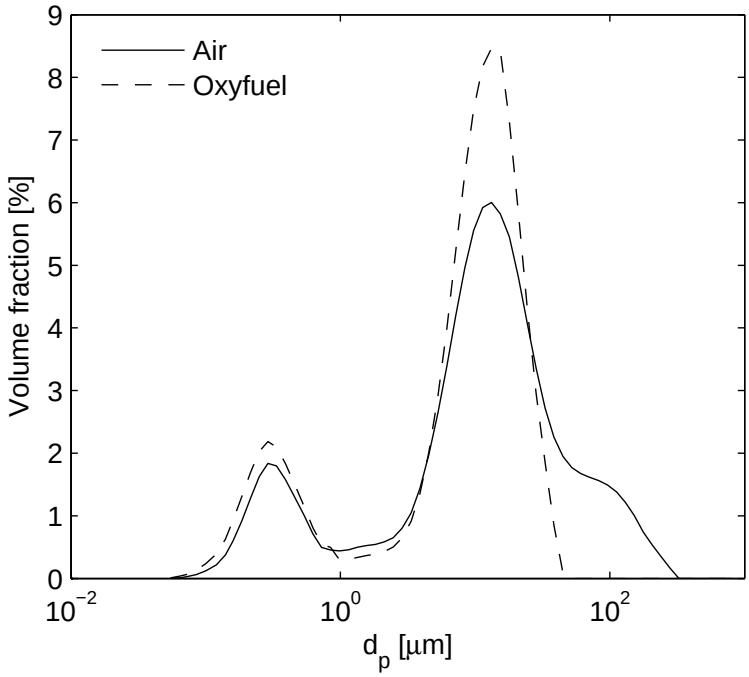


Figure 3.10: Comparison of ash size distributions for coal combustion in air and 30% $O_2/CO_2$ at the reference conditions. The ash is the combined cyclone and filter ash fractions from the ash sampling system. The distribution type is volumetric and is obtained from a Malvern laser diffraction particle size measurement.

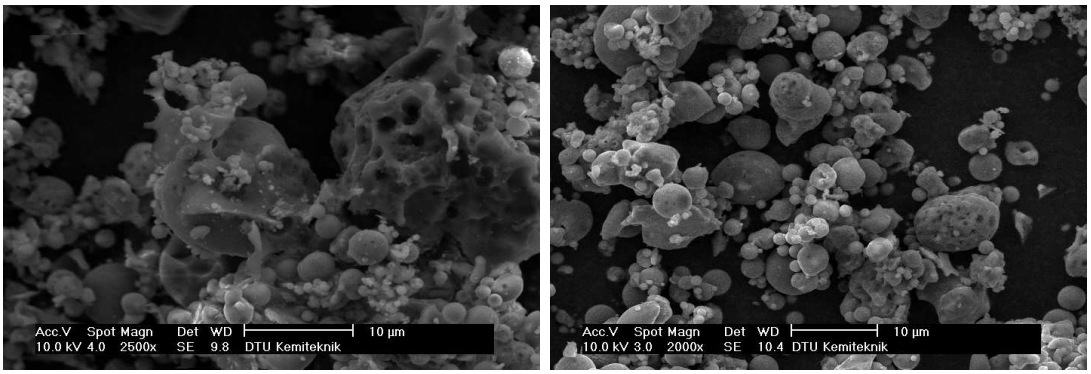


Figure 3.11: SEM images of fly ash. Left: coal combustion in air at $\lambda = 1.25$ ($y_{O_2}^{dry} = 4.4$ %); Right: coal combustion in 30 % $O_2/CO_2$ at $\lambda = 1.3$ ($y_{O_2}^{dry} = 7.3$ %). Even though the applied combustion conditions do not match the chosen reference values the influence on the size distribution of the fine ash particles is assumed to be negligeble.

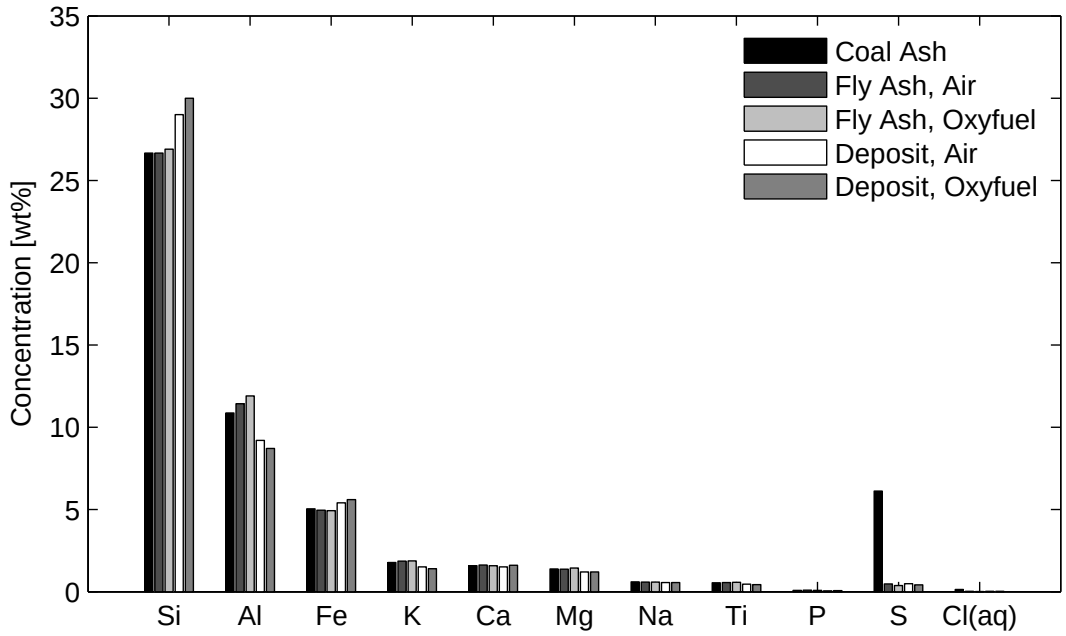


Figure 3.12: Comparison of fly ash and deposit compositions for coal combustion in air and 30% $O_2/CO_2$ at the reference conditions. The uncertainty is about 10 % on the individual values.

Table 3.4: Total carbon (C) and total organic carbon (TOC) contents of combined filter and cyclone ash fractions for air and oxyfuel coal references

| | Air | Oxyfuel |
|---|---|---|
| C (total) | $5.6 \pm 0.5$ | $2.6 \pm 0.2$ |
| TOC | $5.4 \pm 0.3$ | $2.4 \pm 0.2$ |

the air and oxyfuel ashes. The difference between the two values is a measure of the carbonate content of the ash. No difference can be observed between the two combustion oxidants and for the applied setup, oxyfuel combustion will thus not lead to increased carbonate formation in the fly ash. The appearance of the deposits from the two atmospheres is likewise similar as seen in Figure 3.13 on the following page. The upstream part of the deposits was loose and powdery, and easily removable from the deposit probe. The downstream part of the deposit could be identified as a condensed layer. The potential difference in the composition of upstream and downstream deposit fractions was not determined as the two fractions were mixed prior to analysis. However, the difference can be expected to be negligible.

Nothing in the data indicates that the change from air to $O_2/CO_2$ as oxidant will lead to significant differences in the mineralogy of the fly ash or deposits.

Figure 3.13: View of deposits from the side. The deposit probe has a diameter of 16 mm and the thickness of the upstream deposits is about 1 mm. Top: coal/air combustion; Bottom: coal/oxyfuel combustion. The upstream part of the probe faces upwards in the picture. Colour differences are a consequence of the picture recording.

Table 3.5: Average deposit fluxes as well as flue gas and deposit probe temperatures for air and oxyfuel coal references

| Oxidant | Upstream [g/m$^2$·hr] | Downstream [g/m$^2$·hr] | Average [g/m$^2$·hr] | $T_{probe}$ [°C] | $T_{FG}$ [°C] |
|---|---|---|---|---|---|
| Air | 107 | 11 | 59 | 500 | 900 |
| Oxyfuel | 75 | 3 | 39 | 500 | 950 |

The deposits were sampled during a period of about 2 hours. Based on the mass of deposits collected from the upstream and downstream halves of the probe the deposit flux for each atmosphere has been determined. Table 3.5 shows the results. The uncertainty on the fluxes to the downstream part of the probe are relatively large due to very small sample sizes. There is an indication that the deposit flux is smaller during oxyfuel combustion than in air. Due to very low flue gas velocities and small particle sizes the difference cannot be explained by variations in inertial impaction on the probe. Due to the fact that only one data set exist for each atmosphere, it is unknown whether the observed difference is within the experimental uncertainty. However, no obvious explanation to the difference exists.

## 3.4 Summary and Conclusions

Reference operating conditions for coal combustion in air and $O_2/CO_2$ at a thermal load of 30 kW have been defined. In order to yield experimental results comparable to full-scale boilers a target of a loss-on-ignition of maximum 5 % was set up for the fuel burnout efficiency. The target was reached for air-firing at a stoichiometric oxygen excess ratio of $\lambda = 1.3$ corresponding to 5 % $O_2$ in the burnout stages of combustion (measured in the dry exit flue gas).

The $O_2$ concentration in the char burnout stage (*i.e.* 5 vol%) were applied as the standard of reference during the work related to defining the reference operating parameters for oxyfuel combustion. Three different oxidant compositions (25, 30, and 35 % $O_2$ in $CO_2$) were investigated with respect to burnout efficiency, flame temperature profiles, and emissions. The investigations showed that a match of temperatures could be obtained with an inlet $O_2$ concentration between 25 and 30 %. An oxidant composition of 30 % $O_2$ in $CO_2$ was chosen as the reference case due to slightly improved burnout efficiency compared to 25 % $O_2$ in $CO_2$.

A comparison of the air and oxyfuel reference cases showed no significant differences between burnout efficiencies or emissions of CO and $SO_2$ even though there was a tendency for improved burnout. NO emissions from oxyfuel combustion was reduced approximately 28 % compared to combustion in air. The reduced NO emission is suggested to be a consequence of three effects; (1) higher NO levels in the flue gas promoting gas-phase reduction due to NO reacting with other nitrogen-containing species; (2) Increased reduction of NO over char due to significantly higher levels of CO in the flame zone; and (3) the application of a high-$NO_x$ burner in combination with the alterations to the radical pool caused by the significantly increased concentration of $CO_2$. The composition of fly ash and deposits do not change with the change in combustion atmosphere. The deposit flux was, however, observed to be reduced about 30 % in oxyfuel compared to air combustion. No explanation was found for the difference in deposit flux. Good agreement between the results obtained in this work and results reported in open literature for comparable once-through reactors was observed.

# Chapter 4

# OxyFuel Combustion for Below-Zero $CO_2$ Emissions – Co-Firing Coal and Biomass

Co-firing coal with biomass is a relatively easy way of reducing $CO_2$ emissions from fossil fuel fired power plants. However, the biomass share of the fuel blend is typically kept low ($<$ 20 wt%) in order to ensure that residual products can be utilized, to prevent deactivation of SCR catalysts, and to reduce superheater corrosion risks. Oxyfuel combustion can be applied to biomass as well as coal and the use of $CO_2$ neutral fuels induces the potential of achieving an overall negative $CO_2$ emission from the power plant. The objective of this chapter is to illustrate the impact on the combustion characteristics including flame temperature, burnout, emissions, as well as fly ash and deposit characteristics when pure biomass (straw) and blends of coal and biomass are combusted in air and oxyfuel atmospheres. All experiments described in the following have been performed with equal thermal input (30 kW) and at the reference oxygen excess of 5 % in the dry flue gas. For oxyfuel experiments the inlet oxygen concentration is fixed at 30 %.

## 4.1 Flame Temperature – Effect of Fuel Change

Due to the differences in fuel characteristics between coal and straw, differences in ignition, flame shape, and temperature profiles are expected. The utilized straw has a significantly higher content of volatiles as well as a larger average particle size compared to the coal, see Table 2.2 on page 20. This section provides results from two different temperature measurement techniques; Thermocouple and FTIR; applied in the characterization of the effect of fuel change.

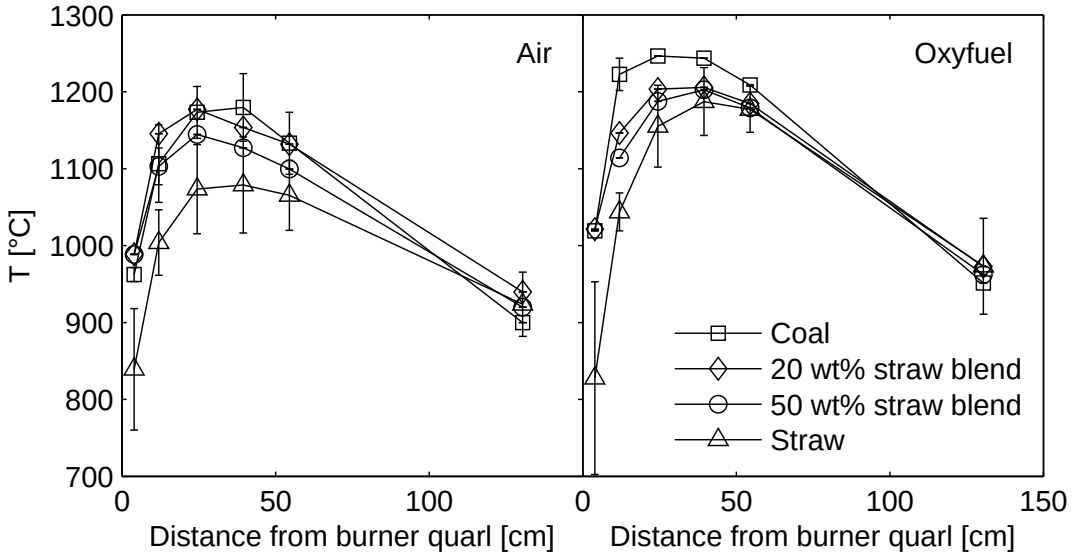


Figure 4.1: Reactor centreline temperature profiles measured with S-type thermocouple for co-firing experiments in air and in the oxyfuel atmosphere with 30 % $O_2$. Errorbars correspond to two times the standard deviation for repeated measurements.

### 4.1.1 Simple Flue Gas Temperature Measurements

Simple temperature measurements are performed with an S-type thermocouple as described in Section 2.3.2.5. Figure 4.1 shows reactor centre line profiles for the four investigated fuel blends for both air and 30 % $O_2/CO_2$ as oxidant. Figure 4.2 on the facing page shows a direct comparison of the temperature profiles for the pure fuels in the two combustion atmospheres. For both combustion atmospheres, near burner temperatures increase with increasing coal share of the fuel. The temperature difference between pure straw and the other three fuels when burned in air is significant and the presence of up to 50 wt% straw in the coal/straw blend does not significantly change the temperature profile compared to pure coal firing. The temperature profile for straw combustion in both atmospheres shows the characteristics of delayed ignition compared to the coal containing flames, *i.e.* a steeper temperature gradient in the first 3 measurement positions. Visual inspections of the flame proved this since a distinct, cold fuel jet was observable at port 1 with flame ignition initiating at port 2. For the remaining fuel blends ignition was observable at port 1. Peak flame temperatures are generally positioned between ports 3 and 4 (25 to 40 cm from the burner quarl). The peak flame temperature position for pure straw was likewise moved downstream from the burner relative to the remaining fuels.

The oxyfuel temperature profiles show similar peak flame temperature positions to the air profiles. However, in each specific position the temperature is generally higher than for air as oxidant as was also shown for pure coal in Section

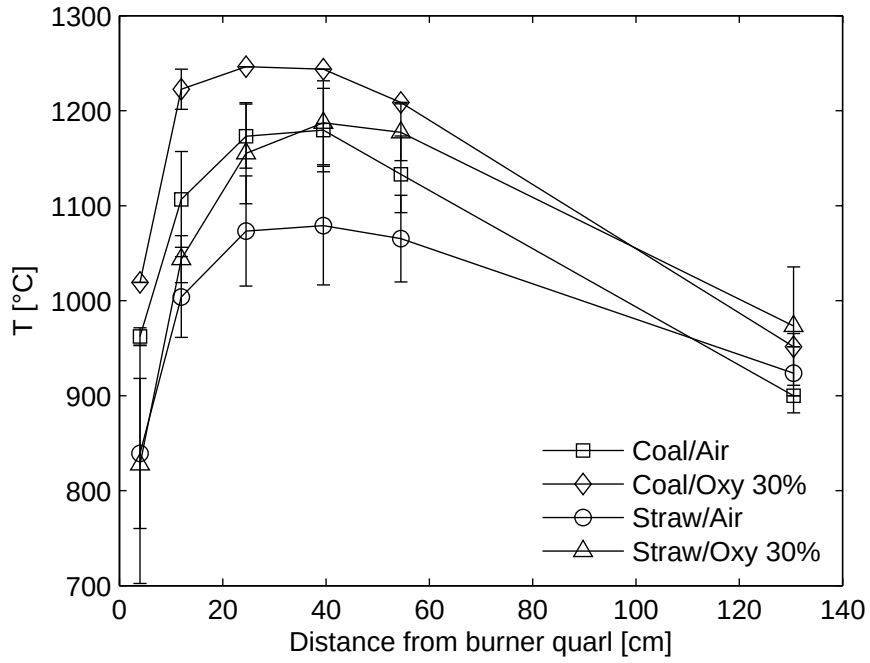


Figure 4.2: Comparison of reactor centre temperature profiles measured with S-type thermocouple for coal and straw combustion in air and the reference oxyfuel atmosphere. Error bars correspond to two times the standard deviation for repeated measurements.

3.2.2. The effect of changing combustion atmosphere is most pronounced for pure straw combustion where a temperature difference of more than 100 °C is measured in ports 4 and 5, see Fig. 4.2. Contrary to the case of air-firing, pure coal yields higher temperatures than blends. For the blends the straw content seems to have an insignificant effect on temperature. Compared to air combustion, less difference between coal-containing fuels and pure straw for the last three measurement points (ports 4, 5, and 7) exists in the oxyfuel case.

### 4.1.2 FTIR Measurements of Gas Phase Temperature

FTIR temperature mappings, see Section 2.3.2.6, have been performed for pure coal and the 50 wt% straw blend in air and 30 % $O_2/CO_2$ and for pure straw combustion in 30 % $O_2/CO_2$. However, during straw combustion only measurements with the beam stop were performed and for coal/oxyfuel combustion only ports 2 and 4 were mapped without the beam stop. Figure 4.3 on the next page compares the measured profiles for coal and the 50 wt% straw blend. A trend similar to the one observed from the simple temperature measurements with oxyfuel yielding higher centreline temperatures than combustion in air is seen. Also, the 50 wt% straw blend generally yields slightly lower temperatures than pure coal. For all fuels, peak temperatures reaching 1600-1700 °C are observed and the

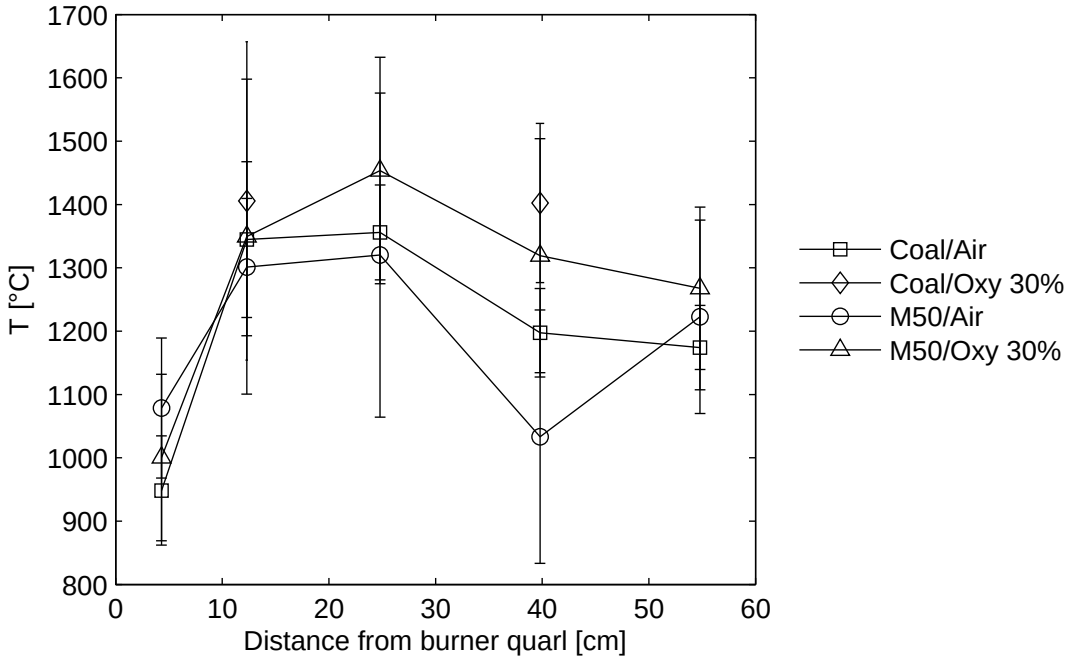


Figure 4.3: Comparison of reactor centre temperature profiles measured with the FTIR probe for combustion of coal and the 50 wt% straw blend in air and the reference oxyfuel atmosphere. Error bars correspond to two times the standard deviation for each time series and is a measure of the level of fluctuations in the given measurement position.

gas-phase temperatures are generally higher than what was observed from the thermocouple measurements which were not corrected for radiation. Since the furnace walls are cooled their radiative flux to the thermocouple will act to lower the measured temperature. The M50/air temperature shows an unexplainable drop at 40 cm from the burner. This is most likely due to either problems during the conversion of the obtained spectra to temperatures or errors during the measurement.

## 4.2 The Impact of Fuel Properties on Burnout

Co-firing coal with up to about 20 wt% straw is seen to improve the carbon burnout in full-scale plants [76]. Occasionally, unburned straw particles (from the nodes of the straw) can be observed in the fly ash. However, the overall burnout efficiency is not affected significantly by this.

Fly ash samples collected for combustion of the four investigated fuel blends in air and the reference oxyfuel atmosphere supports this trend, when the straw share does not exceed 20 wt%. Figure 4.4 on the following page shows the loss-on-ignition analysis results and the calculated carbon burnout efficiency for each condition as function of the fuel straw share. The carbon burnout efficiency (CB) is determined from (4.1).

$$\begin{aligned} \mathrm{CB} &= \frac{m_{C,\,fuel} - m_{C,\,ash}}{m_{C,\,fuel}} \\ \mathrm{CB} &= \frac{x_{C,\,fuel} - \frac{x_{C,\,ash}}{(1-x_{C,\,ash})}\, x_{ash,\,SF}}{x_{C,\,fuel}} \end{aligned} \tag{4.1}$$

where $m_{C,\,Fuel}$ is the amount of carbon fed with the fuel (kg/kg fuel) and $m_{C,\,ash}$ is the amount of carbon leaving the reactor with the fly ash (kg/kg fuel). It is assumed that all ash entering the reactor leaves as fly ash, *i.e.* deposition within the reactor is neglected. Since ash particles that are retained as deposits within the reactor are assumed to yield full burnout, see the discussion related to the carbon balance in Section 2.4.1, this assumption will lead to a conservative estimate of the burnout efficiency since the amount of carbon retained in fly ash is slightly overestimated. $x_{C,\,fuel}$ is the carbon content of the fuel given by the ultimate analysis. $x_{C,\,ash}$ is the measured carbon content of the fly ash sample and $x_{ash,\,SF}$ is the ash content of the fuel.

For both combustion atmospheres increasing the fuel straw share beyond 20 wt% leads to reduced burnout. The reduced burnout efficiency is mainly due to an increased amount of large straw and straw char particles being transported through the furnace with limited conversion of the fixed carbon content. Table 4.1 on page 81 illustrates the differences between the bottom ashes for the eight fuel/oxidant combinations investigated. From the pictures it is evident that

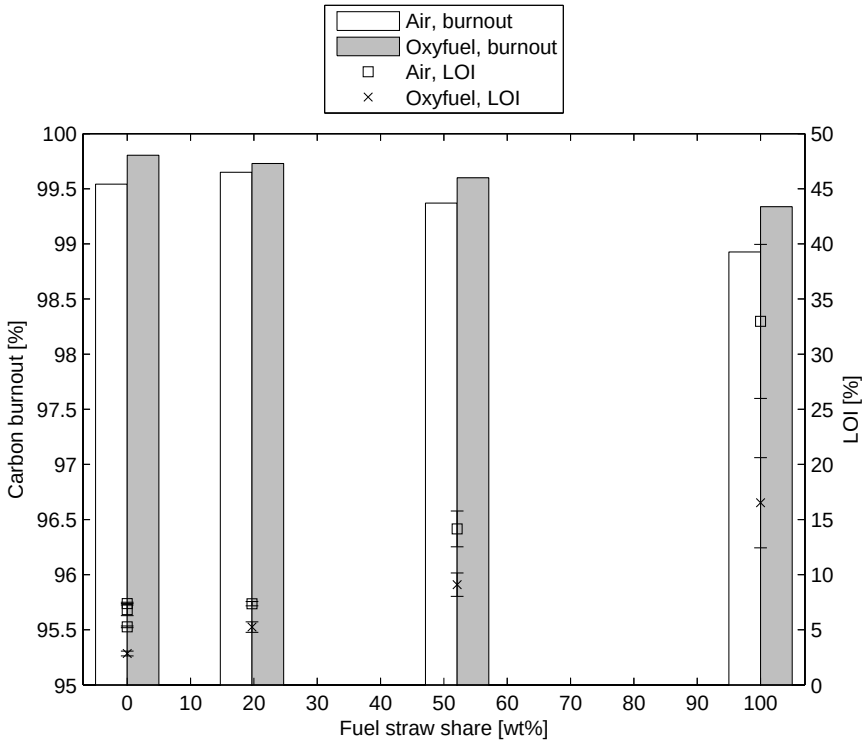


Figure 4.4: Calculated carbon burnout and loss-on-ignition analysis of fly ash as function of fuel straw share. Comparison of air and oxyfuel environments at the reference operating conditions. The error bars correspond to two standard deviations on the LOI analysis.

Table 4.1: Appearance of bottom ash samples collected from the setup. Top row: Air combustion experiments, bottom row: oxyfuel combustion experiments. Fuel straw share increases from left to right. Each picture has dimensions of approximately 20x20 mm.

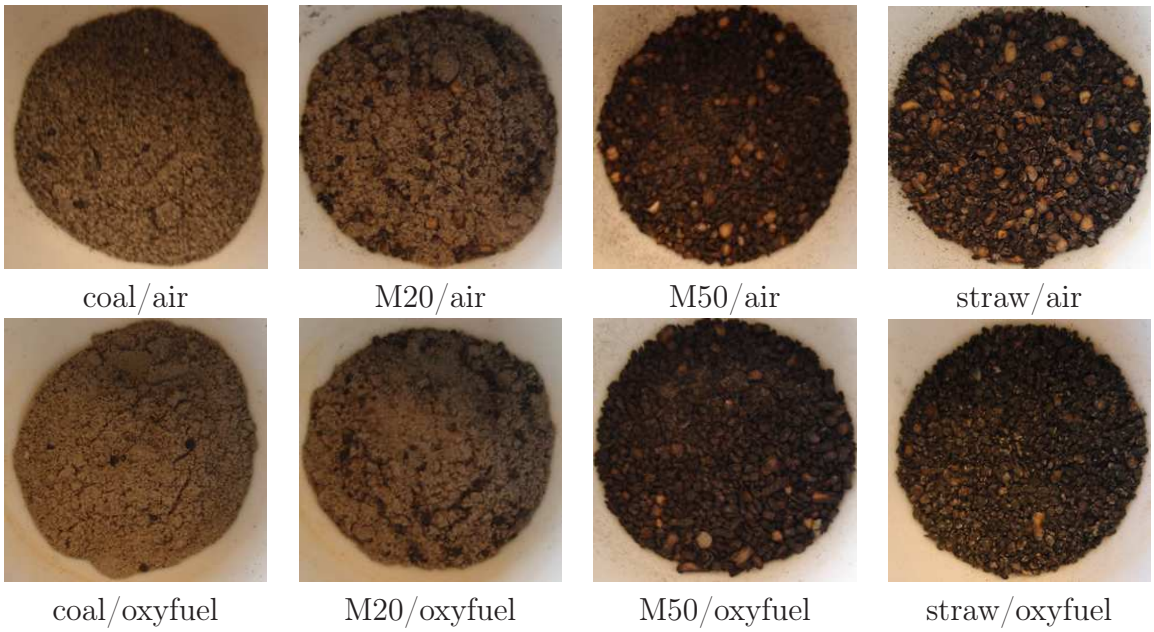


an increasing number of large straw particles ($d_p = 0.5 - 1$ mm) are transported through the furnace without being burned. Especially the increasing fraction of particles which still appear yellow and only have been blackened at the edges for the air experiments are contributing to the decreasing burnout efficiency and increasing LOI with increasing fuel straw share. Due to the lower fuel ash content of straw compared to coal (4.4 versus 9.6 %) the LOI values for the pure straw fly ashes appear very large even though the overall burnout is about 99 %. The increasing uncertainty in the values for increasing straw share is due to the high fraction of straw char particles in the bottom ash fraction making it increasingly difficult to extract a representative sample for analysis. The LOI value for straw/air is an average of 4 measurements (3 for the oxyfuel experiment).

The most likely explanation to the appearance of yellow particles is that they shoot directly through the flame without ignition. Visual inspection of the flame from the bottom of the reactor likewise revealed a significant portion of visible particles below the flame, see Figure 4.5 on the following page. Note that the pictures illustrate instantaneous flame shapes. Due to the swirling motion of the oxidant the fuel particles can be observed to burn in a rotating band down through the furnace and hence the flame is not axisymmetric.

Figure 4.6 on page 83 shows estimated heating profiles of straw particles of three characteristic sizes under the assumption that they do not ignite. The tem-

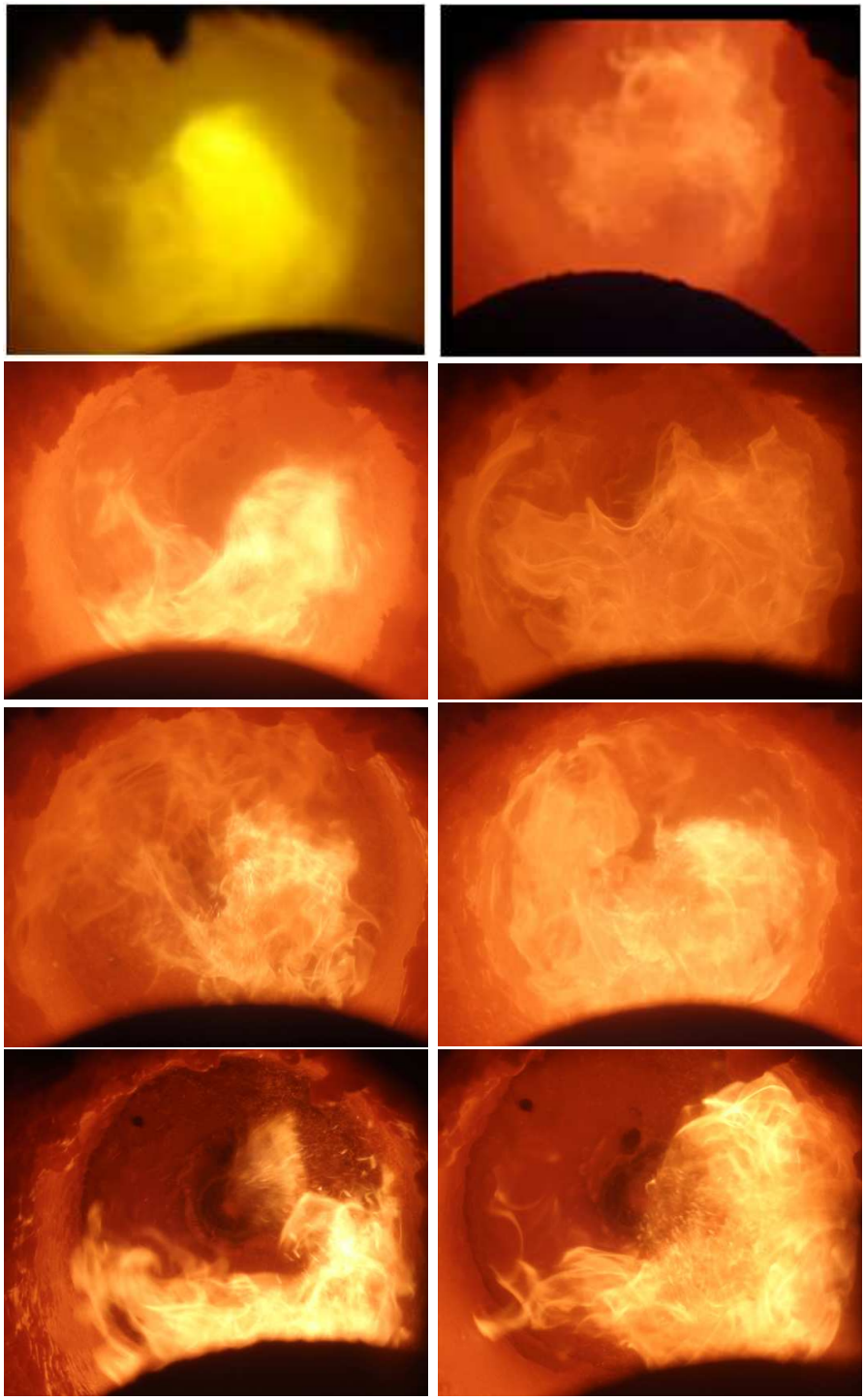

Figure 4.5: Appearance of flames recorded through the bottom of the reactor. Left column: Air combustion experiments, right column: oxyfuel combustion experiments. Top row: pure coal; second row: fuel straw share: 20 wt%; third row: fuel straw share: 50 wt%; bottom row: pure straw.

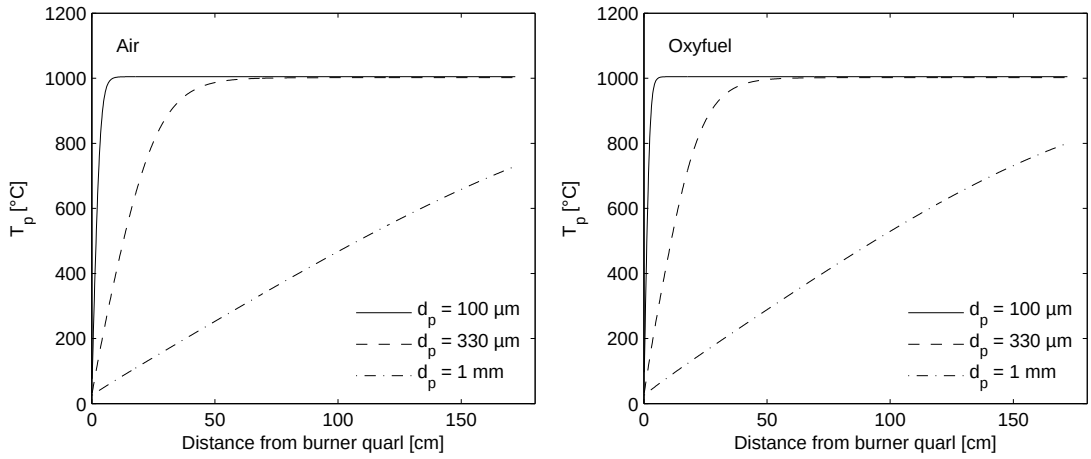


Figure 4.6: Heating profiles for straw particles of different size, assuming isothermal temperature gradient through particle and heating by both radiation and convection. Comparison of combustion in the reference air and oxyfuel atmospheres.

perature profiles are determined from combined radiative and convective heating of the particles by means of the energy balance shown in Eq. (4.2).

$$m_p C_{p,p} \frac{dT_p}{dt} = \pi d_p^2 \cdot \left( h \left( T_g - T_p \right) + \epsilon_p \sigma \left( T_w^4 - T_p^4 \right) \right) \tag{4.2}$$

Appendix D provides an overview of the parameters and the values applied.

The heating profiles show significant differences between the three particle sizes. Whereas the smaller particles reach temperatures of 1000 °C within the first 10 cm of the reactor, the largest particles are heated considerably slower. The slow heating of the 1 mm particles means that they reach the lower part of the furnace before being heated enough to ignite. In that position the partial pressure of oxygen surrounding the particles have dropped to about 5 vol%, further decreasing the ignitability of the particles. The result is that large straw particles leave the reactor with no or a very small degree of conversion as observed experimentally. Besides the effect of the size of the particles on the heating rate, their velocity relative to the flue gas will differ due to the difference in mass with increasing diameter. Table 4.2 on the following page shows average terminal velocities of the investigated particle sizes and their residence time within the furnace. The data further elucidate the problems encountered with large straw particles regarding burnout since the residence time is very limited. Due to the smaller flue gas flow during oxyfuel combustion the residence time is longer and hence the burnout should increase. The large increase in the terminal velocity of large particles compared to the smaller size fractions is especially a problem with respect to down-fired reactors as the one applied in this work. In full-scale boilers were the flue gas moves in the upward direction, the increased terminal velocity of large particles actually will increase their average residence time within the

Table 4.2: Terminal velocity, $u_t$, and average residence time, $\tau_p$, of large straw particles in furnace

| | Air | | Oxyfuel | |
|---|---|---|---|---|
| $d_p$ [$\mu$m] | $u_t$ [m/s] | $\tau_p$ [s] | $u_t$ [m/s] | $\tau_p$ [s] |
| 100 | 0.05 | 2.42 | 0.05 | 3.25 |
| 330 | 0.59 | 1.38 | 0.61 | 1.58 |
| 1000 | 2.61 | 0.53 | 2.34 | 0.61 |

boiler compared to the smaller particles. For similar conditions, the burnout of large particles in full-scale boilers is thus expected to improve compared to what has been shown in this work.

The burnout efficiency is consistently higher during oxyfuel combustion than when using air as oxidant. The difference between the two atmospheres seems to increase with increasing fuel straw share. This indicates the relatively higher importance of the combined effect of the higher inlet $O_2$ concentration, increased maximum flue gas temperature, and increased residence time during oxyfuel combustion for the burnout of large straw char particles. Figure 4.7 on the next page shows the radial profiles of CO for the first 55 cm of the furnace (ports 1-5). The figure illustrates the change in flame length and width with the change in fuel composition. Downstream of the flame the CO is typically very low due to sufficient $O_2$ to oxidize CO to $CO_2$. However, near the flame front the concentration of CO can reach very high levels. For pure coal, the centreline concentration of CO (position 0 cm) drops to zero in port 5, whereas combustion of pure straw shows significant levels of CO (about 5% on average) at this distance from the burner. The flame length of pure straw is thus considerably larger than for pure coal elucidating the increasing importance of increased residence time on the burnout efficiency for increasing fuel straw share.

The exit flue gas CO emission as function of the fuel straw share is seen in Figure 4.8 on page 86. The figure shows a trend for pure straw experiments to yield increased CO emissions, the trend is however not consistent due to the large spread on the data. For several of the pure straw experiments the CO emission rate is observed to increase during the course of the experiment. The emission is also very sensitive towards external disturbances of the furnace, *e.g.* frequent changes to the pressure due to opening of measurement ports. From an overall perspective it is possible to obtain satisfactory low CO emissions for all fuel/oxidant combinations taking the relatively small size of the experimental setup into consideration.

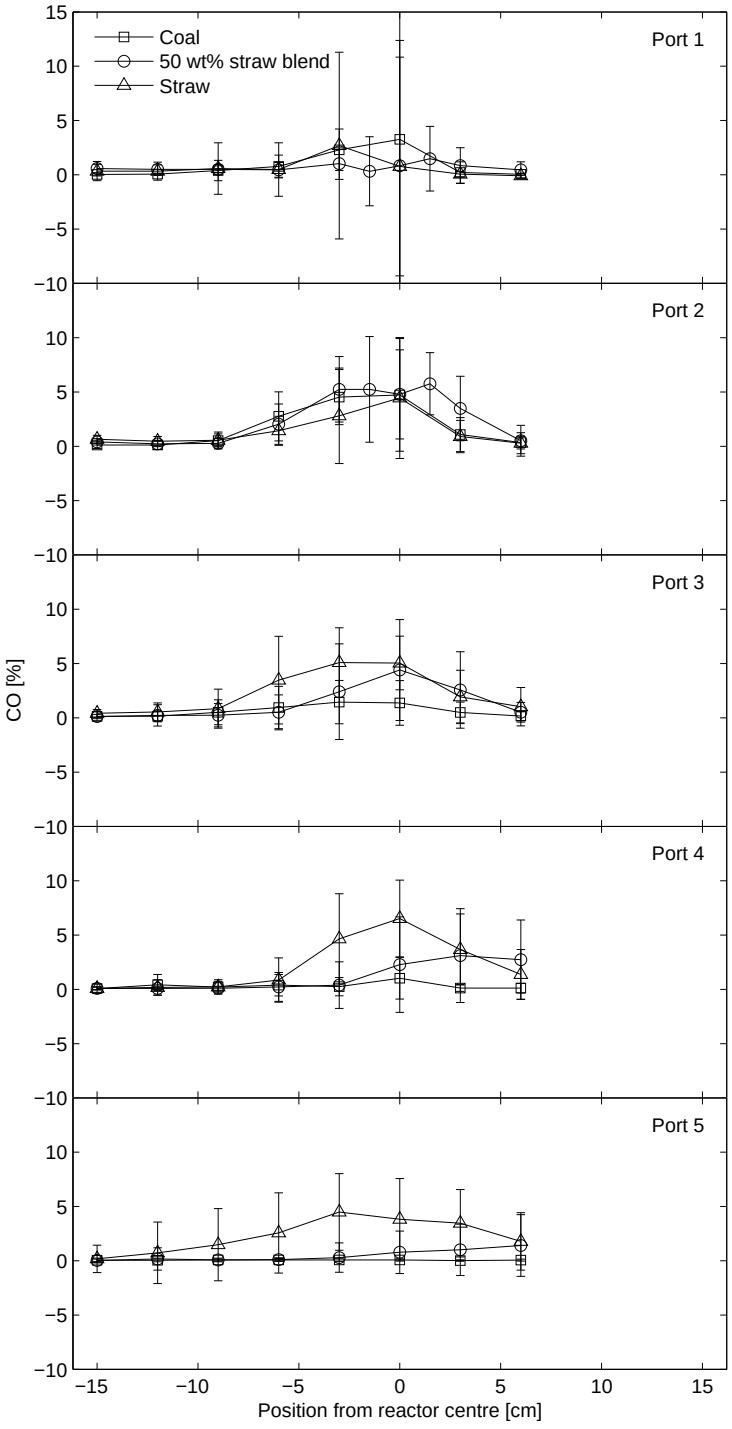


Figure 4.7: Radial profiles of CO concentrations for combustion of coal, straw and the 50 wt% straw blend in the reference oxyfuel atmosphere. The profiles are measured with the FTIR probe. Error bars correspond to two times the standard deviation on the 60 measurements in each position and is a measure of the level of fluctuations.

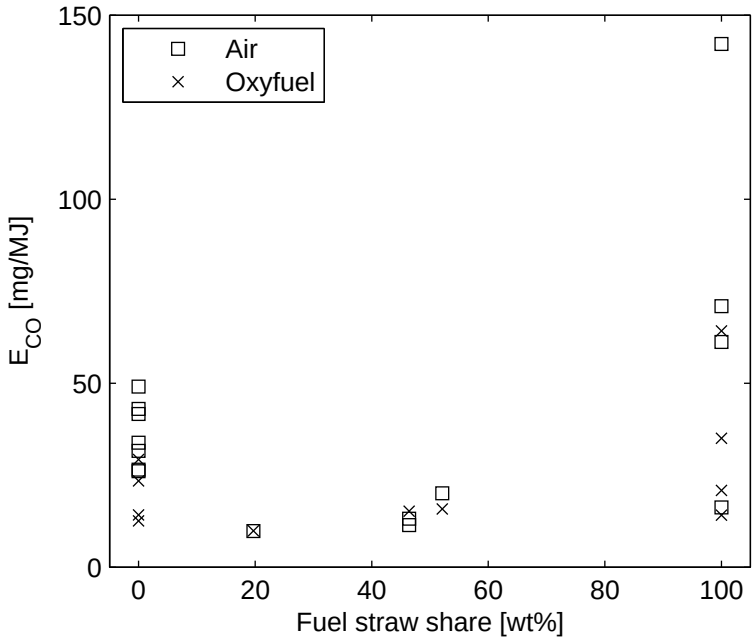


Figure 4.8: CO emission rates as function of fuel straw share. Comparison of air and oxyfuel environments at the reference operating conditions. The error bars correspond to two standard deviations on the LOI analysis.

## 4.3 Emission of NO and $SO_2$ for Varying Fuel Composition

Coal and straw contain significantly different amounts of N and S. Table 4.3 on the next page compares the values for the fuels used during the experimental investigations. The comparison is made both on a mass and an energy basis. Due to the fact that all experiments have been performed at constant thermal input to the reactor and thus varying fuel flows according to the difference in the heating value of coal and straw, the difference between the fuels is most precisely illustrated on an energy basis. Regardless of the reference basis, coal has the highest content of both elements. Especially with respect to sulphur the difference is marked. Based on the differences in fuel composition, the emissions of NO and $SO_2$ during combustion can be expected to differ.

### 4.3.1 NO Emissions

Figure 4.9 on the facing page shows the calculated emission rates of NO as a function of the fuel straw share for both air-firing and oxyfuel combustion. The figure also contains the trend lines for the data which show similar descending slopes. As observed for the coal reference experiments, the change from air com-

Table 4.3: Fuel-N and Fuel-S contents of the applied coal and straw on a mass and energy basis

| | Coal | Straw |
|---|---|---|
| N [wt%, daf] | 1.69 | 0.49 |
| S [wt%, daf] | 0.73 | 0.09 |
| N [g/MJ, LHV] | 0.53 | 0.27 |
| S [g/MJ, LHV] | 0.23 | 0.05 |

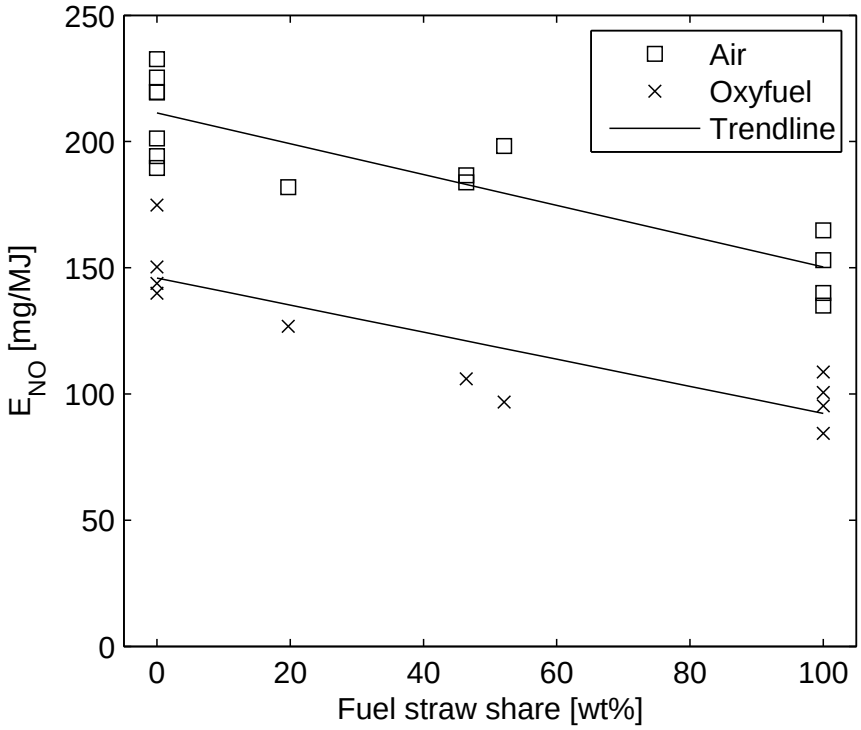


Figure 4.9: Emission rates of NO as a function of the weight based straw share of the fuel. Comparison of air and oxyfuel environments at the reference operating conditions.

Table 4.4: Average reduction of NO emission rate during oxyfuel combustion compared to air-firing

| Fuel | Reduction [%] |
|---|---|
| Coal | 28 |
| 20 wt% straw blend | 30 |
| 50 wt% straw blend | 47 |
| Straw | 34 |
| Overall | 35 |

bustion to oxyfuel combustion leads to reduced NO emission for all fuel blends investigated. Table 4.4 shows the average reductions for the individual fuels and the overall value determined as the average with equal weight to each fuel. The reduced NO emission is suggested to be a consequence of three effects; (1) higher NO levels in the flue gas promoting gas-phase reduction due to NO reacting with other nitrogen-containing species; (2) Increased reduction of NO over char due to significantly higher levels of CO in the flame zone; and (3) the application of a high-$NO_x$ burner in combination with the alterations to the radical pool caused by the significantly increased concentration of $CO_2$. The tendency of decreasing NO emission rates with increasing fuel straw share has likewise been observed during full-scale experiments with up to 20 % co-firing of straw (thermal basis) in air [76, 77].

The difference in emission rates when changing from one fuel to another could be due to the decreasing Fuel-N content when changing from coal to straw and the trends thus include the fact that less N is available for conversion to NO. However, contrary to the full-scale results reported by Pedersen et al. [77], the conversion ratio of Fuel-N to NO increases with increasing straw share, *i.e.* decreasing fuel-N content, as seen in Figure 4.10 on the facing page. This difference is most likely due to the fact that the burners are dissimilar. The full-scale boiler operates with oxidant staging whereas the experimental setup is operated with the burner in high-$NO_x$ mode. With low-$NO_x$ burners it is exploited that volatile-N species are relatively easily reduced to $N_2$ compared to char-N which almost exclusively forms NO at the oxidizing conditions during burnout [70]. The ratio of volatile-N to char-N increases with increasing straw share explaining the reduction in the overall Fuel-N to NO conversion ratio with increasing straw share observed in full-scale. The high-$NO_x$ burner, on the other hand, yields mixing of fuel and oxidant at oxidizing conditions. At these conditions, it is generally known [70] that a decreasing Fuel-N content will yield an increasing Fuel-N to NO conversion. The reaction between NO and N-containing, reducing species in the gas phase, *e.g.* $NH_3$, forming $N_2$ is a second order reaction and thus proceed at a higher rate with an increase in the concentrations of NO and/or $NH_3$ within the flame,

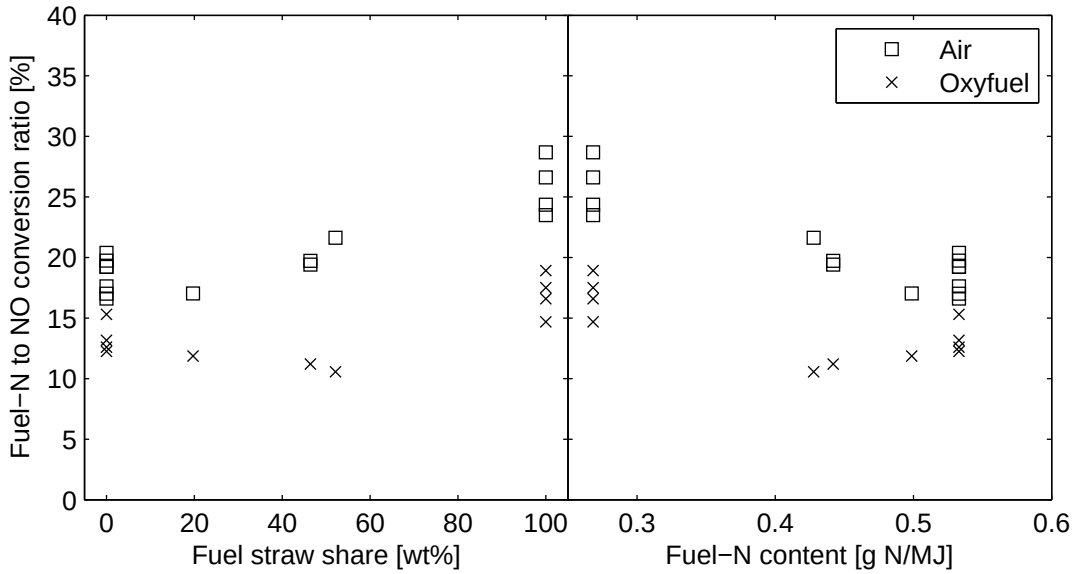


Figure 4.10: Fuel-N to NO conversion ratios as a function of the weight based straw share of the fuel (left) and the N content of the fuel based on heating value (right) - pure straw data to the left and coal data to the right. Comparison of air and oxyfuel environments at the reference operating conditions.

*i.e.* for increasing Fuel-N content. This shift in mechanisms leads to an overall increase in the Fuel-N to NO conversion ratio with increasing fuel straw share. Parameters such as flame temperature and the mixing of fuel and oxidant in the near-burner region which has an impact on *e.g.* the point of fuel ignition, and the release profile of Fuel-N which is dependent on the size of the individual fuel particles could also potentially influence the NO formation. The observed change in flame shape when varying the fuel composition will likewise have an impact on the formation of NO.

### 4.3.2 $SO_2$ Emissions

During combustion, essentially all organically bound sulphur and sulfides (mostly pyrite, $FeS_2$) are released to gas phase as $SO_2$ whereas sulfates are only released during char combustion [69]. Sulphur can also remain in residual ash without being released to gas phase. Depending on the characteristics of the residual ash, primarily the K/Si ratio, the $SO_2$ released to the gas phase can be captured in the ash as sulphate salts of alkali and alkali earth metals or be transported through the boiler in the gas phase due to lack of available alkali. Figure 4.11 on the next page provides a simplified description of the interaction between alkali and alkali earth metals (exemplified by potassium), gas phase $SO_2$, and silica-containing ash particles in the fuel. The figure shows that $SO_2$ competes with ash particles

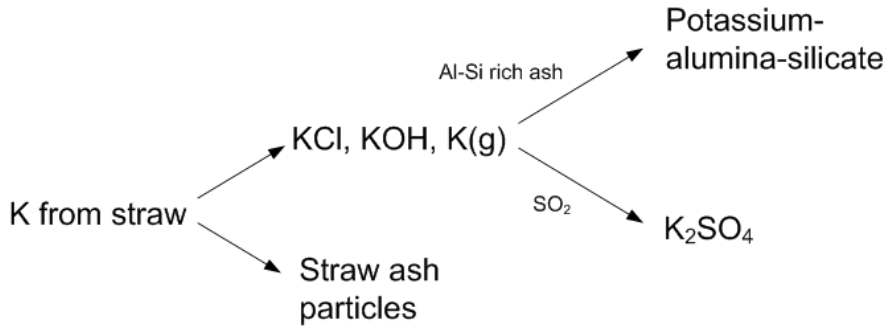


Figure 4.11: Simplified description of the mechanism for potassium transformation during combustion.

rich in Al and Si for potassium released to the gas phase. The emission rate of $SO_2$ is thus directly dependent on the amount of coal ash (Al-Si rich), the amount of S in the fuel (*i.e.* the $SO_2$ concentration during early stages of combustion), and the amount of potassium in the fuel (increases significantly with increasing straw share) [78].

The specific emission of $SO_2$ determined for the four fuel blends in the two reference combustion atmospheres is shown in Figure 4.12 on the facing page. The figure also contains the coinciding trend lines for the air and oxyfuel data and the theoretical emission rate for $SO_2$ determined under the assumption of full conversion of Fuel-S to $SO_2$, see (4.3).

$$E_{SO_2,\,theo} = \frac{\gamma \cdot M_{SO_2}}{LHV} \tag{4.3}$$

where $\gamma$ is the molar content of S in the fuel [kmole/kg], $M_{SO_2}$ is the molar mass of $SO_2$, and LHV is the lower heating value of the fuel. The theoretical line is not linear since both $\gamma$ and LHV are linear functions (weighted averages) of the fuel straw share.

The measured emission rate of $SO_2$ shows a linearly decreasing trend with increasing fuel straw share. For all four fuel blends the measured emission lies below the theoretical curve emphasizing the retention of sulphur in solid phases, fly ash and deposits, within the system.

The ratio between the measured $SO_2$ emissions and the theoretical curve, *i.e.* the Fuel-S to $SO_2$ conversion ratio, is seen in Figure 4.13 on the next page. Contrary to Figure 4.12 on the facing page we can observe a non-linear trend with respect to the fuel straw share. However, when plotting the conversion ratio against the Fuel-S content on an energy basis (right-hand-side of Figure 4.13) a linear correlation is observed. Due to the different heating values of the applied coal and straw and the fact that the thermal input to the burner has been kept

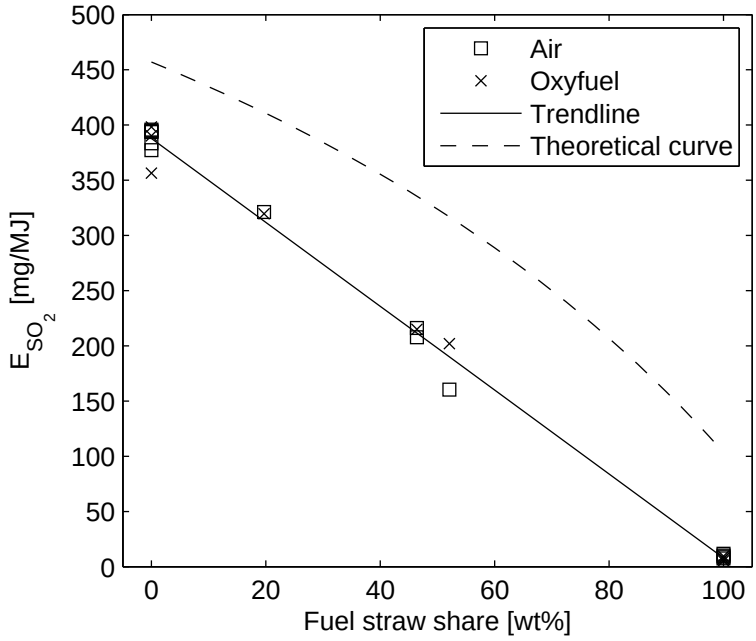


Figure 4.12: Emission rates of $SO_2$ as a function of the weight based straw share of the fuel. Comparison of air and oxyfuel environments at the reference operating conditions.

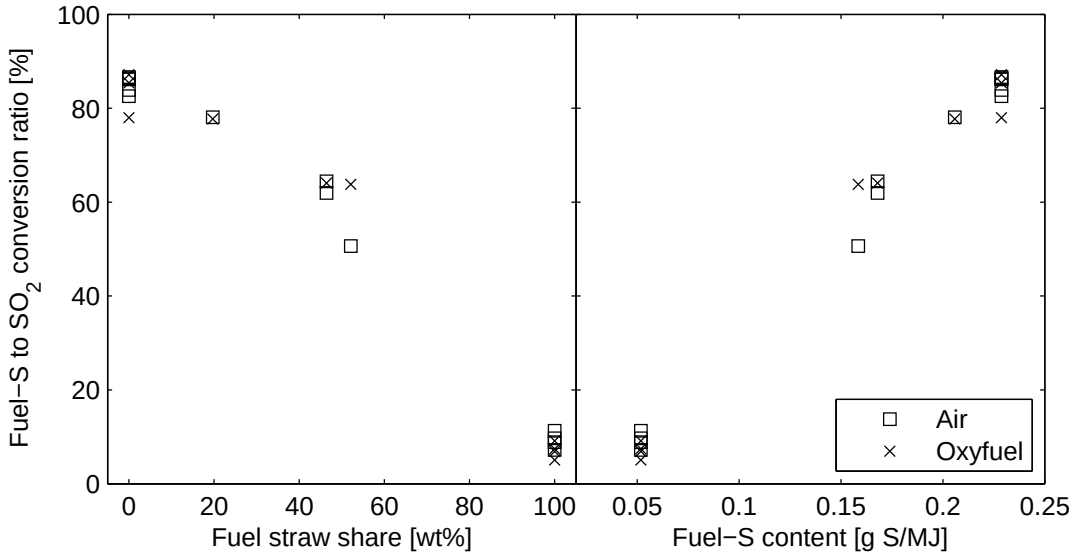


Figure 4.13: Fuel-S to $SO_2$ conversion ratios as a function of the weight based straw share of the fuel (left) and the S content of the fuel based on heating value (right) - pure straw data to the left and coal data to the right. Comparison of air and oxyfuel environments at the reference operating conditions.

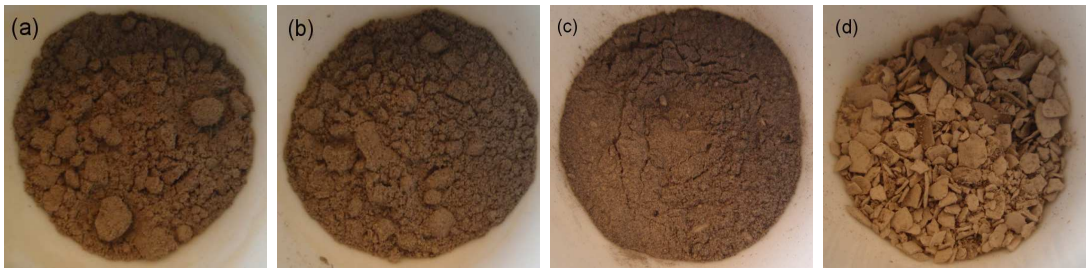


Figure 4.14: Appearance of ash samples collected from setup. (a) combined cyclone and filter ash samples from combustion of the 20 wt% straw blend. (b) combined cyclone and filter ash samples from combustion of the 50 wt% straw blend. (c) cyclone ash from combustion of pure straw. (d) filter ash from combustion of pure straw. Ash from combustion of pure coal resembles the samples for the coal-containing blends. Each picture has dimension of 20x20 mm.

constant irrespective of the fuel type a comparison on energy basis is more suited than the typically applied mass basis.

The variation in the Fuel-S to $SO_2$ conversion ratio with fuel composition is mainly due to differences in the composition of the fuel ash. The K/Si ratio in the fuel is a linear function of the fuel straw share. For pure coal and pure straw the ratios are 0.05 and 0.79, respectively. As expected from the mechanism in Figure 4.11, the $SO_2$ emission thus decreases with increasing fuel straw share both as a consequence of an increased K/Si ratio enabling formation of potassium sulphate and due to decreasing Fuel-S content. The mechanism is further investigated in relation to the treatment of the quality of fly ash in Section 4.4.

## 4.4 Ash and Deposits – Formation and Composition

The change in fuel characteristics when co-firing coal with increasing shares of straw will have an impact on the formation and composition of the produced fly ash and the deposits formed within the furnace.

### 4.4.1 Visual Appearance and Physical Properties of Fly Ash and Deposit Samples

The main part of the fly ash collected during the experiments is contained in the cyclone and filter ash fractions as was seen in Figure 2.10 on page 32. Figure 4.14 shows the appearance of these samples. The ash samples generally have a greyish-brown colour indicative of the high burnout efficiency in the experiments and resemble well ash collected in full-scale plants burning coal. The ashes from combustion of pure straw deviates from the remaining fuels in both colour and

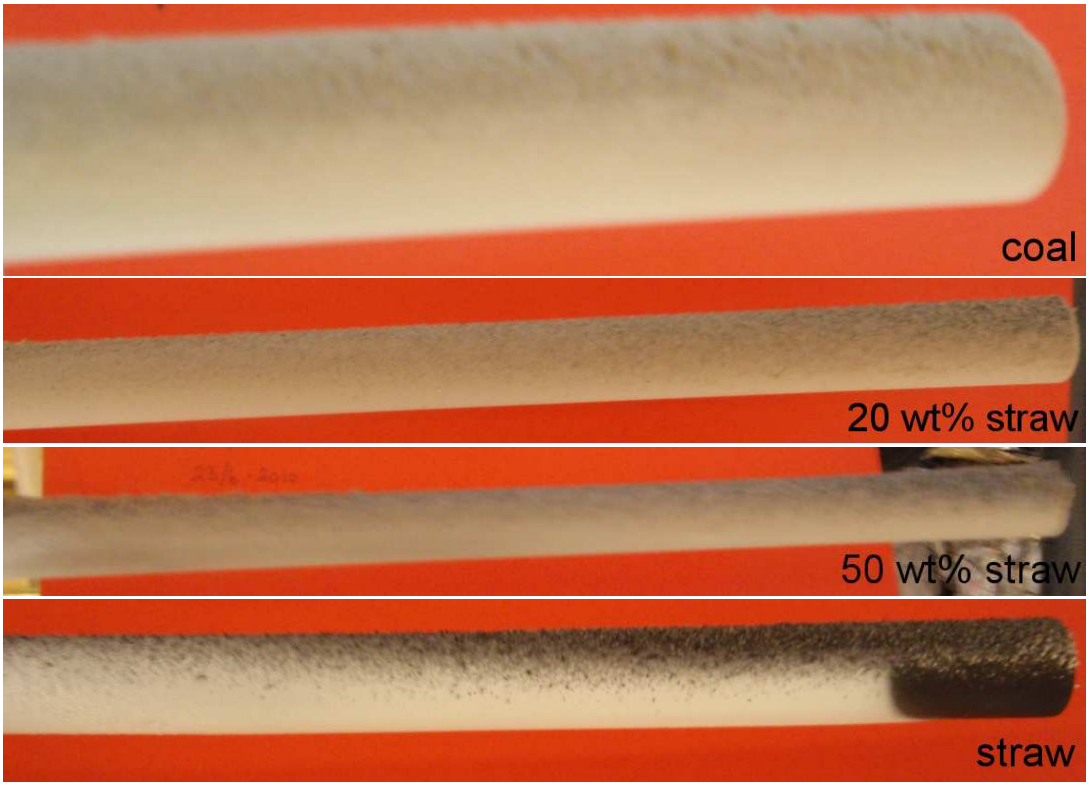


Figure 4.15: Side view of deposits. The deposit probe has a diameter of 16 mm. The top of the probe faces in the upstream direction,*i.e.* the flue gas flow is downwards in the pictures. Pictures have been recorded with different zoom.

morphology. The cyclone ash is more loose and flows easier than the combined ashes from combustion of the coal-containing fuels. It likewise has a stronger tendency to become static electric than the ashes from the coal-containing fuels. The filter ash, on the other hand, is very brittle and significantly lighter in colour. The filter ash is presumably formed from aerosols in the flue gas or from condensation of gas phase species on the filter cake due to the low temperature (about 100 °C) at the filter.

Figure 4.15 illustrates the visual appearance of the deposits collected for each fuel. Only one example is shown for each fuel as the change in oxidant type did not influence the visual and physical appearance of the deposits. The colour of the deposit from pure coal combustion is light greyish-brown and the upstream part is very loose and powdery, and easy to remove from the probe. The downstream part is a thin, homogeneous layer which clearly consists of condensed matter. The deposits from combustion of the 20 and 50 wt% straw blends differ from the pure coal deposit only with respect to the thickness of the upstream layer. As seen from the picture of the 50 wt% straw blend, a thicker layer of

ash particles builds up at the ends of the probe in the upstream direction. The uneven distribution across the probe is most likely due the swirling motion of the flame moving ash particles from the centre of the reactor towards the walls. The flue gas temperature variation across the reactor at the deposit probe position in port 7 is assumed to be negligeble due to the flat profiles measured in port 5 for both oxidant types. The visual and physical appearance of the deposit from pure straw combustion deviates significantly from the remaining deposits shown in the figure. The downstream part is completely white which is indicative of a high content of salts. The upstream part is hard, almost completely sintered, and more difficult to remove from the probe than the remaining deposits which were all powdery. At the same time, the colour is darker than for the coal-containing fuel blends. The dark colour is typical for deposits containing $SiO_2$. As was the case for the 50 wt% straw blend the upstream deposit shows an unequal weight distribution across the probe with higher deposition towards the ends (reactor walls). The deposit thickness is however smaller for the pure straw case since the sintering acts to reduce the porosity of the deposit.

Based on the visual appearance of the deposits, co-firing up to 50 wt% straw should not induce problems with respect to the removal of deposits within full-scale boilers. However, firing of pure straw would most likely necessitate an increased frequency in soot-blowing.

### 4.4.2 Deposit Fluxes

Table 4.5 on the facing page compares the calculated deposit fluxes for each fuel/oxidant combination investigated. Contrary to the observation for the coal reference experiments in Section 3.3.2, oxyfuel combustion yields higher deposit fluxes than combustion in air for the straw-containing fuels. If the difference is larger than the experimental uncertainty, the most probable reason for the shift in the deposition propensity is a change in the sticking efficiency. Due to the presence of straw ash particles which generally have lower deformation temperatures than ash from pure coal combustion [79] the higher flue gas temperatures during oxyfuel combustion than during combustion in air for the same fuel will increase the stickiness of the deposit and ash particles.

A change in the fuel straw share for each of the combustion atmospheres induces no difference in the deposit flux for the blends, whereas pure straw combustion yields marked increases in deposition rates. This can also be attributed to the differences in the sticking probability with the change in the chemical composition of the ash particles. For coal-containing fuels the majority of the ash particles consist of alumina-silicates which have higher melting point temperatures than the K-silicates formed in pure straw ashes [80]. The salts which constitute a significant part of the straw ashes have even lower melting points than the silicate-containing compounds. A repetition of deposit sampling during oxyfuel combustion of pure straw have illustrated the effect of the flue gas tem-

Table 4.5: Average deposit fluxes as well as flue gas and deposit probe temperatures for combustion of coal, straw, and their blends in air and oxyfuel atmospheres for an exposure time of 2 hr.

| Fuel | Oxidant | Upstream [g/m$^2$·hr] | Downstream [g/m$^2$·hr] | Average [g/m$^2$·hr] | $T_{probe}$ [°C] | $T_{FG}$ [°C] |
|---|---|---|---|---|---|---|
| Coal | Air | 107 | 11 | 59 | 500 | 900 |
| Coal | Oxy 30 | 75 | 3 | 39 | 500 | 950 |
| 20 wt% straw | Air | 64 | 6 | 35 | 500 | 940 |
| 20 wt% straw | Oxy 30 | 90 | 2 | 46 | 500 | 970 |
| 50 wt% straw | Air | 56 | 9 | 32 | 500 | 920 |
| 50 wt% straw | Oxy 30 | 89 | 4 | 46 | 500 | 960 |
| Straw | Air | 102 | 15 | 59 | 500 | 940 |
| Straw[a] | Air | 153 | 18 | 86 | 500 | 910 |
| Straw | Oxy 30 | 194 | 12 | 103 | 500 | 950 |
| Straw | Oxy 30 | 219 | 17 | 118 | 500 | 995 |

[a] 4.3 hr exposure time

perature. From the data in Table 4.5 it is seen that an increase in the flue gas temperature of about 50 °C yields a 10 % increase in deposit flux.

Prolonged exposure time (4.3 hr as opposed to 2 hr) also leads to an increase in the time-averaged flux for combustion of straw in air. This is due to the fact that the increasing thickness of the deposit leads to a higher surface temperature due to the insulating effect of the underlying deposit layer. The temperature increase at the surface consequently increases the sticking efficiency of the deposit. The deposition rate will thus increase over time.

Increased deposit formation has been observed in full-scale (MKS1) for co-firing of 10 % straw (energy basis). Some slagging problems were seen when 20 % straw was co-fired [81]. However, in another boiler (SSV4), no fouling problems were observed within the first two years of operation with co-firing up to 20 wt% straw with coal and soot-blowing was not increased. [76]

### 4.4.3 Chemical Composition of Fly Ash and Deposit Samples

In addition to the differences in physical properties of the ashes and deposits the chemical composition of the samples is of great importance with respect to characterizing the effect of fuel change. Figure 4.16 on the next page shows the variation in the ash forming elements for each fuel blend. The values for the 20 and 50 wt% straw shares are weighted averages of the compositions of the pure

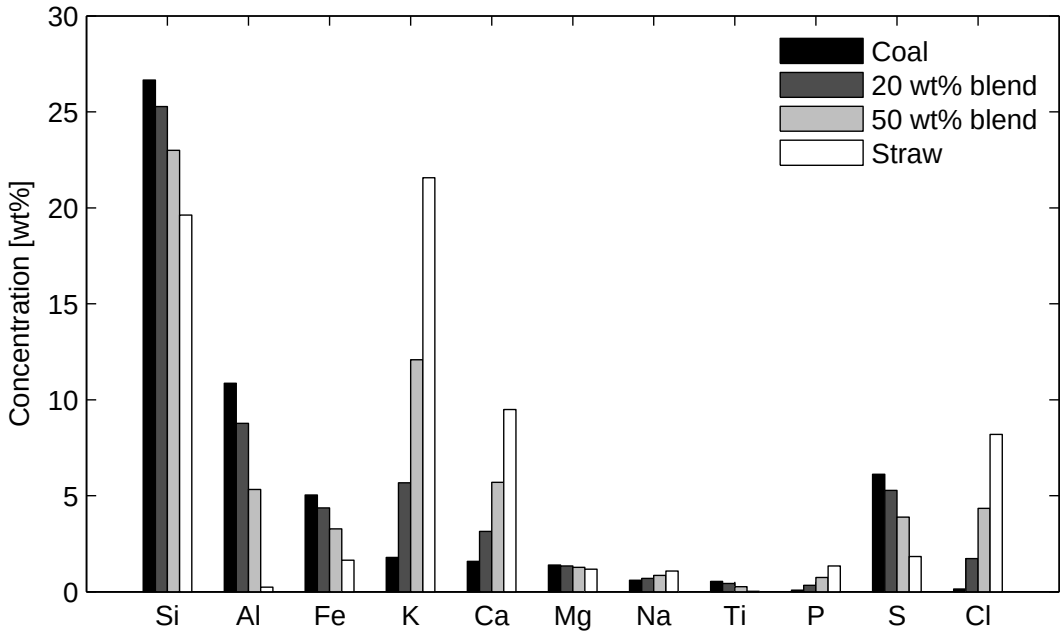


Figure 4.16: Comparison of calculated fuel ash compositions for the four different fuels. The concentrations are determined based on an analysis for the inorganic elements in the fuel sample. The values for the 20 and 50 wt% straw shares are weighted averages of the compositions of the pure fuels.

fuels. The most distinct differences are concerned with the Al, K, Ca, S, and Cl contents. These elements are important when considering the corrosion potential of the ashes and deposits. High concentrations of K, Cl, and S compared to Si and Al will increase the corrosion potential of the solid phase.

Figures 4.17 to 4.20 show the corresponding elemental analysis for the collected fly ash and deposit samples. Cl is shown as the result from the analysis of water soluble species, as this is the same as the total content. The analysis method for water soluble Cl has, however, a lower detection limit. For the pure coal experiments the deposit composition is from the analysis of the combined sample from the upstream and downstream parts of the deposit probe. For the remaining fuel/oxidizer combinations these two samples have been analysed separately.

As described in Section 3.3.2 the differences between fuel ash, fly ash, and deposits for pure coal combustion in both air and the reference oxyfuel atmosphere are insignificant. The high Fuel-S to $SO_2$ conversion ratio of about 85-90 % is the most striking for these data. In fact, for all of the investigated fuel blends, no significant differences between air-firing and oxyfuel combustion can be determined.

Adding 20 wt % straw to the fuel blend, see Figure 4.18, yields a similar low capture rate of S in the fly ash, see *e.g.* Figure 4.23 on page 104, but an increased

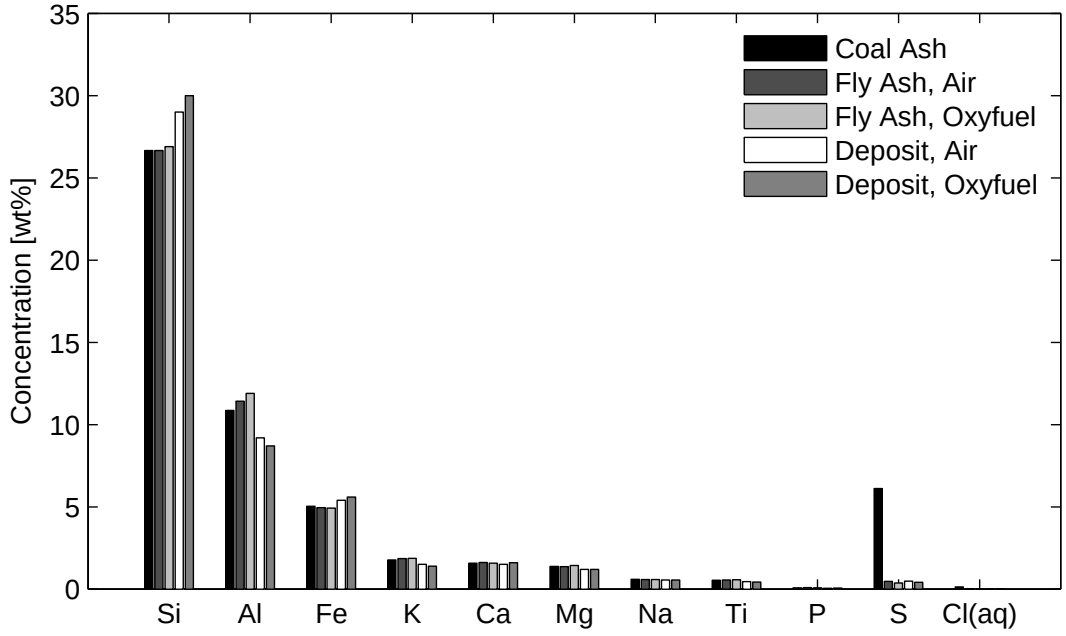


Figure 4.17: Comparison of fly ash and deposit compositions for coal combustion in air and 30% $O_2/CO_2$ at the reference conditions.

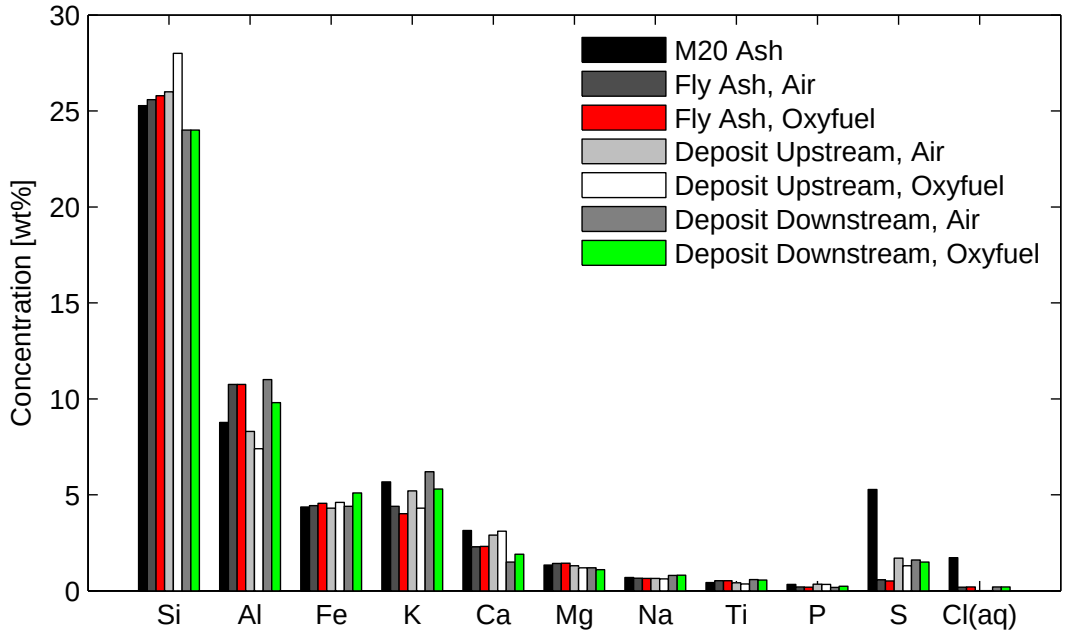


Figure 4.18: Comparison of fly ash and deposit compositions for combustion of the 20 wt % straw/coal blend in air and 30% $O_2/CO_2$ at the reference conditions.

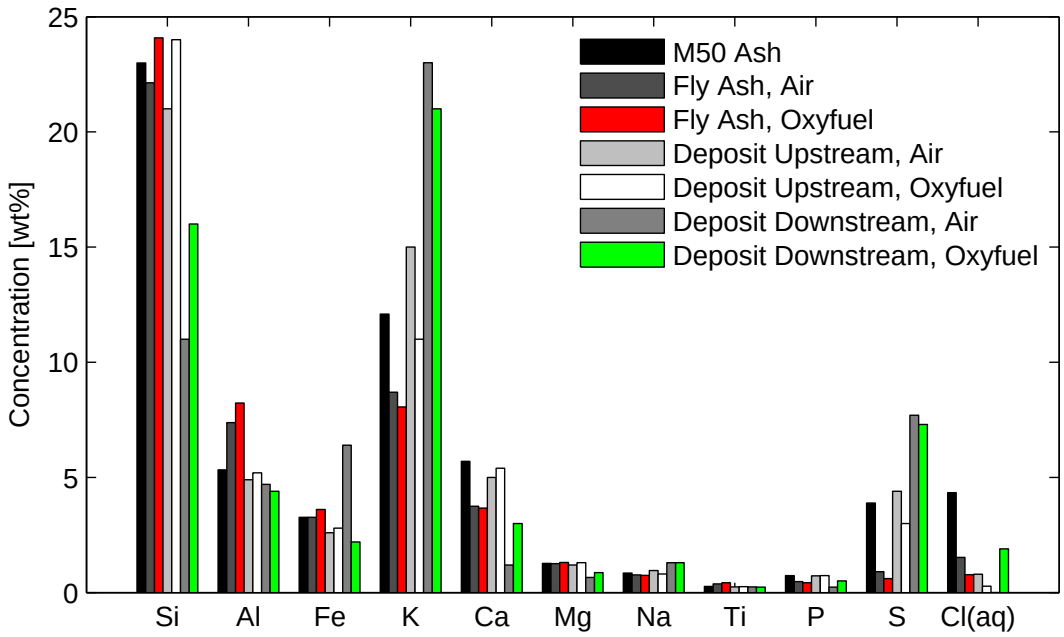


Figure 4.19: Comparison of fly ash and deposit compositions for combustion of the 50 wt % straw/coal blend in air and 30% $O_2/CO_2$ at the reference conditions. Cl data for the downstream deposit sample from combustion in air is not available. However, the level is expected to be similar to the corresponding oxyfuel sample.

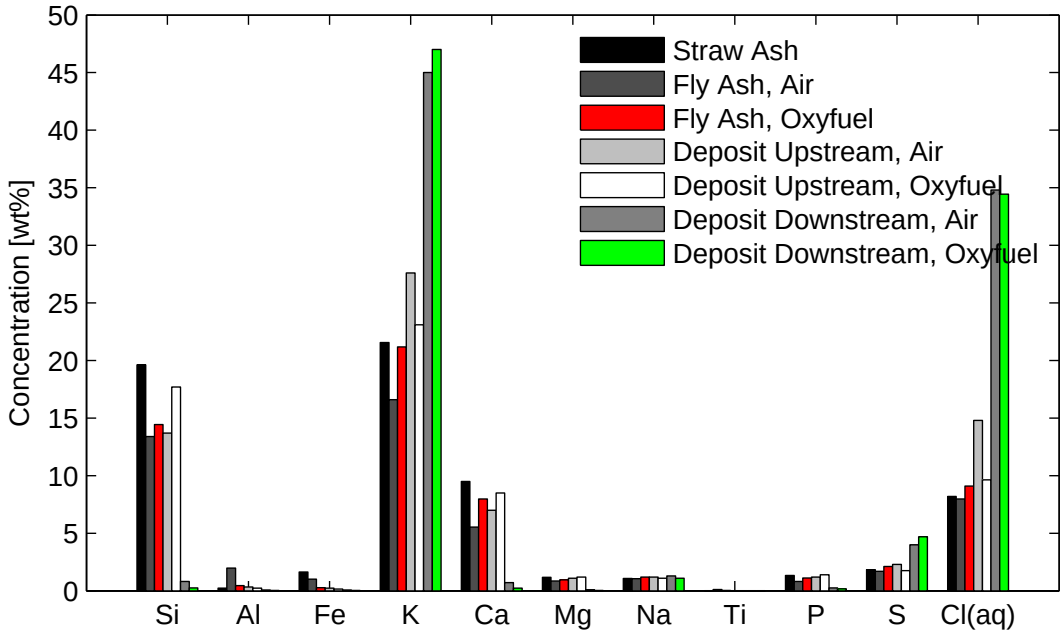


Figure 4.20: Comparison of fly ash and deposit compositions for straw combustion in air and 30% $O_2/CO_2$ at the reference conditions. Experiments SA04_ADT and SO04_ADT.

retention in the entire deposit even though the Fuel-S content has decreased. Since no Cl is present in the fly ash, it is unlikely that the increased S content in the deposit is due to on-site sulphation of KCl. Instead, capture of sulphur by Ca could explain the observation. Cl is absent in the deposits indicating that all K is bound in alumina-silicates or as $K_2SO_4$. The fuel-bound Cl is thus released to gas phase as HCl or $Cl_2$. K in the deposit is equally distributed between the upstream and downstream samples and at the same level as for the fly ash and the fuel indicating that all particles depositing on the probe have similar composition. The figure does not show the distribution between K bound in alumina-silicate compounds and K found in salts. This has a significant impact on the characteristics of the samples and will be treated later in this section. The higher concentration of Al in the downstream deposit samples compared to the upstream samples is not immediately explainable as this element is expected to mainly be associated with large residual ash particles. These particles would primarily deposit on the upstream part of the probe. The trend with higher concentration on the upstream part of the probe compared to the downstream part is seen for both Si and Ca which likewise are assumed to mainly be present in large ash particles due to their low volatility. However, the Si concentration in the downstream deposit is still very high indicating capture of residual ash particles on the downstream part of the probe due to recirculation zones.

The presence of 50 wt % straw in the fuel blend significantly alters the composition of the fly ash and deposit samples compared to the fuels with higher coal-share as seen in Figure 4.19. The ratio of K to Si (and Al) has increased significantly and especially the deposits show high retention of K, most pronounced in the downstream samples indicating condensation of K-rich salts, mostly sulphates which the correspondingly high S contents imply, but also chlorides unlike the case for the fuels with lower straw share. Condensation of Na-rich salts on the downstream side of the probe is likewise observed. Contrary to the observation for the previously described fuel, on-site sulphation of the deposit may have occured during the sampling period implied by the difference in both the S and Cl contents of the fly ash and deposit. In fact, even though the K content of the fly ash has increased the concentration of S in the fly ash is still low, indicating K being bound mainly in silicate compounds or as KCl. The Cl concentration in the fly ash and the deposit samples has increased compared to the 20 wt% straw blend samples (from about 0.1 to about 1 %). No analysis with respect to Cl exists for the downstream deposit sample for air combustion, however, the Cl concentration is assumed to be similar to the oxyfuel sample. As was seen for the 20 wt% straw blend the Al concentrations in both the upstream and downstream deposit samples are similar. However, the Si concentration in the downstream deposit samples is significantly lower than in the upstream samples which has the same Si content as the fly ash. A similar trend is seen for the distribution of Ca between the upstream and downstream of the deposit probe. The very high Fe concentration in the downstream deposit sample for the air experiment is most

likely due to contamination with Fe from the probe during sample collection. This contamination could have a minor impact on the measured concentrations of the remaining elements, however no changes to the conclusions would be made.

Combustion of pure straw leads to fly ash and deposits with a relatively high corrosion potential. Especially the downstream deposits consist almost solely of KCl, and $K_2SO_4$ in smaller amounts due to the very low Fuel-S content compared to the fuel blends containing coal, see Figure 4.20. Less on-site sulphation of the upstream deposit is likewise a result of the lower flue gas concentration of $SO_2$. No significant difference in the concentration of S in the fuel ash, fly ash and upstream deposits can be observed. The corresponding levels of Cl are likewise similar. The release of Cl to the gas phase is thus significantly reduced compared to combustion of coal-containing fuel blends, see also Figure 4.23 on page 104. The near absence of Al means that K-silicates with lower melting points than K-aluminium-silicates are formed. Additionally, Ca competes with K for the Si and thus increases the ratio of water soluble K to total K in fly ash and deposits [80].

In summary, increasing the straw share of a coal/straw blend will induce significant changes to the composition of fly ash and deposits. Most pronounced is the increasing corrosion potential of both ash and deposits due to significant increases in the K and Cl contents. Additionally, the on-site sulphation of deposits is likewise significantly affected by the fuel type. Figure 4.21 on the facing page illustrates these findings by directly comparing the concentrations of K, Cl, and S in deposits and fly ash for the investigated fuel/oxidizer combinations. The figure shows both the total contents of each element and the concentration of the elements in water soluble form. The total K and Cl contents are seen to be equally distributed between the fly ash and the upstream part of the deposit. Increased levels in the downstream part of the deposit compared to the upstream sample is likewise observed indicating that the downstream part of the deposit is mainly made up of aerosols. A comparison of the total and water soluble concentrations of K shows a tendency for the deposits to be enriched in K-containing salts when the fuel contains both straw and coal. This trend could be due to an over representation of KCl aerosols being deposited compared to the amount found in the fly ash. Subsequent on-site sulphation of KCl decreases the Cl concentration in the deposit and increases the concentration of S compared to the fly ash. The sulphur data confirms this as both blends show significantly increased concentrations in the deposits whereas both pure coal and pure straw yield an equal distribution between ash and deposit. A maximum in the sulphur retention in the deposit is seen at 50 wt % straw in the fuel blend due to the combined effect of high alkali and alkali earth metals present in the deposit from the straw and high levels of sulphur available from the coal. The trend is present both at the upstream and downstream of the deposit probe.

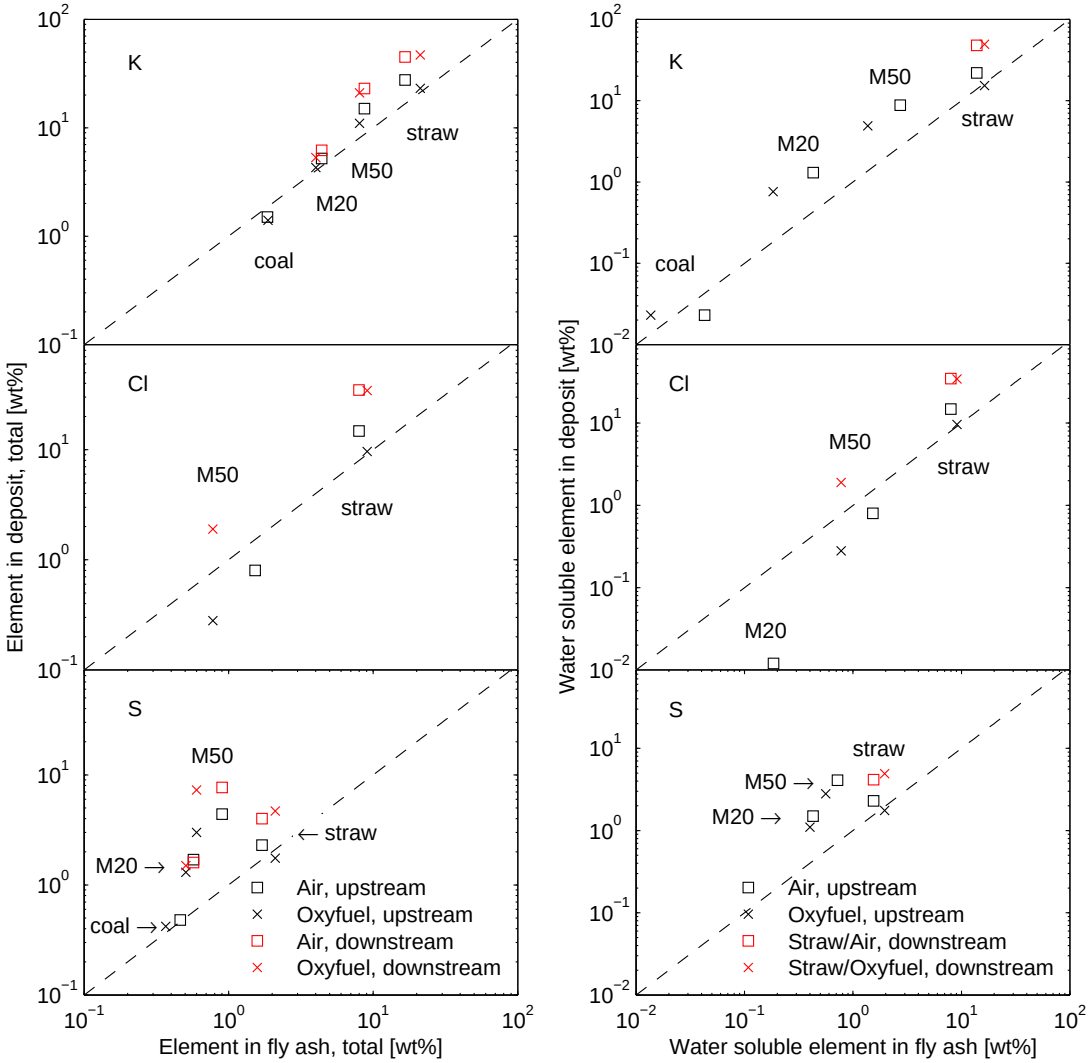


Figure 4.21: Comparison of K, Cl, and S in fly ash and deposits for the four fuel blends. Data shown for air and oxyfuel combustion at the reference operating conditions. Left: total contents, right: water soluble concentrations. The Cl data for the pure coal and 20 wt% straw blend which are below the detection limit are not shown. Water soluble K and S analysis does only exist for the downstream deposit samples for straw as fuel. Water soluble S has not been measured for the pure coal deposits but can be assumed to be equal to the total content.

The corrosive potential of fly ash and deposits is primarily determined by the presence of chlorides and sulphates of alkali and alkali earth metals. Figure 4.22 on the next page shows the concentrations of water soluble K, Ca, Cl, and S in the fly ash samples for each fuel/oxidant combination investigated. The concentration of water soluble K, Cl, and S in the ashes follows the trend from the total contents. With up to 20 wt% straw in the fuel blend only a small increase in salts in the ashes occurs. However, increasing the straw share above 20 wt% leads to significant increases in the alkali salt contents. This indicates surplus of primarily K from the straw compared to the alumina-silicates from the coal ash. The K is released to the gas phase due to the high temperatures in the flame and is thus available for condensation as sulphates or chlorides on ash particles or for reaction with alumina-silicates. Even though the total amount of Ca in the straw fuel and fly ashes is significantly higher than for coal ash the amount found in the fly ash in water soluble form is lower than for the experiments with coal-containing fuels. This could be a consequence of the limited solubility of $CaSO_4$ in water. However, a parallel analysis at a liquid-to-solid (LS) ratio of 50 instead of 100 yielded a higher concentration of $Ca^{2+}$ in the solute and a value well below the solubility of $CaSO_4$ in water of about 2000 mg/L (600 mg $Ca^{2+}$/L) [82]. The results thus seem physically sound even with the solubility limitations occuring due to the presence of additional salts in the solution.

The requirements for fly ash used in concrete are less than 0.1 wt% Cl, less than 3 wt% S measured as $SO_3$, and less than 5 wt% total alkali [63]. For the fly ashes collected from the experiments it is seen that the requirement regarding Cl cannot be fulfilled unless for pure coal combustion. At 20 wt% straw in the fuel blend the Cl content in the fly ash is 0.2 wt%. The limits for total alkali (sum of K and Na) and sulphur are not exceeded for fuel straw shares up to 20 wt%. The relatively large capture efficiency of Cl in the swirl burner setup deviates significantly from full-scale boilers as discussed in Section 4.5.

Figure 4.23 on page 104 shows the retention in water soluble form of K, Ca, Cl, and S fed with the fuel in the fly ash. The retention shows similarly increasing trends for K, Cl, and S as did the absolute concentrations. Within the experimental uncertainty, full capture of both S and Cl is obtained by the fly ash obtained by combustion of pure straw. The lack of complete consistence between this figure and the Fuel-S to $SO_2$ conversion ratios shown in Figure 4.13 on page 91 is due to the small error on the mass balances. The K and S data confirms the competition between the capture of K in water insoluble alumina-silicates when coal ash is present and the increasing capture efficiency in water soluble sulphates (and chlorides) when the fuel straw share increases, as discussed in relation to Figure 4.11 on page 90.

Ca retention in water soluble form exhibits the opposite trend of the other elements in that almost none of the fuel-bound Ca is found in water soluble form in the fly ash for pure straw combustion whereas about 50 % of the Ca fed with the pure coal is retained in salts. The residual ash from straw combustion consists

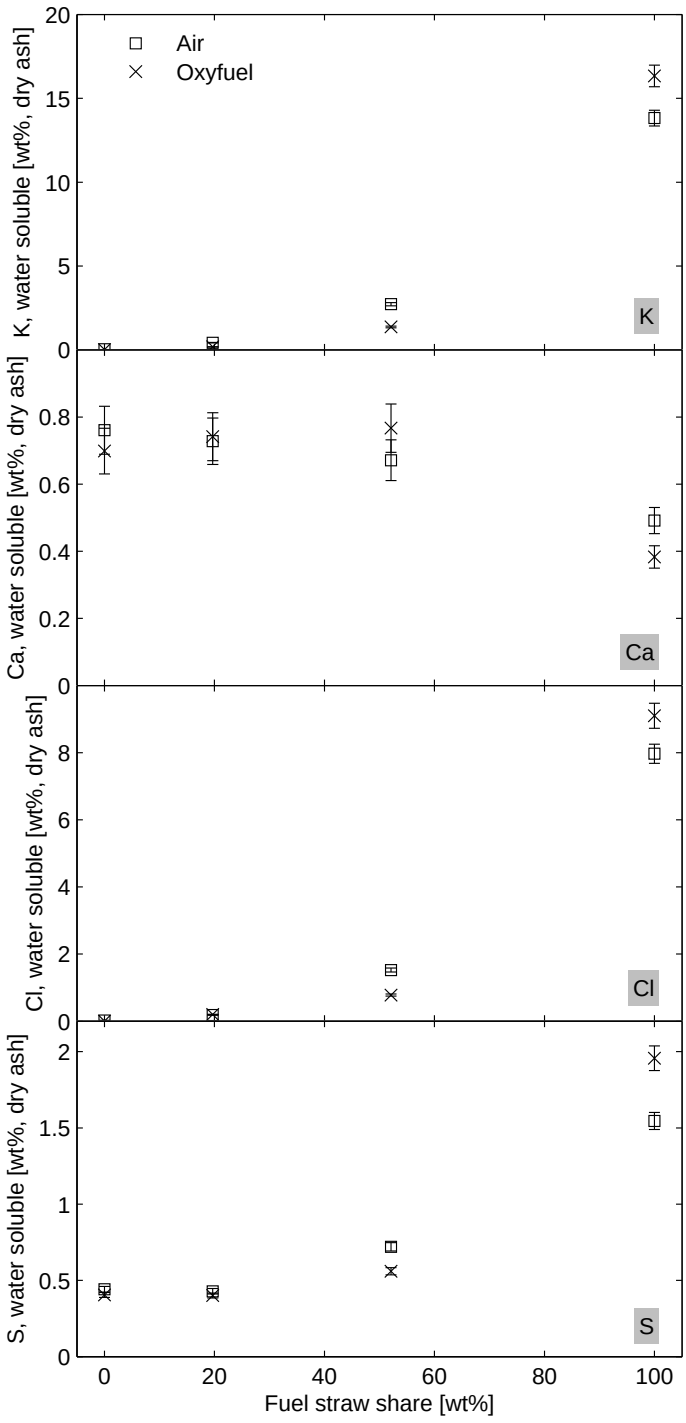


Figure 4.22: Concentration of water soluble K, Ca, Cl, and S in fly ash as a function of the weight based straw share of the fuel. Comparison of air and oxyfuel environments at the reference operating conditions. The error bars correspond to two times the standard deviation on the ash analysis. The analysis have been performed with liquid-to-solid ratios of 100.

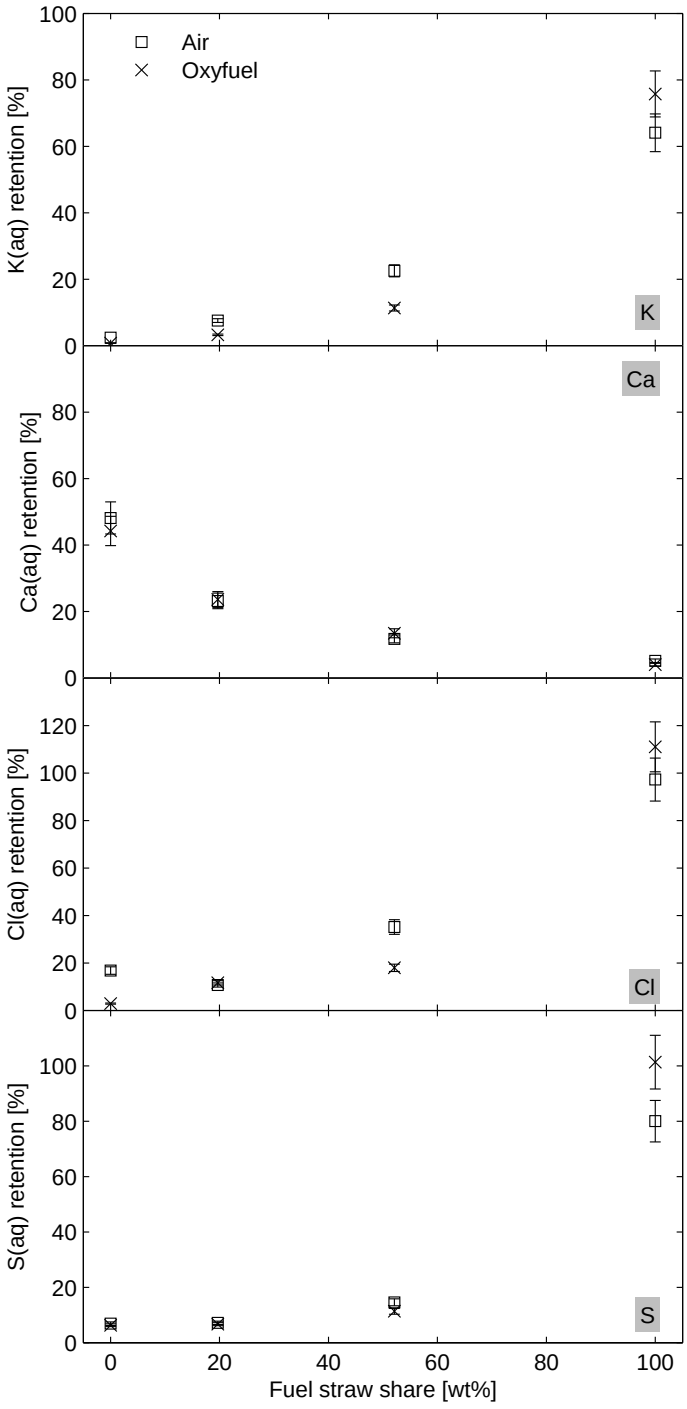


Figure 4.23: Capture of K, Ca, Cl, and S in water soluble form in fly ash as percentage of the amount of the element fed with the fuel and as a function of the weight based straw share of the fuel. Comparison of air and oxyfuel environments at the reference operating conditions. The error bars correspond to two times the standard deviation on the calculated value determined from the law of propagation of uncertainties.

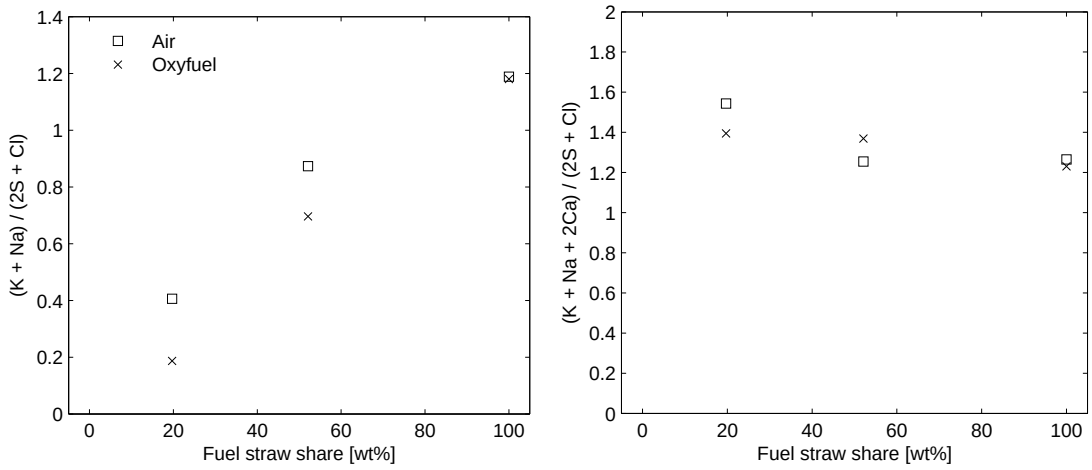


Figure 4.24: Stoichiometric ratio of water soluble alkali and alkali earth metals to sulphur and chloride in fly ashes as function of the fuel straw share.

primarily of Ca-Si compounds. As mentioned earlier, Ca competes with K for Si making the straw ash significantly less efficient for self-retention of gas-phase K in a water insoluble form compared to coal ash which has a higher Si and a lower Ca content. This is evident from the K data as between 60 and 80 % of the K fed with the straw is bound as salts in the ash, see Figure 4.23. The surplus of alkali metals in the straw ash (20 %) to form sulphate and chloride salts is seen in the left-hand-side of Figure 4.24. The figure shows that there is a deficit of water soluble alkali in the fly ash from combustion of the straw/coal blends to the amount of S and Cl. The right-hand-side of Figure 4.24 shows that the surplus of S and Cl is bound to alkali earth metals (represented by Ca).

## 4.5 Comparison to Full-Scale data

### 4.5.1 Comparable Fuels

Co-firing of straw and coal of the same type as utilized in the present work has been performed at the Studstrup power plant (SSV4) in Denmark as reported by Sander and Wieck-Hansen [78]. Fly ash was sampled from the flue gas duct upstream of the electrostatic precipitator and analysed for the content of water soluble elements (K, Na, Ca, Mg, Cl, P, and S). Between 0 and 20 wt% straw was fired and the boiler load was varied in the range 30-100 %. Figure 4.25 on the following page shows a comparison of the concentration and percentage retention of water soluble K and Cl in the ash samples and the data obtained in the present experiments. Due to the large influence of the weather conditions during the harvest season, the content of potassium and chlorine in straw varies significantly over the years. The potassium content of the straw used in this work

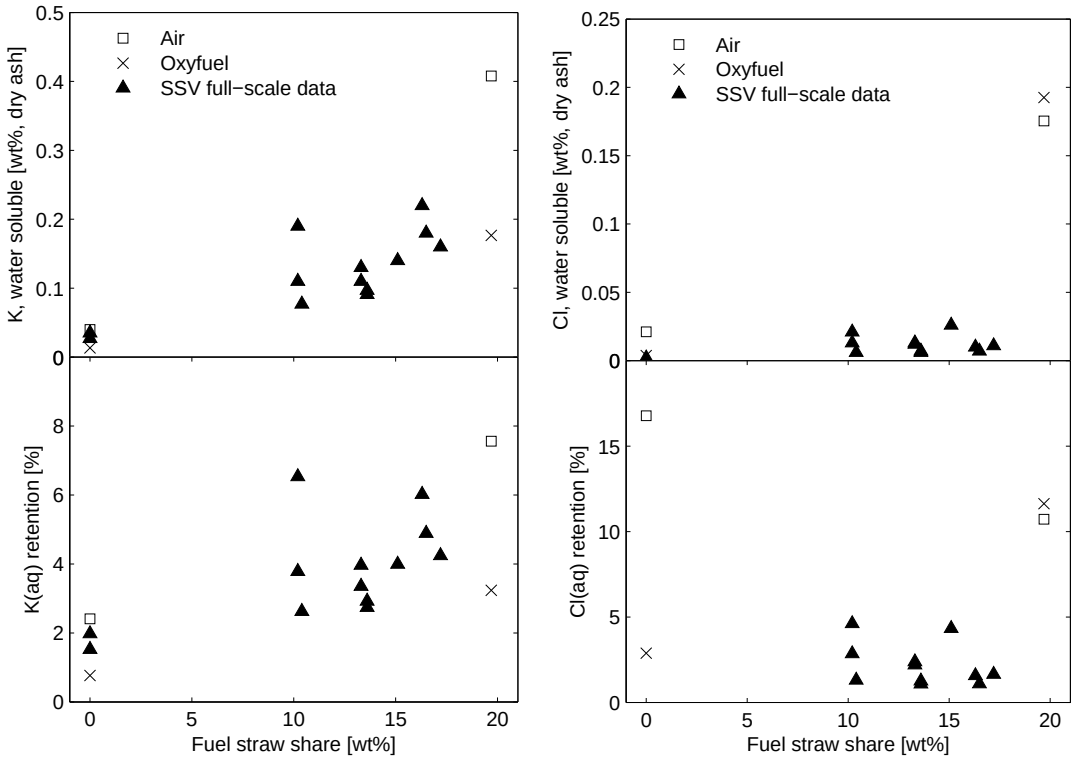


Figure 4.25: Concentration of water soluble K and Cl in fly ash and the percentage share of water soluble K and Cl in fly ash compared to K and Cl fed with the fuel as a function of the weight based straw share of the fuel. Comparison of air and oxyfuel environments at the reference operating conditions with full-scale data from Studstrup power plant (SSV) for comparable fuels (straw and Colombian coal (COCERR)).

Table 4.6: Characteristic fuel parameters and their importance in ash transformations during coal/straw co-firing

| Fuel ash | Possible implication during ash transformation |
|---|---|
| K | Amount of K ending up in fly ash |
| K/Si | Availability of silicate and aluminosilicate to react with potassium salts |
| K/(S+Si) | Availability of silicate and aluminosilicate to react with potassium salts, and the extent of potassium sulphation |
| S/Cl | The fraction of potassium in form of $K_2SO_4$ and KCl |

is about 2/3 of the amount in the full-scale experiments (1 wt% and 1.5 wt%, respectively). Despite this difference, a good agreement between the full-scale and semi-technical scale data is observed with respect to the K content. The swirl burner air data generally yields higher levels of water soluble K than full-scale and the oxyfuel data are situated in the lower range of the full-scale data. This could suggest that the lower flame and flue gas temperatures obtained in the swirl burner during air-firing compared to full-scale flames reduces the reactions between K in the gas phase and Al-Si compounds in the ash particles. Better agreement is thus seen for oxyfuel combustion due to the higher temperatures obtained here. The retention of Cl in the fly ash from the full-scale boiler is relatively low compared to the fly ash obtained in the present work. This supports the assumption of decreased retention of potassium in alumina-silicates in the small-scale setup. Another explanation to the discrepancy could be differences in the degree of sulphation of the fly ash. The following section provides a more general comparison of the fly ashes obtained in the present work to full-scale experiments with co-firing of coal and biomass (primarily straw).

### 4.5.2 General Comparison of Fly Ash Quality to Full-Scale Co-Firing Experiments with Air as Oxidant

Zheng et al. [80] made a detailed study of the transformation of ash during co-firing of coal and straw. The study included lab-scale combustion experiments in an entrained-flow reactor and a literature review of full-scale experiments primarily performed on Danish power plants. The study considered the interaction effects occurring between coal and straw ashes and the resulting effect on the fly ash. Zheng et al. [80] identified a number of characteristic fuel parameters which can be used to predict the quality of the fly ash. The parameters and their importance during ash transformations are given in Table 4.6.

Figure 4.26 on the following page shows the linear dependence between potassium in the fuel and the total amount of potassium in the fly ash for both the data shown in [80] for bituminous coals and from this work. A relatively good

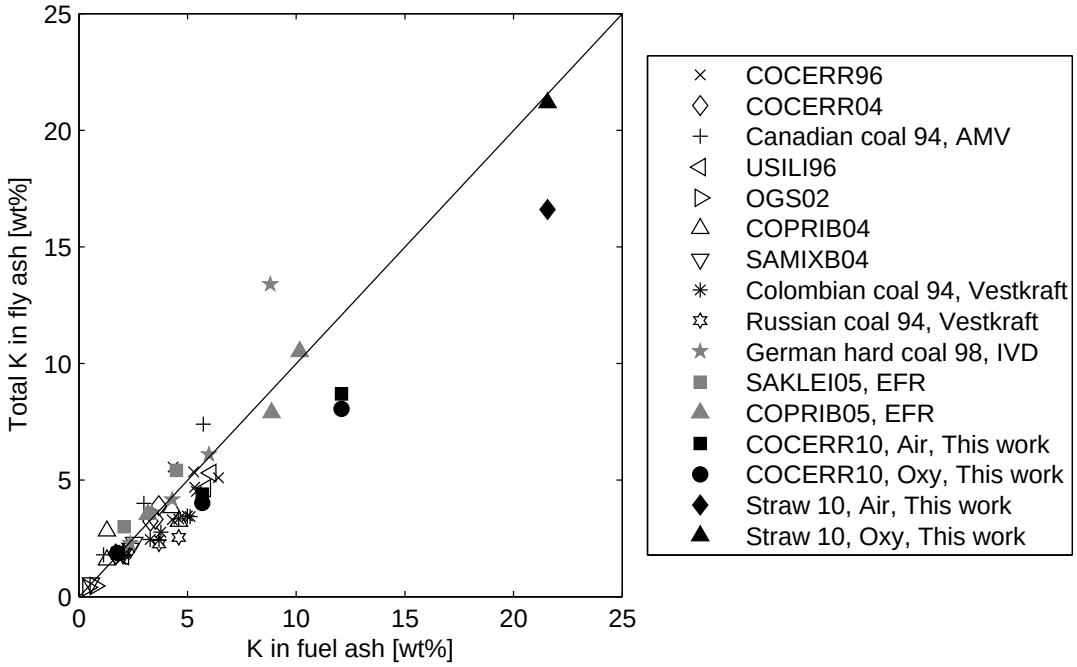


Figure 4.26: Total K in fly ashes as function of the K content of the fuel ash. Open symbols: literature data from [80]; closed, grey symbols: semi-technical and entrained flow reactor (EFR) data from [80]; closed, black symbols: semi-technical scale data from this work.

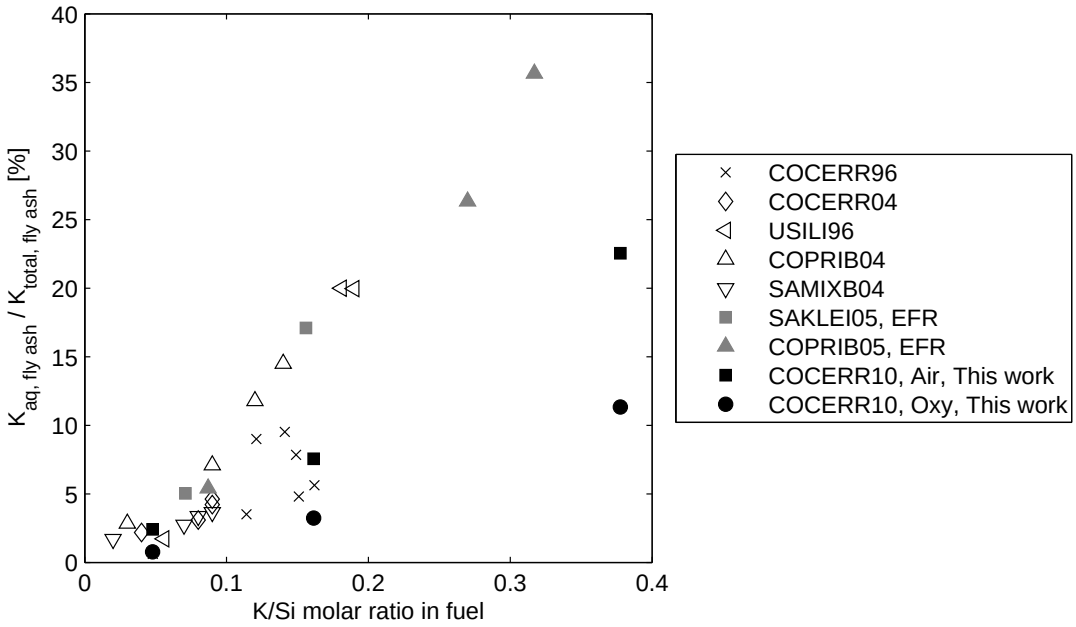


Figure 4.27: Percentage share of water soluble K in fly ash to total K in fly ash as a function of the K/Si ratio of the fuel for coal/straw co-firing. Open symbols: literature data from [80]; closed, grey symbols: Entrained flow reactor (EFR) data from [80]; closed, black symbols: semi-technical scale data from this work.

agreement with the full-scale data is observed for this work with up to 20 wt% straw in the fuel blend. Co-firing with high straw shares (increasing K in fuel ash) and combustion of pure straw tend to decrease the relative conversion of Fuel-K to fly ash potassium (this work). This deviation supports the increased level of total K in deposits compared to fly ash for the 50 wt% straw blend (air and oxyfuel) and the pure straw (air) shown in Figure 4.21 on page 101. For high fuel straw shares K is generally retained to a larger degree in deposits than in fly ash in the semi-technical scale setup. The observed split between fly ash and in-furnace deposits in the experimental setup of about 50:50 yields enough deposits to support this explanation.

The availability of silicate and aluminosilicate to react with potassium salts (K/Si molar ratio in fuel) has a significant effect on the amount of water soluble potassium found in the fly ash as seen in Figure 4.27. The retention of potassium in water soluble salts increases with increasing K/Si ratio, *i.e.* decreasing Si availability. A comparison of both the data from this work and the entrained flow reactor experiments show very good agreement to the full-scale trends for similar coals (COCERR and COPRIB). The best agreement for the data from this work is seen for the air-firing experiments whereas the oxyfuel combustion experiments, even though they are close to the full-scale data, generally yield lower levels of water soluble K than the trend suggests. The difference between

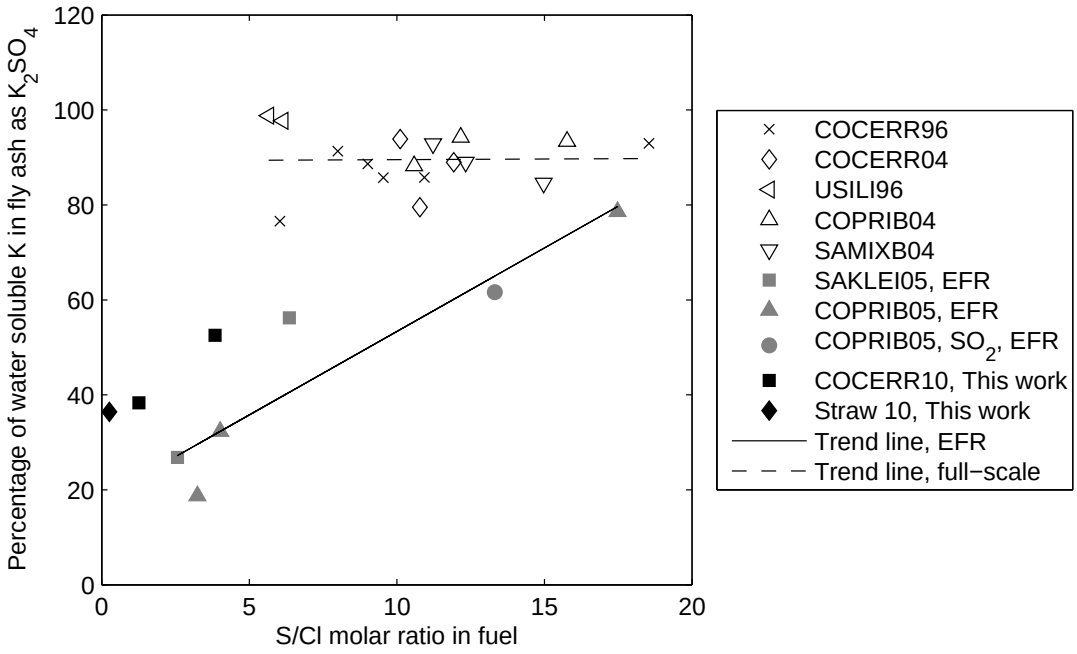


Figure 4.28: Percentage share of water soluble K in fly ash that appears as $K_2SO_4$ as a function of the S/Cl ratio of the fuel. Open symbols: literature data from [80]; closed, grey symbols: Entrained flow reactor (EFR) data from [80]; closed, black symbols: semi-technical scale data from this work. Pure coal data from this work have been omitted.

the air and oxyfuel combustion data is suggested to be caused by the increased, average residence time and increased flame and flue gas temperatures during oxy-fuel combustion possibly leading to an increased capture of K in alumina-silicates, thus decreasing the amount of water soluble K.

The water soluble potassium found in the fly ash is suggested to exist in the form of KCl and $K_2SO_4$. Under the assumption that all Cl found in the fly ash exist as KCl, the amount of potassium found as $K_2SO_4$ can be determined from (4.4).

$$K_{aq,\,K_2SO_4} = 1 - \frac{x_{Cl_{aq},\,ash} \cdot M_K}{x_{K_{aq},\,ash} \cdot M_{Cl}} \tag{4.4}$$

where $x_{Cl_{aq},\,ash}$ and $x_{K_{aq},\,ash}$ are the mass fractions of water soluble Cl and K in the fly ash, and $M_i$ are the corresponding molar weights. The fraction of the Cl being bound to Na in the fly ash is neglected.

Figures 4.28 and 4.29 show the observed difference between full-scale ashes and those obtained in the lab-scale and semi-technical scale experimental setups with respect to the sulphation of chlorides in the fly ash. Whereas the fraction of water soluble K in fly ash from full-scale boilers appears independent of the S/Cl molar ratio in the fuel, both the lab-scale and semi-technical scale experiments yield

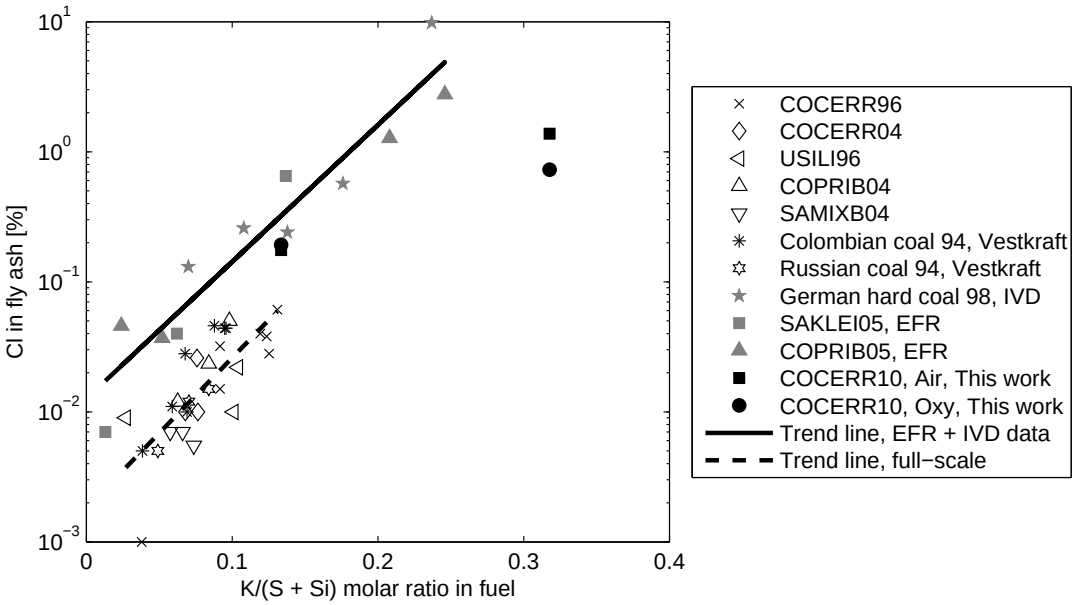


Figure 4.29: Percentage share of water soluble Cl in fly ash as a function of the K/(S + Si) ratio of the fuel. Open symbols: literature data from [80]; closed, grey symbols: semi-technical and entrained flow reactor (EFR) data from [80]; closed, black symbols: semi-technical scale data from this work. Only data for the straw/coal blends are shown for this work.

increasing sulphation propensity with increasing surplus of sulphur compared to Cl. The share of $K_2SO_4$ is higher for the experiments in this work than for the lab-scale setup probably due to a longer residence time in the temperature window where sulphation occurs (about 900 °C). For all of the investigated, straw-containing fuels in this work the degree of sulphation is lower than in full-scale. However, the data sets do not overlap with respect to the S/Cl ratio. A possibility exists, that for very low S/Cl ratios (high straw share) there would be a drop-off in the percentage of K occurring as $K_2SO_4$ due to the increased surplus of Cl in full-scale boilers as well. It is however unknown, if the full-scale fly ashes would resemble the data obtained in this work. Figure 4.29 confirms that the chloride retention in the fly ash is higher for the small-scale setups than for full-scale boilers, *i.e.* a larger percentage of the water soluble K could be expected to be bound in KCl. However, for the experiments with co-firing 50 wt% straw in this work (K/(S + Si) $\sim$ 0.32) the chloride content of the fly ash is closer to the trendline for the full-scale experiments (if extrapolated) than to the other lab-scale data. The reason for this is unknown.

## 4.6 Summary and Conclusions

Combustion of coal/straw blends with straw shares of 0, 20, 50, and 100 % was carried out at the reference air and oxyfuel conditions. The effect of the variation of the fuel composition was investigated with respect to flame temperatures, burnout efficiency, emissions, fly ash characteristics, and deposit formation.

It was shown that increasing fuel straw share yields decreasing flame and flue gas temperatures and increasing flame length. The most pronounced difference occurred with the change from the 50 wt% coal/straw blend to pure straw combustion.

Increasing the fuel straw share likewise had a significant impact on the fuel carbon burnout efficiency. For pure coal a burnout efficiency in air of 99.5 % was obtained while it dropped to 98.9 % for pure straw. Oxyfuel combustion consistently yielded higher burnout efficiencies than in air (99.3-99.8 %) and the difference to the data obtained in air increased with increasing fuel straw share. This is suggested to be a consequence of the relatively higher importance of the combined effect of higher inlet $O_2$ concentration, increased maximum flue gas temperature, and increased residence time when large straw particles ($d_p = 0.5-1$ mm) are fed to the reactor.

The observation made for pure coal with a change from air to oxyfuel combustion leading to a reduction in the emission of NO of about 30 % and to no difference with respect to $SO_2$ was also obtained for straw-containing fuels. However, the emission rates of both NO and $SO_2$ decrease with increasing fuel straw share. The slope is similar for both combustion atmospheres. The decrease is a consequence of the lower amount of Fuel-N and Fuel-S in straw compared to coal. An investigation of the Fuel-N to NO conversion ratio showed that a larger percentage of the Straw-N was converted to NO compared to coal. This is due to the fact that internal, gas-phase reduction of NO to $N_2$, proceeds via a 2nd order reaction whose reaction rate decreases relatively more than the 1st order oxidation of reduced N-species to NO with decreasing concentration of N-species in the gas-phase, *i.e.* decreasing Fuel-N. The Fuel-S to $SO_2$ conversion ratio for combustion of pure straw is essentially zero whereas it is above 80 % for combustion of pure coal. The difference is caused by the competing reactions between Al-Si containing ash particles and $SO_2$ for the potassium present in the parent fuel. At high K/Si ratios (straw), most $SO_2$ released to the gas phase is captured in sulphate salts.

The chemical composition of the collected fly ash samples was highly dependent on the fuel straw share. Significantly increased corrosion potential was observed for pure straw combustion compared to combustion of coal and the 20 wt% straw/coal blend. Due to the relatively low content of Si compared to K in the straw almost full capture of S and Cl as potassium salts in the ash was observed. A tendency for increased capture of water soluble K and S was found in deposits compared to the fly ash, further increasing the corrosion potential for the

straw-containing fuels. The deposition propensity likewise increases significantly when pure straw is burned compared to pure coal and the applied coal/straw blends. The deposit also became more sintered and difficult to remove.

A comparison of the fly ash data from this work to data from full-scale boilers co-firing coal and straw showed good agreement with respect to the capture of potassium in water soluble form in the fly ash. However, deviations were observed with respect to the degree of sulphation of the fly ash with full-scale plants achieving higher amount of $K_2SO_4$ in the fly ash than the semi-technical setups applied in this work and reported in literature.

# Chapter 5

# Special Topics

This chapter presents results regarding the combustion fundamentals for pure fuels (coal or straw) related to two different areas of the oxyfuel power plant process. The first part of the chapter treats the results related to the fate of N and S during simulated recirculation of flue gas prior to flue gas cleaning. The second part of the chapter describes results obtained during an investigation regarding the potential for improvement of the process economy of a retrofitted oxyfuel power plant by reducing the overall level of excess oxygen.

## 5.1 Sulphur and Nitrogen Chemistry in OxyCoal Combustion with Simulated Recirculated Flue Gas

The flue gas cleaning strategy for an oxyfuel power plant will have a significant impact on the level of pollutants such as NO and $SO_2$ within the boiler. If the recirculated flue gas is taken downstream of the $DeNO_x$ and desulphurization units the composition of the flue gas within the boiler would resemble what has been measured in the once-through experiments presented in Chapters 3 and 4. However, if flue gas is recirculated to the boiler prior to desulphurization and without $NO_x$ removal accumulation of NO and $SO_2$ will occur in the flue gas. This section investigates the impact of the most often suggested process design of an oxyfuel power plant with recirculation of flue gas to the boiler prior to desulpurization and without $NO_x$ removal on the nitrogen and sulphur species, *i.e.* emissions of NO and $SO_2$, as well as the impact on the ash and deposits quality. The experiments are performed using pure coal as fuel and at the reference operating conditions determined in Chapter 3.

### 5.1.1 Specific Experimental Methods and Considerations

The experimental setup applied in this work is a once-through setup and does thus not enable a physical recirculation of flue gas in its current configuration. Instead, NO and $SO_2$ can be added to the secondary, tangential oxidant flow in varying amounts. During the experiments the $SO_2$ and NO concentrations in the total oxidant flow have been varied in the range 0–3500 ppm and 0–2000 ppm, respectively. The operation of the experimental setup corresponds to recirculation of dry flue gas since no steam is added to the oxidant.

#### 5.1.1.1 Addition of NO and $SO_2$ to Oxidant

During experiments with NO and/or $SO_2$ addition to the secondary tangential oxidant the flow of each species is set according to simultaneous measurements of the species concentration in the oxidant flow. Based on the measurements the overall concentration of the species, $y_i^{ox}$, in the entire oxidant flow can be determined from (5.1).

$$y_i^{ox} = \frac{y_i^{tan} F_{ox}^{tan}}{F_{ox}} \tag{5.1}$$

$y_i^{tan}$ is the mole fraction of species $i$ in the tangential flow, $F_{ox}^{tan}$, and $F_{ox}$ is the total flow rate of oxidant.

#### 5.1.1.2 Flue Gas Dilution

During the experiment with high concentrations of NO and/or $SO_2$ in the oxidant (CO17_ADNS with 2000 ppm NO and 3500 ppm $SO_2$) it was necessary to dilute the flue gas prior to analysis. The largest available upper limit on the measurement range on the online gas analysers for the two gases were 2500 ppm. The dilution was performed with an injector-type dilution panel. The diluting gas was pure $N_2$. Figure 5.1 on the next page shows the measured flue gas concentrations during the experiment. In order to correct the raw data the dilution ratio should be known. The dilution ratio could not be set directly at the dilution panel and is thus determined from the measurements on the oxidant which has a known composition. These measurements are located prior to the shaded areas in Figure 5.1. Neglecting the added species, the oxidant consists of 30 % $O_2$ and 70 % $CO_2$. From the measurements of $O_2$ and $CO_2$ in the oxidant the dilution ratio (DR) can be determined:

$$\mathrm{DR}_{\mathrm{O_2}} = \frac{0.30}{y_{\mathrm{O_2}}^{\mathrm{diluted}}} = 11.6 \pm 0.3 \tag{5.2}$$

$$\mathrm{DR}_{\mathrm{CO_2}} = \frac{0.70}{y_{\mathrm{CO_2}}^{\mathrm{diluted}}} = 12.3 \pm 0.2 \tag{5.3}$$

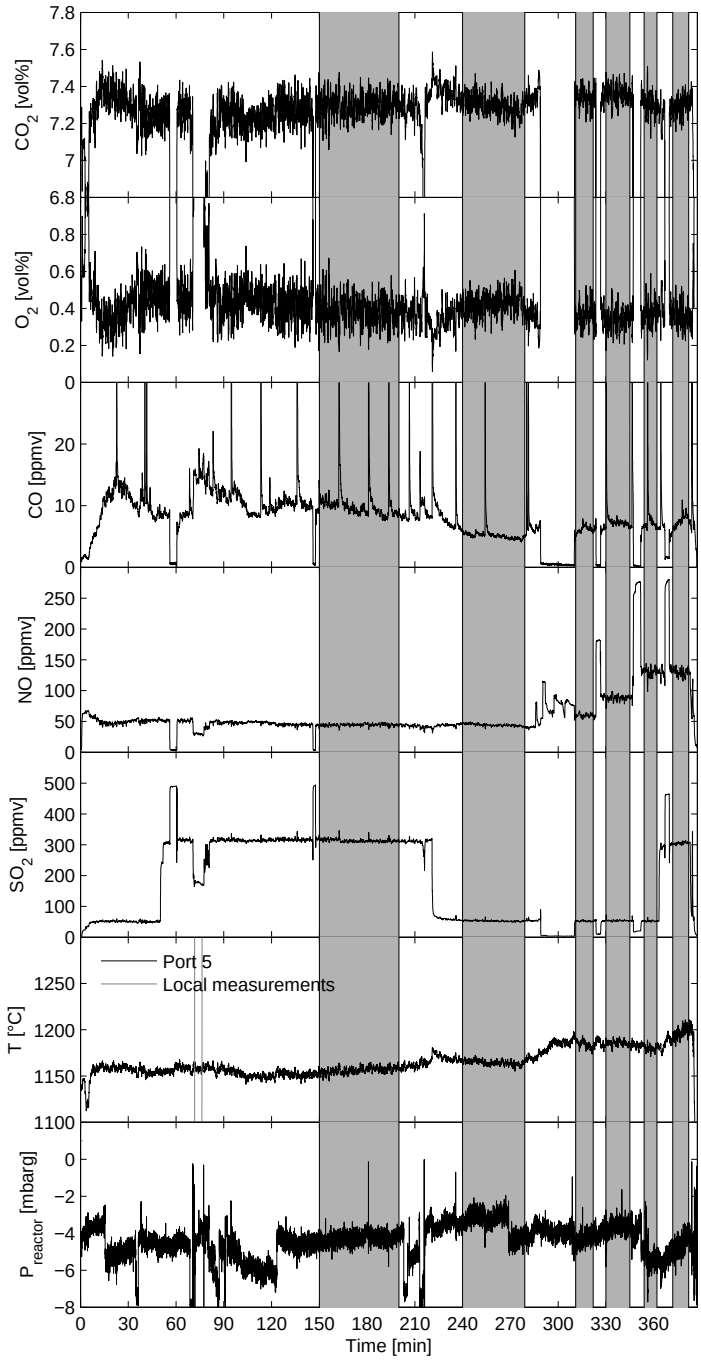


Figure 5.1: Diluted concentrations of major flue gas components ($CO_2$, $O_2$, CO, NO, and $SO_2$) as function of time for experiment CO17_ADNS, as well as the pressure at the top of the reaction chamber, the reference temperature measured at the reactor wall at a vertical position about 55 cm from the burner (port 5), and the local temperature measurements conducted with the S-type thermocouple probe. The shaded areas indicate the part of the data which are used during further data analysis.

The uncertainties on the determined ratios are due to fluctuating concentrations of the individual species during the measurement periods. The flue gas emision data are corrected by multiplying with the mean of the determined dilution ratios (DR = 12.0). It should be noted that the uncertainty on the measurements is increased significantly due to the dilution.

### 5.1.2 Simulated Recirculation of NO in Semi-Technical Scale

A large fraction of NO introduced with the recirculated flue gas to the furnace through the burner during oxyfuel combustion will be reduced to $N_2$ due to re-burning reactions [59]. A high gas phase concentration of NO during combustion could also reduce the percentage conversion of Fuel-N to NO. The relevant reactions are shown below. HCN is used as synonym for reduced N-species in the gas phase.

$$\mathrm{NO} + \mathrm{HCN} \rightleftharpoons \mathrm{N_2} + \ldots \tag{5.4}$$

$$\mathrm{HCN} + \mathrm{O_2} \rightleftharpoons \mathrm{NO} + \ldots \tag{5.5}$$

The split between gas-phase NO being reduced and Fuel-N not forming NO is unknown.

Figure 5.2 on the facing page compares the actual inlet NO concentrations used in the individual experiments with the measured exit flue gas concentration of NO corrected for the dilution by false air ingress. Three levels of NO in the oxidant have been tested; 550, 1300, and 2000 ppmv. With 2000 ppm NO in the oxidant the effect of a simultaneous high concentration of $SO_2$ (3500 ppmv) was also investigated. In the interval 0–1300 ppmv NO in the oxidant the concentration of NO in the flue gas increases linearly. Above 1300 ppmv NO in the oxidant a larger fraction of the NO doped to the oxidant appears to go unconverted through the furnace. The addition of 3500 ppmv $SO_2$ to the oxidant decreases the exit flue gas NO level when all other conditions are kept constant. This is in accordance with results reported in literature [83] which indicate that the presence of high levels of $SO_2$ may enhance the rate of consumption of NO in the gas phase. The formation of significant levels of radicals like SO, SH, and S at high temperature acts to reduce NO present in the gas phase [83].

Figure 5.3 on the next page shows the apparent conversion of NO introduced with the oxidant to $N_2$ under the assumption that the Fuel-N to NO conversion rate does not change compared to the case with no NO in the oxidant. The reduction, $\eta_{NO}$, is determined from Eq. (5.6).

$$\eta_{NO} = \frac{n_{NO,in} + n_{NO,0} - n_{NO,FG}}{n_{NO,in}} \tag{5.6}$$

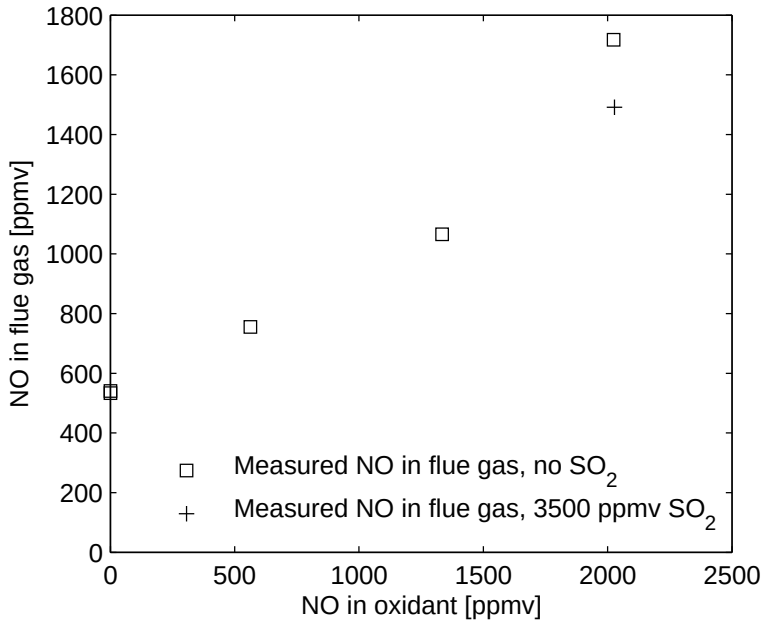


Figure 5.2: Comparison of the concentration of doped NO in the oxidant and the NO concentration measured in the resulting flue gas.

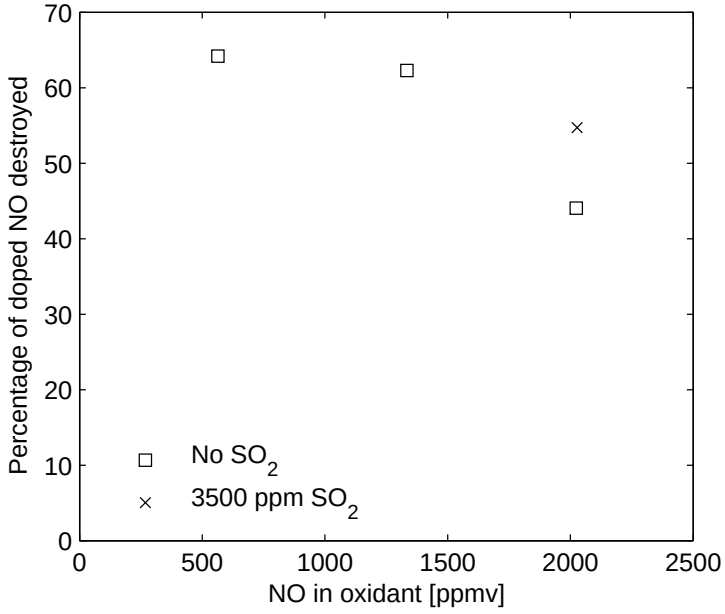


Figure 5.3: Apparent reduction of NO recirculated through the burner shown as the fraction of the NO in the oxidant which has been destroyed as a function of the concentration in the oxidant.

where $n_{NO,in}$ is the amount of NO introduced with the oxidant [mole/s], $n_{NO,0}$ is the amount of NO formed from Fuel-N when no NO is doped to the oxidant, and $n_{NO,FG}$ is the amount of NO in the flue gas.

The conversion efficiency decreases with increasing gas-phase NO concentration. For an inlet NO concentration of 550 and 1300 ppm about 62-65 % of the NO is reduced to $N_2$. These results are in good agreement with results presented by Liu et al. [84] from a comparable setup which yields reduction efficiencies between 68 and 82 % for an inlet NO concentration of about 500 ppmv. Liu et al. observed that the reduction efficiency increases with decreasing coal reactivity, *i.e.* decreasing burnout. This is most likely due to the increased amount of char present during combustion which reduces NO through the reactions:

$$\mathrm{NO + C} \rightarrow 0.5\,\mathrm{N_2 + CO} \tag{5.7}$$

$$\mathrm{NO + CO} \rightarrow 0.5\,\mathrm{N_2 + CO_2} \tag{5.8}$$

For a burnout efficiency similar to the one obtained in this work ($>$ 99 %) and with similar stoichiometric oxygen excess (1.2 versus 1.19 for this work) the NO reduction efficiency obtained in [84] was 68-70 %. The reported results by Liu et al. [84] likewise show only a marginal decrease in the reduction efficiency with an increase in the inlet NO concentration from 500 ppmv to 1000 ppmv when the NO is introduced with the secondary oxidant flow like in this work.

Increasing the inlet NO concentration from 1300 to 2000 ppmv yields a decrease in the reduction efficiency. These results are in contrast to the general observation that increased NO levels in the flame yields increased reduction of NO to $N_2$ [70] due to the fact that reactions of the type shown in (5.4) have second-order rate expressions. The results shown here indicate that the NO reduction potential of the flame is approaching its capacity when the NO concentration increases above a certain level. It is possible that, instead of NO, the concentration of reduced N-species becomes the limiting reactant since the applied burner is operated in high-$NO_x$ mode.

The simultaneous presence of 3500 ppmv $SO_2$ and 2000 ppmv NO in the oxidant yields a 10 % point increase in the reduction efficiency of NO, from 44 to 54 %, compared to the case with only NO present in the oxidant flow.

The variation of the inlet NO concentration independently of the main oxidant composition is only relevant in a once-through reactor. For a setup with actual recirculation of the flue gas the inlet NO concentration at steady state operation will be determined by the chosen recirculation ratio, *i.e.* the inlet $O_2$ concentration at the burner. Figure 5.4 on the facing page illustrates the flows and the main gas species present in each flow for oxyfuel combustion with recirculation and without false air ingress. The part of the system positioned within the dashed square corresponds to a once-through setup as the one used in this work.

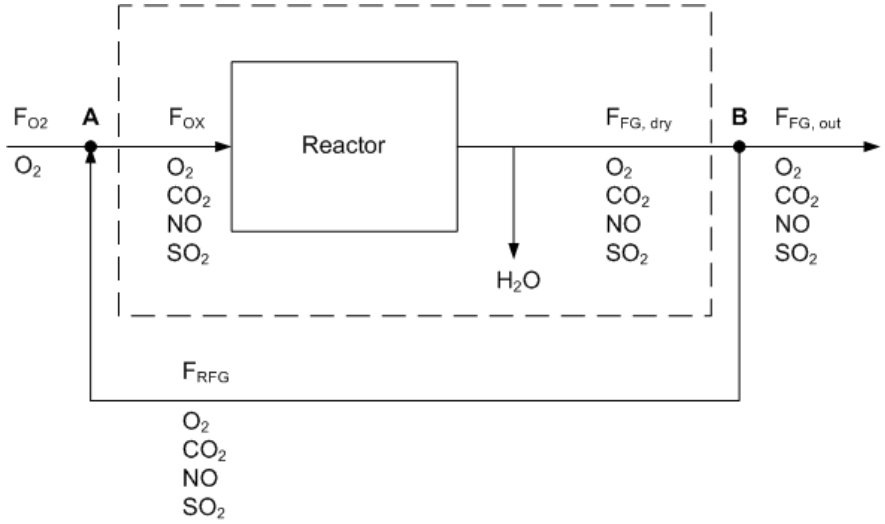


Figure 5.4: Flow diagram for an oxyfuel combustion reactor with recirculation of flue gas indicating the gas species present in each subflow. The part of the system situated within the dashed square corresponds to a once-through reactor.

Based on the measured NO concentration in the flue gas ($F_{FG,\,dry}$) for varying inlet NO concentrations it is possible to calculate the steady state concentration of NO at the reactor inlet if flue gas recirculation was performed. A comparison of the calculated inlet concentration and the actual concentration of NO doped to the oxidant will enable a determination of the inlet NO concentration at steady state during recirculation. The mole fraction of NO at the inlet, $y^{calc}_{NO,\,in}$, can be determined from (5.9).

$$y^{calc}_{NO,\,in} = \frac{y^{RFG}_{NO} \cdot F_{RFG}}{F_{ox}} \tag{5.9}$$

where $y^{RFG}_{NO}$ is the mole fraction of NO in the recirculated flue gas, $F_{RFG}$ is the flow of dry, recirculated flue gas, and $F_{ox}$ is the total amount of oxidizer sent to the burner. The concentration of NO in the recirculated flue gas corresponds to the concentration in the entire flue gas flow leaving the reactor and is determined from the measured concentration, $y^{dry}_{NO}$, by Eq. (5.10).

$$y^{RFG}_{NO} = \frac{y^{dry}_{NO} \cdot F_{FG,\,dry,\,FA}}{F_{FG,\,dry}} \tag{5.10}$$

The measured concentration, $y^{dry}_{NO}$, is corrected for the flue gas dilution occurring due to the ingress of false air (FA) into the experimental setup.

The ratio between the recirculated flue gas flow and the total oxidant flow is determined from the mass balances in (5.11) and (5.12).

Overall balance for oxidant mixing point (point **A**):

$$F_{O2} + F_{RFG} = F_{ox} \tag{5.11}$$

$F_{O2}$ is the flow of oxygen from the air separation unit (ASU). For simplicity it is assumed to be 100 % pure $O_2$.

$O_2$ balance at oxidant mixing point (point **A**):

$$F_{O2} + y_{O_2}^{dry} \cdot F_{RFG} = y_{O_2}^{ox} \cdot F_{ox} \tag{5.12}$$

The concentration of $O_2$ in the recirculated flue gas, $y_{o_2}^{dry}$, is about 5 % for the actual experiments and the oxidant inlet $O_2$ concentration, $y_{O_2}^{ox}$, is 30 %. The recirculation rate of flue gas, $RR$ see (5.13), is about 70 %.

$$RR = \frac{F_{RFG}}{F_{FG,\,dry}} \tag{5.13}$$

The calculated mole fraction of NO in the oxidant for a setup with flue gas recirculation, based on known quantities, can thus be determined from:

$$y_{NO,\,in}^{calc} = \frac{y_{NO}^{dry} \cdot F_{FG,\,dry,\,FA}\left(1 - y_{O_2}^{ox}\right)}{F_{FG,\,dry}\left(1 - y_{O_2}^{dry}\right)} \tag{5.14}$$

Figure 5.5 on the next page compares the calculated inlet values based on the measured flue gas concentration with the actual inlet NO concentrations used in the individual experiments. The figure also shows the measured exit flue gas concentrations from Fig. 5.2. For low, doped inlet NO concentrations ($<$ 550 ppmv) the calculated inlet concentration is higher than the actually applied level, whereas for inlet concentrations above 550 ppmv the calculated levels are below the actual levels. This implies that the inlet NO concentration at steady state if flue gas recirculation was established would be around 550 ppmv, *i.e.* where the line with a slope of 1 (dashed line) crosses the trend line through the data points. The concentration of NO in the dry exit flue gas at steady state would thus be about 750 ppmv corresponding to an emission rate of 203 mg/MJ at the furnace exit ($F_{FG,\,dry}$) and 50 mg/MJ in the flue gas ($F_{FG,\,out}$) transported to the chimney (or other downstream processes). Compared to the once-through experiments with no addition of NO to the oxidant which have a NO emission rate of about 150 mg/MJ the recirculation of flue gas induces a reduction of the NO emission of about 67 %. An overall NO emission rate of 50 mg/MJ correspond well to the lower range of levels reported in literature for pilot scale and semi-technical scale experimental facilities with flue gas recirculation [59].

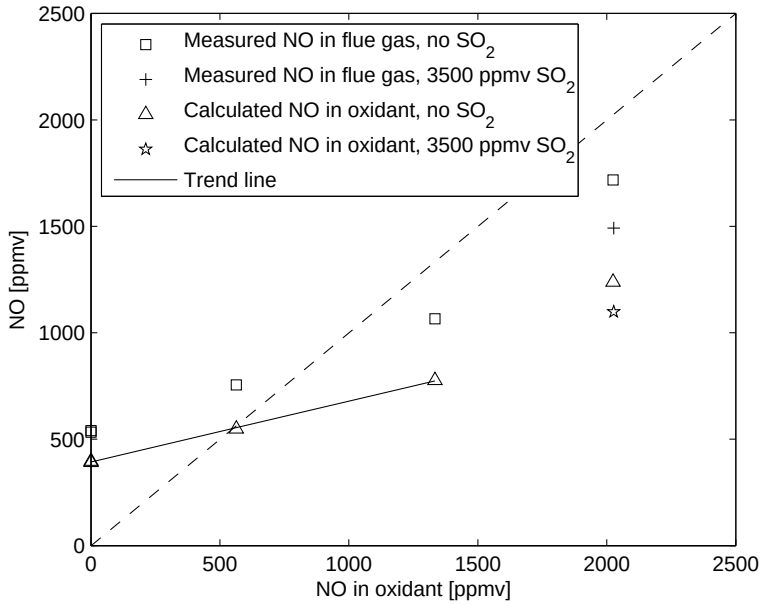


Figure 5.5: Comparison of the concentration of doped NO in the oxidant and the calculated concentration in the oxidant if flue gas with an NO concentration equal to the one measured in the resulting flue gas was recirculated to the burner.

### 5.1.3 Simulated Recirculation of $SO_2$ in Semi-Technical Scale

Unlike NO, $SO_2$ introduced through the burner in oxyfuel combustion will not be subject to reburning reactions. Instead, a significantly increased concentration of $SO_2$ within the furnace would be the result of accumulation due to the recirculation of $SO_2$-containing flue gas [59]. Generally, the reported $SO_2$ levels in flue gas from experimental setups with flue gas recirculation is lower than anticipated. This decrease is typically associated with increased retention of sulphur in fly ash and deposits and absorption in the flue gas condensate. This section investigates the impacts of increased in-furnace $SO_2$ concentrations on the flue gas $SO_2$ concentration and the retention of sulphur in ash and deposits. The concentration of doped $SO_2$ in the oxidant has been varied from 0 to 3500 ppmv. At 3500 ppmv the effect of a simultaneous high concentration of NO (2000 ppmv) was investigated.

#### 5.1.3.1 Sulphur Retention in Ash and Deposits

The amount of sulphur doped to the oxidant which is removed from the gas phase during combustion is expected to mainly be captured by fly ash and deposits. An increase in the concentration of $SO_3$ is also expected since about 0.1-1 % of the $SO_2$ is oxidized to $SO_3$ in the flue gas [69]. However, the increase in the $SO_3$ concentration in the flue gas with increasing in-furnace $SO_2$ levels is

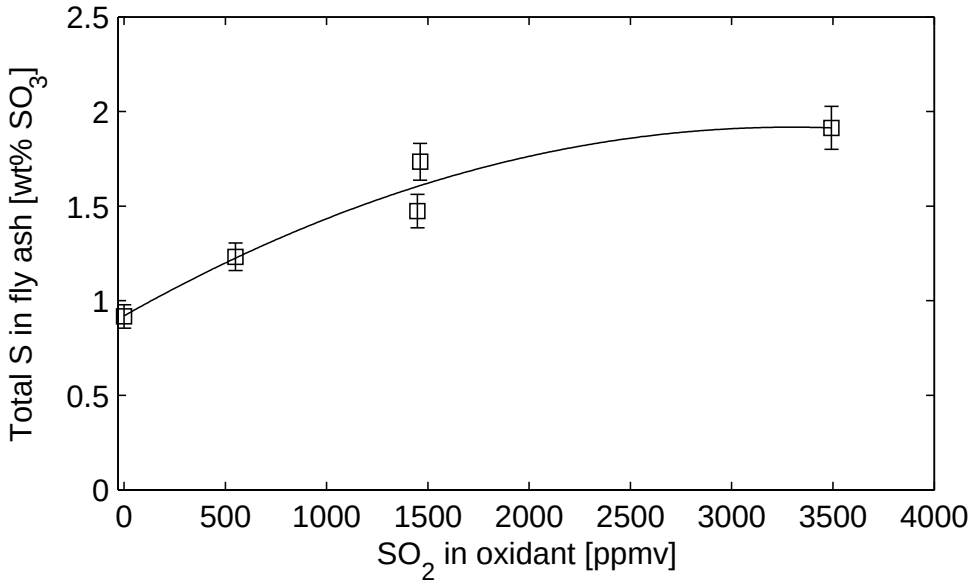


Figure 5.6: Relation between the total amount of sulphur captured in fly ash, measured as $SO_3$, and the concentration of $SO_2$ in the oxidant. Error bars correspond to two times the standard deviation in the analysis. The data have been fitted with a second order polynomial trend line.

insignificant with respect to the overall mass balance for sulphur in the system. Figure 5.6 shows the increasing retention of sulphur in the fly ash with increasing $SO_2$ concentration in the oxidant. Increasing the oxidant $SO_2$ concentration from 0 ppmv to 3500 ppmv yields an about 100 % increase in the sulphur content of the fly ash. The data corresponds well with the findings by Fleig et al. [69], that a high in-furnace $SO_2$ concentration in oxyfuel combustion with FGR favours sulphation and stabilises the sulphates formed. The non-linear trend in the fly ash sulphur content indicates the approach to the capacity of the ash to capture sulphur. Figure 5.7 on the next page shows the ratio of water soluble alkali and alkali earth metals to sulphur in the ash. A stoichiometric ratio is reached at approximately 1500 ppmv $SO_2$ in the oxidant and it can thus be anticipated that a further increase in the flue gas concentration of $SO_2$ beyond 3500 ppmv would not yield a significant increase in the sulphur content of the fly ash.

One of the critical aspects regarding the implementation of the oxyfuel combustion technology in power plants is the quality of the fly ash. In order to observe to the criteria of maximum 3 wt% S in fly ash (measured as $SO_3$) for utilisation of fly ash in concrete [63] it has been a question whether flue gas recirculation prior to desulphurization was possible. The data in Figure 5.6 shows that the quality criteria can be met with a considerable safety margin for the coal used in this work. The coal has a relatively low sulphur content (0.62 wt%, as received) and for coals with higher sulphur contents the significant increase in

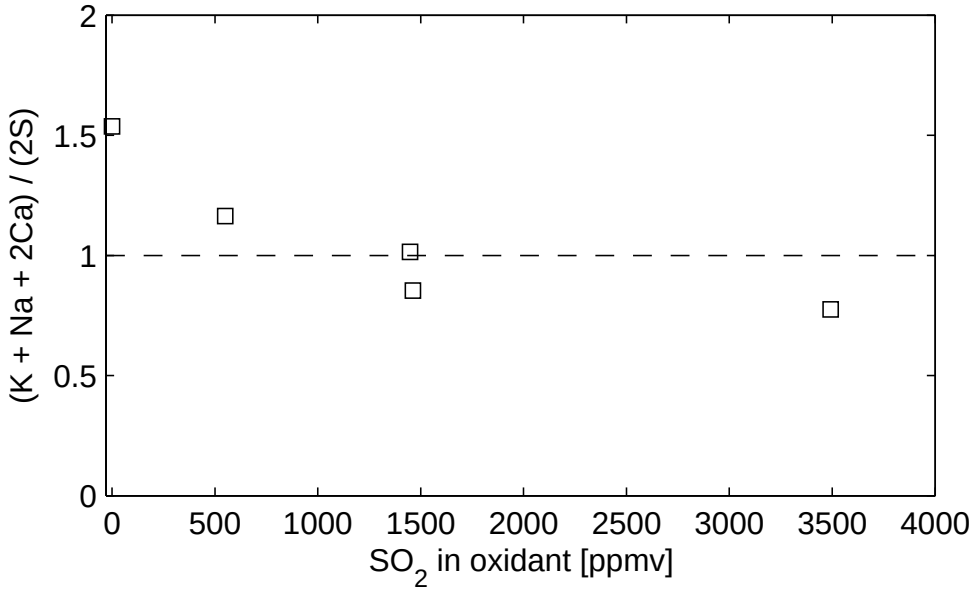


Figure 5.7: Stoichiometric ratio of water soluble alkali and alkali earth metals to sulphur in fly ash samples as function of the concentration of $SO_2$ in the oxidant.

the sulphur retention by the fly ash with increasing in-furnace $SO_2$ levels could pose a problem with respect to its utilization.

The three fly ash fractions; bottom, cyclone, and filter ashes, see Section 2.3.2.2, were analysed separately. The analysis indicated that sulphur is captured preferentially in the smaller particles, as the S content of the ash fractions increases in the order: Bottom ash $<$ Cyclone ash $<$ Filter ash for all experiments. This corresponds well with formation of sulphate-rich aerosols which mainly will end up in the filter ash fraction.

Table 5.1 on the following page shows the measured sulphur concentrations in the collected deposits and the calculated deposit fluxes. Similarly to the fly ash, the sulphur content of the deposits is observed to increase with increasing level of $SO_2$ in the flue gas. Except for one experimental run, the increase is linearly correlated to the fly ash sulphur content, as seen in Figure 5.8 on the next page. The data point that falls outside the trend of equal sulphur content in fly ash and deposit has an exposure time which is only about half as long (1.3 hr) as for the other experiments (2 hr). The most plausible cause to the deviation from the trend is the reduced sampling time and the relatively low yield of fly ash, 30 versus typically 50 %, see Figure 2.10 on page 32, which induces a significant uncertainty on the result.

Table 5.1: Average deposit fluxes as well as flue gas and deposit probe temperatures for exposure times of 1-2 hr and total S content in deposit for combustion of coal in the reference oxyfuel atmosphere with doping of $SO_2$ to the oxidant.

| Inlet $SO_2$ [ppmv] | Exposure time [hr] | Up-stream | Down-stream | Average | $T_{probe}$ [°C] | $T_{FG}$ [°C] | $S_{tot}$ [wt%] |
|---|---|---|---|---|---|---|---|
| 0 | 2.3 | 75 | 3 | 39 | 500 | 950 | 0.42 |
| 550 | 2.0 | 62 | 8 | 35 | 500 | - | 0.50 |
| 1460 | 1.3 | 64 | 5 | 34 | 500 | - | 0.50 |
| 1450 | 2.0 | 74 | 8 | 41 | 500 | 880 | 0.51 |
| 3500 | 2.2 | 67 | 10 | 38 | 500 | 810 | 0.68 |

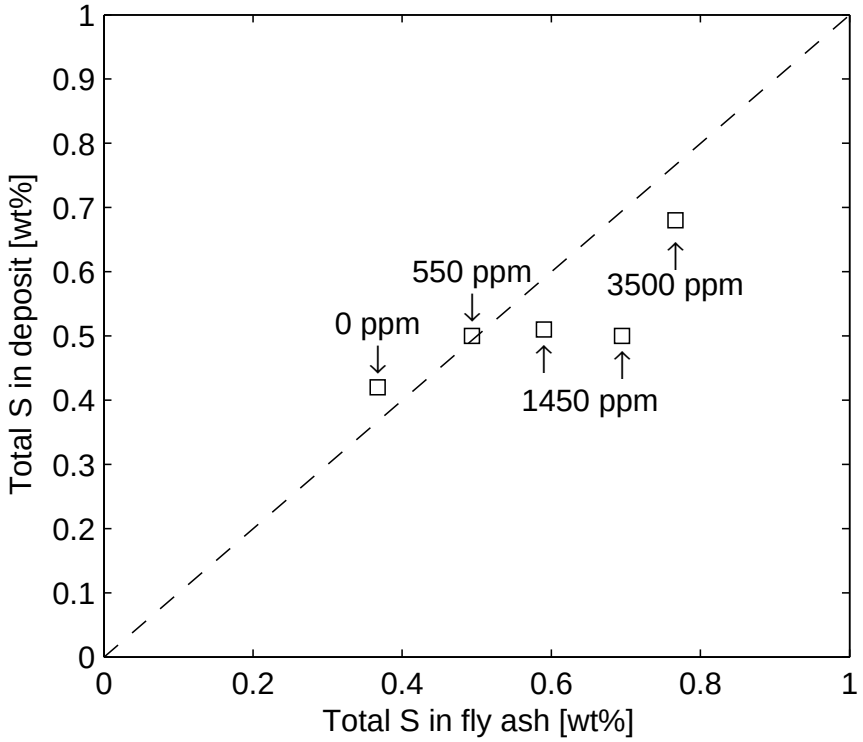


Figure 5.8: Comparison of the total sulphur content of related fly ash and deposit samples. The oxidant $SO_2$ concentration is stated for each data point.

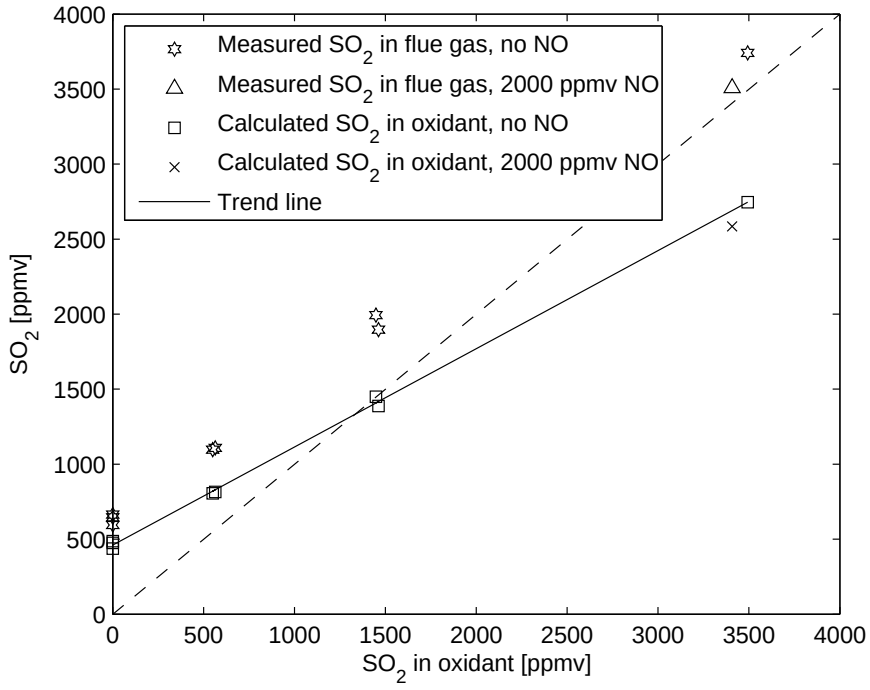


Figure 5.9: Comparison of the concentration of doped $SO_2$ in the oxidant and the calculated concentration in the oxidant if flue gas with a $SO_2$ concentration equal to the one measured in the resulting flue gas was recirculated to the burner. The experiments have been performed both with and without simultaneous addition of NO to the oxidant.

#### 5.1.3.2 Impact of Increased Furnace $SO_2$ Level on the $SO_2$ Emission

Figure 5.9 shows the relationships between the doped inlet concentration of $SO_2$ and the flue gas $SO_2$ concentration as well as the calculated $SO_2$ concentration in the oxidant if flue gas recirculation was performed. A linearly increasing trend is seen for the calculated oxidant concentrations. The steady state inlet concentration if the experimental setup was equipped with flue gas recirculation would be about 1500 ppmv and the flue gas concentration would be about 1950 ppmv at the reference operating conditions. Compared to the experiments without $SO_2$ addition to the oxidant the in-furnace $SO_2$ concentration thus increases with a factor of 3 (from 645 ppmv). The exit furnace emission rate of $SO_2$ would be 1130 mg/MJ which corresponds to about 280 mg/MJ after the point of flue gas recirculation. Compared to the once-through experiments which have an $SO_2$ emission rate of about 390 mg/MJ the recirculation of flue gas induces an overall reduction of the $SO_2$ emission of about 28 %. An overall $SO_2$ emission rate of 280 mg/MJ correspond well to results reported in literature for combustion of coals with similar sulphur contents combusted in pilot scale and semi-technical scale experimental facilities with flue gas recirculation [72, 73]. At high burnout efficiencies the $SO_2$ emission rate is determined only by the sulphur content of

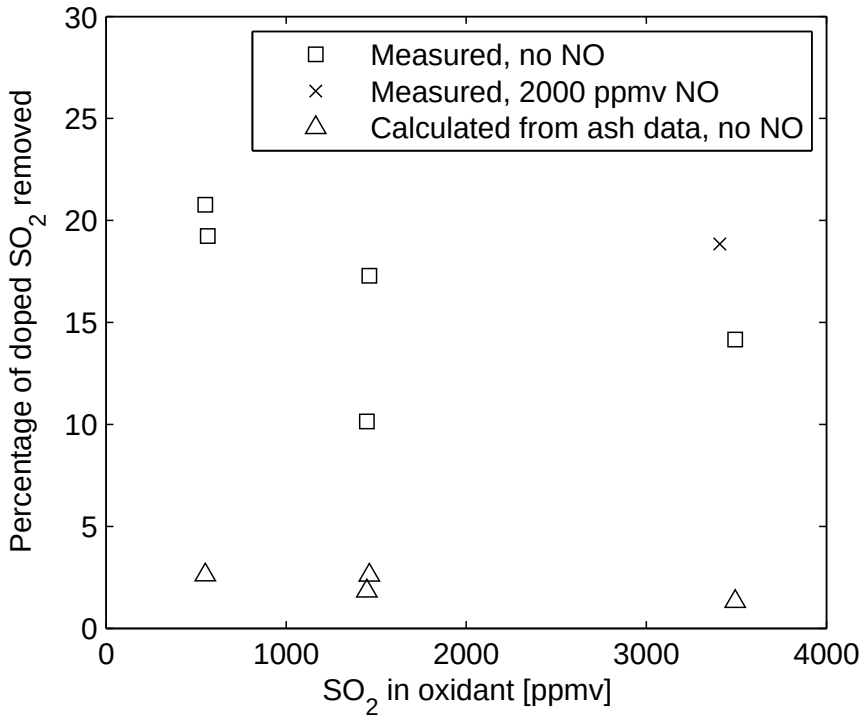


Figure 5.10: Apparent removal from the gas phase of $SO_2$ introduced through the burner as a function of the concentration in the oxidant. The experiments have been performed both with and without simultaneous addition of NO to the oxidant. The figure shows both removal efficiencies based on the measured flue gas concentration of $SO_2$ and based on the amount of sulphur measured in the fly ash samples.

the coal.

The presence of 2000 ppmv NO does not seem to have a significant effect on the gas phase sulphur chemistry.

Figure 5.10 shows the percentage of the doped $SO_2$ which has been removed from the gas phase during the combustion. The removal has been determined according to the procedure described in Section 5.1.2. The observed reduction is between 10 and 20 % and tends to decrease with increasing in-furnace $SO_2$ level. The decrease indicates the approach to the capacity limit for sulphur retention in fly ash and deposits when the in-furnace $SO_2$ concentration becomes very large. The removal of $SO_2$ from the gas phase during combustion is significantly smaller than for NO which is a consequence of the different removal mechanisms – capture by solid phases versus gas phase reactions. An explanation to the large difference between the points at 1500 ppmv $SO_2$ in the oxidant has not been found.

A comparison of the flue gas and fly ash samples shows that the removal efficiency which can be determined based on the measured sulphur levels in the

fly ash correlates poorly to the values based on the flue gas measurements with respect to the absolute values, see Fig. 5.10. The trend of decreasing removal efficiency with increasing in-furnace $SO_2$ level is, however, the same. This deviation is indicative of a significant source of error on the flue gas $SO_2$ measurements. A loss of $SO_2$ occurs in the flue gas sampling system prior to analysis, either due to absorption in the condensate or by reaction with moist ash. Alternatively, the $SO_2$ levels in the oxidant have been overestimated.

### 5.1.4 Summary and Conclusions

Dry flue gas recirculation for an oxyfuel combustion system without removal of NO and $SO_2$ has been simulated in the once-through experimental setup used in this work. NO and $SO_2$ levels of 0-2000 ppmv and 0-3500 ppmv, respectively, have been applied during combustion of pure coal.

The investigation showed that the steady state NO concentration in the oxidant would be around 550 ppmv if flue gas gas was recirculated. This implies that about 65 % of the NO in the recirculated flue gas is reduced to $N_2$ during combustion. The NO emission rate is likewise reduced to about 1/3 (50 mg/MJ) of the level for once-through operation which corresponds well to results reported in literature for experimental facilities with actual flue gas recirculation.

Simultaneous presence of NO and high levels of $SO_2$ leads to an increased reduction of NO formed in the gas phase. At 2000 ppmv NO in the inlet addition of 3500 ppmv $SO_2$ increases the reduction efficiency of NO with 10 % points.

The simulated recirculation of $SO_2$ showed that the in-furnace $SO_2$ level increases with a factor of 3 due to accumulation and the fact that only 10-20 % of the $SO_2$ is removed from the gas phase during combustion. At steady state the inlet $SO_2$ level would be about 1500 ppmv and the flue gas concentration about 1950 ppmv for the coal applied in this work. Unlike NO which is reduced due to reburning reactions, $SO_2$ is removed mainly due to capture by fly ash and deposits. The data showed an increasing capture with increasing flue gas $SO_2$ level and at steady state the amount of sulphur in the fly ash would increase about 60 % compared to the case with no $SO_2$ in the oxidant. However, due to the fact that a coal with a relatively low sulphur content (0.62 wt%, as received) has been applied, the requirement of a maximum content of 3 wt% $SO_3$ in the fly ash can be met with significant safety margen.

The capture of sulphur by fly ash and deposits is seen to be similar and the increase in the in-furnace $SO_2$ level was not observed to have an effect on the rate of formation of deposits.

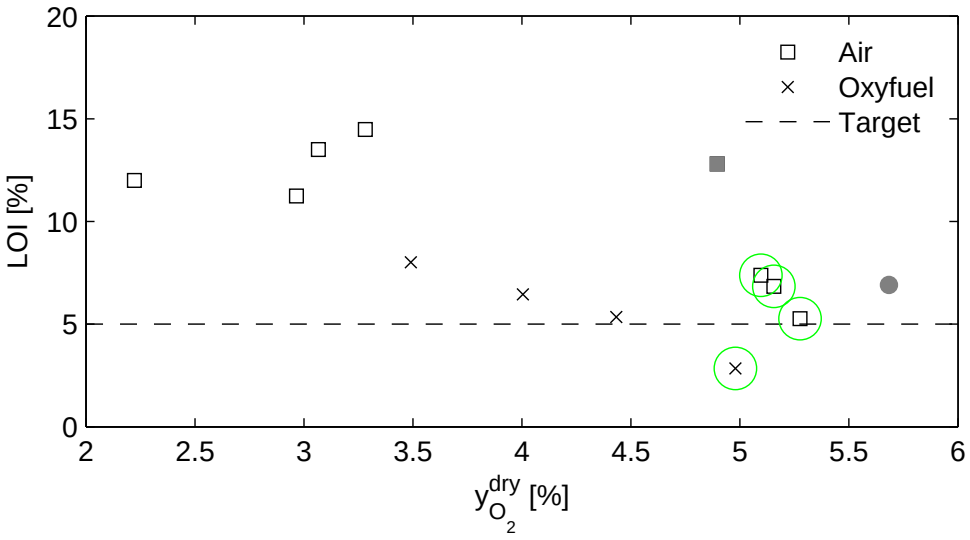


Figure 5.11: Comparison of loss-on-ignition (LOI) for coal combustion in air and 30% $O_2/CO_2$ at different flue gas oxygen levels. Data points marked with green circles are the experiments with realized operating conditions corresponding to the chosen reference parameters (CA10, CA14, CA16, and CO09). The air experiment marked in grey and the oxyfuel experiment marked with a grey circle fall outside the trend for the remaining experiments according to the discussion in Sections 3.1.2 and 3.2.1.

## 5.2 Improving Process Economics

The major penalty to the oxyfuel combustion process economy is at present the high operating expenses associated with cryogenic oxygen production [59]. This section provides results for both coal and straw combustion showing that there is a potential for reducing oxygen excess in oxyfuel combustion compared to conventional air-firing and hence improve process economics. The analysis is made under the assumption that a conventional air-blown power plant is retrofitted to oxyfuel combustion and that a design criteria is that the exit flue gas oxygen concentration is kept at the same level as in the original plant. A key issue in relation to the reduction of oxygen excess is that the change is not made at expense of the quality of the combustion process, *i.e.* giving rise to increased emissions or reduced burnout.

### 5.2.1 Comparing Air and OxyCoal Burnout and Emission Rates as Function of Oxygen Excess

Figure 5.11 shows a comparison of the development in fly ash loss-on-ignition as function of the combustion stoichiometry for air and 30 % $O_2/CO_2$ experiments. The general trend in the data is that the burnout efficiency for comparable flue

gas oxygen levels is higher during oxyfuel combustion than in air for a plant of a given size. It is thus possible to decrease the oxygen excess level to some degree in an oxyfuel power plant compared to the corresponding plant using air as oxidant without compromising fuel burnout. A potential requirement is that the residence time in the retrofitted oxyfuel plant is increased relative to the air conditions with the same factor of about 1.5 as has been the case for the experiments displayed here.

Figure 5.12 on the following page shows comparisons of the NO, $SO_2$, and CO emission rates for air and oxyfuel combustion as function of the oxygen concentration in the dry exit flue gas. Based on the available data, reducing the oxygen excess does not induce significant changes to the emission rates of the polluting species and no limitations should be put up for the reduction in oxygen excess.

For the experimental setup, a reduction from about 5 % to about 4.5 % $O_2$ in the dry flue gas is possible without compromising fuel burnout (LOI = 5 %). Under the assumption that the same relative reduction of the oxygen excess can be applied at a full-scale power plant, the associated decrease in the oxygen demand for the power plant can be estimated from (5.15).

$$\begin{aligned} \mathrm{O}_{2,\,\mathrm{saved}} &= \frac{\mathrm{F}_{\mathrm{O}_2,\,\mathrm{Oxy\ 30/5}} - \mathrm{F}_{\mathrm{O}_2,\,\mathrm{Oxy\ 30/4.5}}}{\mathrm{F}_{\mathrm{O}_2,\,\mathrm{Oxy\ 30/5}}} \\ &= \frac{\lambda_{30/5} - \lambda_{30/4.5}}{\lambda_{30/5}} \\ &= \frac{1.19 - 1.17}{1.19} = \mathbf{2}\ \% \end{aligned} \tag{5.15}$$

where $F_{O_2,\,Oxy\ XX/YY}$ is the required oxygen flow to the boiler for an oxidant with $XX$ % $O_2$ (remaining $CO_2$) and an oxygen excess corresponding to $YY$ % $O_2$ in the dry flue gas.

Even though the saving may seem insignificant, it may induce a marked reduction of the operating expenses for an oxyfuel power plant. The potential for reducing the oxygen excess in full-scale is very dependent on the possibility of achieving good mixing of oxidant and fuel within the boiler.

### 5.2.2 Taking Advantage of the Extra Degree of Freedom in OxyStraw Combustion

For the coal experiments discussed above the concentration of oxygen at the burner inlet was fixed. However, oxyfuel combustion has the advantage over air-firing that the oxygen excess and inlet oxygen concentration are no longer dependent variables. This section describes an investigation which exploits the

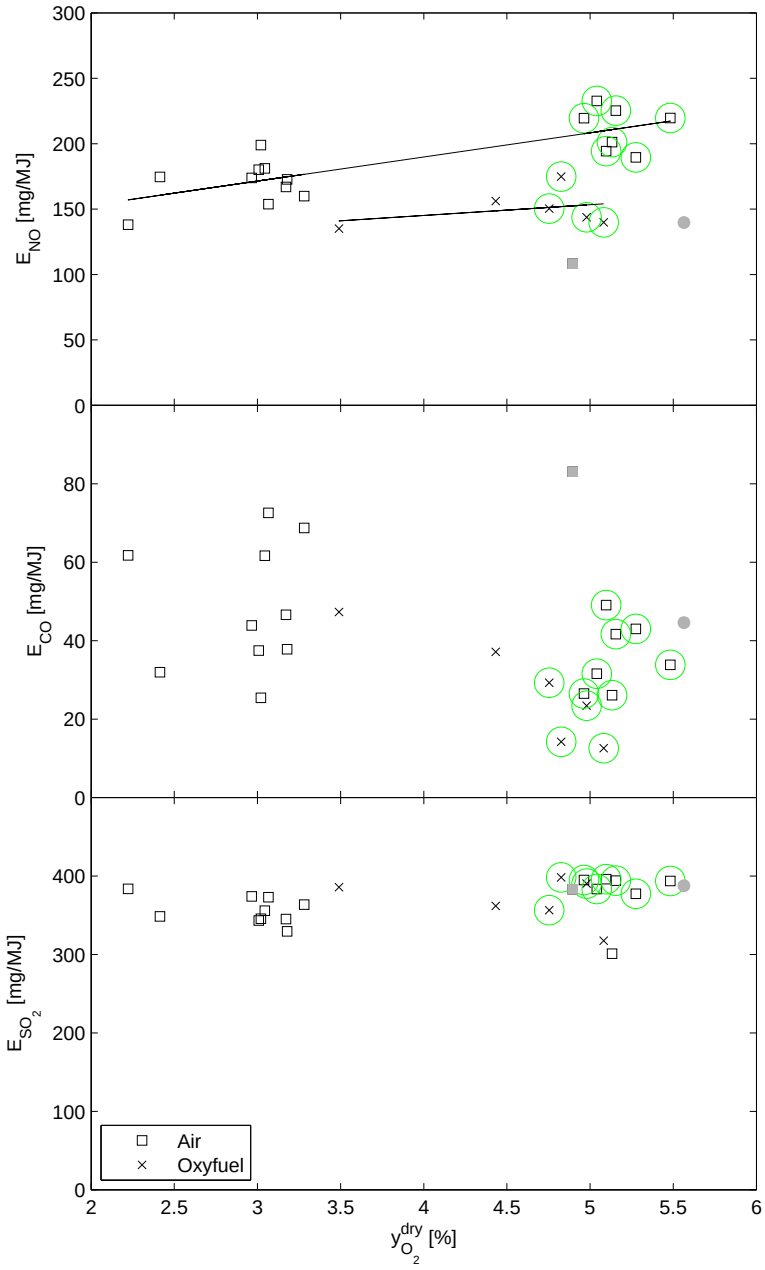


Figure 5.12: Comparison of the emission rate of NO, CO, and $SO_2$ for coal combustion in air and 30% $O_2/CO_2$ at different stoichiometries. Data points marked with green circles are the experiments with realized operating conditions corresponding to the chosen reference parameters (CA10, CA12-17, CO09, CO10, CO12, and CO18). CA17 and CO18 have been omitted in the $SO_2$ plot according to the discussion in Section 2.4.2. The air experiment marked in grey and the oxyfuel experiment marked with a grey circle fall outside the trend for the remaining experiments according to the discussion in Sections 3.1.2 and 3.2.1. These points have been omitted in the determination of trend lines.

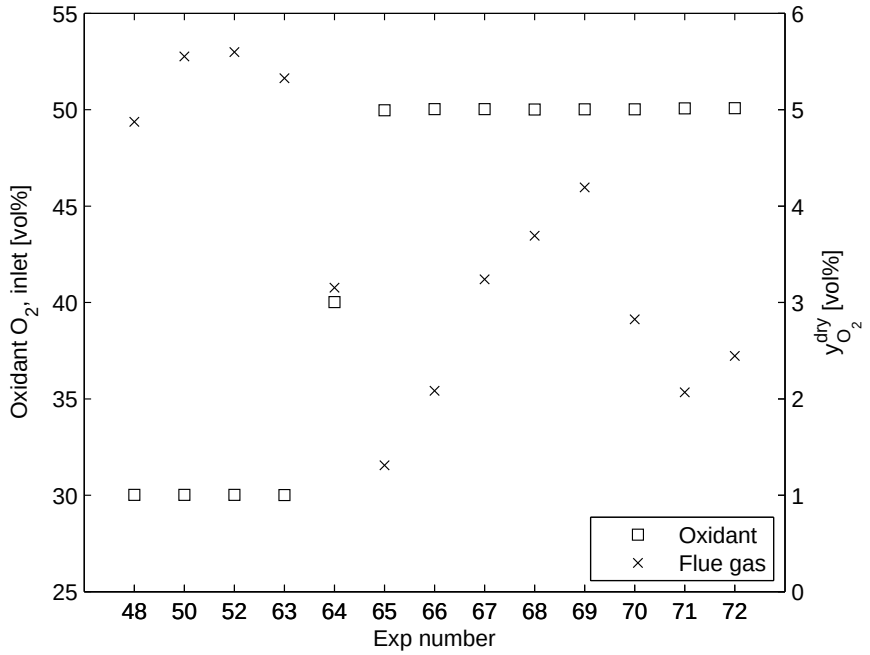


Figure 5.13: Related values of oxidant $O_2$ concentration and theoretical $O_2$ concentration in the dry exit flue gas as function of the experiment number (chronological order).

effect of increasing inlet oxygen concentration while simultaneously reducing the flue gas oxygen level. The investigation is performed with pure straw as fuel. The choice of straw over coal is made with the aim of investigating the savings potential for the most difficult fuel where large particles causes challenges during burnout.

Figure 5.13 provides an overview of the combustion conditions for the series of experiments in the investigation. Only experiments 63, 64, and 72 includes fly ash sampling while the remaining experiments are used solely for evaluation of emissions.

The development in fly ash loss-on-ignition when changing combustion conditions is seen in Figure 5.14 on the following page. The oxidant and stoichiometry is given as *e.g.* Oxy 40/3 meaning that the oxygen concentration at the inlet is 40 % and the corresponding concentration in the dry flue gas is 3 %. The change from air-firing to oxyfuel combustion yields a significant improvement in burnout for all combustion conditions. For all oxyfuel experiments no change in the burnout efficiency is observed with the change in conditions. The decreasing trend in the uncertainty on the measurements with increasing inlet $O_2$ concentration is a consequence of decreasing occurrence of char particles in the bottom ash fraction.

Changing the oxyfuel combustion conditions from a 30 % $O_2/CO_2$ oxidant mix-

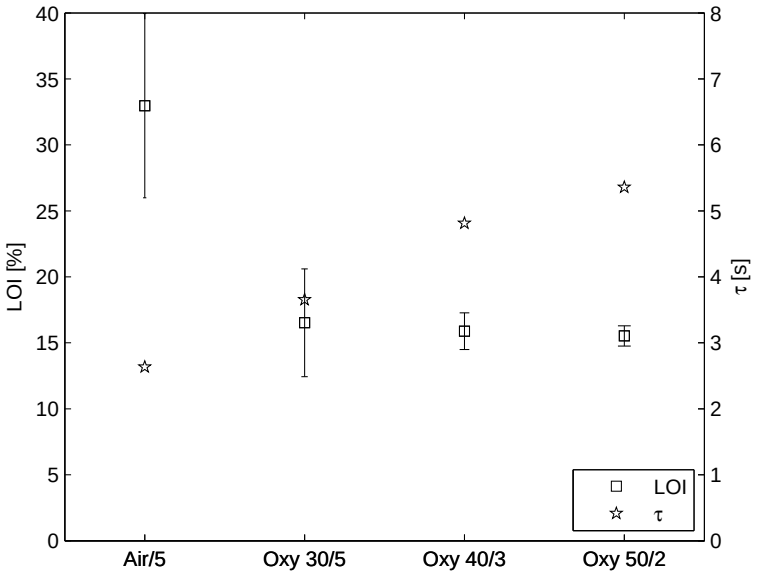


Figure 5.14: Comparison of loss-on-ignition (LOI) and average gas and particle residence time for straw combustion in air and oxyfuel atmospheres with varying oxidant compositions and stoichiometries. Error bars correspond to two times the uncertainty on the LOI analysis.

ture with an oxygen excess corresponding to 5 % $O_2$ in the dry flue gas to a 50 % $O_2/CO_2$ oxidant mixture with an oxygen excess corresponding to 2.4 % $O_2$ in the dry flue gas would yield an approximately 13 % decrease in the required oxygen demand, as shown below.

$$\begin{aligned} O_{2,\,\text{saved}} &= \frac{F_{O_2,\,\text{Oxy }30/5} - F_{O_2,\,\text{Oxy }50/2}}{F_{O_2,\,\text{Oxy }30/5}} \\ &= \frac{\lambda_{30/5} - \lambda_{50/2}}{\lambda_{30/5}} \\ &= \frac{1.21 - 1.05}{1.21} = \mathbf{13}\ \% \end{aligned} \tag{5.16}$$

Compared to the coal case described previously which had a potential of a 2 % reduction in oxygen production demand, the 13 % reduction in oxygen demand shown here implies a great potential in favour of the oxyfuel technology.

#### 5.2.2.1 Implications of Major Changes to OxyFuel Combustion Conditions

The change of the operating conditions described above has a number of implications on the combustion process. First of all, the increase in the initial oxygen concentration in the reactor yields a smaller flue gas volume flow and

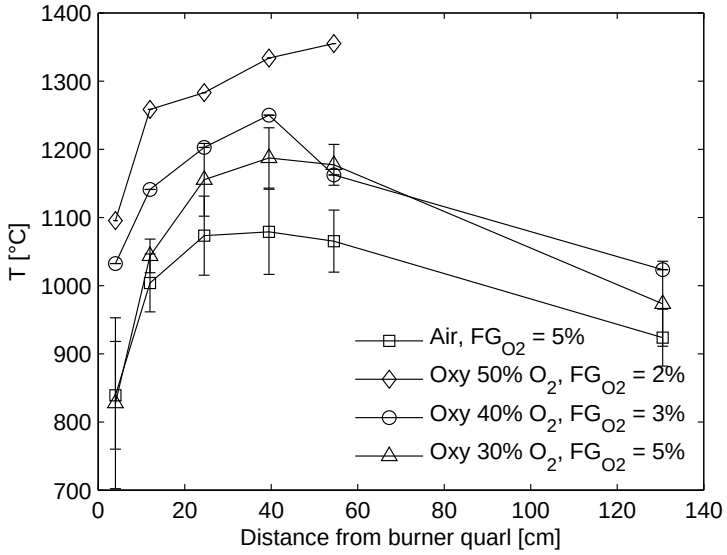


Figure 5.15: Reactor centre temperature profiles measured with S-type thermocouple for pure straw combustion in air and oxyfuel atmospheres with different inlet oxygen concentrations and stoichiometry. Errorbars correspond to two times the standard deviation for repeated measurements.

hence an increased residence time for the fuel particles within the reactor as seen in Figure 5.14 on the preceding page. The increase in residence time is one of the important factors necessary for keeping a satisfying burnout efficiency even though the oxygen excess is decreased.

The increasing oxygen partial pressure in the flame zone has a significant impact on the flue gas temperature in the furnace. Figure 5.15 shows reactor centre temperature profiles for the investigated combustion conditions. A flame temperature difference of about 300 °C is observable between air combustion and combustion in 50 % $O_2/CO_2$. This temperature increase will aid the fuel conversion rate but at the same time, it is a critical parameter with respect to full-scale boilers. Significantly increased temperatures in the radiative section of the boiler could lead to problems with the boiler walls as these are not capable of withstanding these higher temperatures without tube failures. Protection of the boiler materials could prove necessary, *e.g.* by recirculating cold flue gas close to the walls. This protection strategy would decrease the overall residence time in the boiler and could thus reduce the burnout efficiency.

The effect of varying oxidant composition and stoichiometry on emissions is shown in Figure 5.16 on the next page. The change from air combustion to combustion in a 30 % $O_2/CO_2$ oxidant leads to a decrease in NO emission. Increasing the oxygen concentration at the inlet from 30 to 40 % and decreasing oxygen excess yields a further decrease of the NO emission without any change to CO or $SO_2$

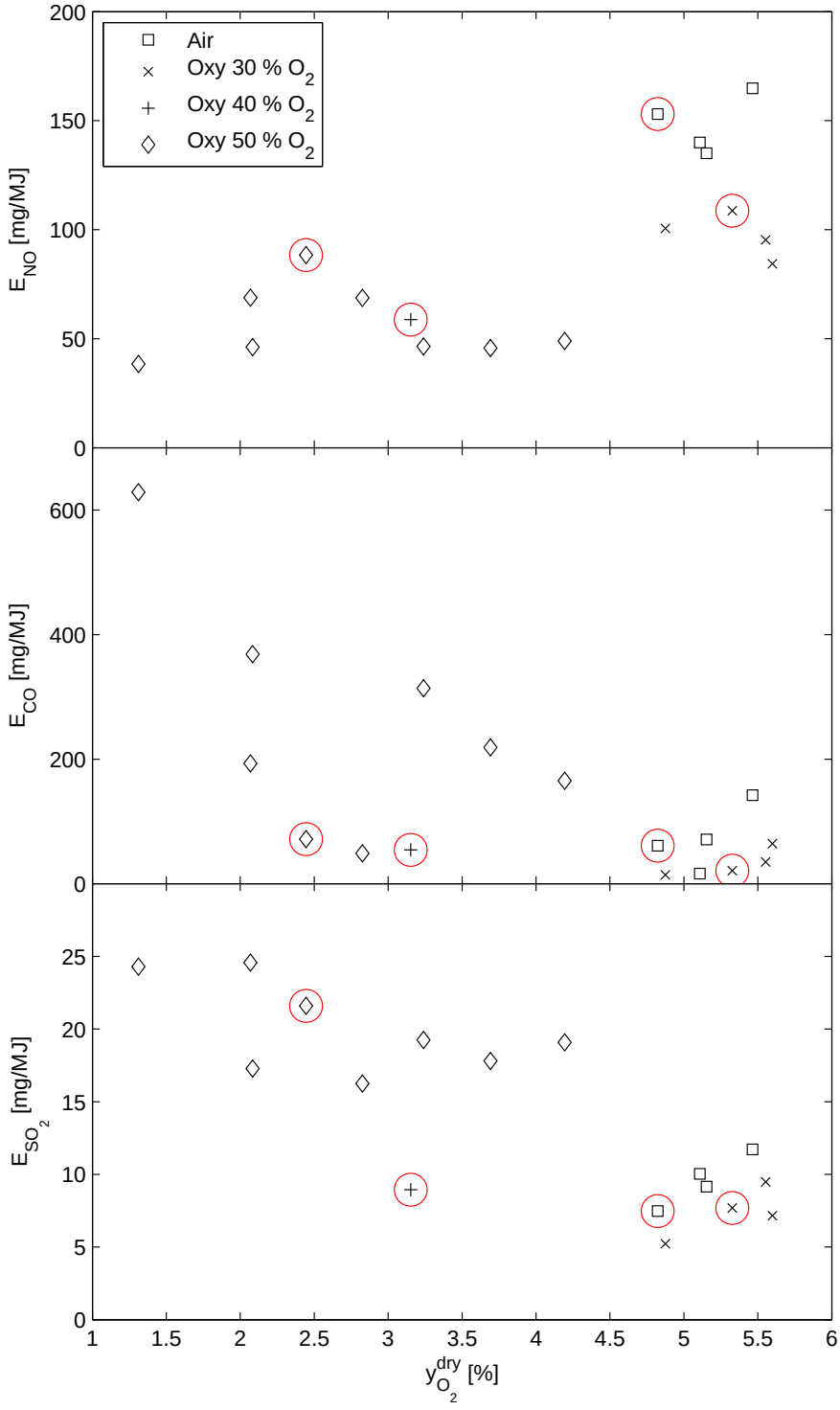


Figure 5.16: Comparison of the emission rate of NO, CO, and $SO_2$ for straw combustion in air and oxyfuel atmospheres with varying oxidant compositions and stoichiometries. The points marked with red circles are the experiments with fly ash sampling.

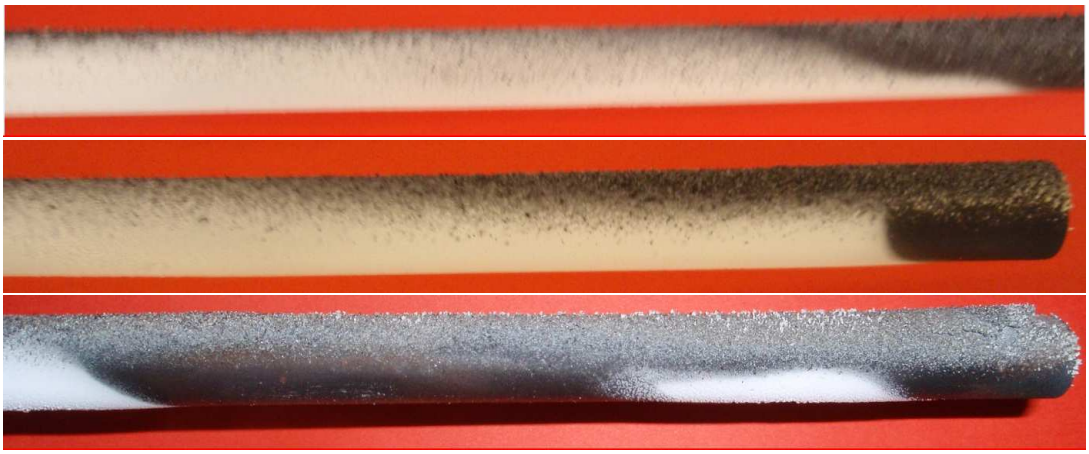

Figure 5.17: Sideview of deposits. The deposit probe has a diameter of 16 mm. Top: Straw combustion in air; Middle: Straw combustion in 30 % $O_2/CO_2$; Bottom: Straw combustion in 40 % $O_2/CO_2$. Colour differences are a consequence of the picture recording.

emissions. The experiments performed with 50 % $O_2$ at the inlet show no clear trend in NO and CO emissions. This is a consequence of necessary changes to the individual burner flow settings (increasing ratio of primary oxidant to total oxidant and decreasing secondary axial flow) in order to stabilize the flame. The high CO emissions cover high frequencies of CO peaks due to instabilities in the transport of the solid fuel through the burner. Increasing the primary oxidant flow lead to less frequent CO peaks due to more smooth fuel feeding. The fly ash was sampled at conditions with low CO emission but increased NO emission compared to the combustion with 40 % $O_2$ at the inlet. However, the NO emission does not exceed the value for the reference state with 30 % $O_2$ at the inlet. There seems to be a higher $SO_2$ emission for the experiments with 50 % $O_2$ at the inlet but all levels are very low and in reality within the measurement uncertainty.

Besides fly ash, a deposit sample was collected for all but the Oxy 50/2 conditions. The visual appearance of the deposits is seen in Figure 5.17. For all conditions the deposit on the upstream part of the probe is dominated by residual ash particles reaching the surface and sticking to the thin, soft layer of condensed salts build up following the insertion of the probe in the reactor. For the air and Oxy 30/5 deposits a large fraction of the upstream deposit is white. This is not the case for the Oxy 40/3 conditions which is assumed to be a consequence of the higher flue gas temperature. For all combustion conditions the upstream part of the deposit is highly sintered and increasingly difficult to remove as the oxygen concentration was increased. Condensation of salts on the downstream part of the probe is seen to be almost equally distributed along the probe for the air and Oxy 30/5 conditions whereas for the Oxy 40/3 conditions areas without

Table 5.2: Average deposit fluxes as well as flue gas and deposit probe temperatures for straw combustion in air and oxyfuel atmospheres for an exposure time of 2 hr.

| Oxidant | Upstream [g/m$^2$·hr] | Downstream [g/m$^2$·hr] | Average [g/m$^2$·hr] | $T_{probe}$ [℃] | $T_{FG}$ [℃] |
|---|---|---|---|---|---|
| Air | 102 | 15 | 59 | 500 | 940 |
| Oxy 30/5[a] | $206 \pm 35$ | $14 \pm 7$ | $110 \pm 21$ | 500 | $970 \pm 30$ |
| Oxy 40/3 | 295 | 16 | 156 | 500 | 1025 |

[a] Average ± two standard deviations for two repetitions (exp SO02 and SO04)

condensation is observed. The absence of condensed salts in the latter case is most likely due to differences in the flue gas flow conditions around the probe since the temperature difference across the probe is small.

Table 5.2 shows the calculated deposit fluxes based on the collected samples. A significant increase in the average fluxes are seen with each change in combustion conditions. Part of the explanation to the increase is the increase in flue gas temperature at the deposit sampling position, $T_{FG}$. From air combustion to Oxy 30/5 the temperature increases about 30 ℃ and a further increase of about 60 ℃ is again seen with the change to Oxy 40/3. The increase in gas phase temperature will increase the stickiness of the ash particles and hence increase the deposition on the upstream part of the probe. Within the experimental uncertainty, no change to the downstream deposit flux (condensation) can be observed.

### 5.2.3 Summary and Conclusions

The potential for improving the process economy of an oxyfuel power plant by reducing the overall level of excess oxygen for combustion has been investigated. The investigation covered experiments with pure coal and pure straw combustion in air and oxyfuel atmospheres with varying oxidant composition and oxygen excess level.

For the case of matching flame temperature between air and oxyfuel atmospheres (30 % $O_2/CO_2$) it has been shown with coal as fuel that similar burnout to the air reference can be achieved in the swirl burner setup during oxyfuel combustion with lower oxygen excess level. A potential decrease in oxygen demand of 2 % was determined for these conditions and no problems regarding pollutants emissions were observed.

Advantage was taken of the fact that the oxidant oxygen concentration and the oxygen excess level can be fixed independently during oxyfuel combustion during a series of experiments with pure straw as fuel. The inlet oxygen concentration was increased in two steps from 30 % to 40 and 50 % and the oxygen excess level was decreased from 5 % in the dry flue gas to 3 and 2.4 %. Loss-on-ignition analysis on fly ash samples showed that comparable burnout was obtained for

all three combustion conditions and the potential decrease in oxygen demand for the combustion process was about 13 % for the swirl burner setup. Compared to the coal experiments, significant differences to the combustion fundamentals were observed for this strategy. Flame temperatures and, as a results of higher temperature, deposit fluxes increased significantly with increasing inlet oxygen concentration. Both aspects could impose challenges to full-scale oxyfuel power plants and further investigations are needed in order to determine whether this would be ditrimental to this strategy for reducing the process operating costs. The emission rates of NO, $SO_2$, and CO did not change with the change in combustion conditions. However, it is questionable if significant thermal $NO_x$ formation could be avoided in a full-scale plant with a considerably larger degree of false air ingress to the high-temperature zones for the case of the very high inlet oxygen concentration.

# Chapter 6

# Conclusions

The results reported in this thesis cover five important aspects with respect to the operation of a power plant, both the conventional air-blown type and oxyfuel combustion plants; (1) Combustion fundamentals, including in-furnace temperature profiles and burnout; (2) Emissions of polluting species (NO, $SO_2$, and CO); (3) Quality of residual products, here only fly ash is considered; (4) Slagging and fouling, focusing on the deposit formation propensities and deposit composition for different fuels at different operating conditions; (5) Process economics, targeting the area of an oxyfuel power plant with the largest potential of reducing operating expenses – the oxygen demand.

The above areas have been investigated experimentally in a once-through, 30 kW semi-technical scale setup which simulates combustion in suspension-fired boilers. Four different fuels have been applied; a pulverized, bituminous Colombian coal; pulverized, Danish cereal straw pellets; and two coal/straw blends with straw shares of 20 and 50 wt%. The fuels have been burned in air and synthetic $O_2/CO_2$ mixtures simulating recirculation of dry flue gas in an oxyfuel power plant.

### Combustion Fundamentals

A match of flue gas temperature profiles and burnout efficiency was obtained for combustion of the bituminous coal in air and an 30 % $O_2/CO_2$ mixture at an oxygen level of 5 % in the dry, exit flue gas. At these conditions the burnout efficiency was sufficiently high ($> 99.5$ %) in order for the fly ash to be comparable to fly ash from full-scale power plants.

Co-firing coal with straw and combustion of pure straw yields significant changes to the combustion conditions compared to the case with pure coal as fuel. For very high straw shares ($> 50$ %) the flue gas temperature decreases significantly due to delayed ignition and hence, the flame length increases significantly. The occurence of large straw particles (originating from straw nodes) travelling almost unconverted through the experimental setup leads to a decrease

in burnout efficiency, from 99.5 to 98.9 % for combustion in air and from 99.8 to 99.3 % during oxyfuel combustion.

### Emissions

Whereas no significant change to the CO and $SO_2$ emissions are associated with the change in combustion atmosphere, the emission rate of NO was reduced 35 % on average during oxyfuel combustion compared to the conventional air-firing. Three mechanisms were suggested to explain this reduction; increased internal NO reduction due to reduced dilution of NO in the gas phase, increased reduction of NO over char promoted by high CO levels in the flame, and the influence of high concentrations of $CO_2$ on the radical pool promoting reduction of NO when fuel and oxidant are mixed at oxidizing conditions.

Also, the change in fuel type affects the emission rates of NO and $SO_2$. For a given combustion atmosphere increasing the straw share of the fuel reduces both NO and $SO_2$ emission rates. For NO this is in accordance with the decreasing Fuel-N content with increasing fuel straw share. At the same time, the Fuel-N to NO conversion ratio increases with decreasing Fuel-N content due to the reduced reduction of NO in the gas phase from other gaseous N-containing species. The relative difference in the NO emission between air and oxyfuel combustion increases with increasing fuel straw share. The reduced emission of $SO_2$ with increasing fuel straw share is a consequence of a higher availability of water soluble potassium in fly ash and deposits capable of capturing $SO_2$ from the gas phase. A linear correlation between the Fuel-S to $SO_2$ conversion ratio and the Fuel-S content on LHV basis as well as the K/Si ratio of the fuel was observed.

The effect of the plant configuration, *i.e.* the position of the withdrawal of flue gas for recirculation downstream of the boiler, on the emission of NO and $SO_2$ was investigated. Recirculation of untreated flue gas was simulated by doping NO and $SO_2$ to the oxidant in different amounts. The results showed that about 75 % reduction of the NO emission rate compared to air-firing could be obtained while the presence of high levels of $SO_2$ within the boiler will increase the capture of sulphur ($SO_3$) in the fly ash and deposits by up to 100 %. However, less than 5 % of the recirculated $SO_2$ is removed from the gas-phase due to capture by solid phases.

### Fly Ash Quality and Deposit Formation

One of the main concerns regarding the oxyfuel combustion technology is the risk of compromising the fly ash quality with respect to its applicability as an additive in concrete production. In this respect, the most often suggested plant configuration with recirculation of flue gas prior to desulphurization induces a risk of increasing the amount of sulphur in the fly ash above the permissible level of 3 wt% $SO_3$. The results obtained in this work show that simulating a recirculation

of $SO_2$ to the boiler yielded an increase of about 60 % in the amount of sulphur captured in the fly ash. The applied coal has a relatively low sulphur content (0.62 wt%, as received) and even with the increased retention (1.6 wt% $SO_3$ in the fly ash), the requirements could be met with considerable margin.

Co-firing of coal with straw has significant effects on the fly ash quality. Compared to the applied coal the straw has a markedly different content of K, Ca, Al, S, and Cl. A considerable increase in the corrosion potential is observed due to formation of water soluble alkali and alkali earth sulphates and chlorides in the ash with increasing straw share above 20 wt%.

A comparison of the fly ash data from this work to data from full-scale boilers co-firing coal and straw showed good agreement with respect to the capture of potassium in water soluble form in the fly ash. However, deviations were observed with respect to the degree of sulphation of the fly ash with full-scale plants achieving a higher amount of $K_2SO_4$ in the fly ash than the semi-technical setups applied in this work and reported in literature.

Similar deposition propensities have been found for co-firing coal with 20 to 50 wt% straw in each combustion atmosphere. However, significantly increased flux to the deposit probe was observed for combustion of pure straw. The deposit also became more sintered and difficult to remove. The change from combustion in air to oxyfuel combustion increased the deposition rate, most likely due to higher flue gas temperatures at the sampling position. High in-furnace levels of $SO_2$ during oxyfuel combustion lead to increased sulphation of coal deposits.

### Process Economics

The production of near-pure oxygen for oxyfuel power plants constitutes the single-largest penalty to the operating expenses. An investigation was made which showed that it is possible to reduce the excess oxygen level during combustion, and hence the operating costs, by increasing the concentration of oxygen at the burners. For example, the oxygen excess could be reduced to 2.4 % in the exit flue gas at an inlet $O_2$ concentration of 50 vol% while obtaining a burnout of 99.6 % during pure straw combustion. The change to the oxidant composition therefore did not compromise the fuel burnout and further did not increase the emission rates of NO and $SO_2$. It did, however, induce significant changes to the in-furnace temperature profile and increased the rate of deposition of ash on cooled surfaces. Further investigations are needed in order to determine the potential of this strategy for reducing the operating expenses for the oxyfuel process.

### Implications for OxyFuel Combustion

An incentive to the execution of this work was to investigate whether any show-stoppers regarding the oxyfuel combustion technology could be identified. A

number of critical aspects were found from which the potential changes to the combustion conditions have been investigated experimentally. The main concerns were associated with the risk of increased fire-side corrosion and the risk of a reduction in fly ash quality.

The results from this work has not brought forth any disqualifying characteristics of the oxyfuel combustion process rendering it unsuited for implementation as carbon capture technology in suspension-fired power plants.

# Chapter 7

# Suggestions for Further Work

This work has shown that it is indeed possible to achieve similar combustion conditions with air and an $O_2/CO_2$ mixture as oxidant. In order to further investigate the applicability of the oxyfuel combustion technology in large scale for carbon capture the following areas are of interest:

- The effect on burnout efficiency when solid fuels burned in the oxyfuel atmosphere are subject to similar residence times within the furnace as found during air-firing. This will be of interest in relation to design of green-field plants where a reduced boiler size typically is suggested.
- More detailed studies on the sulphur chemistry:
  - Closure of the sulphur mass balance during recirculation of high levels of $SO_2$. Closure of sulphur balances is typically very difficult and further work could be performed in order to understand the deviations observed in this work.
  - The effect of changes to the fuel (coal) ash composition with respect to the capture of sulphur by fly ash and deposits. Fly ash from combustion of coals with high alkali and sulphur contents could potentially exceed the limit for sulphur regarding its applicability in concrete if flue gas is recirculated to the boiler prior to desulphurization.
  - The impact of wet versus dry flue gas recycling on the sulphur uptake in fly ash and deposits.
- Even though the $NO_x$ chemistry of oxyfuel combustion has been intensively studied the specific mechanisms responsible for the differences observed between combustion in air and oxyfuel atmospheres and their relative importance have not been completely established.
- The observed differences in deposition propensity for the two combustion atmospheres are worth further analysis since slagging and fouling are of great importance to the operation of full-scale boilers.

- Due to the ongoing efforts to replace coal with biomass in power plants more research into all of the areas investigated in this work should be further elucidated. Especially co-firing at high straw shares ($> 50$ wt%) in suspension-fired boilers is relatively unexplored and the results obtained in this work have shown interesting trends regarding ash and deposits chemistry.

- The initial work on a potential improvement of the process economy of an oxyfuel power plant by reducing the demand for oxygen shown in this work needs further investigations, amongst others on the consequence to the boiler heat uptake, deposit formation, emission levels, etc. The investigations should aid in the determination of whether this strategy should be pursued further.

- The flame mappings – temperature and gas phase composition measurements – conducted during this work are well suited for validation of *e.g.* Computational Fluid Dynamics (CFD) models of the oxyfuel combustion process. A validated model is an important tool in the design process for plant retrofits or new-builds.

# Bibliography


[1] Energy Agency (IEA) International. *World Energy Outlook 2007 – China and India Insights*. IEA Publications, 2007.

[2] Energy Agency (IEA) International. *World Energy Outlook 2008*. IEA Publications, 2008.

[3] K Kavouridis and N Koukouzas. Coal and sustainable energy supply challenges and barriers. *Energy Policy*, 36(2):693–703, 2008.

[4] BJP Buhre, LK Elliott, CD Sheng, RP Gupta, and TF Wall. Oxy-fuel combustion technology for coal-fired power generation. *Prog Energy Combust Sci*, 31(4):283–307, 2005.

[5] TF Wall. Combustion processes for carbon capture. *Proc Combust Inst*, 31 (1):31–47, 2007.

[6] S Solomon, D Qin, M Manning, Z Chen, M Marquis, KB Averyt, M Tignor, and HL Miller, editors. *IPCC, 2007: Climate Change 2007: The Physical Science Basis. Contribution of Working Group I to the Fourth Assessment Report of the Intergovernmental Panel on Climate Change*. Cambridge University Press, Cambridge, United Kingdom and New York, NY, USA, 2007.

[7] S Bachu. $CO_2$ storage in geological media: Role, means, status and barriers to deployment. *Prog Energy Combust Sci*, 34(2):254–73, 2008.

[8] J Davison. Performance and costs of power plants with capture and storage of $CO_2$. *Energy*, 32(7):1163–76, 2007.

[9] Y Tan, KV Thambimuthu, MA Douglas, and R Mortazavi. Oxy-fuel combustion research at the CANMET Energy Technology Center. *Proc 2003 5th Int Symp Coal Combust*, pages 550–4, 2003.

[10] K Jordal, M Anheden, J Yan, and L Strömberg. Oxyfuel combustion for coal-fired power generation with $CO_2$ capture – opportunities and challenges. *The 7th International Conference on Greenhouse Gas Control Technologies (GHGT-7). Vancouver, Canada, September*, 2004.

[11] PHM Feron and CA Hendriks. $CO_2$ capture process principles and costs. *Oil Gas Sci Technol*, 60(3):451–9, 2005.

[12] R Tan, G Corragio, and S Santos. Oxy-Coal Combustion with Flue Gas Recycle for the Power Generation Industry – A Literature Review. Study Report, IFRF Doc. No. G 23/y/1, International Flame Research Foundation (IFRF), Velsen Noord, The Netherlands, September 2005.

[13] JN Knudsen, P-J Vilhelmsen, JN Jensen, and O Biede. First year operating experience with a 1 t/h $CO_2$ absorption – pilot plant at Esbjerg coal-fired power plant. *VGB Powertech*, 87(3):57–61, 2007.

[14] JD Figueroa, T Fout, S Plasynski, H McIlvried, and RD Srivastava. Advances in $CO_2$ capture technology – The U.S. Department of Energy's Carbon Sequestration Program. *Int J Greenhouse Gas Control*, 2(1):9–20, 2008.

[15] RJ Allam and CG Spilsbury. A study of the extraction of $CO_2$ from the flue gas of a 500 MW pulverised coal fired boiler. *Energy Convers Manage*, 33 (5-8):373–8, 1992.

[16] MM Abu-Khader. Recent Progress in $CO_2$ Capture/Sequestration: A Review. *Energy Sources, Part A: Recovery, Utilization, and Environmental Effects*, 28(14):1261–79, 2006.

[17] M Fischedick, W Günster, H Fahlenkamp, H-J Meier, F Neumann, G Oeljeklaus, H Rode, A Schimkat, J Beigel, and D Schüwer. Separation in Power Plants – Do Retrofits Make Sense in Existing Plants? *VGB PowerTech*, 4: 108–17, 2006. In German.

[18] J Gibbins and H Chalmers. Carbon capture and storage. *Energy Policy*, 36 (12):4317–22, 2008.

[19] M Pehnt and J Henkel. Life cycle assessment of carbon dioxide capture and storage from lignite power plants. *Int J Greenhouse Gas Control*, 3(1):49–66, 2009.

[20] MT Sander and CL Mariz. The Fluor Daniel econamine FG process: Past experience and present day focus. *Energy Convers Manage*, 33(5-8):341–8, 1992.

[21] S Reddy, J Scherffius, S Freguia, and C Roberts. Fluor's Econamine FG Plus$^{SM}$ technology – an enhanced amine-based $CO_2$ capture process. In *Proceedings of the second national conference on carbon sequestration*, Alexandria, VA, USA, May 2003. US Department of Energy National Technology Laboratory.

[22] Y Yagi, T Mimura, M Iijima, K Ishida, R Yoshiyama, and T Kamino. Improvements of carbon dioxide capture technology from flue gas. In *Greenhouse gas control technologies. Proceedings of the seventh international conference on greenhouse gas control technologies, 5–9 September 2004*, Vancouver, Canada, 2005. Oxford, UK: Elsevier Ltd.

[23] S Wegerich, A Witt, E Huizeling, and H Rode. Untersuchungen zur Nachrüstung einer $CO_2$-Abscheidetechnologie für das neue E.ON Kraftwerk Maasvlakte 3. In *39. Kraftwerktechnisches Kolloquium, October 11-12, 2007, Dresden, Germany*, 2007.

[24] J Oexmann and A Kather. Post-Combustion $CO_2$-Capture from Coal-fired Power Plants – Wet Chemical Absorption Processes. *VGB PowerTech*, 89 (1/2):92–103, 2009. In German.

[25] M Okawa, N Kimura, T Kiga, S Takano, K Arai, and M Kato. Trial design for a $CO_2$ recovery power plant by burning pulverized coal in $O_2/CO_2$. *Energy Convers Manage*, 38:123–7, 1997.

[26] H Altmann and G-N Stamatelopoulos. Steps towards the Minimisation of $CO_2$ Emissions from Coal-Fired Power Plants. *Conference and Exhibition for the European Power Generation Industry, POWER-GEN Europe 2005, Milan (Italy), June 28-30*, 2005.

[27] RK Varagani, F Châtel-Pélage, P Pranda, M Rostam-Abadi, Y Lu, and AC Bose. Performance Simulation and Cost Assessment of Oxy-Combustion Process for $CO_2$ Capture from Coal-Fired Power Plants. *The Fourth Annual Conference on Carbon Sequestration, May 2-5. Alexandria, VA*, 2005.

[28] D Singh, E Croiset, PL Douglas, and MA Douglas. Techno-economic study of $CO_2$ capture from an existing coal-fired power plant: MEA scrubbing vs. $O_2/CO_2$ recycle combustion. *Energy Convers Manage*, 44(19):3073–91, 2003.

[29] M Ewert. The Significance of Power Stations with $CO_2$ Capture in Planning Future Generation Portfolio. *VGB PowerTech*, 85(10):36–40, 2005. In German.

[30] Unknown. Chilling news for carbon capture [carbon dioxide capture process]. *Modern Power Systems*, 26(12):17–18, 2006.

[31] B Xu, RA Stobbs, V White, RA Wall, J Gibbins, M Iijima, and A MacKenzie. Future $CO_2$ Capture Technology Options for the Canadian Market. Technical Report Report No. COAL R309 BERR/Pub URN 07/1251, Doosan Babcock Energy Limited, March 2007.

[32] R Notz, N Asprion, I Clausen, and H Hasse. Selection and pilot plant tests of new absorbents for post-combustion carbon dioxide capture. *Chem Eng Research Design*, 85(A4):510–15, 2007.

[33] K Damen, M van Troost, A Faaij, and W Turkenburg. A comparison of electricity and hydrogen production systems with $CO_2$ capture and storage. Part A: Review and selection of promising conversion and capture technologies. *Prog Energy Combust Sci*, 32(2):215–46, 2006.

[34] JM Beér. High efficiency electric power generation: The environmental role. *Prog Energy Combust Sci*, 33(2):107–34, 2007.

[35] C Descamps, C Bouallou, and M Kanniche. Efficiency of an Integrated Gasification Combined Cycle (IGCC) power plant including $CO_2$ removal. *Energy*, 33(6):874–81, 2008.

[36] DK McDonald, TJ Flynn, DJ DeVault, R Varagani, S Levesque, and W Castor. 30 $MW_t$ Clean Environment Development Oxy-Coal Combustion Test Program. *The 33rd International Technical Conference on Coal Utilization and Fuel Systems, Clearwater, Florida*, 2008.

[37] M Kanniche, R Gros-Bonnivard, P Jaud, J Valle-Marcos, J-M Amann, and C Bouallou. Pre-combustion, post-combustion and oxy-combustion in thermal power plant for $CO_2$ capture. *Appl Thermal Eng*, 30(1):53–62, 2010.

[38] J Lambertz and J Ewers. Clean Coal Power – The response of power plant engineering to climate protection challenges. *VGB PowerTech*, 86(5):72–7, 2006. In German.

[39] J Gibbins and H Chalmers. Preparing for global rollout: A 'developed country first' demonstration programme for rapid CCS deployment. *Energy Policy*, 36(2):501–7, 2008.

[40] AJ Minchener. Coal gasification for advanced power generation. *Fuel*, 84 (17):2222–35, 2005.

[41] B Gericke, P Kuzmanovski, and K Nassauer. Conceptual Solutions Regarding the Influence of the Oxy-Fuel-Process on Conventional Power Plants (Konzeptüberlegungen bezüglich der Auswirkungen des Oxy-Fuel-Prozesses auf konventionelle Kraftwerksanlagen). *VGB PowerTech*, 86(10):64–72, 2006. In German.

[42] C Chen and ES Rubin. $CO_2$ control technology effects on IGCC plant performance and cost. *Energy Policy*, 37(3):915–24, 2009.

[43] LI Eide and DW Bailey. Precombustion Decarbonisation Processes. *Oil Gas Sci Technol*, 60(3):475–84, 2005.

[44] FL Horn and M Steinberg. Control of carbon dioxide emissions from a power plant (and use in enhanced oil recovery). *Fuel*, 61(5):415–22, 1982.

[45] H Herzog, D Golomb, and S Zemba. Feasibility, modeling and economics of sequestering power plant $CO_2$ emissions in the deep ocean. *Environmental Prog*, 10(1):64–74, 1991.

[46] BM Abraham, JG Asbury, EP Lynch, and APS Teotia. Coal-oxygen process provides $CO_2$ for enhanced recovery. *Oil Gas J*, 80(11):68–70, 75, 1982.

[47] S Nakayama, Y Noguchi, T Kiga, S Miyamae, U Maeda, M Kawai, T Tanaka, K Koyata, and H Makino. Pulverized coal combustion in $O_2/CO_2$ mixtures on a power plant for $CO_2$ recovery. *Energy Convers Manage*, 33(5-8):379–86, 1992.

[48] M Simmons, I Miracca, and K Gerdes. Oxyfuel Technologies for $CO_2$ Capture: A Techno-Economic Overview. *7th International Conference on Greenhouse Gas Control Technologies. Vancouver, Canada, September*, 2004.

[49] F Châtel-Pélage, R Varagani, P Pranda, N Perrin, H Farzan, SJ Vecci, Y Lu, S Chen, M Rostam-Abadi, and AC Bose. Applications of Oxygen for $NO_x$ Control and $CO_2$ Capture in Coal-Fired Power Plants. *Thermal Sci*, 10(3): 119–42, 2006.

[50] M Anheden, J Yan, and G De Smedt. Denitrogenation (or Oxyfuel Concepts). *Oil Gas Sci Technol*, 60(3):485–95, 2005.

[51] DJ Dillon, RS Panesar, RA Wall, RJ Allam, V White, J Gibbins, and MR Haines. Oxy-Combustion Processes for $CO_2$ Capture from Advanced Supercritical PF and NGCC Power Plant. *7th International Conference on Greenhouse Gas Control Technologies. Vancouver, Canada, September*, 2004.

[52] DJ Dillon, V White, RJ Allam, RA Wall, and J Gibbins. Oxy Combustion Processes for $CO_2$ Capture from Power Plant. Engineering Investigation Report, 2005/9, IEA Greenhouse Gas Research and Development Programme, June 2005.

[53] A Kather, M Klostermann, C Hermsdorf, K Mieske, R Eggers, and D Köpke. Konzept für ein 600 $MW_{el}$ Steinkohlekraftwerk mit $CO_2$-Abtrennung auf Basis des Oxyfuel-Prozesses. In *Kraftwerksbetrieb unter künftigen Rahmenbedingungen, 38. Kraftwerkstechnisches Kolloquium, October 24-25, 2006, Dresden, Germany*, 2006.

[54] S Rezvani, Y Huang, D McIlveen-Wright, N Hewitt, and Y Wang. Comparative assessment of sub-critical versus advanced super-critical oxyfuel fired PF boilers with $CO_2$ sequestration facilities. *Fuel*, 86(14):2134–43, 2007.

[55] LI Eide, M Anheden, A Lyngfelt, C Abanades, M Younes, D Clodic, AA Bill, PHM Feron, A Rojey, and F Giroudiere. Novel Capture Processes. *Oil Gas Sci Technol*, 60(3):497–508, 2005.

[56] MM Hossain and HI de Lasa. Chemical-looping combustion (CLC) for inherent $CO_2$ separations–a review. *Chem Eng Sci*, 63(18):4433–51, 2008.

[57] J Davison, P Freund, and A Smith. Putting Carbon Back into the Ground. Technology overview, The IEA Greenhouse Gas R&D Programme, February 2001.

[58] M Farley. Developing oxyfuel capture as a retrofit technology. *Modern Power Systems*, 26(4):20–2, 2006.

[59] MB Toftegaard, J Brix, PA Jensen, P Glarborg, and AD Jensen. Oxy-fuel combustion of solid fuels. *Prog Energy Combust Sci*, 36(5):581–625, 2010.

[60] MB Toftegaard. 045-8 Swirl Burner: Experimental Setup for Air and Oxy-fuel Combustion of Coal and Biomass – Design, Construction, and Commissioning. CHEC Report, 2011.

[61] MB Toftegaard. Introducing Biomass in Carbon Capture Power Plants: Coal and Biomass Combustion in Air and OxyFuel Atmospheres – Experimental Investigations in a Swirl Burner. CHEC Report, R003, 2011.

[62] JA Miller and CT Bowman. Mechanism and modeling of nitrogen chemistry in combustion. *Prog Energy Combust Sci*, 15(4):287–338, 1989.

[63] European Standard. EN 450-1:2005 Fly ash for concrete. Definition, specifications and conformity criteria, 2005.

[64] MB Toftegaard. Data Collection: Coal and Biomass Combustion in Air and OxyFuel Atmospheres – Experimental Investigations in a Swirl Burner. CHEC Report, 2011.

[65] S Clausen. Local measurement of gas temperature with an infrared fibre-optic probe. *Measurement Sci Technol*, 7(6):888–96, 1996.

[66] J Bak and S Clausen. FTIR emission spectroscopy methods and procedures for real time quantitative gas analysis in industrial environments. *Measurement Sci Technol*, 13(2):150–6, 2002.

[67] J Brix, MB Toftegaard, S Clausen, and AD Jensen. Advanced Diagnostics in Oxy-Fuel Combustion Processes – The Use of IR- and FTIR in Pilot- and Laboratory-Scale Reactors. Final Report, PSO project 010069, 2011.

[68] Bo Sander. DONG Energy. Personal Communication, 2010.

[69] D Fleig, K Andersson, F Johnsson, and B Leckner. Conversion of Sulfur during Pulverized Oxy-coal Combustion. *Energy Fuels*, 25(2):647–55, 2011.

[70] P Glarborg, AD Jensen, and JE Johnsson. Fuel nitrogen conversion in solid fuel fired systems. *Prog Energy Combust Sci*, 29(2):89–113, 2003.

[71] H Liu, R Zailani, and BM Gibbs. Comparisons of pulverized coal combustion in air and in mixtures of $O_2/CO_2$. *Fuel*, 84(7-8):833–40, 2005.

[72] E Croiset, K Thambimuthu, and A Palmer. Coal combustion in $O_2/CO_2$ mixtures compared with air. *Canadian J Chem Eng*, 78(2):402–7, 2000.

[73] E Croiset and KV Thambimuthu. $NO_x$ and $SO_2$ emissions from $O_2/CO_2$ recycle coal combustion. *Fuel*, 80(14):2117–21, 2001.

[74] T Mendiara and P Glarborg. Ammonia chemistry in oxy-fuel combustion of methane. *Combust Flame*, 156:1937–49, 2009.

[75] T Mendiara and P Glarborg. Reburn Chemistry in Oxy-fuel Combustion of Methane. *Energy Fuels*, 23(7):3565–72, 2009.

[76] P Overgaard, B Sander, H Junker, K Friborg, and OH Larsen. Two Years' Operational Experience and Further Development of Full-Scale Co-Firing of Straw. In *2nd World Conference and Exhibition on Biomass for Energy, Industry and Climate Protection, Rome, Italy*, 2004.

[77] LS Pedersen, HP Nielsen, S Kiil, LA Hansen, K Dam-Johansen, F Kildsig, J Christensen, and P Jespersen. Full-scale co-firing of straw and coal. *Fuel*, 75(13):1584–90, 1996.

[78] B Sander and K Wieck-Hansen. Full-Scale Investigations on Alkali Chemistry and Ash Utilisation by Co-Firing of Straw. In *14th European Biomass Conference, Paris, France*, pages 1131–34, 2005.

[79] LA Hansen. *Melting and Sintering of Ashes*. PhD thesis, Department of Chemical Engineering, Technical University of Denmark, 1998.

[80] Y Zheng, PA Jensen, AD Jensen, B Sander, and H Junker. Ash transformation during co-firing coal and straw. *Fuel*, 86(7):1008–20, 2007.

[81] M Montgomery and OH Larsen. Field test corrosion experiments in Denmark with biomass fuels. Part 2: Co-firing of straw and coal. *Materials Corrosion*, 53(3):185–94, 2002.

[82] DR Lide (editor-in chief). *Handbook of Chemistry and Physics*. CRC Press, 85th edition, 2004-2005.

[83] P Glarborg. Hidden interactions – Trace species governing combustion and emissions. *Proc Combust Inst*, 31(1):77–98, 2007.

[84] H Liu, R Zailani, and BM Gibbs. Pulverized coal combustion in air and in $O_2/CO_2$ mixtures with $NO_x$ recycle. *Fuel*, 84(16):2109–15, 2005.

[85] A Jensen. Heating and devolatilization of coal particles. note, Department of Chemical Engineering, Technical University of Denmark, 1997.

# Appendix A

# OxyFuel combustion of solid fuels (Review Paper)

Progress in Energy and Combustion Science 36 (2010) 581–625

Contents lists available at ScienceDirect

Progress in Energy and Combustion Science

journal homepage: www.elsevier.com/locate/pecs

# Oxy-fuel combustion of solid fuels

Maja B. Toftegaard [a,b], Jacob Brix [a], Peter A. Jensen [a], Peter Glarborg [a], Anker D. Jensen [a,*]

[a] Department of Chemical and Biochemical Engineering, Technical University of Denmark, DK-2800 Kgs. Lyngby, Denmark
[b] DONG Energy, Kraftvaerksvej 53, DK-7000 Fredericia, Denmark

ARTICLE INFO

*Article history:*
Received 15 May 2009
Accepted 10 February 2010
Available online 31 March 2010

*Keywords:*
Carbon capture and storage
Oxy-fuel combustion
Coal
Biomass
Emissions

ABSTRACT

Oxy-fuel combustion is suggested as one of the possible, promising technologies for capturing $CO_2$ from power plants. The concept of oxy-fuel combustion is removal of nitrogen from the oxidizer to carry out the combustion process in oxygen and, in most concepts, recycled flue gas to lower the flame temperature. The flue gas produced thus consists primarily of carbon dioxide and water. Much research on the different aspects of an oxy-fuel power plant has been performed during the last decade. Focus has mainly been on retrofits of existing pulverized-coal-fired power plant units. Green-field plants which provide additional options for improvement of process economics are however likewise investigated. Of particular interest is the change of the combustion process induced by the exchange of carbon dioxide and water vapor for nitrogen as diluent. This paper reviews the published knowledge on the oxy-fuel process and focuses particularly on the combustion fundamentals, i.e. flame temperatures and heat transfer, ignition and burnout, emissions, and fly ash characteristics. Knowledge is currently available regarding both an entire oxy-fuel power plant and the combustion fundamentals. However, several questions remain unanswered and more research and pilot plant testing of heat transfer profiles, emission levels, the optimum oxygen excess and inlet oxygen concentration levels, high and low-temperature fire-side corrosion, ash quality, plant operability, and models to predict $NO_x$ and $SO_3$ formation is required.



**Contents**



* Corresponding author. Tel.: +45 4525 2841; fax: +45 4588 2258.
*E-mail address:* aj@kt.dtu.dk (A.D. Jensen).

0360-1285/$ – see front matter © 2010 Elsevier Ltd. All rights reserved.
doi:10.1016/j.pecs.2010.02.001

## 1. Introduction

The world, and especially the developing countries such as China and India, is facing an increasing growth in the demand for electrical power [1,2]. New power plants are thus being constructed at a considerable rate in order to keep up with this demand [1–3]. The majority of the recently constructed and planned power plants, on a world-wide basis, are coal-fired [1,2]. Coal is a cheaper and more abundant resource than other fossil fuels such as oil and natural gas while at the same time being a very reliable fuel for power production [4,5].

In the developed countries an increasing part of the energy consumption is being produced from renewable sources of energy; wind, biomass, solar, hydro power, etc. [1]. The main purpose of the shift from a fossil fuel based production to renewable energy is to decrease the emission of greenhouse gases. Especially the emission of $CO_2$ from the combustion of fossil fuels has gained great focus in recent years in connection with the discussions of global warming. Since the beginning of the industrialization in the late part of the 18th century the amount of $CO_2$ in the atmosphere has increased sharply from about 280 to 380 ppm [6], see Fig. 1.

Table 1 lists the current and projected $CO_2$ emissions, in Gton carbon per year, from power generation (both electricity and heat) [1]. Both the emissions and the coal share of the emissions are seen to increase toward 2030 for the world as a whole. Even though the $CO_2$ emissions are seen to increase within Europe the percentage increase is much less pronounced than for the rest of the world and the coal share of the emissions is expected to decrease. Despite the fact that the ultimate goal for most countries is to phase out all fossil fuels in heat and power production as well as in the transport sector, the share of renewable energy sources increases only slowly and the world will depend on fossil fuels for many years to come. A rapid move away from fossil fuels could result in great conflicts concerning water and land use between biomass for energy production, food production, and forestation [7] as well as in serious disruption to the global economy [8]. The latter is mainly caused by the long lifetime of the energy supply infrastructure. In the transitional period, technologies are sought which will enable the continuous usage of fossil fuels but at the same time eliminate the emission of $CO_2$.

### 1.1. Carbon capture and storage

Since power plants constitute large point sources of $CO_2$ emission the main focus is related to their operation. Currently,

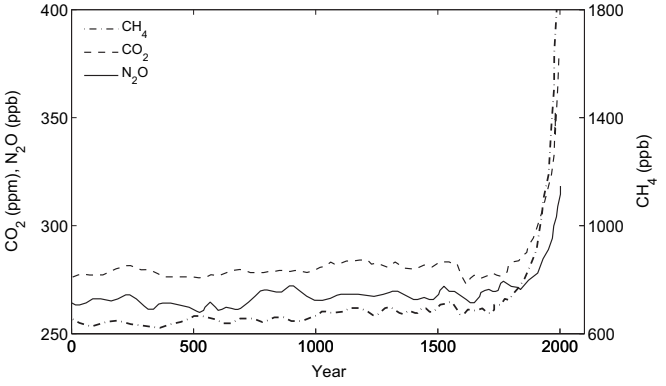


**Fig. 1.** Development in the concentrations of important long-lived greenhouse gases in the atmosphere over the last 2000 years. The increases in concentrations since about year 1750 are attributed to human activities in the industrial era. Data taken from [6].

**Table 1**
Estimated $CO_2$ emissions from power generation (Gton C/year). The numbers in parenthesis indicate the percentage coal share of the emissions. Data taken from [1].

| Region | 2005 | 2015 | 2030 |
|---|---|---|---|
| World | 3.0 (72) | 4.0 (74) | 5.1 (74) |
| European Union | 0.38 (70) | 0.39 (66) | 0.42 (61) |

several possible technologies are being investigated which will enable the so called Carbon Capture and Storage (CCS) from power plants [5,8–14]. Both researchers in universities and other research institutions, most manufacturers of boilers and other power plant related equipment, and many power companies are active. CCS will act as a complimentary technology to the ongoing work related to increasing fuel efficiency and the change toward fuels with lower fossil carbon content, e.g. natural gas and/or biomass. As indicated by the term CCS, the elimination of $CO_2$ emissions include two consecutive operations:

1. Capture of $CO_2$ from the power plant flue gas
2. Storage of the $CO_2$ (incl. transport to storage site)

The estimated cost of separation, capture, and compression of $CO_2$ (point 1) from power plants or other point sources accounts for around 75% of the total cost of a geologic sequestration process [11,15–17].

### 1.2. Carbon storage technologies overview

The disposal technology should ensure a complete elimination of the $CO_2$ from the earth's carbon cycle in order to stabilize the $CO_2$ concentration in the atmosphere. Two types of disposal are defined: sequestration (permanent disposal) or storage (disposal for a significant time period) [7]. These terms are often interchanged in the sense that time periods of more than the order of 10,000 years are considered permanent. Possible storage methods suggested include injection in e.g. depleted oil and gas reservoirs, coal beds, deep saline aquifers, etc. [7,11,17–24]. The estimated storage potential for the suggested options is given in Table 2.

When $CO_2$ is injected below the caprock in oil and gas reservoirs as well as deep saline aquifers it is first trapped by static and hydrodynamic mechanisms. Secondary trapping mechanisms begin operating over time and act to immobilize the $CO_2$ in the reservoir, thereby significantly limiting the risk of leakage [7,15,24–26]. This type of storage is considered secure even in the initial injection phase where the secondary trapping mechanisms contribute only minimally [7].

The large storage potential in deep aquifers without structural traps is only obtainable if the traps are not required for secure storage during the initial phases [19]. Even without this storage volume the remaining sites offer storage capability for potentially the next many hundred of years [19,22], see more below. According to Table 2 the estimated retention time in the underground storage sites is $10^5$–$10^6$ years. The retention time for storage in combination with enhanced oil recovery (EOR) differs between authors and ranges from only 10s of years [20,19] to permanent disposal [7].

**Table 2**
Estimated storage capacities and retention times for $CO_2$ in different types of sinks on a world-wide basis. Data taken from [7,17–22].

| Sink | Storage capacity (Gton C) | Retention time (years) |
|---|---|---|
| Enhanced Oil Recovery (EOR) | 20–65 | 10–$10^6$ |
| Deep aquifers with structural traps | 30–650 | $10^5$–$10^6$ |
| Deep aquifers without structural traps | ~14,000 | $10^5$–$10^6$ |
| Depleted oil and gas wells | 130–500 | $10^5$–$10^6$ |
| Coalbeds | 40–260 | $10^5$–$10^6$ |
| Ocean disposal | 400–1200 | 500–1000 |

Because of the limited retention times and the great risks of explosive release of $CO_2$ back into the atmosphere and/or an alteration of the ocean chemistry in the near vicinity of the disposal sites [7] ocean disposal is regarded a less attractive storage solution.

A comparison of the estimated $CO_2$ emissions from power production, Table 1, and the estimated storage capacities in EOR and saline aquifers, Table 2, yields between 75 and 6000 years of storage on a world-wide basis (2.5 Gton C/year stored). This calculation is based on the fact that due to small size and remote location of many utility plants only a limited fraction of these emissions can be captured and stored cost-effectively. Baes et al. [18] estimate this fraction to be around 50%. CCS is generally not anticipated as a permanent solution to the elimination of anthropogenic $CO_2$ emissions from electricity and heat generation. The lower limit of 75 years of storage capacity should thus be sufficient in order for the industry to change almost entirely toward renewable sources of energy.

### 1.3. Carbon capture technologies overview

The identified technologies for carbon capture can be divided into four main categories [5,11,12,23,27–30], described briefly below. Fig. 2 shows the main operations concerned with the post-, pre-, and oxy-fuel combustion technologies.

*Post-combustion capture:* $CO_2$ is separated from the flue gas of conventional pulverized-coal-fired power plants. The separation is typically performed via chemical absorption with monoethanolamine (MEA) or a sterically hindered amine (KS-1) [23,31–35]. Amine absorption is a proven technology in the process industry [23,34,36,37]. The demonstrated scale of operation is, however, significantly smaller than the typical size of power plants [34] and serious penalties to the plant efficiency exist at the current state of development [5,8,12,16,34,38–43]. The anticipated drop in the net efficiency of the power plant is about 10–14% points [41,34]. Some current research projects investigate the possibility of developing

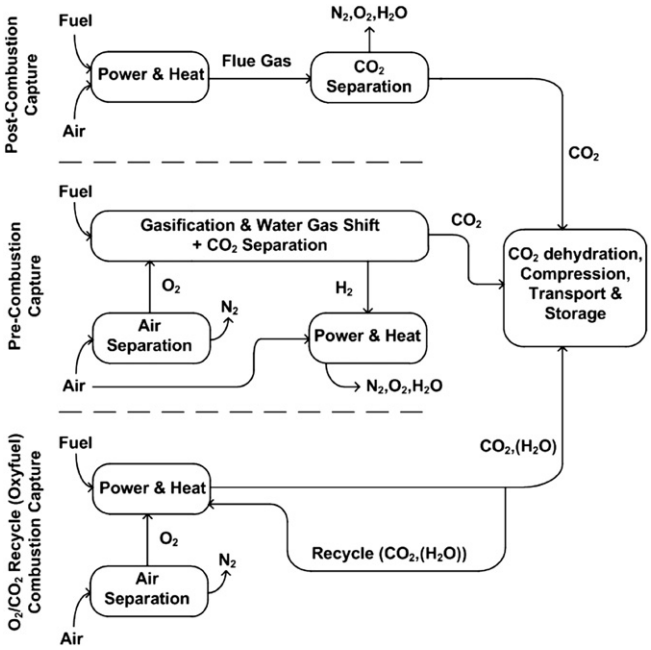


**Fig. 2.** Possible, overall plant configurations for the three main categories of carbon capture technologies. Adopted from [10].

more efficient absorbents [35]. More on the technology can be seen in [5,8,13,29,44–47].

The chilled ammonia process in which an aqueous solution of ammonia constitutes the absorbent has shown promising reductions in energy consumption in laboratory studies, up to 50%, compared to the MEA process [42]. The process benefits from low operating temperatures and precipitation of ammonium bicarbonate ($NH_4HCO_3$) yielding a higher $CO_2$ loading of the absorbent.

Retrofit to existing plants for both process types is considered relatively simple since the capture unit can be added downstream of the boiler and flue gas cleaning systems without any significant changes to the original plant [8,45]. There are, however, strict requirements for removal of $SO_2$ and $NO_2$ from the flue gas prior to the $CO_2$ capture since these components react irreversibly with the absorbent leading to its degradation.

*Pre-combustion capture:* Also termed fuel decarbonisation. The process is typically suggested to be used in connection with Integrated Gasification Combined Cycle (IGCC) power plants where it is termed IGCC–CCS. Coal gasification is applied to obtain a gas (syngas) containing CO, $CO_2$, and $H_2$. The CO is transformed into $CO_2$ by the water-gas shift reaction and can then be separated from the remaining hydrogen containing gas before this is combusted in a gas turbine. Alternatively, $H_2$ can be separated from the syngas and the CO combusted in an $O_2/CO_2$ atmosphere [48]. Some techno-economic calculations [11,30,36,49,50] show that IGCC has promising process economics and plant efficiency characteristics. However, high capital costs are associated with plant construction and IGCC plants are generally much more complicated systems than suspension-fired boilers [51,37]. Only few electricity producing IGCC units exist [29,50,52–54], none of which are equipped with CCS. As a consequence of the few plants and limited operating experience along with the highly integrated nature of the plants compared to the more matured, conventional pulverized-coal-fired power plants, the demonstrated availability for IGCC is significantly less (80–85% versus ~96%, respectively) [5,30,37,50,52,55]. IGCC–CCS is not a viable option for retrofit of existing pf plants [30,51,56,57].

*Oxy-fuel combustion:* By eliminating molecular nitrogen from the combustion medium the flue gas will consist mainly of $CO_2$ and water. The plant configuration typically suggested involves flue gas recirculation to the burners to control the flame temperature to within the acceptable limits of the boiler materials. Implementation of the oxy-fuel combustion technology in existing pulverized-coal-fired power plants will induce a larger change of the plant configuration when comparing to the post-combustion absorption processes mentioned above. This is mainly due to the fact that the combustion chemistry is altered by substituting recycled flue gas (mainly $CO_2$ and water) for nitrogen in the oxidizer. Several of the earlier techno-economic assessment studies indicate that oxy-fuel combustion should be the most energy and cost efficient of the carbon capture technologies [9,16,38,58–63]. This conclusion is mainly based on assumptions of greater boiler efficiency caused by a smaller flue gas volume and the reduced need for flue gas cleaning, i.e. de$NO_x$ and desulphurization, including the derived decrease in capital and operating costs. It is suggested that $SO_x$ and $NO_x$ can be stored along with $CO_2$ in the geospheric sinks [8,12,64,65]. Typically, no experimental validation of these assumptions has been performed. Whether co-storage of $SO_x$ and $NO_x$ is politically acceptable is, however, questionable.

The main disadvantage of the oxy-fuel combustion technology is the need for almost pure oxygen. The available large-scale technology for air separation is based on cryogenic distillation which will impose a very large energy penalty on the plant [65]. The expected efficiency drop is about 7–11 percent points, or about 15–30% of the generated electricity (net power output), depending on the initial plant efficiency [5,8,12,16,27,29,43,58,59,66–69].

*Emerging technologies:* Technologies such as membrane separation, chemical looping combustion, carbonation–calcination cycles, enzyme-based systems, ionic liquids, mineralization, etc. impose the possibility to drastically reduce the cost of electricity and the energy penalty concerned with carbon capture from power plants. The papers by Eide et al. [70], Abu-Khader [28], Hossain and de Lasa [71], and Figueroa et al. [14] provide broad overviews of these technologies and their current state of development.

The choice of technology will depend on several factors. First and foremost the economy and the expected development in plant efficiency is of importance. The maturity, expected availability, operating flexibility, retrofit or green-plant built, local circumstances, utilities preferences, etc. will likewise have to be taken into account. No general acceptance of superiority of one of the presented technologies over the others exists. Several techno-economic studies also indicate that with the current knowledge on the technologies no significant difference in cost within the limits of precision of the applied cost estimates can be determined between amine absorption capture, coal-based IGCC type capture, and oxy-fuel combustion capture [5,8,22,57,66,67,72].

Because of the large changes induced in the power plant by the implementation of oxy-fuel combustion, more research is needed to fully clarify the impacts of the introduction of this technology. Many laboratory scale investigations of the technology have been performed within the last two decades and it is generally accepted that it is possible to burn coal and natural gas in an $O_2/CO_2$ atmosphere. On the other hand, it is likewise recognized that much work still remains in obtaining sufficient insight into the effects on e.g. emissions, residual products such as fly ash, flue gas cleaning, heat transfer, etc.

In 2005, Wall and coworkers [4] published a literature review on the oxy-fuel combustion technology. The work was updated in the broader CCS review by Wall [5] in 2007. The reviews focused mainly on combustion fundamentals, overviews of research groups and their experimental facilities, techno-economic assessments of the technology, and research needs.

The amount of literature on the oxy-fuel technology has increased drastically over the latter years and significant new information is thus now available. The objective of the present review has been to summarize the current knowledge status on the oxy-fuel combustion technology. The current review has two focuses. (1) The possible advantages and challenges associated with retrofitting of existing pulverized-coal-fired power plants to the oxy-fuel combustion technology as well as considerations regarding green-field plants. (2) The reported results from laboratory- and semi-technical scale experiments regarding the combustion process fundamentals, including the flue gas composition and residual products.

## 2. The oxy-fuel combustion technology and retrofit implications

### 2.1. Process overview

In open literature, oxy-fuel combustion with recirculation of flue gas was proposed almost simultaneously by Horn and Steinberg [58] and Abraham et al. [60] in the early eighties. Abraham et al. proposed the process as a possible mean to produce large amounts of $CO_2$ for Enhanced Oil Recovery (EOR) whereas Horn and Steinberg had in mind the reduction of environmental impacts from the use of fossil fuels in energy generation. As such, the technology received renewed interest in the mid-90s in connection with the re-emerging discussions of global warming caused by increased $CO_2$ levels in the atmosphere [12].

Oxy-combustion can in principle be applied to any type of fuel utilized for thermal power production. The research interests have

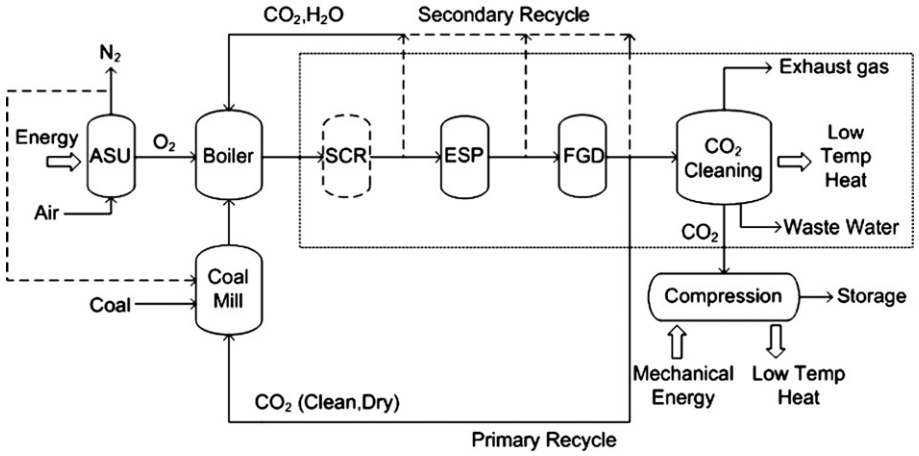


**Fig. 3.** Possible configuration of an oxy-fuel power plant. ASU: Air Separation Unit, SCR: Selective Catalytic Reduction reactor (deNOx), ESP: Electrostatic Precipitator, FGD: Flue Gas Desulphurization. Energy inputs and low-temperature-heat outputs new to the plant in case of a retrofit are indicated.

mainly been focused on coal and natural gas since these are the most abundant fuels. For these specific fuels the technology is typically termed oxy-coal and oxy-natural gas combustion, respectively. Application of CCS through oxy-combustion of biomass or blends of coal and biomass will result in a possible mean of extracting $CO_2$ from the atmosphere and thereby possibly inverting the presumed anthropogenic caused changes to the climate [11,23,30].

As indicated in Section 1.3 a shift from conventional air-firing to oxy-fuel combustion in a power plant will induce multiple changes to the plant configuration. Fig. 3 provides a sketch of a coal-fired oxy-fuel plant with indications of the major process steps and the necessary energy inputs and low-temperature-heat outputs new to the plant when retrofitting an existing coal-fired unit. The sketch covers the original state-of-the-art plant with boiler, coal mills, and flue gas cleaning equipment. The final processing of the $CO_2$ stream, i.e. the removal of water and the non-condensible gases like $O_2$, $N_2$, Ar, etc. to meet the requirements regarding purity of the $CO_2$ stream, as well as the air separation unit (ASU) and the compression step for the $CO_2$ stream before it is transported to the storage site are new to the plant. The discussion in the coming sections is based on the assumption that an underground geological formation, a saline aquifer, is used as storage site. The type of storage will have an impact on the oxy-fuel process, especially the flue gas purification units, through the quality criteria for the $CO_2$ stream.

Table 3 provides the results of our calculation on the approximate daily flows in and out of a 500 $MW_e$ oxy-fuel combustion power plant. The calculations are based on a state-of-the-art electrical efficiency of 46% of the conventional plant (supercritical steam parameters, LHV basis) [49] with a 10 percent point decrease due to oxy-fuel operation. The used reference coal is a high-volatile bituminous coal from Colombia see Table 4 for its properties. The oxygen is assumed to have a purity of 100%, in order to simplify the calculations. The combustion is performed in a mixture of 30% $O_2$ in $CO_2$ with an oxygen excess of 10%, corresponding to an oxygen concentration of 3% in the dry recycle stream. The recycle ratio for the dry flue gas is 0.75. As a preliminary assumption, the condenser will remove 100% of the water in the flue gas. The $CO_2$ capture efficiency is ~92%. The remainder of $CO_2$ is vented to the atmosphere together with the non-condensable gas species in the exhaust gas from the $CO_2$ cleaning unit. Generally, between 90 and 95% capture efficiency is expected for oxy-fuel plants [30].

The survey of the implications of retrofitting for oxy-fuel combustion in the next sections will be starting at the point of delivery of the sequestration-ready $CO_2$. The discussion will proceed with the auxiliary units new to the plant and end up with the original parts of the power plant. In order to limit the survey, the discussions, when relevant, will refer to plants utilizing bituminous and/or sub-bituminous coals. Specific aspects regarding lignite fired plants are excluded.

**Table 3**
Approximate mass streams in a 500 $MW_e$ oxy-fuel combustion power plant with an electric efficiency of 36% on a net heating value (LHV) basis.

| Stream | Mass Flow (ton/day) |
|---|---|
| Oxygen in | 9700 |
| Coal in | 4400 |
| Waste water (from condenser) | 2000 |
| Exhaust gas | 1100 |
| $CO_2$ for sequestration | 10,300 |
| $N_2$ from ASU | 31,800 |

### 2.2. $CO_2$ purity requirements

The exact requirements to the quality of the $CO_2$ stream for different storage scenarios are not yet fully clarified [30,73–75].

**Table 4**
Properties for El Cerrejon bituminous coal (Colombian).

| | |
|---|---|
| LHV, as received (MJ/kg) | 27.09 |
| Moisture, as received (wt%) | 5.0 |
| *Proximate analysis* (wt%, dry) | |
| Ash | 10.1 |
| Volatile | 36.7 |
| Fixed carbon (by difference) | 53.2 |
| *Ultimate analysis* (wt%, daf) | |
| C | 80.70 |
| H | 5.41 |
| N | 1.69 |
| S | 0.73 |
| O (by difference) | 11.47 |
| *Ash composition* (wt%, dry) | |
| Al | 10.89 |
| Ca | 1.58 |
| Fe | 5.05 |
| K | 1.78 |
| Mg | 1.39 |
| Na | 0.59 |
| P | 0.08 |
| Si | 26.73 |
| Ti | 0.53 |
| O (by difference) | 51.37 |

**Table 5**
Suggested $CO_2$ quality specifications from different sources.

| Parameter | Modest quality, aquifer storage | High quality, on-shore storage | U.S. Specifications | Saline formation |
|---|---|---|---|---|
| | Anheden et al. [76] | | Lee and Miller [77] | Fout [78] |
| Pressure | 110 bar | 110 bar | – | 150 bar |
| Temperature | 50 °C | 50 °C | <50 °C | – |
| $CO_2$ | >96 vol% | >96 vol% | >95% | Not limited[b] |
| $H_2O$ | <500 ppm | <50 ppm | <480 ppmv | 150 ppmv |
| $N_2$, Ar | <4 vol%[a] | – | <4% | Not limited[b] |
| $O_2$ | <4 vol%[a] | <100 ppm | <10 ppm | <100 ppmv |
| $SO_2$ | <200 mg/Nm$^3$ | <50 mg/Nm$^3$ | – | <3 vol% |
| $H_2S$ | – | – | <10–200 ppm | <1.3 vol% |
| $NO_x$ | – | – | – | Uncertain |
| $NH_3$ | – | – | – | Not limited |
| CO | – | – | – | Not limited |
| $CH_4$ | – | – | – | <0.8 vol% |
| HC's | – | – | <5% | <5 vol% |
| $H_2$ | – | – | – | Uncertain |
| Glycol | – | – | <0.04 ppmv | – |

[a] Sum of $N_2$, $O_2$, and Ar should be <4 vol%.
[b] No limit but the impacts on compression power and equipment cost need to be considered.

However, Table 5 provides a number of suggestions for purity requirements found in the literature.

Some authors lay down different criteria for different storage sites [76,78], the differences mainly being associated with the content of water, oxygen and $SO_2$. Lee and Miller [77] comment on the individual limits with respect to e.g. the minimum miscibility pressure ($CO_2$, hydrocarbons, and $N_2$), the risk of corrosion ($O_2$, water), as well as materials (temperature), operations (glycol), and safety ($H_2S$). Anheden [76] likewise identifies the aspects which should be taken into account when determining the individual limits. These aspects come down to operational issues, storage integrity, environmental aspects during the full lifetime of the capture and storage chain, health and safety aspects, legal aspects, and economic considerations. The authors state that the requirements arising from exposure limits in case of leakage to air put the strictest restrictions to the process and are, at the same time, the easiest to quantify. The exact requirements will most probably be determined for each individual case of capture and storage.

Jordal and coworkers [10,74] considered the optimum specifications with respect to technical and economical considerations. Not surprisingly, the optima differed. For economic reasons, the preferable option is to co-store as many of the impurities; $SO_x$, $NO_x$, non-condensable gas species, and water, as possible. This will reduce the plant investment and operating costs of the process. The disadvantage could be the requirement for more expensive materials in e.g. compressors and pipelines to withstand the potentially severely corrosive environment. There is, however, an economic optimum for the non-condensables ($N_2$, $O_2$, NO, CO, $H_2$, $CH_4$, Ar, etc.) since co-storage of these species will increase energy and reservoir size requirements as well as capital and operating expenses in the transport chain with an amount proportional to their concentrations [24,73,74]. At the same time the non-condensible gas species will entail an energy and capital penalty when removed from the $CO_2$ stream [73,74]. Technically, there are two general issues which should be considered. First, the purity requirements for transport and storage with respect to corrosion and the risk of structural changes within the storage formations caused by impurities in the $CO_2$ stream. Secondly, the limitations to the present best available technology for flue gas cleaning, i.e. particle removal, water condensation, dehydration, $SO_x$ removal and removal of non-condensible gas species, and how to minimize the loss of $CO_2$ to the atmosphere during the purification process. It is obvious that the technical considerations will set both the lower and upper limits to the purity requirements.

$SO_2$ receives the largest amount of interest with respect to the effect of contaminants on the structure of storage formations. A typical assumption regards the possibility of co-storing the $SO_2$ together with the $CO_2$ because of very similar physical and chemical properties at supercritical conditions [10,58,65,67,75,79]. However, even small amounts of $SO_2$ may cause problems due to the risk of calcium sulphate formation and thus a decreasing porosity of the reservoir rock [26,75,79,80]. Oxygen could likewise lead to the formation of precipitations [74]. On the other hand, if the concerns regarding $SO_2$ in the storage formations prove to be insignificant there would obviously be a possible economic benefit from combined capture and storage of $CO_2$ and $SO_2$ [80]. The current state of flue gas cleaning on modern power plants involves ~85% removal of $NO_x$, ~98% removal of $SO_2$, and ~99.8% removal of particulates [68,30]. The fact that only a finite percentage of the $SO_2$ is removed with the current best available technology elucidates the importance of identifying the correct purity demands through e.g. field tests since these may have a significant impact on the plant configuration, operating conditions and operating costs [43,64]. Besides the chemical effects of impurities in the $CO_2$ on the reservoir rock, $CO_2$ itself has the potential to alter the mechanical properties of the rock [26,17]. Especially calcite ($CaCO_3$) precipitation which can cement the reservoir around the injection well and render further injection impossible should be taken into consideration.

With respect to transportation the greatest concern involves the water content in the $CO_2$ stream [27,64,73,75]. In the presence of water, $CO_2$ can cause so called sweet corrosion [26,17]. Water vapor and $CO_2$ in the presence of liquid water can likewise form solid ice-like crystals known as hydrates [64,73,79,80]. Concurrent presence of both water and $SO_2$ (incl. $H_2S$) in the $CO_2$ stream will increase the risk of sulfuric acid corrosion. If the flue gas is dehydrated to a dew point 5 °C below the temperature required for transport conditions, the sulphur dioxide will behave almost as carbon dioxide in the supercritical state and the two gases should not cause any corrosion problems [26,79,80]. Others report no risk of corrosion at a dew point of less than −60 °C [66]. A requirement for a very low water content in the $CO_2$ is thus present. This can most likely not be achieved by condensation alone and drying by e.g. absorption in a recyclable dehydrant (triethylene glycol) in combination with the last compression step, see Section 2.3, will be necessary [43,65,74,79].

Some researchers believe that all the limiting factors regarding purity of the $CO_2$ stream arise from compression and transportation requirements [67,73,74]. In this respect, the demand of dryness is crucial.

Another aspect regarding the concentrated $CO_2$ stream is the legislative classification. This will depend on the content of contaminants such as $H_2S$, sulphur oxides, $NO_x$, hydrocarbons, etc. Significant quantities of these elements could mean that the stream should be regarded as a hazardous waste [7,19,64,73,74,80]. This could eventually lead to difficulties with respect to locating suitable storage sites or a large penalty concerned with the purification.

### 2.3. $CO_2$ processing

Assuming that $CO_2$ transportation should be in pipelines, the $CO_2$ must be conditioned to both pipeline and reservoir specifications, as described in the above section. Moreover, the stream must be compressed to a high enough pressure to overcome the frictional and static pressure drops and deliver the $CO_2$ at the storage site without risking flashing of gas anywhere in the process [73,75].

The typically suggested conditions of the $CO_2$ stream at the delivery point includes the following ranges of pressures and temperatures; 80–200 bar and 0–50 °C [8,11,25,27,41,56,67,74,81–84]. There is, however, a preference for 100–110 bar and a temperature above the critical value (31.1 °C), see Fig. 4. At these conditions the $CO_2$ is in the supercritical state, even though the presence of impurities will increase the critical pressure of the mixture compared to that of pure $CO_2$ [67].

#### 2.3.1. Compression step

Compression of gases is a highly energy demanding process. This step will induce one of the larger penalties to the plant efficiency in oxy-fuel operation when comparing to conventional air-firing. Generally, ~2–3% point decreases in electrical efficiency, directly associated with the compression step, have been reported [5,16,50,66,67]. Factors such as compressor efficiency, the amount of impurities in the $CO_2$-rich stream, and opportunities for integration with the remaining plant will influence the power consumption [65,85].

Since no specific new problems are expected with respect to the compression of $CO_2$, no demonstration programs are considered to be required [66].

#### 2.3.2. Removal of water and non-condensable gas species

Many existing boilers were not designed to be leak tight and may be difficult to retrofit to oxy-fuel operation where air ingress should be avoided. It is generally reported very difficult to totally avoid air ingress into even small laboratory and pilot scale burners [12,16,63,86–91] and in real size plants it will be almost impossible [62,83,92,93]. The amount of work put into tightening the boiler and flue gas passages will thus be a trade off with the power consumption of the compression unit. Air-fired boilers operate at negative gauge pressure for obvious safety reasons. To avoid air ingress in oxy-fuel boilers one could consider operation at positive gauge pressure. It is, however, questionable whether the avoidance of air ingress can counterbalance the enhanced risk of severe CO and $CO_2$ poisoning of the boiler surroundings and the necessary safety systems to avoid casualties [83]. The amount of air leaking into the boiler and flue gas ducts is believed to constitute around 3% of the flue gas mass flow (1% in boiler and 2% in ESP) [5,40,67,94] for a new-build plant. As the ingress of air typically increases over time, older boilers can have air in-leakage rates of 8–16% [65,67]. Significant air ingress will reduce the $CO_2$ concentration in the flue gas and thus result in increased costs for $CO_2$ cleaning since the non-condensable gases most likely must be removed before (or during) compression. According to Tan et al. [12] the air ingress level should be limited to about 3% in large-scale plants to obtain $CO_2$ concentrations in the flue gas which will enable an economical treatment of the $CO_2$ stream.

This additional need for clean-up, besides air separation, is potentially a significant drawback of the oxy-fuel technology compared to e.g. post-combustion capture with amine absorption which has only one purification step [95]. When the oxy-fuel technology was first proposed purification of the $CO_2$ was not discussed and has most likely not been considered necessary.

The purity of the oxygen for combustion will likewise be a trade off between the ease of liquefaction of the flue gas and the power requirement for the air separation [61,62,67]. Nakayama et al. [61] performed an investigation regarding the combined power requirement for air separation and $CO_2$ liquefaction under the assumption of no air ingress into the system. Fig. 5 shows the relationship between purity of feed oxygen and power consumption for a plant with a gross capacity of 1000 $MW_e$. According to the figure, an oxygen purity of 97.5% will require the lowest overall power consumption. Purities greater than this leads to a significant increase in the air separation energy consumption which the decreased consumption in the liquefaction step cannot counterbalance. Others report optimum purities of 95% [8,43,62,66,67,83,95] taking into account the effect of air ingress. At an oxygen purity of 95% obtained by cryogenic distillation, the

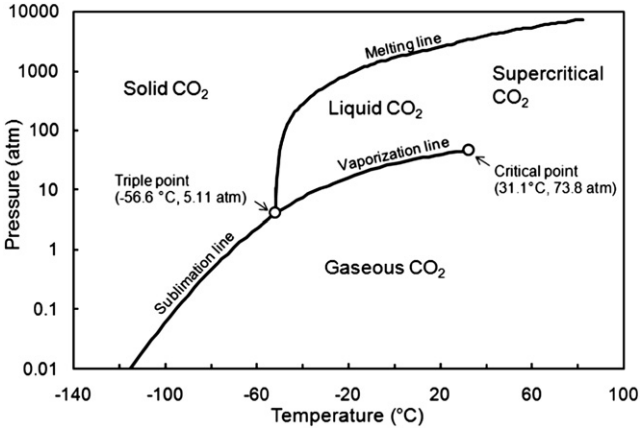


**Fig. 4.** Phase diagram for $CO_2$.

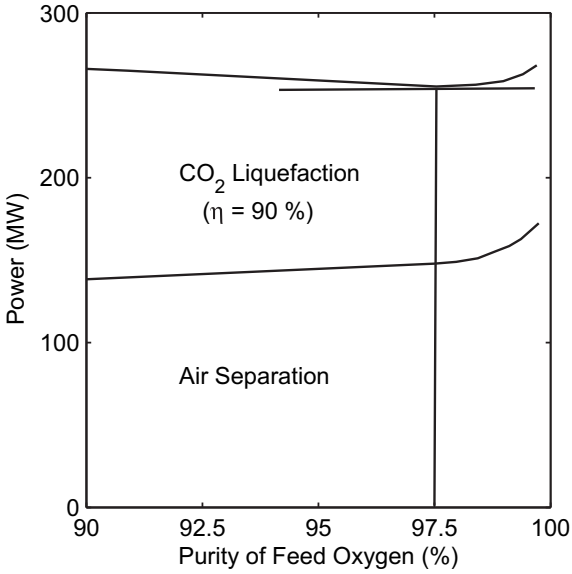


**Fig. 5.** Theoretical relationship between the purity of oxygen fed to the burners and the power consumption for air separation and $CO_2$ liquefaction in a 1000 $MW_e$ (gross) plant. Data taken from [61].

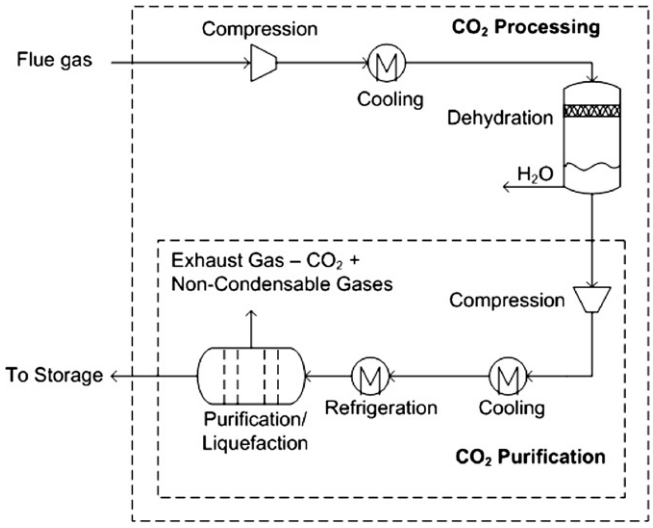


**Fig. 6.** Possible process scheme for $CO_2$ processing and purification, i.e. removal of non-condensable gas species, in an oxy-fuel power plant. Adapted from [85].

remaining impurities present will be argon (3–4 mol%) and nitrogen (1–2 mol%) [67,68]. The almost complete avoidance of nitrogen is beneficial with respect to also reducing $NO_x$ emissions.

Fig. 6 illustrates in more detail suggestions to the $CO_2$ processing and purification steps in an oxy-fuel plant. It is possible that an initial dehydration of the flue gas is performed in combination with the flue gas cleaning step before the initial compression in order to reduce the total flue gas volume and thus costs and equipment size.

After condensation of water vapor, the $CO_2$ stream will have a purity of about 70–95% depending on oxygen purity, oxygen excess, and air ingress into the boiler [4,8,16,40,43,67,91,92,96]. The condensation process will likewise serve to remove water-soluble gas phase components as well as other species with higher boiling points than $CO_2$ [74]. Some $CO_2$ will dissolve in the water and cause a loss in the capture efficiency if not regenerated [74]. If the major part of the flue gas water content is removed at relatively high temperatures and low pressures the loss of $CO_2$ can be kept low [74].

The flue gas processing and purifications system will produce three streams as indicated in Fig. 6; The $CO_2$ stream for compression and sequestration, an exhaust gas containing mainly the non-condensable gas species (Ar, $N_2$, $O_2$, CO, $NO_x$) and some $CO_2$ depending on technology, see more below, and a waste water stream originating from the condensed water.

The exhaust gas stream, around 10–20% of the dry flue gas by volume, is vented to the air. Its composition depends on the chosen cleaning process but is assumed to be about half $CO_2$ and half $N_2$, $O_2$, and Ar. Aspelund and Jordal [73] state that the loss of $CO_2$ to the exhaust stream for a one column system will be 1:1, i.e. 1 mol of $CO_2$ per mole of non-condensable gas.

Depending on the plant configuration, especially whether a desulphurization plant is installed, the waste water stream could be very acidic (sulfuric acid, hydrocloric acid, etc.) and thus extremely corrosive (pH 1.5–3) [10,67,92,97]. The flue gas purification unit should thus be designed acid-proof [82,10] as well as the flue gas pathway [10] due to the risk of low-temperature acid corrosion. Additionally, a fraction of the $CO_2$ (due to its solubility in water) and a large part of the particles remaining after the ESP will be captured in the waste water stream. This stream therefore requires further processing before disposal. This is expected to occur with methods already commercially available [10].

The gas purification unit could e.g. be a flash [40,10] or a distillation unit [27,74,92] since $CO_2$ forms non-azeotropic mixtures with impurities such as $N_2$, $O_2$, and Ar [85]. The thermodynamic properties of the $CO_2$ stream fed to the purification unit will be affected by its content of impurities ($N_2$, $O_2$, Ar, $NO_x$, and $SO_2$). Possible ranges of impurity concentrations are: Ar (0–5%), $N_2$ (0–15%), $O_2$ (0–7%), and $SO_2$ (0–1.5%). The changes are mainly affecting the dew and bubble points, heat capacity as well as the enthalpy and entropy. This again will have an impact on the operating conditions, energy consumption, configuration, and separation performance of the purification system [85]. Generally, removal of $SO_2$ in a flash or distillation system is not preferable since it has a large, negative impact on product purity and energy requirements for even small impurity levels [85] since the thermodynamic properties are very close to that of $CO_2$.

The basic principle in the flash and distillation units is to utilize the differences in boiling point for the different species to separate them. Fig. 7 shows a comparison between the performances of the two purification systems. The figure reveals that for the same recovery rate and feed compositions the distillation process requires less energy and produces a slightly higher-purity $CO_2$ stream than the flash process. This has likewise been reported by Aspelund and Jordal [73,74].

The typical $CO_2$ recovery for oxy-fuel plants is reported at ~90% [12,30,40,43,67]. 100% capture was expected theoretically in one of the earlier studies of the technology [59], under the assumption that the entire flue gas stream could be sequestered in the ocean.

A possibility exists that the initial flue gas cleaning and the $CO_2$ processing steps can be combined in one process unit. This is interesting in the case that desulphurization is neglected within the recycle loop. Air Products Inc. has proposed a process that removes both non-condensable impurities as well as Hg, essentially all $SO_x$

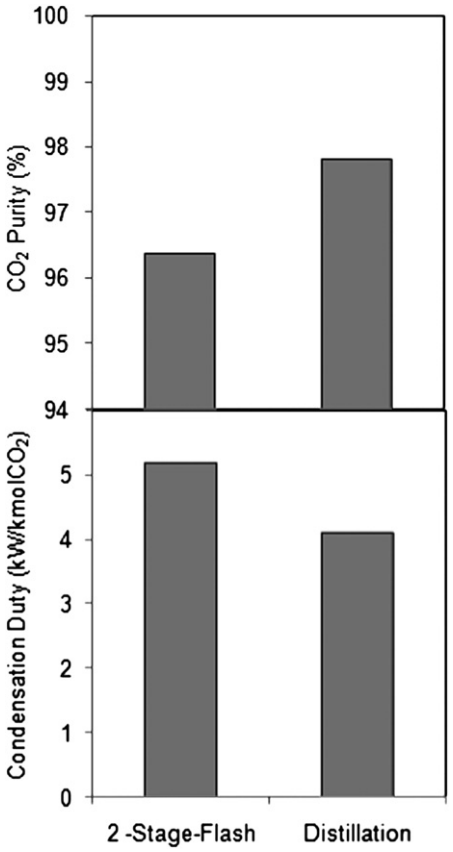


**Fig. 7.** Performance comparison between 2-stage flash and distillation column based on simulations. The $CO_2$ recovery rate is 92.15% and the feed compositions (in mol%) to the purification units are $CO_2$: 76, $O_2$: 6, $N_2$: 15, Ar: 2.5, and $SO_2$: 0.5. Adopted from [85].

and about 90% of the $NO_x$ through the production of waste water containing sulfuric and nitric acid [98].

This compression and purification process has been initially tested in mid-2008 [98]. The tests have confirmed the potential of the process. However, further tests are necessary to gain further understanding of the chemical mechanisms and the kinetics [98]. This is expected to be performed at the Vattenfall Schwarze Pumpe pilot plant [99]. The process should likewise be evaluated against well proven de$NO_x$ and desulphurization technologies [67,43].

### 2.4. Air separation

The air separation unit provides the oxygen for the combustion. The current state of technology development necessitates the application of a cryogenic distillation unit. No other mature technologies exist which can be applied for the necessary size of operation [40,59,65,79,80,82,93,100], see Fig. 8. At the same time, because of mechanical size limitations it will be necessary to build more cryogenic air separation units to operate in parallel. The largest cryogenic ASU plant currently operating (2008) produces 4500 t/d, but design studies for a 7000 t/d have been performed [65]. As seen from Table 3 the oxygen requirement for a 500 $MW_e$ plant is between 9000 and 10,000 t/d, indicating the need for 2–3 parallel ASU plants.

Cryogenic distillation consumes high amounts of energy in the form of electricity. Preliminary calculations indicate that this operation alone requires about 60% of the power consumption for carbon capture and reduces the overall efficiency of the power plant by about 7–9 percentage points [8,10,16,40,43,50,67]. Major improvements are thus required to yield a more efficient oxygen production. It is not likely to find these improvements within the cryogenic technology [62,65,67] and thus alternative technologies like e.g. ion transport membranes (ITMs) should be investigated further. However, it is possible that some synergies can be obtained from an integration of the ASU's with the power plant, i.e. by using the low-temperature heat from the ASU intercoolers for e.g. feed water heating [93].

The availability of the oxygen plant is crucial to the power plant operation. Typical availabilities of 98–99% and only limited time for maintenance are reported from suppliers [65,67]. Another important requirement is the ability to follow the load changes of the power plant. According to Xu et al. [43] the maximum ramp rate for an ASU is 3%/min. The boiler, however, can generally be operated at a ramp of up to 6%/min. At the same time, ASU's are only able to operate at 60–100% load [82,43] and show rather poor efficiencies below 80%. In combination, this gives rise to some operational difficulties, which should be investigated further.

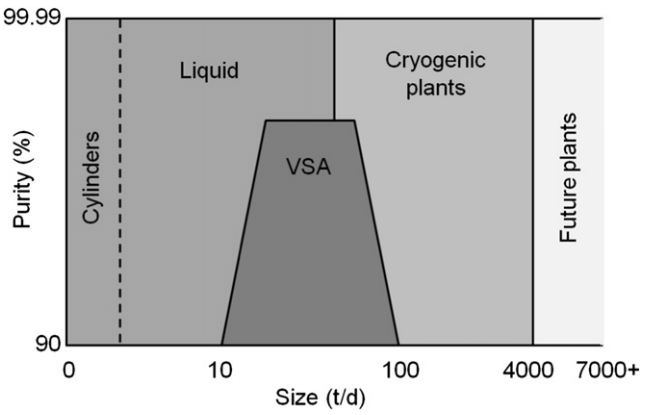


**Fig. 8.** Oxygen supply technologies. Selection as a function of quantity (tonnes per day) and required purity. Cylinders and Liquid: Continuous delivery from manufacturers in either cylinders or for own storage vessel. VSA: Vacuum Swing Adsorption. Future plants could be either cryogenic or based on other technologies, such as e.g. membranes. Adapted from [65].

The introduction of a liquid oxygen storage could provide a solution in which the difference between demand and production during positive load changes in the boiler is taken from the storage and vice versa during decreases in the boiler load [43,92,99]. The storage facility also makes it possible to shift to air-firing mode within a relatively short amount of time without risking boiler trips in case of unexpected ASU shut-down. Even without the load changing challenges, it may be beneficial to decouple the ASU and power plant by introducing oxygen storage. In that way, the liquid oxygen could provide a means of energy storage in periods with high electricity production from e.g. wind mills. The safety issues related to a liquid oxygen storage on a power plant site should be assessed thoroughly however in order to evaluate its applicability. Preliminary studies by Xu et al. [43], suggest to install a tank with a 500 tonne capacity for liquid oxygen at 2.5 bar (about −175 °C), corresponding to approximately 1.5 h of operation of their 413 $MW_e$, net, oxy-fuel reference plant.

For economic reasons it should be considered whether the massive amount of almost pure nitrogen, ~31,800 t/d at low temperature, could be applied for a purpose in the plant or elsewhere.

### 2.5. Flue gas recirculation

The oxygen for combustion is mixed with recycled flue gas to moderate flame temperatures and obtain a boiler heat transfer profile similar to that of air-firing in the case of retrofit. Typically, between 60 and 80% of the flue gas is recycled to the boiler [4,5,8,10,43,66–68,79,80,101,102].

As shown in Fig. 3 two recycle streams will be necessary. The primary recycle is used for fuel transport and corresponds to the primary air in conventional units. It will be about 20% of the total amount of combustion air (RFG + $O_2$) [67]. The secondary stream will constitute the equivalent to the secondary, tertiary, and overfire (if necessary) air flows when oxygen has been added.

A study performed by Kather et al. [68] determined that the temperature of the recirculated flue gas should be between 200 and 350 °C in order to take into account the operation of an ESP and flue gas fan, among others.

#### 2.5.1. Positioning of recycle streams

*2.5.1.1. Primary recycle.* A general consensus exists that the primary recycle stream must be cooled, scrubbed, dried and then reheated to about 250 °C or more before entering the mills [66–68,83,101]. The obvious choice is thus as indicated in Fig. 3 to take this stream after the first condensation step during the flue gas processing.

The reheating is necessary in order for the stream to be able to dry the coal and carry the moisture at the typical mill exit temperature of 60–90 °C [67,68]. If the drying capacity of the primary recycle gas is too small the wet coals will clog the mills. Scrubbing of the flue gas ensures removal of $SO_2$ which would induce corrosion in the mills due to condensation of sulfuric acid at temperatures below 150–160 °C [103]. Xu et al. [43] suggest adding a bypass from upstream the ESP outlet to increase the temperature of the recycle streams approximately 5 K in order to avoid moisture condensation along the recycling ductwork.

*2.5.1.2. Secondary recycle.* Several options exist for the position where the secondary recycle stream is taken. The dashed lines in Fig. 3 indicate these possibilities. Depending on the actual position the heat and water contents along with the concentration of

pollutants ($NO_x$, particles, $SO_x$, etc.) will vary. Even though several reports on oxy-fuel combustion conclude that both de$NO_x$ and desulphurization can be eliminated due to co-sequestration of the impurities with the $CO_2$ [60,61,67] this is not necessarily possible in practice, see Section 2.2. Most probably, the power plant should be able to run in air-firing mode without capture, at least during start-up and shut-down, and thus also needs the flue gas cleaning equipment to obey the legislation regarding emissions. There is, however, the possibility of by-passing the SCR and FGD plants during oxy-fuel operation. It will still be necessary to remove the particulates to avoid accumulation of solids in the boiler and to prevent the flue gas recirculation fan and gas passages from unnecessary wear due to erosion.

Even though oxy-fuel combustion provides the opportunity of highly reduced emissions of $NO_x$ [4,12,16], it is doubtful if the legislations concerning emissions can be fulfilled without some degree of $NO_x$ removal for all future power plants. During start-up and shut-down which most likely will occur at air-firing conditions $NO_x$ removal is likewise regarded necessary. It is possible that the SCR plant can be run at reduced efficiency during oxy-fuel combustion and that operating costs thus can be reduced. The SCR is typically positioned at high-dust conditions. By passing as large an amount as possible of the flue gas around the SCR it is possible to significantly enhance the catalyst lifetime. Even though ammonia is not added to the flue gas, its passage through the SCR catalyst will reduce the catalyst lifetime. It is likely that the extra cost related to the bypass will be counterbalanced by the reduced cost for change of catalyst may be even with an overall saving. An alternative option is the production of a concentrated liquid waste water stream containing both $NO_x$ and $SO_x$ [66] which can be treated to avoid pollutant emissions to the air, see Section 2.3.2.

The acid gases such as sulphur oxides, HCl, and HF are not reduced through the same mechanisms as $NO_x$ in the boiler. Recirculating the flue gas before desulfurization will result in up to an about 3–4 times increase of the sulphur (and chloride) levels in the boiler [4], see Table 6. Since both sulphur and chloride are potentially corrosive this significant increase can cause problems in the boiler components when firing medium to high sulphur containing coals [43]. Significantly increased levels will likewise have a negative impact on a wet desulphurization plant. The change corresponds to firing coals with excessive amounts of S, Cl, F, etc.

Sulphur retention in fly ash is another area of concern. Significantly increased retention can lead to problems utilizing the fly ash for cement and concrete production. The upper limit for sulphur in fly ash used for concrete is 3 wt% measured as $SO_3$ [104]. The limiting value for sulphur in fly ash used in cement production is not regulated by standards but rather determined individually between the cement manufacturer and the fly ash producer. However, the limit is usually not less strict than for concrete purposes. Utilization of fly ash from power plants is becoming increasingly important [105]. The potential risk of contaminating the fly ash with excessive amounts of sulphur is thus very critical to the configuration of an oxy-fuel power plant. In conclusion, the secondary recycle stream will most likely have to be taken downstream of some sort of desulphurization process whether it be a conventional wet FGD plant or another process.

The water content in the secondary recycle could potentially have an impact on the combustion characteristics and the general plant performance and efficiency [102]. This is mainly a consequence of the differences in thermodynamic properties, e.g. heat capacity, between $CO_2$ and water vapor. The effect of wet and dry recycle streams on in-furnace temperatures, ignition, emissions, etc. are discussed in more detail in Section 3. This section will focus on the plant configuration aspects of a wet versus a dry flue gas recycle.

Nakayama et al. [61] proposed five different plant configurations covering both wet and dry recycle, see Fig. 9. The configurations differ in the position of the recycle path and the oxygen preheater. Changing the position of these units will have an impact on the size of both the preheater, the electrostatic precipitator (ESP), and the flue gas cooling unit. The choice of a wet versus a dry recycle will influence the gas recirculation fan (GRF) as will the possibility of recirculating fly ash to the boiler (system A). In relation to the gas recirculation fan, a dry recycle is most favourable since it induces less wear of the fan. On the other hand, a dry recycle will require

**Table 6**
Example of the effect of recycle strategy on $SO_2$ concentration in the flue gas, based on 1000 ppmv without recycle. Data taken from [4].

| Fraction of total flue gas recycled | Sulphur concentration in flue gas |
|---|---|
| 0.7 | 3110 |
| 0.6 | 2370 |
| 0.5 | 1920 |
| 0.4 | 1650 |
| 0.3 | 1390 |
| 0.2 | 1230 |
| 0.1 | 1080 |
| 0 | 1000 |

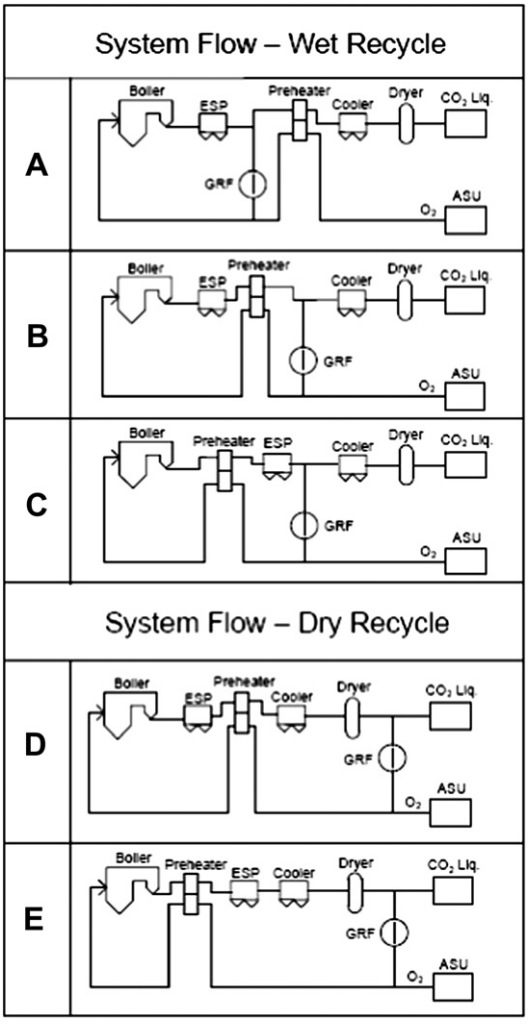


**Fig. 9.** Different, possible configurations for oxy-fuel combustion with either dry or wet recirculated flue gas. The suggested configurations do not include process units for removal of NOx and $SO_2$. ASU: Air Separation Unit; GRF: Gas Recirculation Fan, ESP: Electrostatic Precipitator. Adopted from [61].

approximately four times larger capacities of the preheater, cooling, and drying units compared to the wet recycle case.

Nakayama et al. [61] concluded that a wet recycle taken after the ESP and oxygen preheater (system B) was the most promising configuration. The evaluation is based solely on theoretical considerations and no experiments were performed to test the effect of wet and dry recycle on the combustion process. The suggested configurations include only particle removal for flue gas cleaning, not deNO$_x$ nor desulfurization since these were not considered necessary to obtain the required purity of the $CO_2$ stream. The investigation likewise neglects the fact that some of the recycled flue gas should be used in the coal mills as transport and drying gas.

Dillon et al. [66] likewise assess different recycle arrangements considering both a primary and secondary recycle stream. All of their five arrangements did, however, have the same conditions for the primary recycle, the only difference being the type of equipment for reheating. The authors arrived at a wet, reheated secondary recycle as being the most advantageous option.

As described in Section 2.2, mixtures of $CO_2$ and $H_2O$ are known from the oil and gas industry to cause potential corrosion problems in piping. Corrosion in the flue gas recirculation ducts in case of temperatures below the water dew point is thus an issue that should be addressed when designing an oxy-fuel plant.

For security and availability reasons, Hellfritsch et al. [82] suggest that the flue gas recirculation should consist of multiple independent paths (e.g. 4 of 25% each).

In relation to retrofit of an existing power plant the exact benefits and disadvantages concerned with each of the possible plant configurations regarding secondary recycle position and its water content should be clarified in order to choose the most optimal solution. For green-field plants it is possible that a specific concept could prove to be generally accepted.

### 2.5.2. Oxygen addition

*2.5.2.1. Primary stream.* Fig. 3 indicates that no oxygen is added to the primary recycle before entering the mills. This is mainly due to safety reasons [83]. The highest possible temperature in the coal mills is 120 °C. This limit is set according to materials considerations. In $N_2$ there is no risk of explosions in the mills if the oxygen concentration is below 12%. The use of air during operation in conventional plants can thus be considered a safety risk and is handled through safety precausions. Due to a suggested, inhibitory effect of $CO_2$ on explosions it is possible that the $O_2$ level in the mixture sent through the mills can be raised to above 21% without inducing a risk of explosion [67]. No data are available however.

Even though it is theoretically possible to have relatively high oxygen concentrations in the primary recycle without risking an explosion, some authors advise against it [67]. In practical power plant operation, mills are continually brought in and out of operation to meet the changes in electricity demands. This provides a possibility of transient mismatches between recycle and oxygen flows and thus significant variations in the oxygen concentration. Additionally, equipment failures in control valves, recycle fans, etc. are considered severe security risks [67]. The risk of obtaining significantly higher oxygen concentrations than the safe limit in the coal mills and induce an explosion from ignition of coal dust is thus profound.

With respect to $NO_x$ formation, it is likely that limiting the oxygen concentration in the primary oxidant stream is beneficial since a fuel-rich flame core will be formed. The only concern could thus be flame stabilization. Some preliminary results obtained by IFRF [88,12] suggest, however, that satisfactory ignition and flame stabilization is obtainable when all oxygen is introduced with the secondary oxidant stream. It should be noted that oxygen corresponding to the excess amount, approximately 3 vol%, will be present in the primary recycle.

*2.5.2.2. Secondary stream.* If no oxygen is added to the primary recycle the entire amount should be mixed into the secondary stream. Due to the risk of spontaneous ignition of dust in the recycle stream there will most probably be an upper limit to the concentration of oxygen in this stream as well. If this limit is exceeded it will be necessary to inject oxygen either directly through the burners or the over-fire ports [83].

Mixing of the oxygen stream into the recycled flue gas cannot be considered unproblematic with the amounts relevant for a power plant. It is crucial that the resulting oxidant stream has a homogeneous composition in order to maintain stable burner operation and prevent safety hazards due to injection of large amounts of pure oxygen to the furnace. Generally, it is very important to minimize the risk of having pure oxygen present together with combustibles anywhere in the system. It is questionable if nozzle injection of one stream into the other without e.g. a static mixer will be satisfactory. In the Schwarze Pumpe pilot plant static mixers are used to ensure proper mixing of oxygen and flue gas [106,94]. Some researchers are addressing alternative equipment which will allow proper mixing in the flue gas ducts [91].

Table 7 summarizes the advantages and disadvantages associated with the different options for oxygen introduction to the boiler. Either way the oxygen addition to the boiler is performed it is most likely that new (or modified) burners will need to be developed to obtain efficient and stable combustion in an oxy-fuel plant [67,107–109].

## 2.6. Operation of conventional flue gas cleaning equipment

In case it is necessary to include both desulfurization and deNO$_x$ in an oxy-fuel combustion power plant the operation and performance of these units in atmospheres with high $CO_2$ concentrations should be clarified. These aspects of oxy-fuel combustion seem to be an overlooked area in the research since most investigations neglect these basic units in the plant configuration. Most of those who actually do include these units [4,10,63,80,82] assume that they can operate with exactly the same or even better settings, throughput, and economics as in a conventional plant.

### 2.6.1. Desulphurization

The largest uncertainties regarding operation concerns the desulfurization plant. Below, the series of reactions occurring during the process in a wet plant are provided. First, $SO_2$ is dissolved in the aqueous phase producing hydrogen sulfite, (1). Simultaneously, limestone ($CaCO_3$) is dissolved releasing $CO_2$, (2) and (3). The hydrogen sulfite is oxidized to sulphate in the irreversible reaction given by (4). Finally, gypsum ($CaSO_4 \cdot 2H_2O$) is produced by the reaction between calcium and sulphate ions, (5).

$$SO_2 + H_2O \rightleftharpoons HSO_3^- + H^+ \quad (1)$$

$$CaCO_3 + 2H^+ \rightleftharpoons Ca^{2+} + HCO_3^- + H^+ \quad (2)$$

$$Ca^{2+} + HCO_3^- + H^+ \rightleftharpoons Ca^{2+} + H_2O + CO_2 \quad (3)$$

$$HSO_3^- + 0.5O_2 \rightarrow SO_4^{2-} + H^+ \quad (4)$$

$$SO_4^{2-} + Ca^{2+} + 2H_2O \rightleftharpoons CaSO_4 \cdot 2H_2O \quad (5)$$

Since the wet desulfurization process rely on limestone emitting $CO_2$ during the conversion equilibrium limitations could arise due

to the high $CO_2$ concentration in the flue gas. Likewise, the oxidation of $HSO_3^-$ to $SO_4^{2-}$, (4), in the desulfurisation plant is performed with air in conventional units. Application of air to oxy-fuel desulfurisation would induce an undesirable dilution of the $CO_2$ with nitrogen [68,101,110]. Instead, a portion of the secondary oxidant stream or alternatively pure oxygen could be directed to the desulfurisation unit. The consequences of each of the three possibilities should be investigated. An other alternative could be to construct the desulphurization plant in such a way that the $SO_2$ absorption and the oxidation occur in two separate units [68,76,94,110]. In that case air can be used as oxidizer without the risk of reducing the $CO_2$ concentration in the flue gas.

In the case of a wet recycle the flue gas entering the flue gas desulphurization unit will contain significantly higher amounts of water vapor than in a conventional plant. Even in the case of a dry recycle, the water vapor concentration will increase due to less dilution. The increase in water concentration could lead to an increase of the equilibrium temperature of the gypsum/limestone suspension and thereby influence the kinetics of the desulphurization process. A higher temperature of the suspension could thus lead to a reduction in the degree of desulphurization due to a decrease of the solubility of $SO_2$.

Studies performed by Air Liquide Inc. together with The Babcock & Wilcox Company in the 30 $MW_{th}$ test facility located in Alliance, Ohio [91,51] revealed no noticeable change in the performance of a conventional wet FGD scrubber. Similar conclusions were obtained by Oryshchyn et al. [111] from laboratory-scale experiments.

Due to the fact that only few results on desulphurization in oxy-fuel atmospheres have been published, this is an area of the oxy-fuel process which needs further attention.

The gypsum produced should likewise meet certain quality requirements, see Table 8. The high partial pressure of $CO_2$ in the gas phase could limit the dissolution of the limestone in the solution and thus potentially increase the amount of residual limestone in the gypsum. This could cause problems in the further utilization of the gypsum and would influence process economics negatively.

### 2.6.2. $NO_x$ removal

The concerns regarding removal of $NO_x$ from the flue gas stream are much less than for desulphurization. However, it will still be necessary to verify the performance of e.g. an SCR unit, which is the typical choice for large power plants, if the $NO_x$ reduction obtained during the oxy-fuel combustion is not adequate. An increase in the $CO_2$ concentration above the catalyst is not considered to have an effect on performance. The possibly increased levels of both $SO_2$ and $SO_3$ in the flue gas do, however, impose a risk for reduced performance. $SO_3$ in the flue gas is known to form sticky and corrosive ammonium bisulfate when $NH_3$ is added [113]. Increasing the $SO_3$ level will likewise increase the dew-point temperature for ammonium bisulfate. If the SCR operating temperature falls below the dew point, especially during low load operation, severe clogging of the catalyst must be expected. Additionally, the catalyst acts as an oxidizer and will convert part of the $SO_2$ content of the flue gas to $SO_3$ increasing the risk of ammonium bisulfate formation [113].

**Table 8**
Selected quality requirements for gypsum produced by wet desulphurization of flue gas [112].

| Parameter | Value [wt%] |
|---|---|
| Purity | >95 |
| Residual limestone | <4 |
| Moisture | <10 |

### 2.6.3. Particulate removal

As Suriyawong et al. [114] state, the collection efficiency of particulate removal devices is size dependent. Since oxy-fuel combustion shows the ability of altering the size distribution of ash particles, see Section 3.5, the performance of the electrostatic precipitator (ESP), which is the most common particulate removal system in large-scale power plants, will be subject to changes. For both ultrafine (<100 nm) and sub-micrometer (100 nm < $d_p$ < 1 μm) sized ash particles the penetration (1 − collection efficiency) depends on particle size due to different charging effects and these particles are thus not effectively captured.

A potential change in the size distribution of the fly ash from oxy-fuel combustion is not the only aspect of relevance for ESP performance. The flue gas composition could likewise impose a change in the ion production rate within the ESP and thus lead to a change in collection efficiency. Suriyawong et al. [114] have found that for ESP's with positive coronas it is necessary to increase the applied voltage to obtain similar collection efficiencies in oxy-fuel plants as for air-fired plants. However, when negative coronas are used, there is only an insignificant effect of the ESP performance from the change in flue gas composition in the oxy-fuel plant.

Based on equilibrium calculations Schnurrer et al. [115] conclude that the increased $SO_3$ content in the flue gas is expected to improve the performance of the ESP. This is caused by lower ash resistivity as a result of deposition of sulphate species on the fly ash.

### 2.6.4. Potential improvements for a green-field plant

For a green-field plant there could be an incentive for applying a hot ESP as the first flue gas cleaning unit downstream of the boiler. The hot ESP is generally considered too costly for air-blown units. Removal of the particulates as the first step will, however, yield the possibility of applying a low-dust SCR downstream of the ESP with low catalyst degradation compared to the more conventional high-dust option. The secondary recycle can then potentially be taken in between the ESP and SCR, which additionally reduces the necessary size of the SCR unit. In order to control the sulphur accumulation in the system and thus prevent

**Table 7**
Advantages and disadvantages associated with the different options for oxygen addition to recirculated flue gas.

| Option | Advantage(s) | Disadvantage(s) |
|---|---|---|
| Before coal mills | (1) Sufficient space in recirculation duct to ensure adequate mixing<br>(2) The stream to the mills will be drier than without oxygen<br>(3) With oxygen in primary stream burner design is expected to be closer to that for conventional air burners | (1) Risk of zones with very high-oxygen concentrations if mixing is inadequate and thereby increased risk of combustion/explosions in mills<br>(2) Primary stream will be cooled due to the low temperature of the oxygen |
| After mills, before burners | (1) No risk of explosion in mills<br>(2) Possible to obtain the same oxygen concentration in the burner as is the case for operation on air | (1) Significant risks are associated with the injection of nearly pure oxygen into a high temperature stream of coal and flue gas |
| Directly in burners (either pure oxygen lance or with the secondary stream) | (1) No risk of explosion in mills or flue gas ducts<br>(2) No expenses for mixing in primary stream<br>(3) Oxygen lance provides increased control of the mixing of oxygen and fuel in the near-burner zone | (1) Burner design has to be re-thinked<br>(2) Limited capacity for coal drying in mills |

both corrosion and ammonium bisulfate degradation of the SCR catalyst due to high $SO_3$ levels, a desulphurization unit prior to the SCR should be installed.

The major advantage concerned with the change of sequence of the flue gas cleaning units is to reduce the size of the equipment due to the fact that the flue gas volume is reduced with about 60–80% after the secondary recycle has been taken. In the suggested configuration, the desulphurization unit will, however, not be reduced in size. A disadvantage is that if a wet FGD (the conventional choice) is installed before the SCR, additional cooling and reheating will be necessary. These operations will reduce the plant efficiency.

### 2.7. Boiler and steam cycle

The oxy-fuel boiler is subject to relatively extensive changes regarding chemistry compared to the case of air-firing. The two main, combustion related properties that change during oxy-fuel combustion are [5]:

- Gas radiative properties
- Gas heat capacity

Substituting $CO_2$ (+water vapor) for $N_2$ in the oxidant results in a larger specific heat capacity compared to air, see Table 9. Firing with the same ratio between oxygen and 'inerts' will thus result in a lower flame temperature [118–122] and difficulties in stabilizing the flame [12,123]. In order to obtain a stable flame and the same adiabatic flame temperature in oxy-fuel experiments as in air combustion overall oxygen concentrations between 25 and 42 vol% have been reported necessary [87,97,116,118,120–122,124–126]. The span is somewhat dependent on the coal type and the typical values reported for bituminous coals are 28–35%.

$CO_2$ and water vapor are radiating species as opposed to $N_2$. The radiative heat flux in the flame zone originating from the gas phase is thus expected to increase in oxy-fuel combustion compared to air-firing at comparable gas phase temperatures. The radiative heat flux from solid particles (soot, char, and ash) depends on a number of parameters. Radiation from ash particles depends mainly on the particle temperature whereas radiation from soot and char is influenced by the mixing characteristics of the flame, local $O_2$, $CO_2$, and $H_2O$ concentrations, and temperature.

In coal flames radiation from soot can dominate the heat transfer in the radiative section. The formation rate of soot can be very sensitive to the mixing of fuel and oxidizer in diffusion flames. The near-burner flow dynamics are expected to change in oxy-fuel combustion compared to air-firing due to the changes in flow rates through the burners if conventional burners for air-firing are used. Soot formation and hence the radiation intensity is thus expected to change as well.

#### 2.7.1. Burner operation and flame stabilization

Increasing the oxygen concentration to achieve similar adiabatic flame temperatures to that of air operation is the obvious solution to obtain stable combustion. With this approach the total volumetric flow through the burners and boiler is reduced compared to air-firing because of the overall lower amount of 'inerts'. In order to keep the coal particles in suspension, it has been suggested that the primary flow must have the same linear velocity as in air-firing [83], typically 17 m/s as minimum [116]. Since the density of $CO_2$ likewise is higher than for $N_2$, see Table 9, the mass flow ratio of primary to secondary flows through the burner inlets is increased. This could create an imbalance in the burner aerodynamics compared to air-firing and thus have an impact on ignition, flame shape, and mixing [116]. It is possible that the minimum velocity will depend on the density of the primary stream. A lower value than used in air-firing could then prove to be adequate for oxy-fuel combustion. This would have to be tested in larger-scale setups.

Besides increasing the oxygen concentration to obtain stable combustion, other suggestions have been made:

Liu and Okazaki [127] suggested to stabilize the flame by recirculating additional heat with the flue gas while maintaining an air-like composition of the oxidant. In connection with the application of Ion Transfer Membranes (ITM) for air separation they likewise suggested heat recirculation to obtain stable combustion with oxygen concentrations down to about 15 vol% in the burner inlet. Utilization of ITM membranes will require relatively low oxygen concentrations in the oxidant in order to achieve sufficient driving force in the air separation. The authors claimed that the recirculation of heat should not affect the plant efficiency negatively. There has been no reports of experiments with this approach in larger scale.

Another alternative approach is taken by Toporov et al. [107,108] who work on changing the burner design in order to obtain stable flames at low oxygen concentrations in the $O_2/CO_2$ oxidant mixture. This approach is likewise to enable the use of ITM membranes for air separation instead of a cryogenic unit and thus reduce the penalty on the plant efficiency from about 8 to between 3 and 5% [108]. In order to obtain stable operation their aim is to provide the necessary heat to compensate for the higher heat capacity of the oxidant and the heat used for the endothermic gasification reactions taking place in the near-burner region from the post-flame zone. This is done by promoting under-stoichiometric conditions near the burner region ($\lambda = 0.6$) and having a strong internal recirculation zone to lead hot combustion products back into the burner quarl. A burner design was obtained which allowed stable operation with just below 21% oxygen in the oxidant and an overall stoichiometry of $\lambda = 1.3$. The drawback of this concept is an increase in the recirculation rate of flue gas. However, this is believed to be fully offset by the reduction in power demands for the air separation process [107,108].

#### 2.7.2. Heat uptake

Existing boilers have been carefully designed to match the radiative and convective heat transfer properties of the air-fired combustion process. Especially important is the distribution of heat transfer between the furnace chamber (evaporation) and

**Table 9**
Properties of gases at 1123 °C and atmospheric pressure [116,117].

| | $H_2O$ | $O_2$ | $N_2$ | $CO_2$ | Ratio $CO_2/N_2$ |
|---|---|---|---|---|---|
| Density ($\rho$) [kg/m$^3$] | 0.157 | 0.278 | 0.244 | 0.383 | 1.6 |
| Thermal conductivity ($k$) [W/m K] | 0.136 | 0.087 | 0.082 | 0.097 | 1.2 |
| Specific heat capacity ($c_p$) [kJ/kmol K] | 45.67 | 36.08 | 34.18 | 57.83 | 1.7 |
| Specific heat capacity ($c_p$) [kJ/kg K] | 2.53 | 1.00 | 1.22 | 1.31 | 1.1 |
| Heat sink ($\rho c_p$) [kJ/m$^3$ K] | 0.397 | 0.278 | 0.298 | 0.502 | 1.7 |
| Dynamic viscosity ($\mu$) [kg/m s] | 5.02e-05 | 5.81e-05 | 4.88e-05 | 5.02e-05 | 1.0 |
| Kinematic viscosity ($\nu$) [m$^2$/s] | 3.20e-04 | 2.09e-04 | 2.00e-04 | 1.31e-04 | 0.7 |
| Mass diffusivity of $O_2$ in $X$ ($D_{O_2/X}$) [m$^2$/s] | – | – | 1.7e-04 | 1.3e-04 | 0.8 |

convective part (superheating) but the maximum heat flux to the furnace walls is also important.

The choice of recycle ratio, i.e. the fraction of the total flue gas flow which is recirculated to the boiler, and thus the oxygen concentration in the oxidant affects the heat transfer by controlling the flame temperature and the volume flow through the boiler [65]. The radiative heat transfer is mainly determined from the flame temperature and the gas radiative properties, whereas the convective heat transfer is determined mainly by the Reynolds and Prandtl numbers, the thermal conductivity, and the temperature of the flue gas passing the superheater banks. Fig. 10 shows the connection between the recycle ratio and the adiabatic flame temperature and flue gas volume. In this respect, the flue gas volume is a rough indicator for the convective heat transfer. It is seen that recycle ratios of either 0.61 or 0.76 yield conditions corresponding to air-firing (with $\lambda = 1.15$), although only for one of the parameters. It is thus not possible to simultaneously obtain both an adiabatic flame temperature and a volumetric flue gas flow through the boiler similar to that of air combustion. Section 3.2 will assess the subject of heat transfer in more detail.

*2.7.3. Oxygen excess*

It is important to note that excess oxygen for oxy-fuel combustion carries a much greater penalty than in the air-firing case and that the power consumption in the ASU is directly proportional to the amount of oxygen lead to the boiler [95]. A reduction in the oxygen excess would thus benefit both the ASU and $CO_2$ compression train power demands [66,68,81,95]. In modern power plants the air excess is typically 15–20% ($\lambda = 1.15$–1.2) [68,103,128] corresponding to about 3 vol% $O_2$ in the dry flue gas. The excess is predominantly determined by the uncertainty in the coal mass flow to each burner. By introducing more efficient monitoring of the coal flow to each burner and thus a better control of the oxidizer and fuel flows, it should be possible to reduce the required oxygen excess during oxy-fuel combustion to no more than 10% [68]. At 10% excess oxygen and an oxidizer containing 30% $O_2$ the dry flue gas $O_2$ concentration will likewise be about 3 vol%.

Theoretical considerations regarding the second law efficiency of gas-fired power plants equipped with either oxy-fuel combustion or post-combustion capture have been conducted by Simpson and Simon [95]. Their computations showed that oxy-fuel combustion becomes more favourable with respect to efficiency than post-combustion systems as the oxygen excess level is decreased.

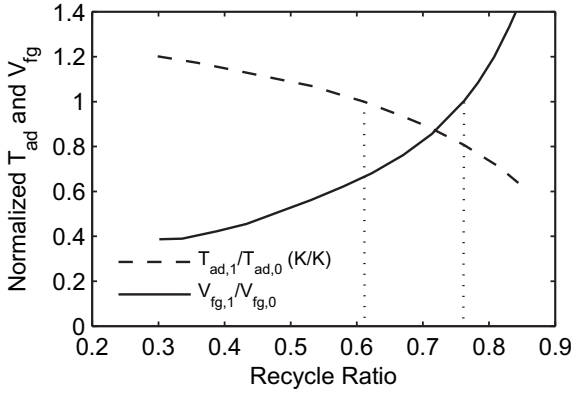


**Fig. 10.** Theoretical considerations on the effect of flue gas recycle ratio on adiabatic flame temperature, $T_{ad}$, and flue gas volume, $V_{fg}$. The reference values, $T_{ad,0}$ and $V_{fg,0}$, are for air combustion. Data taken from [88].

*2.7.4. Fire-side corrosion*

The change in the composition of the combustion medium in oxy-fuel combustion could potentially give rise to increased risk of corrosion. The increased levels of $CO_2$, $H_2O$, and $SO_2$ are expected to change the corrosion potential of the flue gas. Both aspects regarding metal surface oxidation and corrosion under deposits due to changes in deposit compositions are important to investigate [129–131]. Regarding deposits, especially the co-existence of sulphates and carbonates within the deposits could be critical to the boiler tube surfaces [131]. The aspect of carburization of Cr-containing steels due to high partial pressures of $CO_2$ could likewise constitute a challenge to materials lifetimes due to brittleness.

Pirón Abellán et al. [132] studied the oxidation of martensitic steels (Cr-containing alloys) in different $CO_2$ and $H_2O$-containing atmospheres at temperatures between 550 °C and 700 °C in a laboratory setup. They found significant carburization in high $CO_2$ containing atmospheres. They expect the carburization to be governed primarily by the permeability of the protective oxide layer toward $CO_2$. However, the authors show that the presence of water vapor will limit the transport of $CO_2$ through the oxide layer and thus the extent of carburization. The exposure atmospheres contained no $O_2$ and the consequence of the presence of excess oxygen on the obtained results will need to be examined to fully clarify the effect of the change from air-firing to oxy-fuel combustion on fire-side corrosion.

*2.7.5. Aspects regarding green-field plants*

The above discussions are based on the case of a retrofitted conventional air-fired plant to oxy-fuel conditions. For a green-field plant it will be possible to refine the boiler design. The adoption of conditions similar to those of air-firing is not necessarily the most optimal for an oxy-fuel combustion plant. A major target will be a significant reduction or even complete elimination of the rate of external flue gas recirculation. Instead, control of the flame temperature can be obtained from internal recirculation in the boiler [10]. This will likewise have a positive impact on the residence time and thus the burnout of the char particles. The possible avoidance of the external recirculation will reduce the size of the boiler and thus the boiler capital cost significantly [10]. At the same time, efficiency loss due to thermal radiation to the environment and the electricity demand for the flue gas recirculation fans will be reduced.

Maintaining the external recycle is likewise an option. Instead of matching the flame temperature to air-like conditions it would be possible to shift heat transfer to higher temperature throughout the entire boiler, leading to less entropy loss. Higher combustion temperature may lead to more efficient combustion with better burnout at reduced oxygen excess levels. Higher oxygen concentration will at the same time require less flue gas recirculation and thus a smaller volume flow through the boiler.

*2.8. Summary*

The present section has discussed the effects of retrofitting a suspension-fired power plant to oxy-fuel operation. A number of new process units are necessary; an air separation facility to provide the combustion process with almost pure oxygen, ducts and fans for external recirculation of flue gas to the burners in order to control flame temperatures, and a $CO_2$ processing facility including a flue gas condensation unit, compressors, and a purification unit to remove non-condensable species from the product stream.

The review of the literature has shown that even though the cost and efficiency penalties associated with the technology are significant, oxy-fuel combustion of pulverized coal is technically and economically feasible for retrofitting of existing power plants. At the

same time, oxy-fuel combustion for $CO_2$ recovery and sequestration is a competitive power generation technology in relation to post-combustion capture with amines. However, a number of critical aspects regarding the technology and plant configuration have been identified, as listed below. These are the issues which should be investigated in further detail to ensure that the technology is in fact a useful alternative to air-firing and post-combustion capture.

*Plant availability:* The risk of lowering the availability of the plant due to the introduction of the additional auxiliary equipment could be crucial to implementation.

*Plant efficiency:* With the currently available cryogenic technology for large-scale oxygen production the efficiency penalty for an oxy-fuel power plant is significant. Besides alternative air separation technologies, it is necessary to investigate additional measures that will allow the improvement of the electrical efficiency. Reduced oxygen surplus during combustion and a high steam cycle efficiency would have a positive effect on the efficiency.

*Load changes:* The relatively low gradients for load change in the air separation unit compared to those for the thermal cycle could provide a problem with respect to operation of the plant in a system with a large amount of decentralized, non-constant electricity sources, e.g. wind mills. In a world with an increasing fraction of the electricity produced by variable sources, central power plants will be required to run with frequent changes in the load to adjust to the demand for electricity. Additionally, the inability of current air separation units to run at low load without major penalties to the efficiency will require several oxygen plants running in parallel, as well as some sort of storage/buffer capacity.

*Enhanced purification:* The potential need for two purification steps, i.e. both the air separation unit and the pre-compression purification due to leakage of air into the flue gas ducts, could be a major disadvantage to the process. Post-combustion, in comparison, only requires the amine absorption step. The exact requirements for the final $CO_2$ quality are still to be determined and they will dictate the plant configuration with respect to the different purification units.

*Flue gas recycle:* The optimal positioning of the flue gas recycle withdrawal points has not been identified. The choice could have a large impact on both operation, economics, and plant maintenance related to corrosion issues.

*Combustion process:* The significant changes to the combustion process, including the potential effects on heat uptake, fly ash quality and fire-side corrosion likewise provide a challenge.

Several of the above aspects are difficult to examine either theoretically or during small-scale tests. The information and experience obtained from the operation of a larger-scale demonstration plant will greatly improve the knowledge of the process.

The majority of issues regarding the combustion process is, on the other hand, possible to clarify in smaller scale experiments. Much work has already been performed in this area including heat uptake and burner stability measurements as well as aspects regarding coal particle ignition, burnout, flame propagation, radiating properties of the flame, boiler efficiency, and changes in emission levels. In fact, most of the literature related to oxy-fuel combustion is concerned with the combustion chemistry and emissions.

In addition to the changes in the combustion, issues related to corrosion are also very relevant for the evaluation of the process. Because of the increased concentration of $CO_2$ and perhaps $SO_2$ in the flue gas, the risk of enhanced high temperature corrosion compared to conventional air-firing is present.

## 3. Oxy-fuel combustion fundamentals

The following subsections summarize the work performed on oxy-fuel combustion fundamentals by different researchers and reported in the open literature. The assessment will focus on chemical aspects connected to the boiler and other issues directly related to the combustion, e.g. convective and radiative heat transfer, corrosion, and emissions.

### 3.1. Research groups and experimental facilities

Tables 10 and 11 provide an overview of the different groups active within oxy-fuel combustion research. The groups have been divided according to the scale and type of their experiments, i.e. whether they run combustion experiments with flue gas recirculation in semi-technical scale or in once-through, laboratory-scale reactors.

Included in the tables is information on the most important parameters for the experiments; maximum reactor temperature, oxygen concentration, fuel type, and oxygen excess, as well as an interpretation of the aim of the research performed by each group.

### 3.2. Heat and mass transfer effects

The present section covers aspects of the effects of operating parameters such as oxidizer composition and oxygen excess levels on flame temperature and heat transfer in the boiler.

As described in Section 2.7 the differences in the radiative and thermo-physical properties of $CO_2$ and $N_2$, see Table 9, affect the combustion process through alterations of the temperature and mass transfer properties of the gas phase. As a consequence, the heat uptake in a boiler will likewise change compared to that of a conventional air-fired plant.

#### 3.2.1. Flame and gas phase temperatures

Croiset et al. [120] report the results of combustion of two different coals in air and different mixtures of $O_2$ and $CO_2$ in the 0.3 MW oxy-fuel combustion facility at CANMET. The coals tested were a Canadian western sub-bituminous coal (Highvale) and a US eastern bituminous coal. Temperatures along the centre-line have been measured with a suction pyrometer for air-firing and 21, 28, 35, and 42 vol% $O_2$ in $CO_2$, see Fig. 11. The experiments have been performed with an oxygen excess between 1.46 (21% $O_2$) and 1.3 (35% $O_2$) for the Highvale coal. For the Eastern bituminous coal the oxygen excess was between 1.2 (28% $O_2$) and 1.1 (42% $O_2$), corresponding to 5% oxygen in the flue gas (dry). The data in the lower figure show that for the 21% $O_2$ case a direct substitution of $N_2$ for $CO_2$ in the oxidant leads to a considerably lower temperature in the flame zone, a decrease of up to about 300 °C, caused by the higher specific heat capacity of $CO_2$ compared to $N_2$. By increasing the oxygen concentration it is possible to obtain flame and gas phase temperature profiles almost similar to those obtained from conventional combustion in air. The necessary oxygen concentration is somewhat dependent on the type of coal, ~35% for the bituminous coal and ~31% for the sub-bituminous coal. Based on additional experiments the authors conclude that up to 5% nitrogen in the combustion medium has no significant effect on flame temperatures. Comparable results regarding the effect of oxygen concentration on flame temperature have been reported by Wang et al. [118], Liu et al. [121], and Tan et al. [122], among others.

Experiments in a 1.2 MW burner at Ishikawajima-Harima Heavy Industries Co. Ltd. (IHI) [119] explored the effect of wet (16 wt% $H_2O$) and dry primary recycle (for coal transportation) on furnace temperature and flame stability, see Fig. 12. During the experiments the flow rate and composition of the secondary recycle was kept constant. It was found that drying the flue gas increased the gas temperature near the burner by about 150 °C for the same volumetric gas flow rate and thus helped stabilizing the flame by improving ignition stability. The heat capacity of water

**Table 10**
Oxy-fuel combustion research groups working in pilot scale and semi-technical scale with flue-gas recirculation.

| Group | Ref. | Test unit [$MW_{th}$] | Unit description | Inlet $O_2$ [vol%] | Recycle: wet/dry | Coal type | Aim of work (interpretation of the authors) |
|---|---|---|---|---|---|---|---|
| Vattenfall | [133,94,106,134, 92,99] | 30 | Down-fired boiler, single burner | Max 40 | Dry PFGR/ wet SFGR | Lignite, Bituminous, Biomass | Schwarze Pumpe pilot plant. Investigate the entire technology chain of an oxy-fuel combustion power plant in an industrial relevant pilot scale. |
| B&W and Air Liquide | [91,51,131,135] | 30 | B&W Clean Environment Development Facility | – | – | Bituminous, Sub-bituminous, Lignite | Verification of process parameters for full-scale design. |
| ANL | [118,86] | 3 | Tower furnace, single swirl burner | 22–40 | Wet/dry | Sub-bituminous | Determine practical feasibility of the oxy-fuel process from combustion and heat transfer data. |
| IFRF | [88,12] | 2.5 | Horizontal furnace, air staged swirl burner | 21–26 | Wet | Bituminous | Implementation of oxy-firing |
| B&W | [63] | 1.5 | Pilot scale boiler, air staged combustion system | 21–25 | Dry | Sub-bituminous | Feasibility of oxy-firing. Process performance, pollutant formation. |
| IHI | [87,119,136–139, 116,115,128] | 1.2 | Vertical, down-fired furnace, swirl burner | 27 | Wet/dry | 5 Bituminous | Implementation of oxy-firing. Direct injection of $O_2$. Ignition characteristics. Effect of load changes. Ash impacts. |
| E.ON | [140–142] | 1.0 | Combustion Test Facility | Max 24 | Wet | 3 Bituminous | Combustion characteristics, coal ash transformation and deposition, corrosion (50 h tests). |
| IVD | [143–148] | 0.5 | Vertical furnace, swirl burner | 27–30 (dry basis) | Wet | Bituminous, Lignite | Identification of variations in combustion behaviour. Impact on facility components other than furnace. Continuous operation for ~100 h. |
| CANMET | [120,97,89,149,150, 9,151,122] | 0.3 | Vertical combustor, down-fired swirl burner | 28–42 | Wet/dry | Bituminous, Sub-bituminous, Lignite, NG | Emissions from oxy-fuel combustion. Modelling tool validation. Burner and boiler design. |
| Doosan Babcock | [72,152,98] | 0.16 | Vertical furnace, down-fired low-$NO_x$ burner | – | Dry | 6 Bituminous | $NO_x$ Reduction Test Facility (NTRF). Demonstration of oxy-fuel combustion. Supply of flue gas for test of novel flue gas cleaning process. |
| Chalmers | [123,90,153–156] | 0.10 | Down-fired furnace, swirl burner | 25–29 | Dry | Lignite, Propane | Cause of $NO_x$ reduction. Gas-phase reactions. Firing strategies for $NO_x$ reduction. Radiation. |
| CIRCE | [157] | 0.10 | Bubbling Fluidized Bed combustor | 20–40 | Wet | 2 Sub-bituminous, wood, olive residues | Technical feasibility of oxy-fuel combustion of blends of coal and biomass. |
| TU Dresden | [101,110] | 0.05 | Vertical reactor, down-fired burner | 20–30 | – | Lignite | Investigation of combustion related parameters. Validation of CFD model. Production of flue gas for flue gas cleaning test pilot. |

**Table 11**
Overview of oxy-fuel combustion research groups working in once-through laboratory-scale reactors.

| Group | Ref. | Test unit [$kW_{th}$] | Unit description | Max T [°C] | Inlet $O_2$ [vol%] | $\lambda$ | Fuel type | Aim of work (interpretation of the authors) |
|---|---|---|---|---|---|---|---|---|
| Tokyo | [158,127,159] | – | Flat flame burner | 1177 | 21 | 0.7–1.2 | Anthracite/$CH_4$ | Cause of $NO_x$ reduction. Investigate concept of heat recirculation. |
| Nagoya | [96,160,161] | – | Quasi-1D EFR | 1300 | 20–100 | 0.7–3.3 | 3 Bituminous, Semi-Anthracite | Influence of $\lambda$, $O_2$ concentration, temperature, and type of coal with and without initial $NO_x$. |
| Nagoya | [109] | 145 | Bench-scale vertical furnace | > 3000 | 85–88 | 0.9–1.1 | Sub-bituminous | Verify lab-scale results for high-oxygen concentration oxy-fuel combustion with respect to $NO_x$ emission and fuel burnout. Burner design. |
| Leeds | [162,121] | 20 | Down-fired coal combustor | 1350 | 21, 30 | 1.2 | 7 Bituminous | Comparison between air- and oxy-firing. Sensitivity to different fuels. |
| IVD | [163,164,143–148,165] | 20 | EFR | 1400 | 21, 27, 35 | 1.15 | 4 Bituminous, Lignite | Comparison between air- and oxy-firing. Effectiveness of air-staging. Sulphur emissions formation. |
| Sandia | [166,126,167,168] | – | Optical EFR facility | 1730 | 6–36 | – | Bituminous, Sub-bituminous | Ignition devolatilization, and combustion rate of pulverized coal particles. |
| Sandia | [169] | – | Multi-Fuel Combustor (MFC) | 1350 | 12–36 | 6.67 | Bituminous/NG | $NO_x$ formation mechanism. |
| TU Munich | [170,171] | 200 | Side-fired furnace | – | Up to 50 | 0.3–4 | NG | Proof-of-concept for controlled staging in oxy-fuel combustion. |
| DTU | [172–174] | – | Laminar Flow Reactor | 1527 | 0.05–0.4 | 0.25–8 | $CH_4$ | Investigate chemical effects of high concentrations of $CO_2$. Dependence of presence of $NH_3$ and NO. |
| BYU | [124,175,176] | – | Multi-fuel Flow Reactor (MFR), laminar | 1627 | 21–37 | 0.75–1.05 | 2 Bituminous, Sub-bituminous | $NO_x$ formation and reduction. |
| TU Aachen | [177] | 25 | Gas Combustion Chamber | 900 | 14–21 | 1.15 | $CH_4$ | Stabilization of flameless combustion with low $O_2$ concentrations. |
| TU Aachen | [107,108,178,179] | 100 | Lab Scale Oxy-coal Test Rig | 1250 | 19–30 | 1.3 | 2 Lignite, 3 Bituminous | Burner design for stable oxy-fuel combustion at low $O_2$ concentrations. $NO_x$ emissions comparison between flameless and flame combustion. |
| CSIC | [180] | – | Entrained-Flow Reactor | 1100 | 21–35 | 0.75–4 | 2 Bituminous, Anthracite, Semi-anthracite, Biomass | Ignition and burnout of coal/biomass blends. |
| Northeastern Uni. | [181] | 4.2 | Laminar-flow Drop-tube Furnace | 1327 | 20–100 | – | Bituminous, Lignite, Synthetic char | Comparison between air- and oxy-firing. Volatile flame and char burning phenomena. Effect of particle size. |
| Huazhong | [182,183,125] | – | Drop-Tube Furnace | 1500 | 20–40 | – | 5 Bituminous | Ash formation. Comparison between air- and oxy-firing. |
| ECN | [184] | – | Lab-scale Combustion Simulator | 1450 | 25–28 | – | Coal, 2 Biomasses | Coal/biomass blends. Effect of different burner zone residence times on burnout, emissions, and fouling. |
| Utah (UU) | [185] | 29 | U Furnace | 1550 | 21 | 1.15 | 3 Bituminous, Sub-bituminous, Lignite | Fate of char-N during both air- and oxy-fuel firing. |
| Utah (UU) | [186] | 100 | Oxy-Fuel Combustor | 1088 | 21–30 | 1.15 | Bituminous | Provide data for validation of coal-jet ignition model. |
| Washington Uni. in St. Louis | [117,114] | – | Tubular furnace | 1200 | 20–50 | – | Sub-bituminous | Understand effect of oxy-fuel combustion on sub-micrometer particle formation and mercury speciation. |
| Pennsylvania State Uni. | [187] | – | Drop-Tube Reactor | 1550 | 21–30 | 1.25 | 2 Bituminous | Char burnout and CO emissions investigations. |

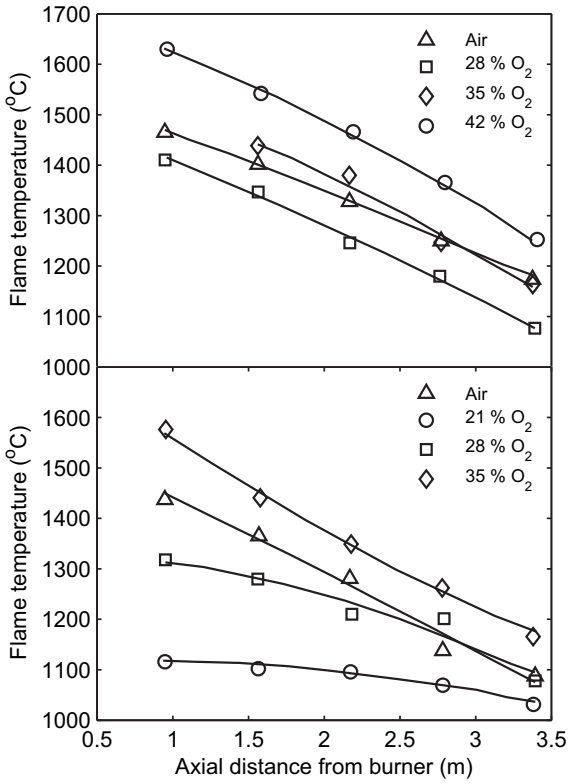


**Fig. 11.** Top: Centre-line axial temperatures for U.S. eastern bituminous coal burned in different $O_2/CO_2$ mixtures. The oxygen excess yields a dry flue gas $O_2$ concentration of 5%. Bottom: Centre-line axial temperatures for Canadian western sub-bituminous coal (Highvale) coal burned in different $O_2/CO_2$ mixtures. The oxygen excess was between 1.46 (21% $O_2$) and 1.3 (35% $O_2$) corresponding to approximately 8% $O_2$ in the dry flue gas. Both set of data are obtained in the CANMET 0.3 MW combuster operated at a firing rate of 0.21 MW. Data taken from [120].

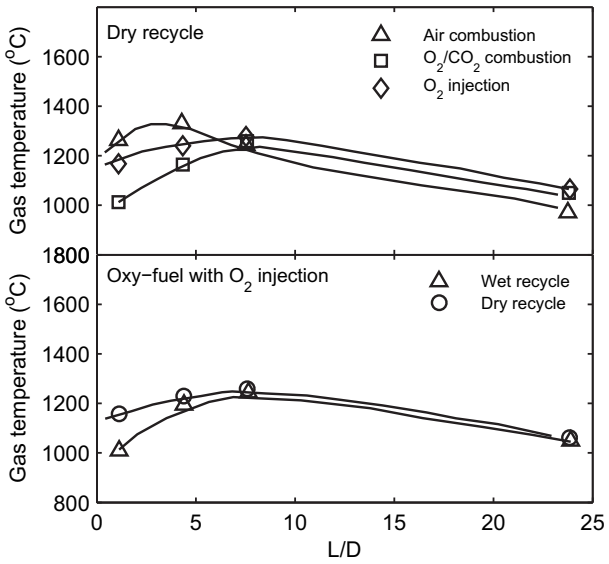


**Fig. 12.** In-flame gas temperature profiles along burner axis in the IHI 1.2 MW burner for a low-volatile bituminous coal (coal A). The overall oxygen concentration in the combustion gas is 27 vol% (30 vol% in the secondary stream). Top: Effect of pure oxygen injecting through burner in the case of a dry primary recycle stream. Bottom: Effect of wet and dry primary recycle stream in the case of direct oxygen injection. Wet flue gas contains 16 wt% $H_2O$. Data taken from [119].

vapor is significantly lower than that of $CO_2$, see Table 9. Taking only this factor into account, the presence of water vapor in the recycle would act to increase the flame temperature, i.e. the opposite effect of what was observed. These findings thus suggest that factors such as radiation and endothermal radical formation (O, OH, H, etc.) dominate the temperature effect of water vapor in the recycle.

Injection of pure oxygen through the centre of the burner likewise increased the gas temperature in the near-burner area compared to a similar experiment with the same $O_2/CO_2$ ratio in the oxidant but without separate oxygen injection.

### 3.2.2. Radiative and convective heat transfer

As mentioned in Section 2.7, it is essential to match the flame and heat transfer characteristics for oxy-fuel combustion to those for air-firing in case of a boiler retrofit. In order not to reduce plant efficiency or induce operational difficulties, the ratio between radiative and convective heat transfer should be maintained similar to that of air-firing as well [12].

*3.2.2.1. Overall heat transfer.* Experiments performed by IFRF [88,12] have shown that a recycle ratio of 0.58 (26 vol% $O_2$) yields radiative and convective heat transfer rates similar to those of air-firing in their experimental setup. The observed, optimum recycle rate is marginally lower than the theoretically determined value, see Fig. 10, which is caused by some degree of air leaking into the boiler and the fact that pure $CO_2$ was used for fuel transportation [88].

Investigations of the possible differences between wet and dry recycle has been performed by the Argonne National Laboratory [86], see Fig. 13. The experiments showed that the optimal $(CO_2 + H_2O)/O_2$ molar ratio is different in each case. The ratio yielding the same overall heat uptake changed from 3.25 (equal to a recycle ratio of 0.68 or 23.8 vol% $O_2$ at the burner inlet) for the wet case to 2.6 (recycle ratio of 0.63 or 27 vol% $O_2$ at the burner inlet) for the dry case. The optimum recycle ratios were likewise validated at reduced load and with a bituminous coal. Wall et al. [128] saw a similar difference between wet and dry recycle. Their values were 28% and 35% for wet and dry recycle, respectively. The difference suggests that the absolute concentration of water vapor in the boiler has a significant effect on overall heat transfer efficiency. The exact reason for this influence is not clear and modelling could provide indications to the influence from different factors such as radiation, thermo-chemical properties of the gases, etc.

*3.2.2.2. Radiative heat transfer.* The main contributor to the heat transfer from a flame from conventional fuels is thermal radiation [4,5]. The radiating species considered for pulverized-coal-fired systems are $H_2O$, $CO_2$, CO, $SO_2$, soot, char, and ash particles [65,86,128,188].

The presence of higher concentrations of $CO_2$, $H_2O$, and $SO_2$ in oxy-fuel combustion will increase the non-luminous radiation [65]. Payne et al. [86] and Khare et al. [116] estimated gas emissivities in both air- and oxy-fuel atmospheres. Even though their estimates are not in exact agreement, they generally find a difference of 0.1 between the two types of environments, e.g. from 0.45 in air to 0.55 in oxy-fuel [116,128].

Because of the higher concentrations of $H_2O$ and $CO_2$ in the furnace and their higher gas emissivities compared to nitrogen, the radiative heat transfer in the boiler will exceed that of conventional air-firing for the same adiabatic flame temperature [4,5,128,155]. In order to obtain the required heat transfer profile in both the radiative and convective passes a slightly lower oxygen concentration than required to reach a comparable adiabatic flame temperature should thus be chosen [4,5,128]. Typical results suggests a decrease of the oxygen concentration of 2–3 vol%. The use of the adiabatic

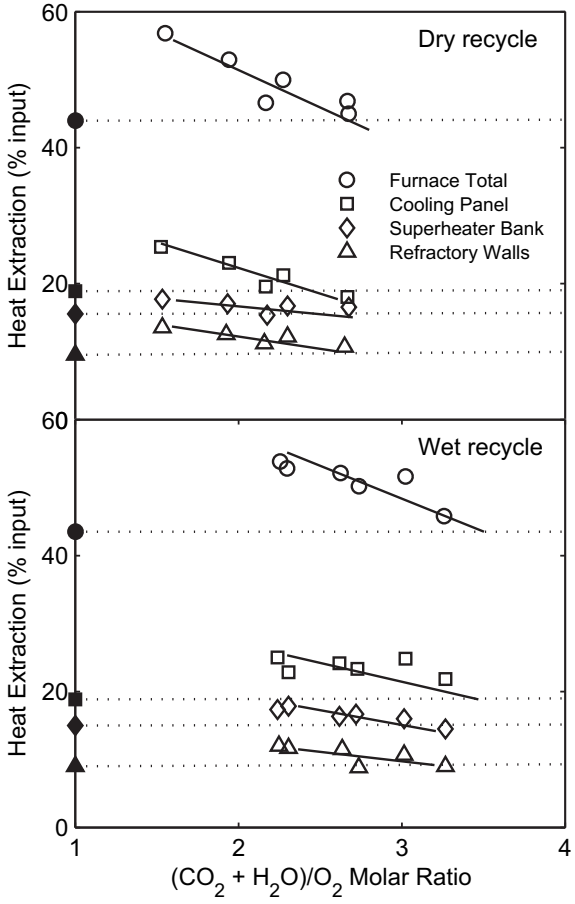


**Fig. 13.** Heat extraction in different furnace sections of a 3 $MW_{th}$ setup as function of the $(CO_2 + H_2O)/O_2$ molar ratio in the flue gas for dry recycle and wet recycle. For the dry case the recycled flue gas contains 5% residual $H_2O$ due to lack of efficiency in the water removal system. Solid symbols correspond to experiments in air. The coal tested is sub-bituminous (Black Thunder). Data taken from [86].

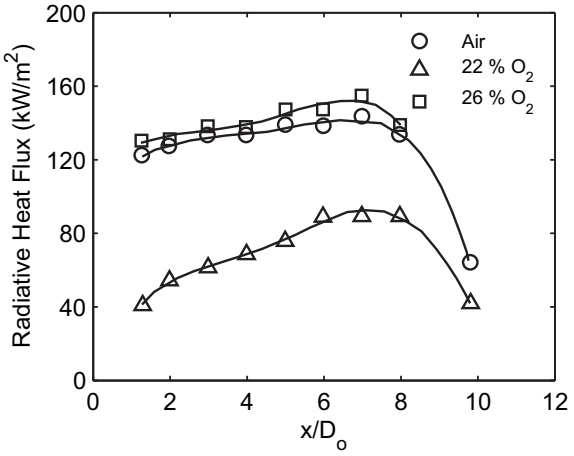


**Fig. 14.** The effect of recycle ratio on the net radiative heat flux along the IFRF 2.5 MW furnace operated with wet flue gas recirculation. Results obtained for a bituminous coal during air combustion and oxy-fuel combustion with oxygen concentrations of 22% and 26% at the inlet. These oxygen concentrations correspond to recycle ratios of 0.73 and 0.58, respectively. Data taken from [88].

flame temperature as a rough indicator of radiative heat transfer characteristics is thus altered compared to air-firing [88,12].

Fig. 14 shows the radiative heat transfer profiles for three different coal flames; the air-firing case, as well as oxy-fuel flames with overall oxygen concentrations in the oxidant of 22 and 26 vol %. The experiments are performed in the IFRF 2.5 $MW_{th}$ furnace. It is seen that 26% $O_2$ in the oxidant yields a profile very similar to that of air-firing, as expected. At the same time, the inlet oxygen concentration of 26% was reported to yield in-flame gas composition trends, combustion performance, flame length, and flame stability comparable to normal air operation.

Experiments on oxy-fuel combustion of propane [153,155] have revealed an up to 30–60% increase in the flame radiation intensity (27% $O_2$) at peak levels compared to air-firing. At the same time, the gas temperature levels are generally slightly lower for the oxy-fuel case. The authors observed that the increased gas emissivity due to enhanced $CO_2$ concentrations could not account for the entire difference. Further investigations showed that the in-flame soot volume fraction increased when shifting to oxy-fuel conditions [153]. Due to the lower volumetric flow rates and higher fuel concentration compared to oxidant in the oxy-fuel combustion the concentration and residence time of soot precursors in the near-burner region are increased. The formation of soot will thus be promoted [155]. These mechanisms for a gaseous fuel most probably also apply to volatiles combustion in coal-fired operation. The relative effect of an enhanced soot formation from volatiles on overall radiation from a solid-fuel flame is not known and could thus be the subject of future research.

Shaddix and Molina [168] measured the soot cloud size for a bituminous and a sub-bituminous coal in both $N_2$ and $CO_2$-based combustion media. Fig. 15 show the results for the bituminous coal. Generally, oxy-fuel combustion leads to larger soot cloud formation compared to the nitrogen based experiments at equivalent oxygen concentrations, confirming the results from Andersson et al. [153,155]. For increasing oxygen partial pressure the soot cloud size decreases for both types of combustion atmospheres.

The effect of in-flame particulates on flame radiative properties is mainly a function of their total mass and temperature. The absolute amount of ash does not change between air- and oxy-firing operation for equal fuel input. The amount of soot in the flame can, on the other hand, change drastically with changes in the near-burner flow dynamics. Changes in the burnout rate of char can likewise affect the location of heat transfer by radiation in the flame zone.

Besides experiments on propane, Andersson et al. [188] conducted radiation intensity measurements in air- and oxy-fuel flames burning lignite. They found that the shift in combustion medium resulted in only a negligible increase in the total radiation intensity at comparable gas phase temperatures. Due to gas-particle overlaps and the fact that particle radiation dominates in solid-fuel flames the effect of increased gas emissivity is limited. Regarding the gas phase, the authors concluded, however, that operating with a wet flue gas recycle would have a much larger impact on radiation intensity in large-scale boilers than the increase in $CO_2$ partial pressure. This observation is in line with that of Nozaki et al. [119].

*3.2.2.3. Convective heat transfer.* The increase in both density and heat capacity of the flue gas from increased concentrations of $CO_2$ and water vapor will increase the heat transfer in the convective section of the boiler [4,5] (for the same volumetric flow and entering temperature as during air-firing). However, in order to obtain an adequate temperature and heat uptake in the radiative section the flue gas flow is reduced due to the necessary increase in oxygen concentration. The resulting heat transfer rate in the convective section is not necessarily reduced in comparison with air-fired conditions as a consequence of the reduced flue gas flow rate. The convective heat transfer is a function of the Reynolds number, the Prandtl number, and the thermal conductivity of the

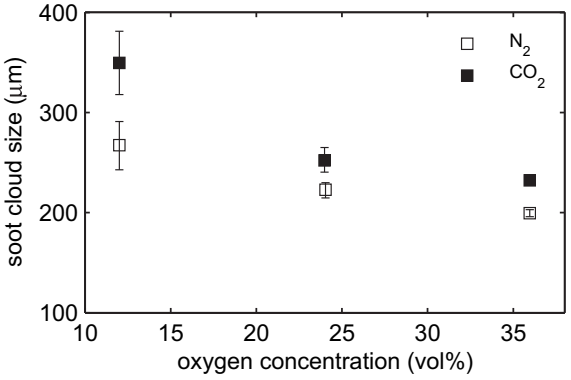


**Fig. 15.** Variation of characteristic soot cloud size during devolatilization of Pittsburgh coal (high-volatile bituminious) for different gas compositions in the Sandia optical EFR facility. Error bars represent 95% statistical error. Data taken from [168].

flue gas. All of the above will change with the change in flue gas composition and the flue gas temperature associated with the shift from air-firing to oxy-fuel combustion. Whether the resulting heat transfer rate in the convective section will match that of the air-firing case is dependent on the specific case. Simulations would be a valuable tool in the evaluation.

### 3.3. The combustion process

#### 3.3.1. Devolatilization and ignition

Volatiles constitute a major fraction of the combustible matter of most coals used for power generation. The combustion of volatiles releases heat which is important for ignition, local stoichiometries, and pollutant emissions [172]. The differences in properties for $N_2$ and $CO_2$ presented in Table 9 suggest that devolatilization and ignition in oxy-fuel combustion will occur at different rates than for combustion in air if $CO_2$ is substituted directly for $N_2$.

Shaddix and Molina [126,168] studied the effects of the presence of $CO_2$ and enhanced oxygen concentrations on the devolatilization and ignition of pulverized Pittsburgh (high-volatile bituminous) and Black Thunder (sub-bituminous) coals in a laminar flow reactor. Fig. 16 shows estimated values of particle devolatilization and ignition times for the Pittsburgh coal at 1700 K in different gas mixtures. From the data it is concluded that the exchange of $CO_2$ for $N_2$ does not significantly affect the devolatilization time for this particular type of experiment. From a consideration of heating an inert particle, the authors reason that for a fixed gas phase temperature the only factor that influences the initial heating of a particle is the thermal conductivity [126,168]. As seen from Table 9 the ratio between the thermal conductivity of $CO_2$ and that of $N_2$ is close to one at 1400 K. Hence, the initial heating profile of particles in each atmosphere will effectively be similar. Since coal devolatilization is an endothermic process with a rate that is strongly dependent on particle temperature and heating rate the specific conditions of the reported experiments suggest that there should be no difference between the different atmospheres, as observed. The result is, however, only valid for the case of equal gas phase temperatures, regardless of the gas phase environment. For a practical boiler this assumption is not necessarily satisfied.

As the oxygen concentration increases the devolatilization as well as the ignition occur more rapidly. In earlier work on air combustion Murphy and Shaddix [166] proposed the increase in the devolatilization rate with increasing oxygen concentration to be the result of (1) a closer proximity of the volatiles flame to the coal particle, and (2) a higher temperature of the volatile flame. Furthermore, modelling considerations suggested increasing

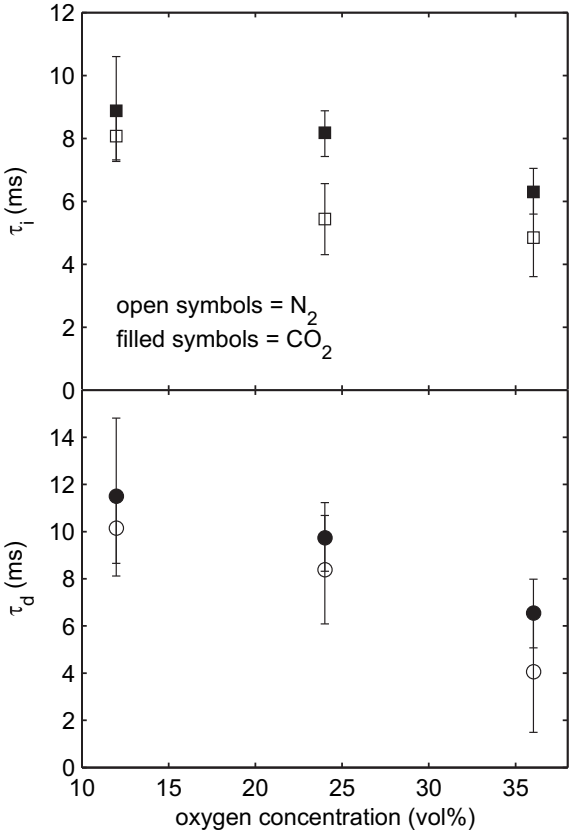


**Fig. 16.** Variation of ignition delay ($\tau_i$) and devolatilization ($\tau_d$) times for Pittsburgh coal burned in different gas mixtures in the optical EFR at Sandia National Laboratories. The data is based on images collected with an ICCD camera. Vertical bars represent the statistical error. Ignition delay was defined as the time elapsed from particle injection into the reactor to the time when 50% of the images correspond to devolatilization. Data taken from [168].

kinetic control for increasing oxygen concentrations. At a low oxygen partial pressure and high temperature, oxygen transport through the gas film surrounding the particles will be rate limiting. At increasing oxygen partial pressures and constant temperature the kinetic rate will remain almost constant whereas the rate of gas film transport will increase linearly with the pressure.

The differences in particle ignition times observed in Fig. 16 is a consequence of the differences in transport properties of the surrounding gas, the combustion heat release, and the reactivity of the local fuel-oxidizer mixture [126,168]. Generally, increasing the mixture reactivity and heat release will decrease the ignition time, whereas an increase in the product of density and heat capacity (the heat sink, $\rho C_p$) leads to an increase in the ignition time. The heat sink for $CO_2$ is substantially larger than for $N_2$, see Table 9, leading to an increase in ignition time for similar oxygen levels. Kiga et al. [136], Kimura et al. [87], and Liu et al. [121] have observed similar delays in the ignition of coal particles when burning in an atmosphere of 21% $O_2$ in $CO_2$. Increasing the oxygen concentration will increase the characteristic reaction rate of the local mixture and thus decrease the ignition time [126,168,189]. Changing from 24 to 36% $O_2$ is seen to have a large, absolute effect on the oxy-fuel mixture. Comparing the results for air- and oxy-fuel combustion reveals that it should be possible to obtain similar devolatilization and ignition properties for oxy-fuel combustion as for conventional air-firing.

Suda et al. [190] measured the flame propagation velocity with respect to different coal concentrations, coal types, and ambient gas compositions in a microgravity facility. Fig. 17 shows the observed

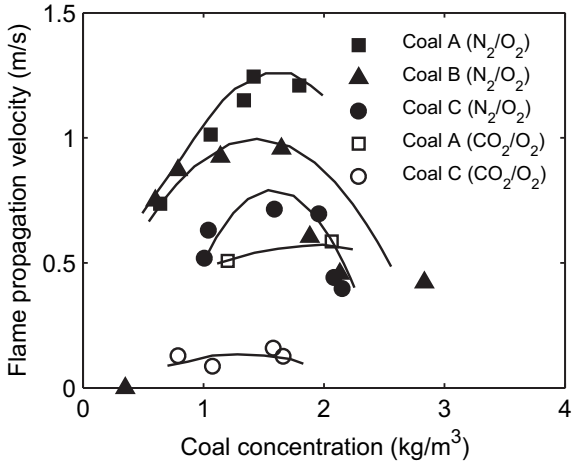


**Fig. 17.** Effect of coal concentration on the flame propagation velocity for three different coals; A, B, and C. Measurements are performed in a microgravity facility. The coals differ in their volatile matter contents. Coal A has the highest amount (46.0 wt%), followed by coal B (36.2 wt%) and then C (32.9 wt%), all on an "as received basis". Coal particle diameters: 53–63 μm, $O_2$ concentration: 40% by volume. Data taken from [190].

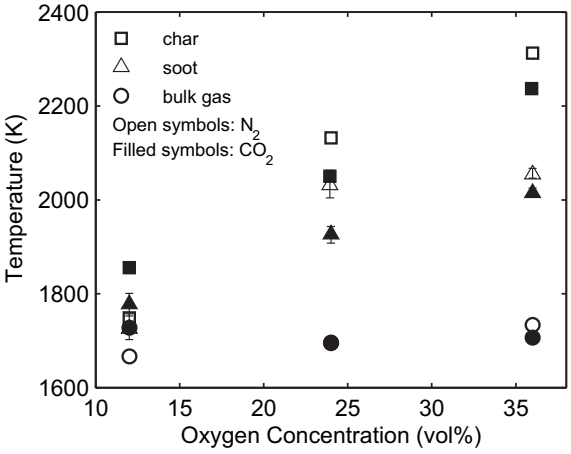


**Fig. 18.** Variation of characteristic soot cloud and char combustion temperature, during devolatilization and subsequent char combustion in different $O_2/N_2$ and $O_2/CO_2$ mixtures. The fuel is a Pittsburgh coal (bituminous) and the experiments are performed in the Sandia EFR facility. Error bars represent 95% statistical error. Data taken from [168].

effect of each parameter. The coal type is seen to have a significant effect on the flame propagation speed in both enriched air- and oxy-fuel environments. Each case operates with 40 vol% $O_2$ in the oxidizer. The difference in coal type is mainly a matter of the volatile content of each coal. The speed is seen to increase with increasing volatile matter content. For a given coal in a given environment an optimum in the propagation speed exists with respect to the coal concentration. The optimum concentration is seen to be approximately similar for all data series. According to the authors, this particle concentration corresponds to an inter-particle distance roughly equal to the flame radius of a single, burning particle [190].

### 3.3.2. Volatile and char burnout

Besides the impact from exchanging $N_2$ with $CO_2$ on the devolatilization and ignition of coal particles the burnout of both char and volatiles is expected to be affected.

The coal burning process is typically limited by both chemical kinetics and external diffusion (Zone II conditions). At 1400 K the diffusivity of $O_2$ in $CO_2$ is only about 75% of that in $N_2$. The lower diffusivity will thus reduce both the burning and heat generation rates for the coal particles [169]. At the same time, the diffusivity is a strong function of temperature. Hence, the effect of the enhanced heat capacity of $CO_2$ and the associated decrease in flame temperature for similar oxygen concentration in oxy-fuel and air combustion will further reduce the burning rate. Fig. 18 shows trends in ambient gas phase as well as soot cloud and char combustion temperatures for different combustion media obtained by Shaddix and Molina [168] in their EFR facility. At equal oxygen concentrations and gas phase temperatures combustion in $O_2/N_2$ mixtures generally yield higher temperatures of both soot clouds and char than in $O_2/CO_2$ mixtures.

The consumption rate of volatiles in oxy-fuel combustion is likewise expected to be slower than in air due to the lower diffusivity of small hydrocarbons in $CO_2$ compared to $N_2$ [122,126,168].

In retrofit respects, burnout in oxy-fuel combustion with comparable adiabatic flame temperatures as in air is expected to improve. This is because of the higher oxygen partial pressure experienced by the burning fuel, possible gasification by $CO_2$ (and $H_2O$), and longer residence times due to the lower gas volumetric flows [5,128]. Other researchers claim that excess $CO_2$ in the vicinity of the burning particle could alter the reaction equilibrium and slow down the burning rate [117]. However, that conclusion is based on a simplified analysis.

*3.3.2.1. Burnout times.* Bejarano and Levendis [181] have conducted a series of experiments with non-intrusive optical multi-colour pyrometry measurements of volatile flame and char burning phenomena in single particle environments. Fig. 19 illustrates average temperatures and burnout times measured for a high-volatile bituminous coal. The data indicate an effect of exchanging $N_2$ for $CO_2$ and the effect of varying the $O_2$ concentration in the oxidizer. The lower diffusivity of $O_2$ in $CO_2$ compared to $N_2$ is the major cause of reducing the burning rate during char combustion [167]. Generally, it is seen that an oxygen mole fraction of 0.3–0.35 yields similar temperature and burnout data for oxy-fuel combustion compared to combustion in air. By comparing the measured and calculated burnout times shown in the figure, Bejarano and Levendis [181] conclude that the char combustion for both air- and oxy-fuel combustion occurs in Zone II.

Wang et al. [118] have shown a significant increase in char burnout rate when increasing the oxygen concentration in $O_2/CO_2$ combustion from 21 to 29%. Similar results were found by Naredi and Pisupati [187] from drop-tube experiments on bituminous coals with 21% and 30% oxygen in the oxidant. Tan et al. [12] refer to studies performed by Takano and coworkers in the IHI 1.2 MW swirl burner which gave similar results. Moreover, a marked reduction in unburned carbon in the fly ash with increasing oxygen level was observed.

In general, the reported investigations have shown that increasing the oxygen concentration in the oxidant for oxy-fuel combustion can compensate for the larger specific heat of $CO_2$ compared to $N_2$. Comparable burnout times are thus achievable.

*3.3.2.2. Gasification reactions.* Both $CO_2$ and $H_2O$ may contribute to the burnout of char particles through gasification reactions, (6) and (7), when these species are present in high concentrations at high temperature [191,166] and the oxygen excess, $\lambda$, is significantly lower than 1.

$$C + CO_2 \rightleftharpoons 2CO \quad (6)$$

$$C + H_2O \rightleftharpoons CO + H_2 \quad (7)$$

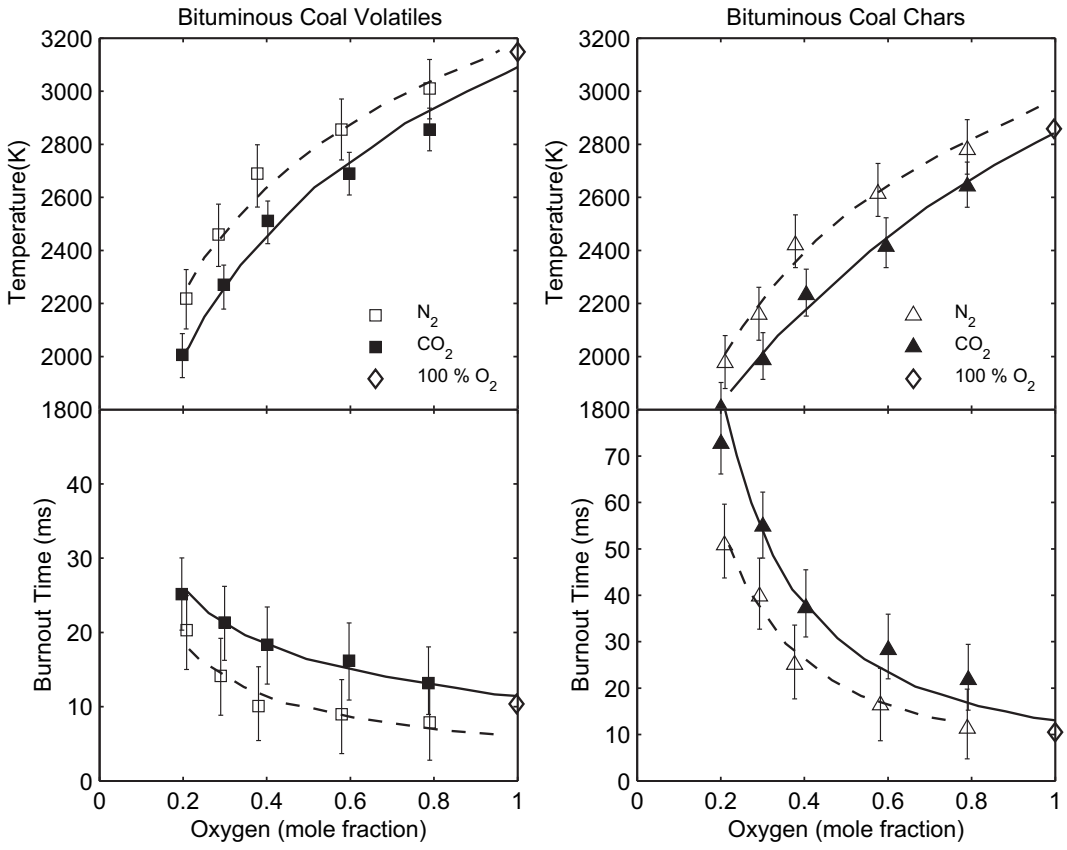


**Fig. 19.** Average particle temperatures (top row) and burnout times (bottom row) for a high-volatile-A bituminous Pittsburgh #8 coal (45–53 μm) burning in $O_2/N_2$ and $O_2/CO_2$ in a laminar-flow drop-tube reactor at $T_{furnace} = 1400$ K. The temperatures shown correspond to ~50% burnout times for each phase. Error bars correspond to one standard deviation, $\sigma$. Data taken from [181].

In low-temperature regions (400–900 °C) gasification does not play a role. This is due to a much lower rate of reaction for gasification with $CO_2$ compared to $O_2$-combustion at these conditions [192].

Results presented by Wall et al. [139,128] indicate that the volatile yield is higher during oxy-fuel combustion than in air. They attribute it to gasification. However, Borrego and Alvarez [193] found the opposite trend during their experiments.

Due to the conflicting results, the possible influence of gasification reactions during oxy-fuel combustion is an area which needs further investigations.

*3.3.2.3. Effect of coal properties.* Liu et al. [162] investigated the burnout efficiency compared to combustion in air for a range of bituminous coals in their 20 kW swirl burner, see Fig. 20. Even though the burnout efficiency differs between the samples it is always higher for combustion in 30% $O_2$/70% $CO_2$ than in air. Generally, the increase in burnout efficiency is between 0.5 and 2%. An examination of the coal characteristics has not revealed any obvious correlation between the burnout efficiency and the proximate or ultimate analysis. The reason for the differences within each coal type is suggested to be the higher oxygen concentration combined with similar temperatures for the oxy-fuel tests. The authors stress that gasification and longer residence times of the burning particles in the combustion chamber could also contribute to the higher burnout efficiency observed [162].

Fig. 21 shows the results of the work performed on burnout characteristics of different coals by Arias et al. [180]. The burnout of both coals show similar trends with changes in the stoichiometry. At fuel-lean conditions the burnout asymptotically approach a value of 100%. It is seen that the burnout of the high-volatile coal generally is a little lower than for the low-volatile coal. This is contrary to what was expected since the high-volatile coal should be more reactive. However, there may be significant uncertainties in the experimentally determined burnout, particularly because of alkali metal volatilization and possible ash carbonization from $CO_2$. For both coals the overall lowest burnout is, as expected, observed for oxy-fuel combustion with a low oxygen content.

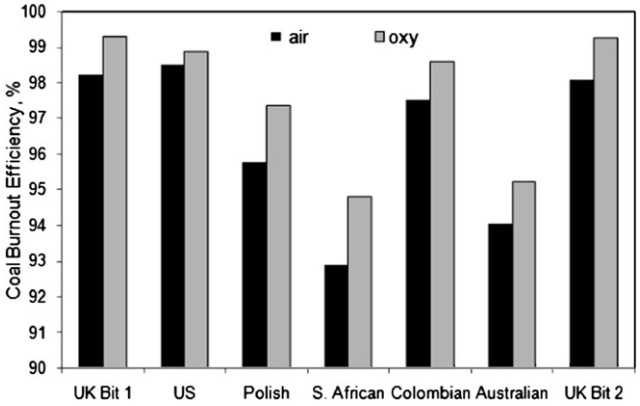


**Fig. 20.** Effect of combustion media on coal burnout efficiency for seven different bituminous coals. Results obtained in a 20 kW down-fired swirl burner. The coals are burned at $\lambda = 1.2$ in air and a mixture of 30% $O_2$ in $CO_2$ (oxy). Data taken from [162].

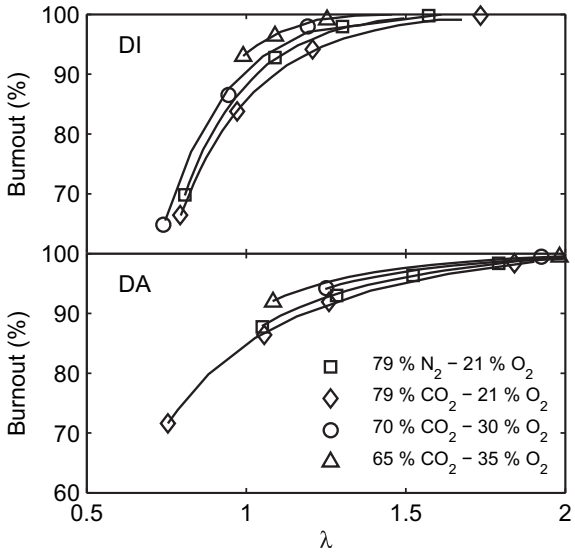


**Fig. 21.** Effect of gas atmosphere and stoichiometry on burnout of a low- and a high-volatile coal (DI and DA, respectively). The experiments are performed in an entrained-flow reactor. Data taken from [180].

*3.3.2.4. Particle size effects.* An investigation of the effect of particle size (45–53 and 75–90 μm) on volatiles and char temperatures has been performed by Bejarano and Levendis [181]. Given that the actual data and the measurement uncertainty has not been stated, the results given in Fig. 22 show only small or insignificant differences between the investigated particle size ranges.

The burnout times for the char particles are seen to depend on the particle size. As expected, the larger the particles the longer the burnout times. The effect of particle size is seen to be more significant in an oxy-fuel environment. A plausible explanation could be the lower diffusivity in $CO_2$ compared to $N_2$. Comparable results have been obtained by Huang et al. [189] from experiments in a TG thermal analyser.

*3.3.2.5. CO.* At high partial pressure and high temperature $CO_2$ can dissociate into CO and $O_2$ through the strongly endothermic reaction, (8), [172].

$$CO_2 \rightleftharpoons CO + 0.5O_2 \quad (8)$$

In the flame zone in oxy-fuel combustion both of the above conditions are present. Gasification of carbon, reaction (6) and (7), could likewise contribute to increase in the production of CO during oxy-fuel combustion. However, among researchers there is a difference in opinion on whether it is the thermal dissociation, [175], or the gasification reactions, [149], that play the dominant role in the significant increase in CO concentration in the flame compared to air-firing.

An even more important pathway to the increase in CO concentrations in the flame zone of oxy-fuel flames could be the reaction between $CO_2$ and H radicals, see reaction (9). The increased level of $CO_2$ induces a possible alteration of the composition of the O/H radical pool during oxy-fuel combustion due to the competition between $O_2$ and $CO_2$ for H radicals, (9) and (10) [172,194].

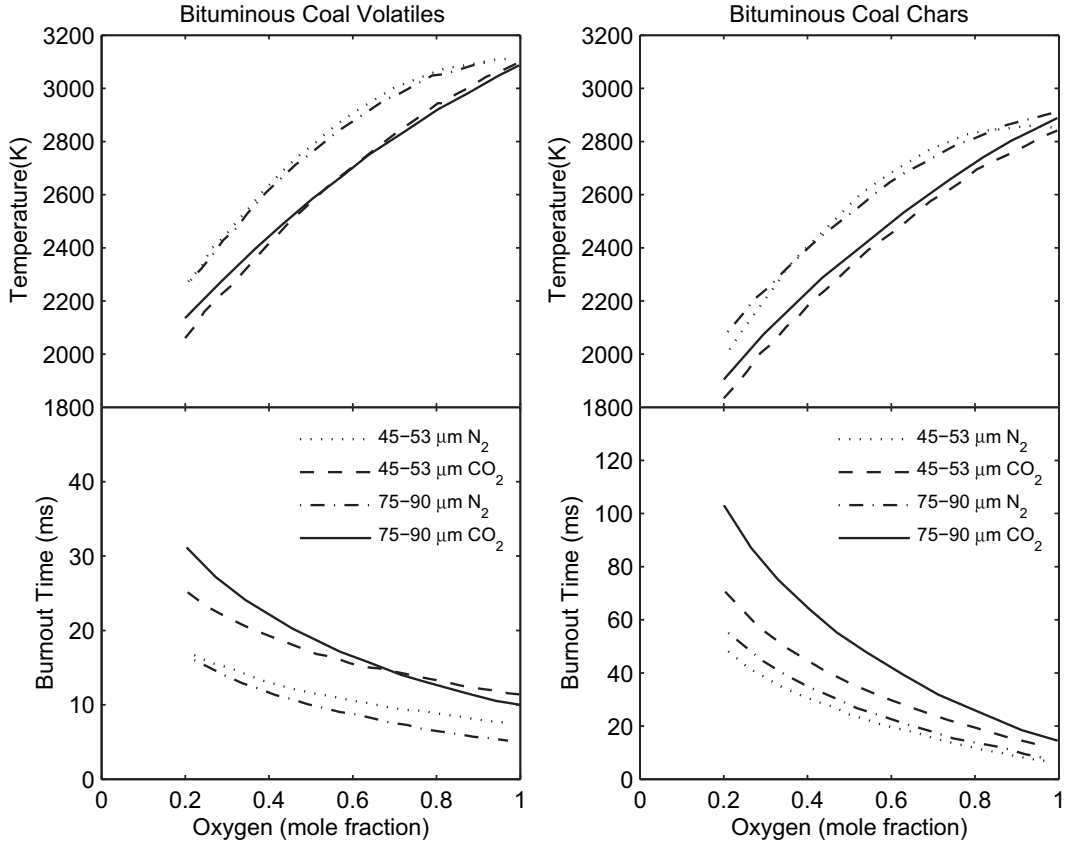


**Fig. 22.** Trends in average temperatures (top row) and burnout times (bottom row) for a high-volatile-A bituminous Pittsburgh #8 coal of two different size cuts (45–53 and 75–90 μm) burning in $O_2/N_2$ and $O_2/CO_2$ in a laminar-flow drop-tube reactor at $T_{furnace} = 1400$ K. The temperatures shown corresponds to ca. 50% burnout. Data taken from [181].

$$H + CO_2 \rightleftharpoons CO + OH \quad (9)$$

$$H + O_2 \rightleftharpoons O + OH \quad (10)$$

Due to the high partial pressure of $CO_2$ in oxy-fuel combustion the ratio of OH to both O and H will increase and the total amount of radicals is expected to decrease compared to air-blown combustion. Besides the reaction with H radicals, reaction of $CO_2$ with $CH_2$ radicals will likewise contribute to enhance the concentration of CO in the flame zone [172,194–196].

Whether the emission of CO from oxy-fuel combustion is larger than from air-firing has been subject to investigation. Because of its severe toxicity it is important that oxy-fuel combustion does not lead to an increased CO emission. Wang et al. [118] report no significant difference in the CO concentration levels both within the latter part of the flame zone and in the exhaust from a 3 $MW_{th}$ horizontal furnace for both air- and oxy-fuel combustion experiments with comparable flame temperatures. A five time increase in the CO level within the flame was expected however based on a modelling study. For an oxy-fuel experiment with an air-like composition of the oxidant the CO concentration in the flame zone was expected to be slightly larger than for air combustion based on modelling. The observed values for the oxy-fuel experiment were lower than calculated. All experiments yielded full burnout of CO before the exhaust.

Experiments performed in the IFRF 2.5 $MW_{th}$ furnace by Woycenko et al. [88] show significantly increased CO levels within the flame zone. Still, the combustion of CO has completed before the furnace exit and no significant CO emission is observed. Similar results were obtained by Scheffknecht and coworkers [164,148] and Liu et al. [121] even when the excess oxygen level was slightly higher for the latter oxy-fuel test. Changing the oxygen concentration from 30 to 21% increased the CO emission from 34 to 200 ppmv, due to delayed ignition and lower peak temperature.

Experiments on natural gas combustion performed by Glarborg and coworkers [172–174] indicate that the high levels of $CO_2$ in oxy-fuel atmospheres prevent complete oxidation of fuel (CO) to $CO_2$ at high temperatures even when excess oxygen is present. However, the effect is most pronounced at fuel-rich or stoichiometric conditions. There is no indication that high $CO_2$ levels influence CO oxidation at low temperatures when oxygen is in excess and hence there should be no increased risk of high CO emissions from a gas-fired oxy-fuel plant if mixing of fuel and oxidant is adequate.

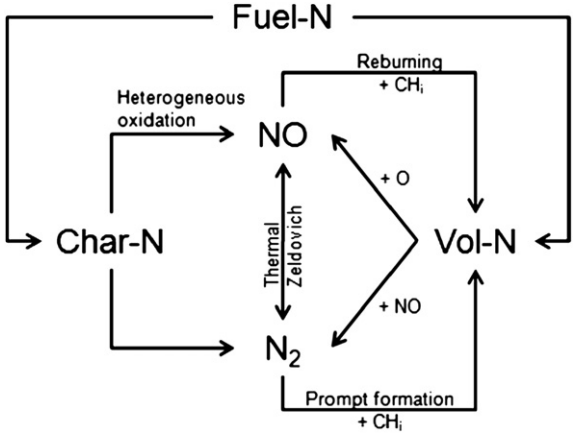


**Fig. 23.** The overall mechanism of NO formation and reduction. Vol-N is an intermediate gaseous compound, e.g. HCN or $NH_3$.

*3.3.2.6. Summary.* The difference in the thermo-chemical properties of $N_2$ and $CO_2$ affects the combustion process. At 21% $O_2$ in $CO_2$ devolatilization, ignition, and burnout proceeds at a lower rate than in air. However, increasing the oxygen concentration in the oxy-fuel environment to about 30% to obtain the same adiabatic flame temperature as in air yields similar devolatilization, ignition, and combustion rates as seen in air combustion. At comparable adiabatic flame temperatures oxy-fuel combustion is reported to yield improved burnout of char. This is most likely due to longer residence times and higher partial pressures of oxygen in the vicinity of the burning particles. Even though contribution of gasification by $CO_2$ and/or $H_2O$ to the increased burnout is suggested several times in literature, it is questionable if this effect is of significant importance for the conversion of the fuel.

CO levels in the flame zone are generally reported to increase significantly in oxy-fuel combustion compared to air-firing. Even though the high $CO_2$ levels prevent CO from being oxidized at high temperatures complete conversion is expected when excess oxygen is present during cool-down of the flue gas.

### 3.4. Gaseous pollutants emissions

The following subsections discuss the reported knowledge on the most important gaseous emissions besides CO from oxy-fuel combustion; $NO_x$, $SO_2$, and $SO_3$. Trace elements in the gaseous phase, e.g. Hg, Cd, As, and Se, are likewise treated. No results have been published regarding emissions of HCl and HF.

#### 3.4.1. $NO_x$

*3.4.1.1. $NO_x$ formation.* In conventional air combustion the generally accepted pathways for $NO_x$ formation are the following three mechanisms [197–199], see e.g. Fig. 23:

*Thermal:* Thermal NO formation results from $N_2$ and $O_2$ reacting at high temperatures (above 1500 °C) to form NO. The mechanism involves three reactions, known as the extended Zeldovich mechanism.

$$N_2 + O \rightleftharpoons NO + N \quad (11)$$

$$O_2 + N \rightleftharpoons NO + O \quad (12)$$

$$N + OH \rightleftharpoons NO + H \quad (13)$$

*Prompt:* Prompt NO is formed when hydrocarbon radicals in fuel-rich zones attack molecular nitrogen to form cyanide species, which subsequently form NO when oxidized. These reactions can take place at temperatures lower than is required for thermal NO formation.

*Fuel:* Fuel NO is derived from nitrogen in the fuel reacting through either volatile-N or char-N. Nitrogen released with the volatiles further decomposes into cyanide and amine species. These intermediate species may react to produce $N_2$ or NO, depending on the conditions. Char-N reacts through heterogeneous reactions and intermediate CN species to eventually produce NO or $N_2$. Detailed understanding of the reaction pathways for the conversion of char-N has not been established and is still an area of active research. The split between NO and $N_2$ on an overall level depends on factors such as the nitrogen content of the coal, its rank and volatility, as well as the stoichiometry.

It is generally assumed that up to 20% of the total $NO_x$ formed from pulverized coal combustion in air is due to thermal $NO_x$ and about 80–100% is derived from fuel-N while the prompt $NO_x$ mechanism is negligble, depending on the quantity of fuel-bound nitrogen species [199]. The low level of molecular nitrogen in oxy-fuel combustion will

suppress the formation of thermal and prompt $NO_x$ and hence potentially lower the overall $NO_x$ emission rate.

The general conclusion in published literature is that the amount of $NO_x$ emitted from an oxy-fuel plant can be reduced to somewhere between one-third and half of that from combustion in air [51,63,87,88,91,97,119,120,128,162]. However, the application of an oxygen concentration higher than 21% to obtain adequate flame temperatures could result in an enhancement of fuel-$NO_x$ formation [122].

The potential for reducing the $NO_x$ emissions from a power plant considerably compared to air-firing [4,200] has been one of the key drivers in oxy-fuel combustion research, particularly in USA [5] and thus, $NO_x$ chemistry has been one of the most heavily investigated areas within the oxy-fuel combustion technology. Normann et al. [201] have recently published a review on emission control of nitrogen oxides from oxy-fuel combustion.

The potential for a significant decrease in $NO_x$ formation is mainly important for oxy-fuel power plants with a configuration of the flue gas clean-up train which releases the impurities, including $NO_x$, to the atmosphere. If instead a $CO_2$ cleaning process is chosen which captures $NO_x$ and produces e.g. nitric acid the $NO_x$ formation rate is of less importance although it will affect process economics. In any case, if $NO_x$ formation can be reduced without significant negative consequence to the remaining combustion process it is desirable.

*3.4.1.2. Mechanism for the reduction of $NO_x$ during oxy-fuel combustion.* The majority of homogeneous $NO_x$ chemistry is taking place in the devolatilization and near-flame zone. The implications of oxy-fuel combustion on the homogeneous $NO_x$ formation and destruction are therefore likely to be alterations in equilibria and reaction pathways caused by higher concentrations of $CO_2$ and $NO_x$ in this part of the furnace. If the recycled flue gas is wet the higher partial pressure of $H_2O$ will likewise interfere through its influence on radical formation and destruction. The enhanced levels of $CO_2$ and $NO_x$ are also expected to affect the heterogeneous formation and reduction of NO. In addition to chemical effects, changes in the mixing patterns between fuel and oxidizer are likely to affect the nitrogen chemistry. In the following, these mechanisms for reduction of $NO_x$ in oxy-fuel combustion are discussed.

*Effect of the increased NO concentrations (reburning):* Recirculation of NO with the flue gas through the burner would be expected to lead to a considerable reduction of the nitrogen oxides emission through processes similar to those of reburning. Reburning is a chemically complex process in which nitric oxide is abated using fuel as reducing agent [202]. The process involves partial oxidation of the reburning fuel under fuel-rich conditions, reduction of NO by reaction with fuel fragments, and subsequent conversion of the intermediate nitrogenous species.

The reduction of NO may involve the following types of reaction:

1. $NO_x$ is reduced to cyanide and amine intermediates by reaction with hydrocarbon radicals, formed from the volatiles released from the coal particles in the early flame zone.
2. $NO_x$ is converted to $N_2$ through reactions with other reactive nitrogen species (XN), such as cyanides and amines. The XN species may be formed either from from the hydrocarbon-NO reactions or from release of N-volatiles in the early flame.
3. $NO_x$ is converted to $N_2$ by heterogeneous reactions on char or soot.

From experiments performed in a small-scale laboratory reactor, Okazaki and Ando [158] evaluated the relative impact of these mechanisms for NO reduction. They concluded that reburn type reactions, i.e. reactions of recycled $NO_x$ with hydrocarbons, is the dominant mechanism in reducing $NO_x$ emissions and that it accounts for 50–80% of the decrease in NO observed in oxy-fuel combustion. Reactions of $NO_x$ with N-volatiles were estimated to contribute 10–50% to the NO reduction. The reduction of NO on char in oxy-fuel combustion was found to be of minor importance, but their results may be biased by the choice of a char with a low reactivity (formed from anthracite).

*Effect of the low $N_2$ concentration:* At a very low concentration of $N_2$ in the oxidizer, the thermal $NO_x$ formation mechanism can be disregarded since the oxy-fuel combustion atmosphere will be oversaturated with NO at all times [123,156]. For this reason the Zeldovich reactions will be reversed and serve to convert NO to $N_2$.

A modelling study using detailed chemical kinetics on oxy-fuel combustion of lignite performed by Andersson et al. [90] indicates that while the formation of NO from fuel-N is the same or even slightly higher for oxy-fuel combustion compared to combustion in air, the destruction mechanisms at oxy-fuel conditions are enhanced compared to air conditions, leading to an overall reduction in the NO emission. At high temperatures (>1500 °C), the near-elimination of molecular nitrogen in oxy-fuel combustion facilitates reduction of NO by the Zeldovich mechanism. In order to obtain an effective reduction of NO by the reverse Zeldovich mechanism, a sub-stoichiometric combustion and/or an insignificant amount of air ingress into the furnace is required (air-staging to promote long enough residence time) [156]. At the same time, applying a wet flue gas recycle will increase the $NO_x$ reduction potential [156].

*Effect of the increased $CO_2$ concentration:* Only few studies have been reported on the impact of high $CO_2$ concentrations on the nitrogen chemistry in oxy-fuel combustion. Mendiara and Glarborg [174,173] investigated the implications of the alterations to the radical pool as described in Section 3.3.2 on NO formation and destruction. They considered oxidation of methane doped with either $NH_3$ (used to simulate volatile-N) [174] or NO [173] in a laminar flow reactor. According to their results, $CO_2$ acts to promote NO formation from volatile-N under fuel-rich conditions whereas it inhibits NO at both stoichiometric and fuel-lean conditions. At low oxygen concentrations formation of NO is favoured by the increase in OH-concentration. At conditions with oxygen excess, the reduced formation of NO is caused by the limitation of the O/H radical pool, particularly O. In reburning, a high concentration of $CO_2$ had only a small impact on the NO reduction efficiency under reducing conditions, while at stoichiometric conditions $CO_2$ slightly enhanced removal of NO.

Okazaki and Ando [158] pointed to the increased importance of reduction of $NO_x$ on char surfaces due to reaction with CO. The CO levels increase because of the high $CO_2$ concentration as described in Section 3.3.2. The promoting effect of CO on $NO_x$ reduction on char is well documented [199,203–206], but this mechanism is mostly important at fluidized bed conditions [198], i.e. at temperatures well below those characteristic of pulverized fuel combustion.

A change in selectivity of the release of char-N to NO has been suggested by Park et al. [207]. They investigated nitrogen release from pulverized bituminous coal char during the reaction with $O_2$, $CO_2$, and $H_2O$ using Ar as carrier gas in a fixed bed flow reactor. Their experiments showed that increasing the concentration of $CO_2$ in an $H_2O$ and $O_2$ free environment reduced the char-N to NO release ratio. In contrast to gasification with $H_2O$, no HCN or $NH_3$ were measured when $CO_2$ was the reactant. These experiments thus suggest that the increased levels of $CO_2$ during oxy-fuel char combustion may suppress the formation of NO and its precursors.

*Effect of changes to the flame and fuel/oxidizer mixing pattern:* Implementation of oxy-fuel combustion may bring about changes in the flame structure and the fuel/oxidizer mixing pattern. These

changes will depend on the burner geometry and the degree of recirculation and the composition of the flue gas.

Mackrory et al. [124,175] identify the following mechanisms that may enhance $NO_x$ reduction in oxy-fuel combustion:

- Less secondary oxidizer entrainment into the burner's recirculation zone due to a more detached flame, i.e. reduced oxygen availability and limited initial NO formation.
- Temperature increase in the fuel-rich zone will increase the rate of NO destruction. At higher temperatures the conversion of volatile-N proceeds faster toward $N_2$ than NO.
- Reduced NO formation from char since more fuel-N is released with the volatiles.
- Indirect effects through changes in reaction rates (combustion) and temperatures from the enhanced importance of gasification reactions.

Their overall conclusion is that faster NO destruction in oxy-fuel combustion appears to be at least partially due to the higher CO and NO concentrations.

*3.4.1.3. Summary of reported, experimental results.* Table 12 provides a summary of the reported results on $NO_x$ emission from oxy-fuel combustion in setups with flue gas recirculation compared with that from air-firing. Most of the experiments yield a decrease in the $NO_x$ emission rate during oxy-fuel combustion. However, some experiments show an increase which is suggested to be caused by the fact that the mechanism of fuel-$NO_x$ formation is very sensitive to the method with which oxygen and fuel is mixed in the flame [122,124,151]. As oxy-fuel burners are typically adopted from air-firing principles the resulting fluid dynamics of the flame can be disadvantageous with respect to $NO_x$ emissions even though the flames are stable.

In the following sections the reported results on $NO_x$ emissions from oxy-fuel combustion are divided according to the effects of different operating conditions and design aspects. Results from both once-through laboratory reactors and setups with flue gas recirculation are included. In each section a further subdivision is made, separating the different types of experimental setups, i.e. EFR type experiments from swirling flames. The underlying mechanisms of $NO_x$ formation and destruction do not change between setup types. However, scaling effects and the fact that mixing of fuel and oxidizer in larger burners is crucial to $NO_x$ formation will influence the absolute levels of $NO_x$ emitted. A direct comparison of small laboratory-scale setups and larger swirl burners with respect to $NO_x$ concentrations and emission rates is thus not possible. A clear example of this is the experiments performed by Hasatani et al. [161,109]. They burned a sub-bituminous Indonesian coal in an oxy-fuel environment with oxygen concentrations between 85 and 88 vol% in both an entrained-flow reactor [161] and in a 145 $kW_{th}$ vertical furnace [109]. They observed $NO_x$ concentrations of 4700 ppm and 1500 ppm, respectively, for otherwise similar combustion conditions.

*3.4.1.4. Effects of changes in the oxygen concentration, oxygen excess, flue gas recycling ratio, and gas phase temperature.* Experiments on $NO_x$ emissions from oxy-fuel combustion of a high-volatile bituminous coal in the IFRF 2.5 $MW_{th}$ furnace were performed in the early nineties by Woycenko et al. [88]. As shown in Fig. 24 they observed considerably higher $NO_x$ concentrations during oxy-fuel combustion with 26 vol% $O_2$ in the oxidant than in the air-firing case. However, the total mass of $NO_x$ formed per energy input of coal [mg/MJ], also termed the emission rate, was significantly lower in the oxy-fuel case which was assigned to the near-elimination of thermal $NO_x$ formation and reburning of recirculated $NO_x$.

Further experiments showed that an increase of the concentration of oxygen in the oxidant, and thus the flame temperature, yielded an increase in both the flue gas $NO_x$ concentration and the emission rate. The increase in oxygen concentration was performed by decreasing the flue gas recycle ratio. Similar trends of reduced

**Table 12**
Summary of $NO_x$ emission results from experiments in pilot scale and semi-technical scale with flue-gas recirculation.

| Author(s) | Fuel input (MW) | Inlet $O_2$, Oxy (%) | Emission (mg/MJ) | Conversion ratio (%) | Conclusion(s) |
|---|---|---|---|---|---|
| Payne et al. [86] | 3 | Dry: 28<br>wet: 24 | Air: 560<br>Oxy,<br>dry: 160<br>Oxy,<br>wet: 95 | – | $NO_x$ formation is reduced by approximately 70% for dry recycle and 80% for wet recycle compared to air-firing. |
| Woycenko et al. [88] | 2.1 | 26 | Air: 320<br>Oxy: 50–150 | Air: 30<br>Oxy: 5–14 | $NO_x$ formation is lower in oxy-coal combustion with flue-gas recirculation than in air case. |
| Châtel-Pélage et al. [63] | 1.5 | 25 | Air: 100–175[a]<br>Oxy: 25–55 | – | Potential for drastic $NO_x$ reduction of up to 60–70% |
| Kimura and coworkers [87,119] | 1.2 | 27 | Air: 340<br>Oxy: <90 | Air: 30–33<br>Oxy: <8 | $NO_x$ conversion ratio in oxy-fuel combustion is significantly lower than that in normal air combustion because the recycled $NO_x$ is rapidly reduced to HCN or $NH_3$ in the combustion zone (reburning). |
| Scheffknecht and coworkers [144] | 0.5 | 27–30 | Air: 90–350[b]<br>Oxy: 55–325 | – | $NO_x$ emission rate increases for increasing burner stoichiometry and is always higher for air combustion than oxy-fuel combustion for comparable operation conditions. |
| Croiset and coworkers [120,97] | 0.21 | 28, 35, 42 | Air: 340<br>Oxy: 100–210 | Air: 35[c]<br>Oxy: 10–22 | High $NO_x$ concentration inside the furnace but lower $NO_x$ emission rate with the flue gas than for air-firing. |
| Chui et al. [150,151] | 0.21 | 28 | Air: 110<br>Oxy: 62–150 | Air: 14<br>Oxy: 8–19 | $NO_x$ formation is strongly dependent on burner design, i.e. the near-burner flow field. $NO_x$ emission from oxy-fuel combustion can change from lower to higher than in the air-firing case. |
| Tan et al. [122] | 0.21 | 35 | Air: 211–269<br>Oxy: 68–233 | Air: 21–31<br>Oxy: 8–24 | $NO_x$ emissions dependent on coal type. Lignite, sub-bituminous, and bituminous coals tested. Specially designed burner for oxy-firing significantly reduces the $NO_x$ emission rate. |
| Andersson et al. [90] | 0.1 | 25, 27, 29 | Air: 150<br>Oxy: 40–50 | Air: 24<br>Oxy: 7–8 | The reduction in NO emissions for oxy-fuel combustion is due to an increased destruction of formed and recycled NO compared to air-firing. The conversion of fuel-N to NO is similar or even slightly higher during oxy-fuel combustion than in air. |

[a] The interval reflects the variation between $\lambda = 0.68$ and 1.2 for the air tests and $\lambda = 0.85$–1.05 for oxy-fuel tests.
[b] The interval reflects the variation between $\lambda_{burner} = 0.75$ and 1.15 for both the air- and oxy-fuel tests.
[c] Conversion made using coal HHV.

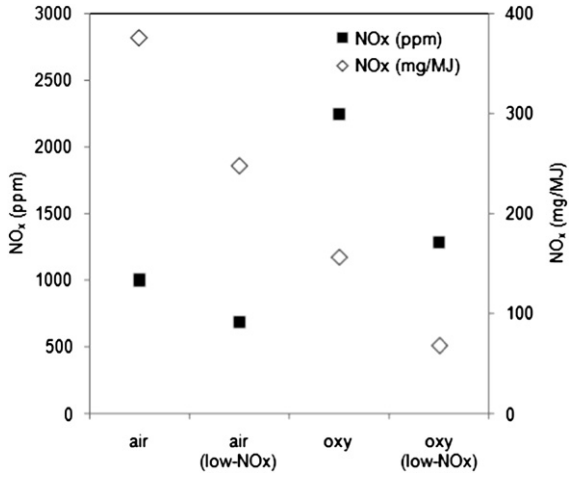


**Fig. 24.** NO emissions and flue gas concentrations for air-firing and oxy-fuel combustion (oxy) with and without low-$NO_x$ burner technology. The fuel, a high-volatile bituminous coal (Göttelborn), is burned in the IFRF 2.5 $MW_{th}$ furnace. The combustion is performed at an overall stoichiometry of $\lambda = 1.15$ and the inlet oxygen concentration in the oxy-fuel experiments is 26%, corresponding to a recirculation ratio of 0.58. The $NO_x$ concentration is in the dry flue gas and is normalized to 0% $O_2$. Data taken from [88].

$NO_x$ emission rates during oxy-fuel combustion compared to air-firing have been reported for different fuels in laminar flow reactors [174], entrained-flow reactors [96,160,161,169], and swirling flames [72,90,97,120,121,164].

According to Hu et al. [161] there are two opposing factors influencing $NO_x$ formation and reduction in coal combustion; the oxidation of fuel-N by oxygen and other oxidizing species, and the reduction of $NO_x$ by reducing agents, such as hydrocarbons from pyrolysis and resident char. They have performed a series of experiments in their entrained-flow reactor analysing the influence of oxygen concentration, oxygen excess, and gas phase temperature to clarify the importance of each parameter on $NO_x$ formation and destruction. Fig. 25 shows, as expected, that the $NO_x$ concentration generally increases with increasing oxygen concentration, partly due to decreased dilution, and shows a peak at near stoichiometric conditions. The $NO_x$ emission rate (bottom row), however, increases approximately linearly near $\lambda = 1$ when changing from fuel-rich to fuel-lean conditions. At high oxygen excess for all oxidant compositions the $NO_x$ emission rates approach asymptotic values. Increasing the gas phase temperature results in both increasing $NO_x$ concentrations and emission rates for all stoichiometric values. As accentuated in Fig. 26 for a temperature of 1273 K, it is likewise seen that the emission rate yields a slight peak at around 50% $O_2$ in the oxidizer, however most significantly for fuel-lean conditions. Hu et al. [96] state that this phenomenon is a consequence of the concentration of reducing agents increasing proportionally to the increase in $O_2$ concentration (decreasing recycle ratio). At low oxygen concentrations (<50 vol%) they thus assume oxidation to dominate and $NO_x$ emissions to increase with increasing $O_2$ concentration. For $O_2$ concentrations above 50%, reduction by reducing species should play the dominant role and $NO_x$ emissions decrease with increasing $O_2$ concentration [96].

The concentration of reducing agents does undoubtedly contribute to the behaviour in Fig. 26 but other factors may likewise contribute. As the oxygen concentration is increased the reaction between char and oxygen proceeds faster which will result in higher particle temperatures. The fractional conversion of char-N to NO has been reported to increase initially with temperature [199] until the point where the oxygen-char reaction approaches the diffusion limited regime. A further increase in particle temperature

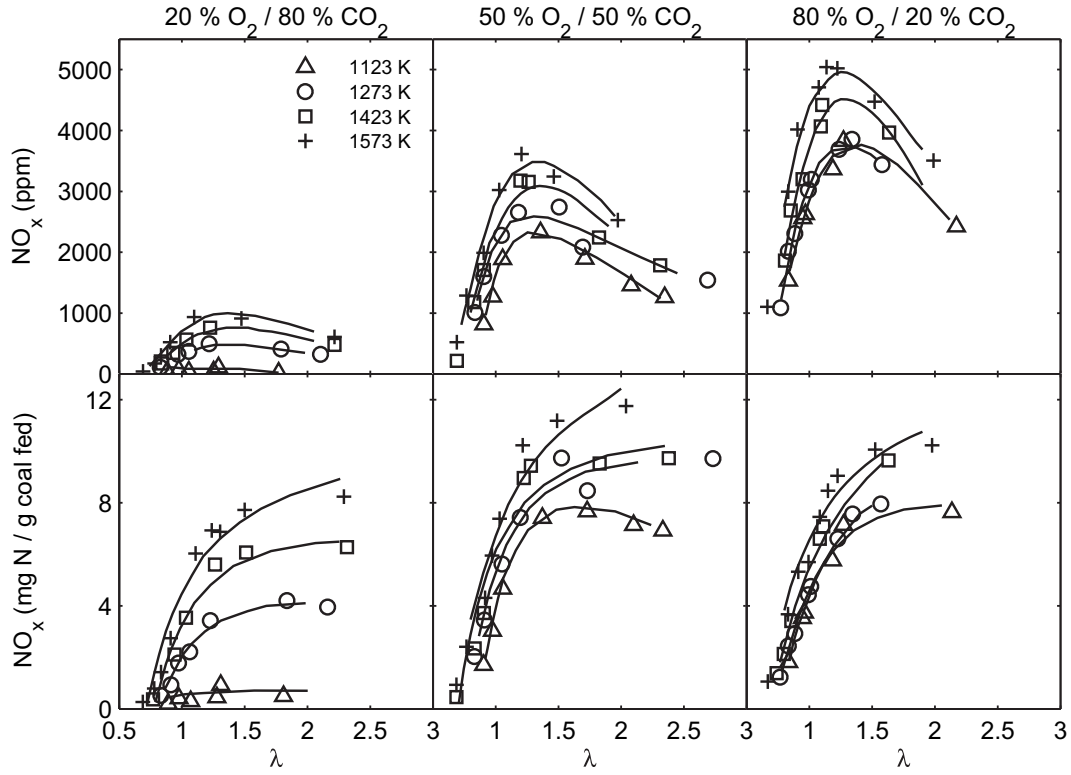


**Fig. 25.** $NO_x$ emission versus stoichiometric ratio and temperature at different $O_2$ concentrations for $CO_2$-based oxidizers. Experiments performed on a bituminous coal in an entrained-flow reactor with a coal flow rate of up to 180 g/h. The $NO_x$ concentrations in ppm are given as measured. Data taken from [96].

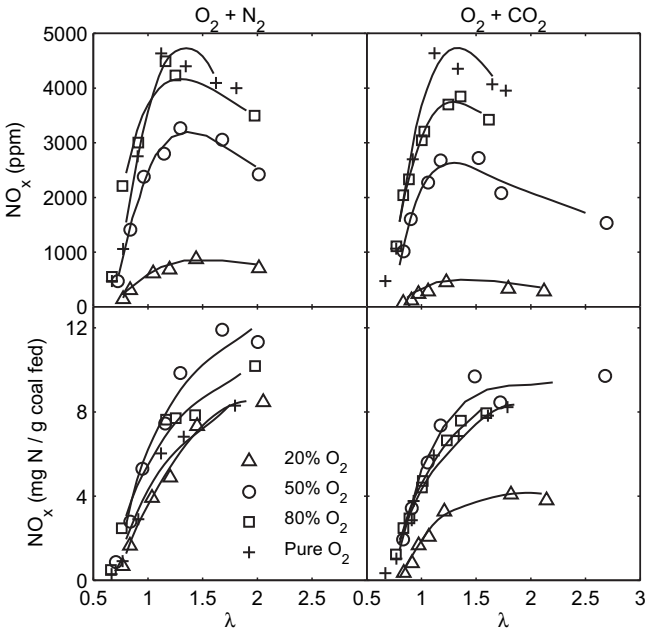


**Fig. 26.** $NO_x$ emissions as a function of stoichiometric ratio at different $O_2$ concentrations for $N_2$ and $CO_2$-based inlet gases at 1273 K. Experiments performed on a bituminous coal in an entrained-flow reactor with a coal flow rate of up to 180 g/h. The $NO_x$ concentrations in ppm are given as measured. Data taken from [96].

will mainly increase the rate of NO reduction by char [199], in fact what is observed from the data in the figure.

Nozaki et al. [119] showed that air- and oxy-fuel combustion of a low-volatile bituminous coal yielded similar $NO_x$ profiles in their 1.2 MW burner with flue gas recirculation, even though $NO_x$ was recirculated to the burner during oxy-fuel firing. The experiments were performed with fixed firing rate and excess oxygen conditions at the burner. Measurements of HCN and $NH_3$ along the burner axis showed significantly increased levels of $NH_3$ in oxy-fuel combustion compared to air-firing, see Fig. 27. The authors concluded that $NO_x$ recycled with the flue gas is reduced primarily to $NH_3$ and $N_2$ in the early part of the flame. Experiments with direct oxygen injection in the burner revealed a significant increase in the HCN concentration in the flame zone. Nozaki et al. [119] assume this to be caused by increased devolatilization arising from a higher flame temperature compared to the oxy-fuel case without direct oxygen injection. Air-firing and oxy-fuel combustion without oxygen injection yielded similar HCN profiles even though the flame temperatures were significantly different. Based on the described observation, oxy-fuel combustion leads to higher concentrations of the intermediate cyano and amine species in the $NO_x$ formation mechanism in the flame zone compared to air-firing. At the same time, oxy-fuel combustion yields similar concentrations of $NO_x$ in the exhaust gas compared to air-firing and thus reduced $NO_x$ emission rates due to the lower volume of flue gas.

*3.4.1.5. Effect of flue gas composition.* Most laboratory-scale experiments on oxy-fuel combustion are performed in once-through reactors, where the recirculated flue gas is simulated by pure $CO_2$. It is relevant to compare the results of once-through experiments to those with flue gas recirculation to clarify whether there are significant differences which should be accounted for.

The experiments reported by Croiset and coworkers [97] yield a 40–50% decrease in $NO_x$ emission rates when flue gas is recycled, compared to once-through runs, see Fig. 28. The experiments were performed in the CANMET 0.3 $MW_{th}$ vertical combustor facility at

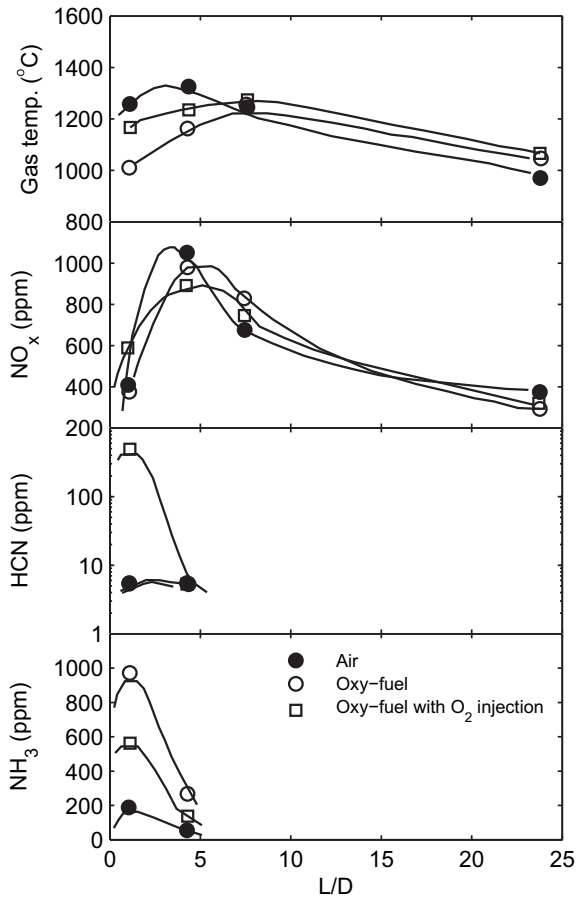


**Fig. 27.** Gas temperature, $NO_x$, HCN, and $NH_3$ concentrations along the burner axis for air combustion, oxy-fuel combustion, and oxy-fuel combustion with direct oxygen injection through the burner in the IHI 1.2 MW furnace. $O_2$ concentration is 0% in primary stream, 30% in secondary stream, and thus 27% overall. The coal is low-volatile bituminous (Coal A) and the recycle streams are dry. Data taken from [119].

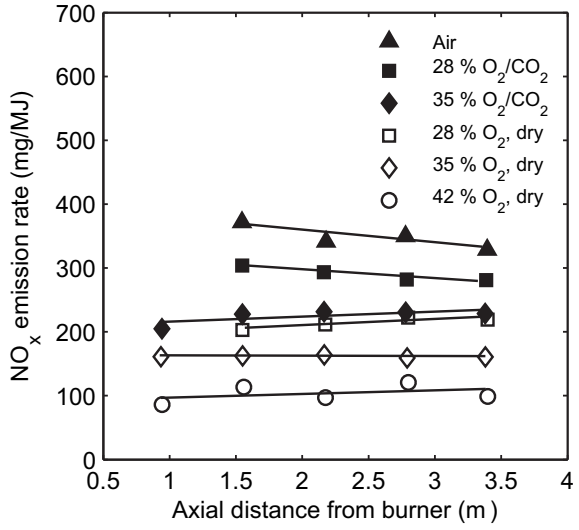


**Fig. 28.** Centre-line axial $NO_x$ concentration (shown as the emission rate) for a US eastern bituminous coal burned in the CANMET 0.3 $MW_{th}$ vertical combustor facility at a firing rate of 0.21 MW with 5 vol% excess oxygen in the dry flue gas. Comparison of air combustion as well as oxy-fuel experiments with flue gas recycle (open symbols) and once-through runs ($O_2/CO_2$, filled symbols). Oxy-fuel experiments with flue gas recycle are provided for the case with a dry recycle stream ($O_2$, dry). The recirculation ratios are 0.63 (28% $O_2$), 0.51 (35% $O_2$), and 0.40 (42% $O_2$). Data taken from [97].

a firing rate of 0.21 MW with 5 vol% excess oxygen in the dry flue gas. Oxygen concentrations in the inlet of 28, 35, and 42% were tested.

The results reported in the literature generally show that combustion in air yields the highest $NO_x$ emissions, oxy-fuel combustion based on synthetic gas mixtures ($CO_2 + O_2$) yields lower emission rates at comparable conditions, whereas oxy-fuel combustion with recirculation of flue gas yields the lowest emission rates.

*Wet versus Dry Recycle*: Payne et al. [86] observed that the reduction efficiency of $NO_x$ through reburning in a 3 $MW_{th}$ oxy-fuel sub-bituminous coal flame appeared to be higher when a wet instead of a dry recycle was applied. The reduction was 80% and 70%, respectively, compared to results obtained for air-blown combustion. During the experiments the flue gas oxygen concentration and the firing rate were fixed.

Nozaki et al. [119] likewise investigated the effect of wet and dry flue gas recycle for the primary flow, i.e. the flow for coal transportation, in their 1.2 $MW_{th}$ burner. The experiments were performed with fixed firing rate and excess oxygen at the burner. Fig. 29 shows measurements of gas phase temperature as well as $NO_x$, HCN, and $NH_3$ concentrations along the burner axis. The $NO_x$ concentration in both experiments peaks at the same level, although the formation of $NO_x$ is shifted further down the reactor in the case of a wet, primary recycle. This can be attributed to the significant reduction in flame temperature in the first measurement point. At the same time, both the HCN and $NH_3$ concentrations are markedly higher for the dry recycle compared to the wet. This is likewise attributable to the differences in temperature profiles and hence the effect on the homogeneous gas phase chemistry dominating $NO_x$ formation in the flame zone.

*Initial $NO_x$ Concentration*: As indicated in Section 3.4.1.2 it is likely that high $NO_x$ concentrations at the onset of both devolatilization and char combustion will limit the formation of further NO in the flame.

Liu et al. [162] determined the difference in reduction efficiency for experiments on a bituminous coal with 500 and 1000 ppmv $NO_x$ in the oxidant $O_2/CO_2$ mixture in their 20 kW swirl-stabilized once-through burner setup. They saw that the change in reduction efficiency between the two levels of $NO_x$ was less than 1% and thus within the experimental uncertainty. For their specific operating conditions, the $NO_x$ concentration in the oxidant was thus not a limiting parameter in the reduction process.

Based on experiments in air, Spinti and Pershing [185] have shown that the apparent conversion of char-N to $NO_x$ is a strong function of the initial $NO_x$ level at the onset of char combustion in the range of 0–900 ppm $NO_x$ on a dry basis. Likewise, the excess oxygen level affected the conversion rate, see Fig. 30. To remove the effect of volatile-N to $NO_x$ conversion during the experiments the authors burned premade chars in methane. The char particles were withdrawn from a pulverized-coal flame just after devolatilization was terminated. For the conditions tested, increasing the initial $NO_x$ concentration had a greater effect on the reduction of the apparent conversion of char-N to $NO_x$ than decreasing the oxygen excess level. In air combustion which is the case for the described experiments, a high initial $NO_x$ level translates to a high conversion of volatile-N to $NO_x$. This will have a negative impact on the process through an increase of the overall $NO_x$ emission rate. In oxy-fuel combustion a high initial $NO_x$ concentration at the base of the flame will most likely almost entirely originate from the recirculated flue gas. The apparent conversion of char-N to $NO_x$ during oxy-fuel combustion could thus decrease as the concentration of $NO_x$ in the oxidant increases, e.g. due to a reduced recycle ratio.

Fig. 31 shows computations of the total $NO_x$ emission as a function of the conversion of volatile-N to $NO_x$ and the fraction of coal-N released during devolatilization in air. It is seen that the lowest overall emission rate is achieved when the volatile-N to $NO_x$

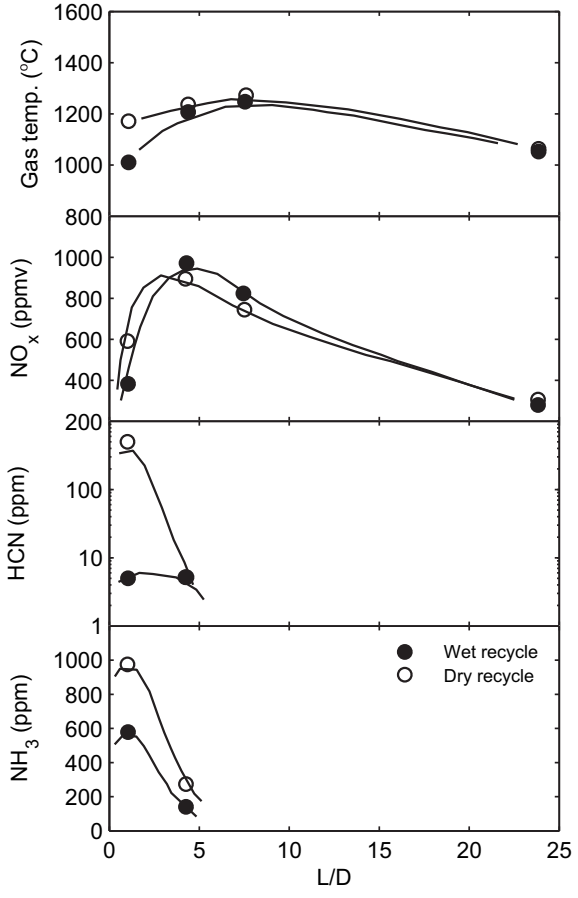


**Fig. 29.** Effect of wet versus dry recycle of primary gas on gas temperature, $NO_x$, HCN, and $NH_3$ concentrations along the burner axis in the IHI 1.2 MW furnace. The setup is operated in oxy-fuel mode with direct $O_2$ injection through the burner and with a low-volatile bituminous coal (Coal A). Data taken from [119].

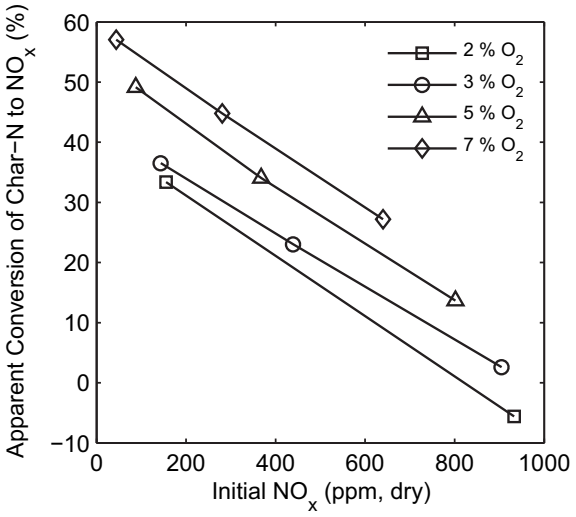


**Fig. 30.** Comparison of the effects of excess $O_2$ and of initial gas phase $NO_x$ concentration on the conversion of char-N to $NO_x$ for an Illinois #6 coal char combusted in air in a 29 kW furnace. Data taken from [185].

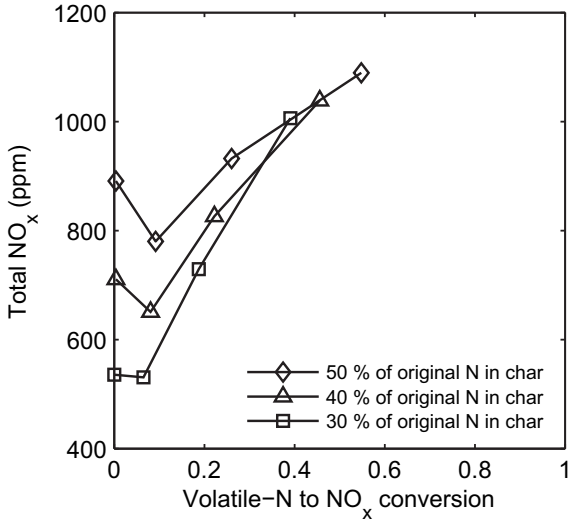


**Fig. 31.** Estimated $NO_x$ emissions from Illinois #6 coal combusted in air. Results are based on modelling. Data taken from [185].

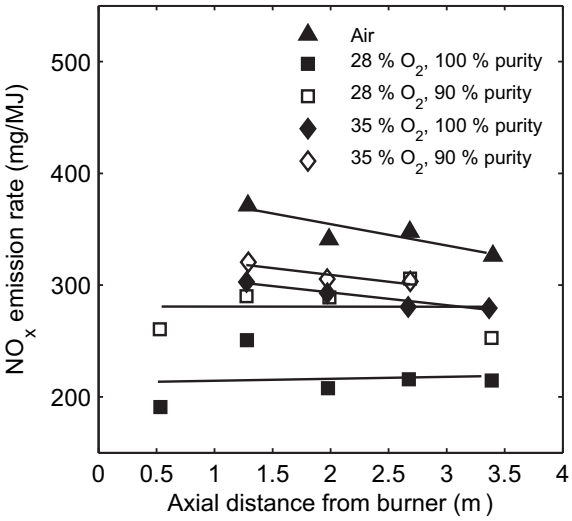


**Fig. 32.** Centre-line axial $NO_x$ concentration (shown as the emission rate) for a US eastern bituminous coal. Comparison of air combustion and once-through ($O_2/CO_2$) oxy-fuel experiments with different oxygen purities in the CANMET 0.3 $MW_{th}$ vertical combustor facility. The experiments were performed at a fixed firing rate of 0.21 MW and with an excess oxygen level corresponding to 5 vol% $O_2$ in the dried flue gas. Data taken from [120].

conversion is low and as much of the coal-N content as possible is released with the volatiles. The governing assumption applied in the modelling was that char-N to $NO_x$ conversion decreases with increasing initial $NO_x$ level during combustion.

Based on the observations above it seems that a high concentration of $NO_x$ in the recirculated flue gas could increase the reduction rate of $NO_x$ in the flame and thus lead to a further reduction of the emission rate.

*3.4.1.6. Effect of oxygen purity and air penetration.* Croiset et al. [120] have determined the $NO_x$ emission rates from air-firing and once-through oxy-fuel combustion experiments of a US eastern bituminous coal with two different oxygen purities, 90 and 100% (remaining is $N_2$). The experiments were performed in the CANMET 0.3 MW combustion facility at a firing rate of 0.21 MW and with temperature profiles as shown in Fig. 11. As expected, the $NO_x$ emission rate increases with decreasing oxygen purity, see Fig. 32. The difference between data obtained with an oxygen purity of 90% and 100% in the experiments with an oxygen concentration of 28% versus those obtained with 35% oxygen at the inlet is quite significant. There is, however, no obvious explanation to the deviations.

The data indicate that a less clean inlet $O_2/CO_2$ mixture (increased $N_2$ content) or air entrainment near the burners may give rise to increased $NO_x$ emission due to thermal NO formation.

*3.4.1.7. Influence of oxidant staging.* The use of oxidant staging in oxy-fuel combustion as a primary measure to reduce $NO_x$ emissions introduces a necessity for optimization due to the fact that the oxidant stream will contain $NO_x$.

Liu et al. [121,162] have investigated the effect of staging on the reduction of $NO_x$ emissions from both air and oxy-fuel combustion in a once-through reactor. The authors focused on the effect of staging and $NO_x$ recycling position on the reduction of recycled $NO_x$. Fig. 33 shows their results for the bituminous coal, Polish Blend. It is obvious that both the combustion media, air or oxy-fuel, the operating mode, with or without staging, and the NO recycling location influences the reduction efficiency. Focusing on the position where $NO_x$ is recycled there is no significant difference between the primary and secondary oxidant streams, which both are introduced through the burner. The tertiary stream constitutes the staging stream. Recycling of $NO_x$ through the tertiary stream markedly reduces the reduction efficiency, down to the range of 44–54% [162] as also shown by Scheffknecht and coworkers [144,148,164] in comparable experiments.

For a commercial oxy-fuel plant $NO_x$ would be present in all oxidant streams. The use of over-fire air would then potentially decrease the rate of reduction of $NO_x$. On the other hand, a significant fraction of the $NO_x$ present in the recycled flue gas will be

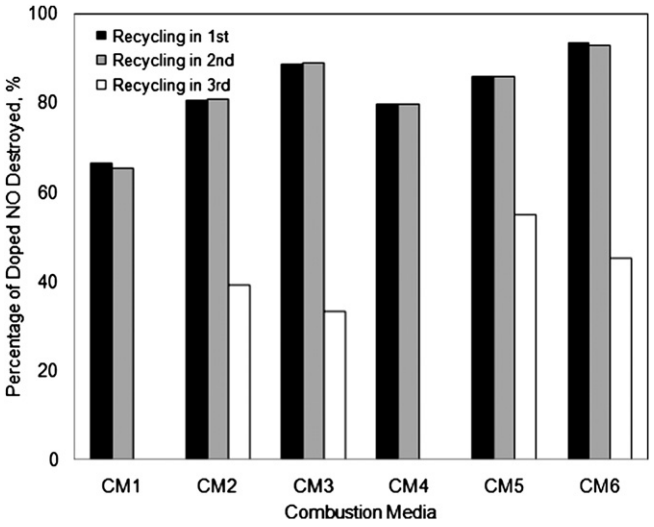


**Fig. 33.** Effects of combustion medium, staging position, and oxidant stream chosen for NO recirculation (doping) on the reduction efficiency of recycled NO. Experiments are performed on a bituminous coal, Polish Blend, in a 20 kW swirl-stabilized once-through burner setup. Five percent of NO in $N_2$ was added and mixed to the different streams of oxidants to simulate the NOx recycle. The concentration of the simulated recycled NO was in the range of 500–700 ppmv. 1st, 2nd, and 3rd refer to primary, secondary, and tertiary oxidant streams. The recycling locations (injection of the tertiary oxidant stream), Level 1 and 2, are 570 and 880 mm downstream of the burner, respectively. CM1: 1st & 2nd – Air, $\lambda = \lambda_{burner} = 1.20$; CM2: 1st & 2nd – Air, $\lambda = 1.20$, $\lambda_{burner} = 0.80$, Level 1; CM3: 1st & 2nd – Air, $\lambda = 1.20$, $\lambda_{burner} = 0.80$, Level 2; CM4: 1st & 2nd – 30% O2/70% $CO_2$, $\lambda = \lambda_{burner} = 1.20$; CM5: 1st & 2nd – 30% $O_2$/70% $CO_2$, $\lambda = 1.20$, $\lambda_{burner} = 0.80$, Level 1; CM6: 1st & 2nd – 30% $O_2$/70% $CO_2$, $\lambda = 1.20$, $\lambda_{burner} = 0.80$, Level 2. Data taken from [162].

introduced through the burners and thus experience fuel-rich conditions for a longer period of time. The optimum degree of over-fire oxidant still remains to be determined and would, at the same time, be dependent on the burner design.

*3.4.1.8. Coal properties.* The effect of coal properties on the formation and reduction of $NO_x$ in oxy-fuel combustion has been investigated by several researchers. In entrained-flow reactor type experiments both Hu et al. [161] and Shaddix and Molina [169] have observed increasing $NO_x$ emission with decreasing rank of the coals. The coals investigated range from semi-anthracite over high-volatile bituminous to sub-bituminous. Shaddix and Molina [169] attributed the trend to the higher volatile content, higher char combustion temperature, and the lower fuel-N content for the lower ranking coals.

Mackrory and Tree [175] have observed that the difference between the $NO_x$ emissions in air- and oxy-fuel combustion in their laminar flow reactor increases with the rank of the coal. Their observations are based on experiments performed with one sub-bituminous coal and two high-volatile bituminous coals, Illinois # 6 and Pittsburgh # 8.

Seven different bituminous coals were investigated in a 20 kW swirl-stabilized once-through burner setup by Liu et al. [162]. The authors measured the coal-N to NO conversion ratio between oxy-fuel combustion with 30% $O_2$ in $CO_2$ and in air. Their data showed no clear correlation between the conversion ratio and the coal rank, volatile matter, nitrogen content, etc. Instead, as shown in Fig. 34, there seems to be a dependence of the char reactivity. Increasing reactivity leads to a relatively larger conversion of coal-N to NO at oxy-fuel conditions. This could be attributed to the observation of Liu et al. [162] that reactive coals produced slightly higher temperatures in the combustion zone. According to Liu et al. this will promote $NO_x$ formation at the fuel-lean conditions at which the tests have been run. For the less reactive coals more unburnt char exists in the flame zone which may promote reduction of the previously formed $NO_x$.

A large portion of the recycled $NO_x$ in an oxy-fuel plant could be $NO_2$ due to oxidation of NO in the downstream processes [160,161]. Fig. 35 shows the results of interchanging NO for $NO_2$ in the synthetic, recycled flue gas applied in the entrained-flow reactor experiments by Hu et al. [160,161] for two different coals. For the high-volatile coal, Prima, the figure demonstrates no significant differences between the two species with respect to the stoichiometric ratio. However, for the medium-volatile coal, Datong, the reduction efficiency in the fuel-lean region is markedly lower for $NO_2$ than for NO. There are some uncertainties regarding the specific mechanism for the reduction of $NO_2$ in the flame [160,161] even though suggestions to direct reduction via free radicals or through initial conversion to NO have been given. The results by Hu et al. [160,161] indicate that the volatile matter in the coal has a dominant effect.

Fig. 36 shows burner axis profiles of gas temperature, as well as $NO_x$, HCN, and $NH_3$ concentrations for two different coals burned in air and oxy-fuel environments ($O_2$ concentration of 27 vol% at inlet) in a 1.2 $MW_{th}$ furnace [119]. The coals differ in their volatiles content. It is obvious from the peaks in the temperature profiles that the low-volatile coal (A) ignites further downstream than the medium-volatile coal (B). The gas phase temperature just outside the burner mouth ($L/D = 0$) for the two coals thus differs by approximately 200 °C. For each coal, the $NO_x$ concentration profile is very similar regardless of the combustion environment. It must thus be the coal properties determining the $NO_x$ formation, with the low-volatile coal producing more $NO_x$. This observation is contrary to the results presented above. It is likewise seen that the coal volatile content has an impact on the HCN and $NH_3$ profiles. They report that the coal with the higher volatiles content forms significantly more HCN during combustion than the low-volatile coal which on the other hand produces a very high concentration of ammonia in the early flame zone during oxy-fuel combustion.

The limited investigations of the influence of coal properties on $NO_x$ formation during oxy-fuel combustion indicate that the relative production of $NO_x$ at oxy-fuel conditions compared to when combustion is performed in air increases with increasing reactivity of the coal char. The effect could be caused by a greater sensitivity to char combustion temperature of the $NO_x$ formation mechanism in an oxy-fuel environment than in air.

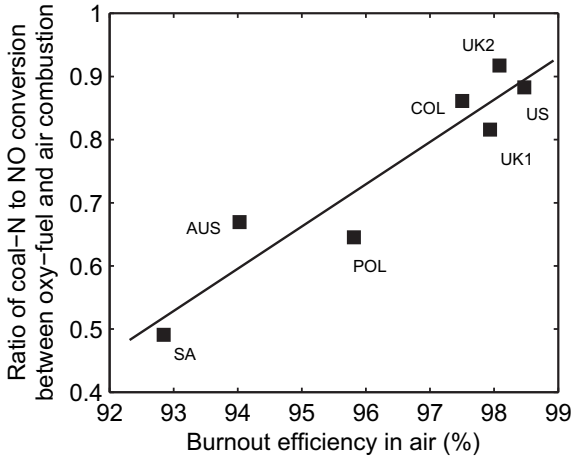


**Fig. 34.** The dependence of the ratio of coal-N to $NO_x$ conversion between coal combustion in 30% $O_2$/70% $CO_2$ and coal combustion in air on the coal burnout efficiency in air for seven different bituminous coals. Experiments are performed in a 20 kW swirl-stabilized once-through burner setup with an overall stoichiometric value of 1.2. SA: South African, AUS: Australian, POL: Polish Blend, COL: Colombian, UK1(2): UK Bituminous 1 (or 2), US: US Blend. Data taken from [162].

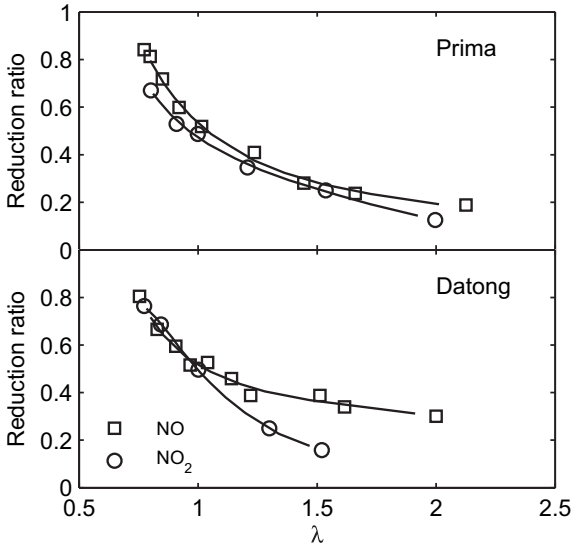


**Fig. 35.** Reduction ratios of recycled NO and recycled $NO_2$ as a function of stoichiometry obtained in an entrained-flow reactor. The reduction ratio at a given stoichiometry is obtained from the difference in $NO_x$ emission between an experiment with and without recirculation of $NO_x$. The operating conditions are: recycling ratio of 0.4; $T = 1373$ K; fixed residence time of 2 s; concentration of $NO_x$ in the inlet gas of 1000 ppm for recycled-$NO_x$ experiments. Prima: high-volatile bituminous Indonesian coal; Datong: medium-volatile bituminous Chinese coal. Data taken from [161].

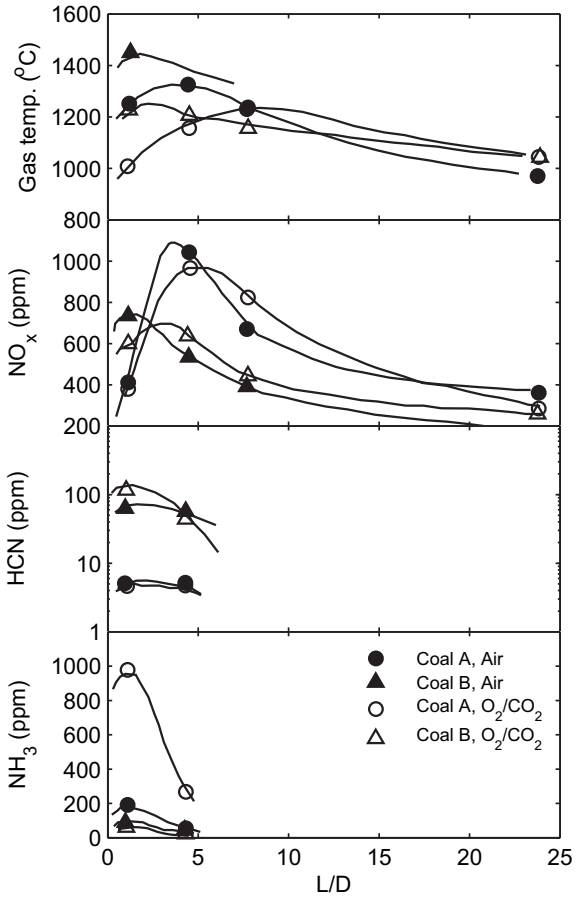


**Fig. 36.** Effect of coal volatiles content on gas temperature, $NO_x$, HCN, and $NH_3$ concentrations along the burner axis in a 1.2 MW furnace. Coal A, low-volatile bituminous, 26.1% volatile matter. Coal B, medium-volatile bituminous, 41.2% volatile matter. $O_2$ concentration is 0% in primary stream, 30% in secondary stream, and 27% overall at inlet, $\lambda = 1.2$. The recirculated flue gas in the oxy-fuel experiments contains up to 200 ppm $NO_x$. Data taken from [119].

*3.4.1.9. Effect of burner configuration for swirling flames.* Fig. 24 showed that exchanging a conventional burner for a low-$NO_x$ burner in oxy-fuel combustion yielded a 56% reduction in the $NO_x$ emission rate. Thus, $NO_x$ formation in oxy-fuel combustion depends on the burner configuration and especially the flow field in the near-burner zone, just as is the case during conventional air combustion.

Experiments performed by Chui et al. [150] in the CANMET 0.3 MW vertical combustor research facility show that $NO_x$ emissions are highly dependent on the burner swirl number, i.e. flow dynamics. Increasing the swirl number from 1 to 2 decreases the $NO_x$ formation by 34%. However, for the range of swirl numbers applied in the experiments $NO_x$ emissions during oxy-fuel combustion was higher than for air-firing, 140–150 versus 110 mg/MJ. This was true for both burner configurations tested. Because of safety limitations, the amount of oxygen mixed into the secondary oxidizer stream was restricted to 28% on a dry basis. For the same reason, the primary stream contained little or no oxygen. To obtain the necessary overall oxygen concentration during combustion a portion of the total oxygen demand was injected as pure oxygen through a special annuli in the burners. The burners provided stable flames but the injection of pure oxygen caused the release of volatiles and fuel-N from the Canadian sub-bituminous coal tested to occur in the $O_2$-rich portion of the flame. An improved burner design subsequently tested by Chui et al. [151] reduced the $NO_x$ emission down to 40 mg/MJ at oxy-fuel conditions and improved the remaining combustion characteristics as well.

Due to the strong influence from the near-burner flow field on $NO_x$ emissions from swirling flames it will be difficult to transfer the results from the changes to the specific burner configurations obtained by Chui et al. [150,151] to a general trend for other oxy-fuel burners.

Based on experiments regarding char-N to $NO_x$ conversion and modelling investigations, Spinti and Pershing [185] suggest the following measures in order to obtain the largest possible reduction in $NO_x$ emissions. (*i*) a burner which yields a fuel-rich flame core, (*ii*) high temperatures during devolatilization, and (*iii*) a char oxidation zone with temperatures as low as possible in combination with low excess $O_2$ and adequate residence time for char burnout at the lower gas temperatures. This is not different from the case of air-firing. However, because of the changes in mass flow rates in the primary and secondary inlets, see Section 2.7.1, the optimal burner design for oxy-fuel combustion is not necessarily similar to that developed for conventional air-firing.

### *3.4.2. $SO_x$*

Sulphur emissions and the effect on ash properties and boiler-tube corrosion in oxy-fuel combustion from significantly increased levels of gas-phase-S in the boiler have received increasing attention in the recent years.

There have been contradictory observations on the $SO_2$ emissions from oxy-fuel combustion. Some researchers experimentally show a decrease when comparing to combustion in air [88,96,97,128,136,138] whereas others on the basis of either experiments [121,113] or equilibrium calculations [149] report no differences.

Kiga et al. [136] reported oxy-fuel experiments performed in the IHI 1.2 $MW_{th}$ combustion facility with recirculation of dry flue gas. The investigations showed that the conversion of the coal sulphur content, measured as the amount of S in the outlet divided by the amount going in with the coal, decreased markedly in oxy-fuel combustion compared to air-firing operation. Even though the authors were not able to close the mass balance for sulphur the results indicated that the major part of the difference could be attributed to removal of S through condensation as $H_2SO_4$ in low-temperature ducts and by retention in ash particles.

Zheng and Furimsky [149] modelled the formation of $SO_2$ and $SO_3$ based on equilibrium considerations during both air- and oxy-fuel combustion. They found that practically all of the sulphur content in coals is released as $SO_2$ and $SO_3$ irrespectively of the combustion medium, as $CO_2$ plays an insignificant role for the release compared to oxygen. With respect to recycle ratio and oxygen excess, their simulations yielded an increased amount of $SO_3$ with an increase in the amount of available oxygen.

Generally, the disagreements observed between experimental findings and the computations based on equilibrium modelling are expected to be a consequence of computations reflecting conditions immediately after combustion and not accounting for changes occurring further downstream. Another plausible explanation is the fact that some of the processes could be kinetically controlled, e.g. the heterogeneous reactions controlling retention of S in ash and other deposits, a fact that is not captured in the simulations.

Table 13 provides a summary of the results on $SO_2$ emissions from semi-technical and pilot scale experiments with flue gas recirculation.

In the following sections the reported results on $SO_2$ emissions from oxy-fuel combustion are divided according to the effects of different operating conditions and design aspects. The subject of boiler-tube corrosion due to the presence of sulphur in the flue gas is likewise treated.

**Table 13**
Summary of $SO_2$ emission results from experiments in pilot scale and semi-technical scale with flue-gas recirculation.

| Author(s) | Fuel input (MW) | Inlet $O_2$, Oxy (%) | Emission (mg/MJ) | Conversion ratio | Conclusion(s) |
|---|---|---|---|---|---|
| Woycenko et al. [88] | 2.1 | 26 | Air: 645<br>Oxy: 375–418 | Air: 100%<br>Oxy: 60–67% | The conversion ratio of fuel-S into $SO_2$ is lower for oxy-fuel combustion than air. |
| Wall et al. [138,128] | 1.2 | 27 | Air: 150–416<br>Oxy: 100–291 | Air: 63–83%<br>Oxy: 40–53% | Lower $SO_2$ emission in oxy-fuel than in air, level dependent on coal type. Increased $SO_3$ concentrations increases acid dew point from ~ 133 to ~ 156 °C. |
| Croiset and coworkers [120,97] | 0.21 | 28, 35 | Air: 300–320<br>Oxy: 260–275 | Air: 91%<br>Oxy: 56–65% | $SO_2$ emissions independent of wet and dry recycle even though removal through condensate was expected. Drop in conversion rate attributed to conversion to $SO_3$ and/or retention in ash and deposits. Coal sulphur content most important factor to determine $SO_x$ emission. |
| Tan et al. [122] | 0.21 | 35 | – | – | $SO_2$ emission rates slightly lower for oxy-fuel combustion than in air even though the concentration was 3–4 times higher in the oxy-fuel case. |
| Scheffknecht and coworkers [144,145,147] | 0.5 | 27–30 | – | Air: –Oxy: 96–100% | Negligible reduction of $SO_2$ in the radiative section of a boiler. Higher $SO_2$ concentrations yields higher $H_2S$ formation in fuel-rich zones. Calcium-rich coals show greater tendency to capture S. |

*3.4.2.1. Effects of changes in the oxygen concentration, oxygen excess, flue gas recycling ratio, and gas phase temperature.* Hu et al. [96] focus on the effect of oxidizer composition, stoichiometry, and flame temperature in their investigations of $SO_2$ emissions in an entrained-flow reactor with a coal feed rate up to 180 g/h. They encountered the highest conversion ratios at or near stoichiometric conditions, see Fig. 37. The decrease in S conversion at fuel-rich conditions is assumed to be due to retention in unburned coal and formation of other, reduced S-containing species (e.g. $H_2S$, COS, and $CS_2$). These species were not measured. The reduction in $SO_2$ emissions at fuel-lean conditions compared to stoichiometric conditions has not been explained but could partly be due to increased conversion to $SO_3$.

According to Liu et al. [121] $SO_2$ emissions are not significantly affected by the use of staging or changes in the combustion media.

*3.4.2.2. Effect of the composition of the recirculated flue gas.* Croiset and coworkers [120,97] reported experiments regarding $SO_2$ emissions from the combustion of a US eastern bituminous and a Canadian sub-bituminous (Highvale) coal in the 0.3 MW CANMET oxy-fuel combustion facility. Fig. 38 shows $SO_2$ emission rates for air-fired experiments, once-through experiments (synthetic flue gas denoted $O_2/CO_2$), and dry flue gas recycle ($O_2$, dry) experiments. The data for the bituminous coal in the figure show similar emission rates for experiments with air and the synthetic $O_2/CO_2$ mixture. For the recycle experiments with 28 and 35 vol% $O_2$, however, the emission rates were slightly lower.

Comparing gas phase concentrations instead of emission rates reveal that the measured $SO_2$ concentrations in the burner during oxy-fuel combustion with a recycle fraction of about 60 vol% were approximately 3 times higher than for air-firing [97]. The theoretical increase in the $SO_2$ concentration was about a factor of 4. The authors concluded that the conversion of sulphur into $SO_2$ was independent of oxygen concentration and that retention in ash and/or further oxidation into $SO_3$ could explain the difference. Ash analysis showed that less than 3% of the initial S-content in the coal was

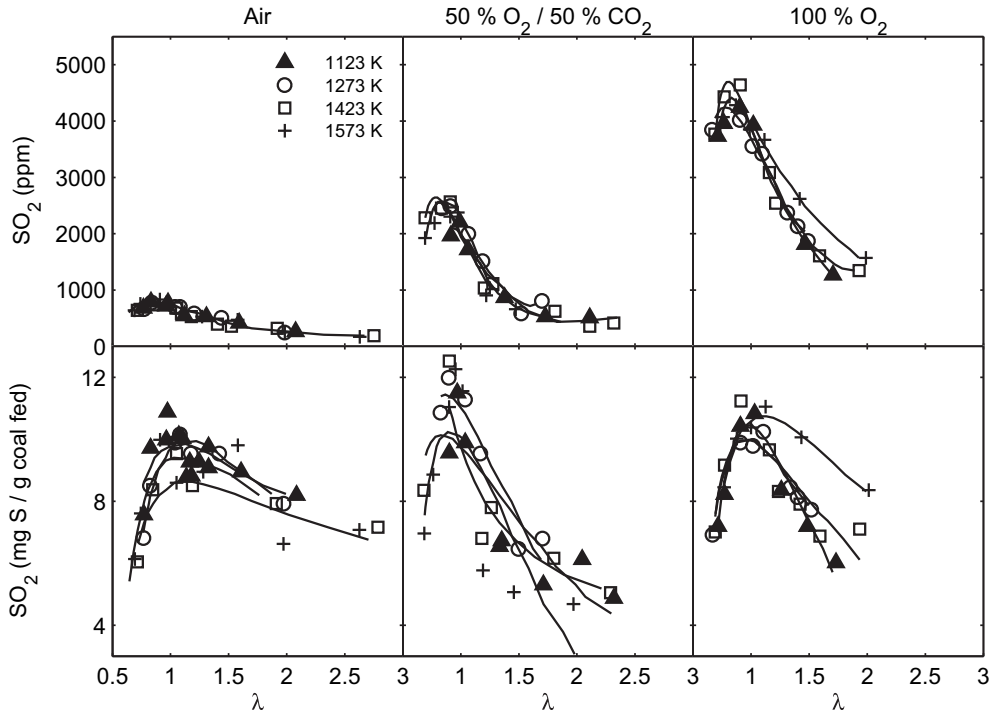


**Fig. 37.** $SO_2$ emissions versus stoichiometric ratio and temperature at different $O_2$ concentrations for $N_2$ and $CO_2$-based oxidizers. Experiments are performed in an entrained-flow reactor with a coal feed rate of up to 180 g/h. The $SO_2$ concentrations in ppm are given as measured. Data taken from [96].

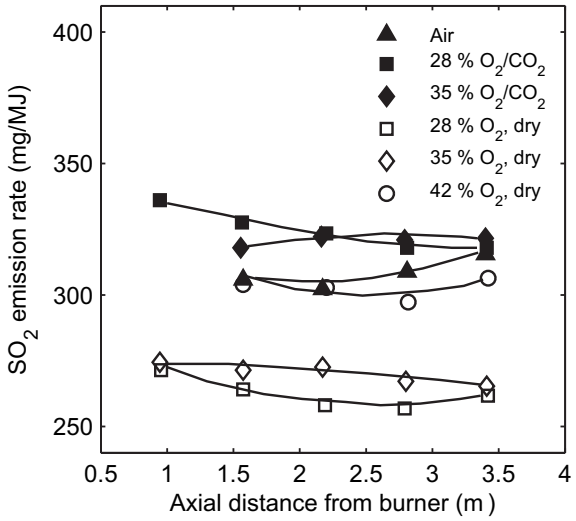


**Fig. 38.** Centre-line axial $SO_2$ concentration (shown as the emission rate) for an Eastern bituminous coal burned in the CANMET 0.3 MW vertical combustor research facility at a firing rate of 0.21 MW with 5 vol% excess oxygen in the dry flue gas. Comparison of air combustion as well as oxy-fuel experiments with flue gas recycle (open symbols) and once-through runs ($O_2$/$CO_2$, filled symbols). Oxy-fuel experiments with flue gas recycle are provided for the case with a dry recycle stream ($O_2$, dry). The recirculation ratios are 0.63 (28% $O_2$), 0.51 (35% $O_2$), and 0.40 (42% $O_2$). Data taken from [97].

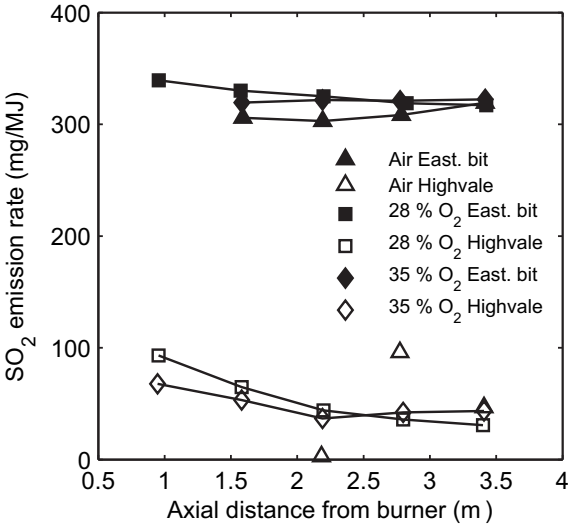


**Fig. 39.** Centre-line axial $SO_2$ emission rate. Comparison of Highvale sub-bituminous and US eastern bituminous coals. The experimental setup is the CANMET 0.3 MW vertical combustor research facility operated in once-through mode at a firing rate of 0.21 MW with 5 vol% excess oxygen in the dry flue gas. Data taken from [120].

present in the ash. However, the condensed water did have a sulphate content of above 3000 mg/L and a pH between 2 and 3. The high sulphate concentration in the condensate indicates high $SO_3$ levels in the flue gas. In the work by Mönckert et al. [147] the sulphur retention in calcium containing coals is shown to increase with increasing $SO_2$ concentration in the recycled flue gas. This is due to the formation of $CaSO_4$.

Experimental runs with wet flue gas recycle were likewise performed by Croiset and Thambimuthu [97] but showed no significant difference to the dry case. The authors, however, expected a lower emission rate for the latter case since some $SO_2$ should be removed with the waste water during the flue gas condensation.

*3.4.2.3. Effect of coal sulphur content.* Comparing the data in Fig. 39 leads to the conclusion that the specific $SO_2$ emissions are almost exclusively dependent on the coal type, i.e. sulphur content. The Eastern bituminous coal has a sulphur content of 0.96 wt% (dry basis) whereas the sub-bituminous coal (Highvale) contains 0.24 wt% (dry basis) [120]. The relative differences due to changes in combustion medium and oxygen concentration are thus negligible in this context.

*3.4.2.4. The $SO_2$ to $SO_3$ conversion and sulphur-induced corrosion.* In later work from CANMET, Tan et al. [122] reported further results on the conversion of $SO_2$ to $SO_3$ in the flue gas. They showed that the conversion was about 5% whereas it is typically between 1 and 5% in conventional air-firing systems [113,122,147] depending on the combustion conditions and the sulphur content of the coal. These values have likewise been found by Scheffknecht and coworkers [145]. Klostermann [113] and Mönckert et al. [147] report that $SO_3$ formation is promoted by both high oxygen and high water levels in the flue gas. In the case of a flue gas recycle without prior $SO_2$ removal the amount of $SO_3$ in the boiler can thus reach high values (up to about 85 ppmv [147]) and thus increase the risk of sulphur corrosion in the regions of the system which operate below the acid dew point.

Because of the potentially higher $SO_3$ concentrations in the flue gas, the acid dew point will increase accordingly [115,138,145,147,148]. Increases of about 20–40 °C from ~130 to ~160 °C have been reported [113,138,145]. Schnurrer et al. [115] found a similar trend from their thermo-chemical equilibrium calculations. An earlier formation of sulfuric acid in the flue gas ducts will increase the risk of flue gas side corrosion in the low-temperature parts considerably. Schnurrer et al. suggest using a dry flue gas recycle to decrease the concentration of water in the flue gas and thus the amount of acid that can form.

Scheffknecht and coworkers [144,145,147,148] investigated the impact of recirculation of $SO_2$ (by doping the oxidant stream in their 20 kW EFR) on the transformation of $SO_2$ in the radiant section of a boiler. They found only a negligible reduction in the concentration of the recycled $SO_2$. However, high concentrations of $SO_2$ in the furnace was found to increase the concentration of $H_2S$ in the fuel-rich regions for both air- and oxy-fuel firing conditions, see Fig. 40, inducing a higher risk of corrosion. The $H_2S$ to $SO_2$ ratio in the oxy-fuel experiments were lower than in air even though the absolute concentration was higher.

*3.4.2.5. In-boiler desulphurization.* In a series of papers Liu and coworkers [127,208,209] address the ability of oxy-fuel combustion

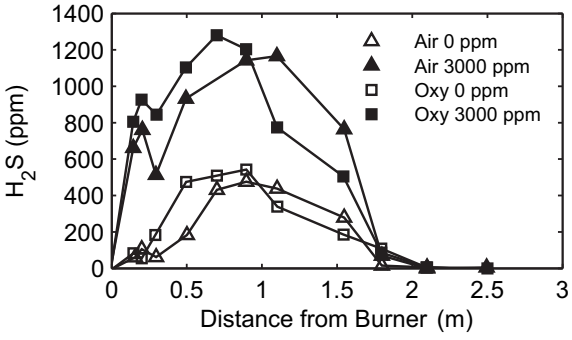


**Fig. 40.** $H_2S$ concentration profiles along burner axis for air- and oxy-fuel combustion experiments on lignite. The experiments were performed in an 20 kW entrained-flow reactor with and without doping of the oxidizer with 3000 ppm $SO_2$. Data taken from [144].

to drastically reduce the emissions of $SO_2$ from combustion of coal. They suggest in-boiler desulphurization by injection of limestone. The combination of both high $SO_2$ and $CO_2$ partial pressures should ensure high reactivity of the limestone toward $SO_2$. The authors explain the increased reactivity by two factors: (1) high $SO_2$ limits $CaSO_4$ decomposition and (2) high $CO_2$ limits decarbonisation of limestone before sulphation whereby direct sulphation of limestone without decarbonisation is favoured. The direct sulphation will minimize the diffusion resistance through the solid phase (no pore clogging) and hence a larger part of each limestone particle will participate in the desulphurization reaction.

Even though the experiments show significantly increased reactivity of the limestone toward $SO_2$ for a sulphur containing flue gas recycle compared to conventional air-fired conditions, this strategy is not likely to be adopted in power plants which produce fly ash for cement and concrete production due to the associated mixing of gypsum and fly ash.

*3.4.2.6. Summary.* The substitution of $N_2$ by $CO_2$ in oxy-fuel combustion does not affect the release of sulphur from the coal during combustion. However, the increased oxygen partial pressure necessary to maintain an appropriate flame temperature increases the formation rate of $SO_3$. During operation with a flue gas recycle without $SO_2$ removal the $SO_2$ and thus the $SO_3$ levels in the boiler and flue gas ducts increase significantly which will enhance the risk of sulphur-induced corrosion at both high and low temperatures. High in-boiler concentrations of sulphur oxides can likewise increase retention of S in the fly ash. Increased retention will reduce the $SO_2$ emission rate but could at the same time yield problems with further utilization of the fly ash in cement and concrete production.

### 3.4.3. Trace elements

The subject of trace element emissions during oxy-fuel combustion is generally seen to have drawn minor attention compared to other of the fundamental combustion issues investigated. Because of the scarcity of published results within this area of research none of the results described below have been confirmed by other research groups.

According to the equilibrium calculations performed by Zheng and Furimsky [149] the Hg-, Cd-, As-, and Se-containing emissions are only insignificantly affected by the combustion medium. However, in case of incomplete elimination of these species in the flue gas cleaning equipment situated before the flue gas recycle point elevated concentrations will occur in the boiler and thus in the flue gas stream to be treated before sequestration.

Suriyawong et al. [117] measured the mercury emission from air- and oxy-fuel combustion of a sub-bituminous coal in a laminar reactor and determined the ratio between the elemental and oxidized forms. Fig. 41 shows their results.

The data lie within typically agreed intervals of sub-bituminous coals, i.e. 10–20% of the total mercury emissions are in the oxidized states with the remainder in the elemental state. The concentrations measured are within the range of uncertainty of the mercury content in the coals which indicate that burning coal at oxy-fuel conditions does not have a significant effect on neither the vaporization nor the speciation at the furnace exit.

At CANMET, ongoing research addresses mercury removal technologies for oxy-fuel combustion [9].

## 3.5. Ash and deposition chemistry

The transformations of coal mineral matter during combustion are significantly affected by the temperature and the gas phase composition surrounding the coal particles [125]. The change in combustion atmosphere and the potential change in local particle temperature between oxy-fuel combustion and air-fired combustion may thus have an effect on the ash formation mechanisms and hence the ash composition and quality.

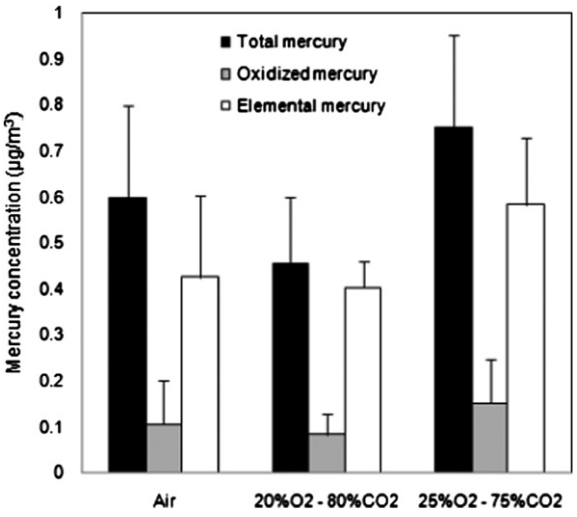


**Fig. 41.** Mercury concentration measured at the furnace exit of a laminar reactor. Experiments are performed with a sub-bituminous coal in air and for two $O_2/CO_2$ mixtures with a fixed reactor temperature of 1200 °C. The total Hg concentration is divided into the fraction consisting of metallic (elemental) Hg and the oxidized forms. Data taken from [117].

### 3.5.1. Particle formation mechanisms

Fig. 42 shows the mineral transformation and particle formation pathways for both fine (sub-micrometer, mode around 0.1 μm) and coarse particles during coal combustion. There are two pathways for the formation of sub-micrometer particles; (1) direct vaporization of volatile metals, e.g. Na, Pb, Cd, and Hg, which react in the gas phase and subsequently nucleate or condense on the surface of existing particles; (2) non-volatile species like e.g. silica oxides can be reduced to sub-oxides, e.g. as in reaction (14). These sub-oxides have a lower melting point and are devolatilized and rapidly reoxidized in the gas phase causing an oversaturated mixture.

$$MeO_x + CO \rightleftharpoons MeO_{x-1} + CO_2 \quad (14)$$

Particle formation occurs mainly through nucleation whereas growth is dominated by condensation and collision mechanisms. The sub-micrometer particle formation mechanisms are complex functions of such factors as coal type, combustion temperature, fuel to oxidizer ratio, and residence time. This is likewise the case for the resulting particle size distributions [117].

Coarse ash particles are formed from the non-volatile mineral inclusions in the coal which are not released as sub-oxides. These inclusions can coalesce and form a glassy matrix or remain in their original state if the temperature does not exceed their melting points [117].

The main fraction of the fines will consist of spherical particles due to their origin from gas phase species. On the other hand, the shapes of the coarse particles may vary from spherical or near-spherical to irregular, depending mainly on the char particle temperatures during combustion, i.e. whether they have been melted.

### 3.5.2. The effects of gas composition on particle formation

Combustion at oxy-fuel conditions with an air-like composition of the oxidant will result in a lower adiabatic flame temperature and hence a reduction of the coal burning rate compared to combustion in air, see Sections 2.7, 3.2, and 3.3. The vaporization of both volatile metals and metal sub-oxides as well as the particle

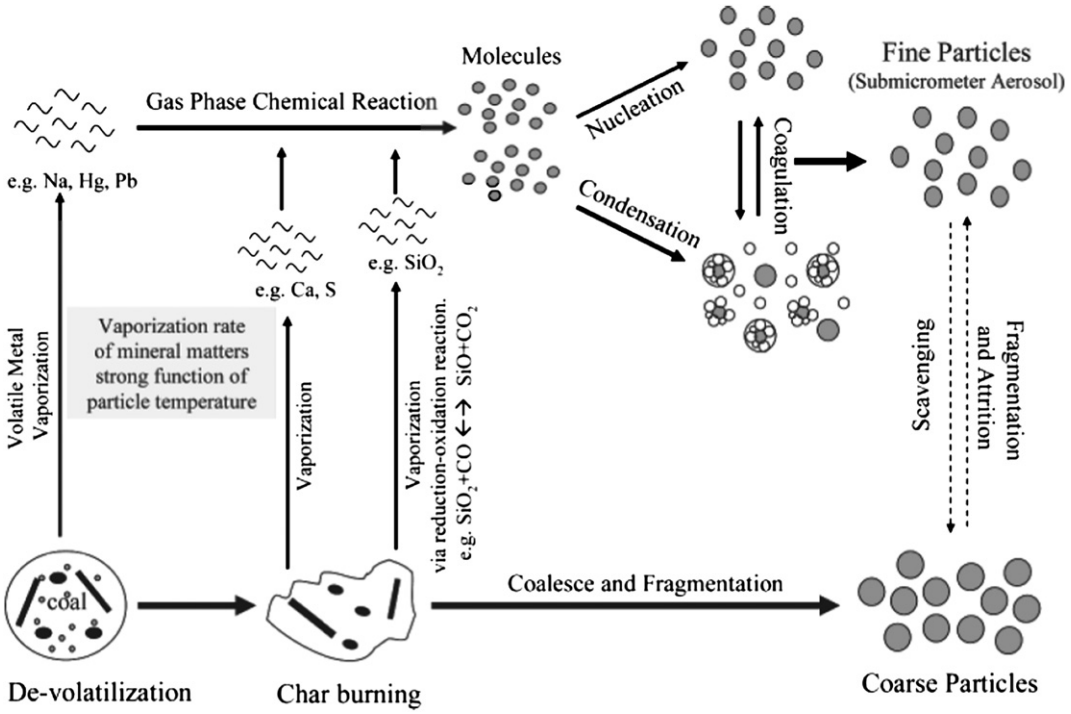


**Fig. 42.** Mineral transformation and particle formation pathways during coal combustion [117].

formation rates will thus be significantly smaller, as observed by Suriyawong et al. [117] and Sheng and coworkers [125,182,183]. From their investigations, Suriyawong et al. found that the ratio between fine and coarse particles shifted significantly toward fewer sub-micrometer particles in this particular oxy-fuel case. The mean size of the fine particles likewise became smaller because the particles have less time to grow when ignition and combustion is delayed, see Fig. 43. The bottom part of the figure shows the amount of various elements in the fine ash. It is generally observed that a smaller amount of ash forming elements have vaporized from the coal in the case of oxy-fuel conditions causing the lower number concentration. At the same time, the ratios between the different elements have changed. Particularly calcium and iron are released to the gas phase to a much lesser extent than in air. Suriyawong et al. [117] explain this phenomenon in the way that the increased concentration of $CO_2$ in the bulk gas will shift the sub-oxides formation equilibrium toward the oxides, see reaction (14), and thus reduce the formation of sub-micrometer particles through this pathway. The reduced particle surface temperature is, however, of significant importance. Sheng et al. [182] likewise determined the compositions of their ashes. They observed a similar shift in the ratio between volatile and less volatile species in the sub-micron ash for oxy-fuel combustion with an air-like oxidant composition. Increasing the oxygen concentration diminished the difference between air and oxy-fuel combustion. Differences in the oxygen concentration and thus the combustion temperature of the coal and char particles can alter the distribution between the main phases slightly, as more or less of the included minerals melt into a glass phase [183,125].

Increasing the $O_2$ concentration in $CO_2$ from 20 to 50% increases the particle surface temperature during combustion from 1772 K to 2679 K [117]. As a result, the particle size distribution of the sub-micrometer-sized fraction of ash particles is shifted toward larger sizes, see Fig. 44.

Sheng et al. [183] observed the same trend for their Chinese coals. They likewise concluded that the temperature difference between air and oxy-fuel combustion with 20% $O_2$ in $CO_2$ might alter the particle fragmentation and coalescence mechanisms in addition to lowering the ash vaporization rate. However, the particle number concentration in the less than 50 nm range does not change.

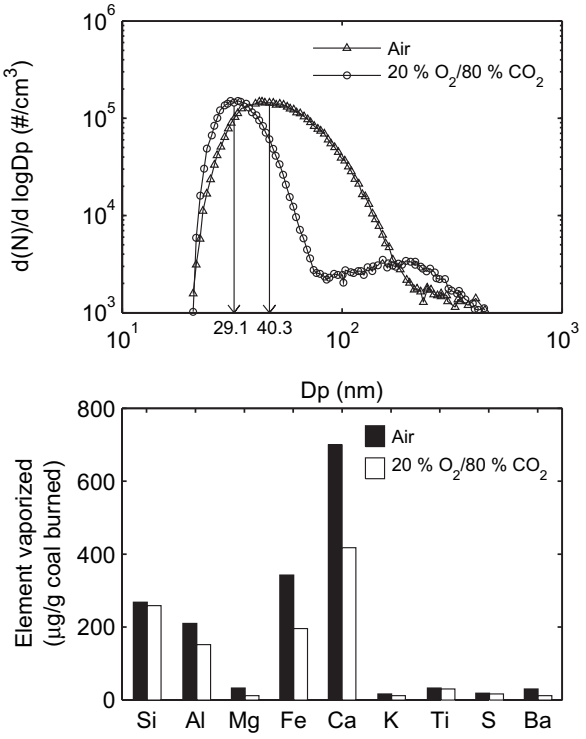


**Fig. 43.** Top: Sub-micrometer particle size distribution from air and 20% $O_2$/80% $CO_2$ combustion of a sub-bituminous coal obtained in a laminar flow reactor with a fixed temperature of 1200 °C. Bottom: Measured elemental compositions in sub-micrometer-sized ash from the same experiments. Data taken from [117].

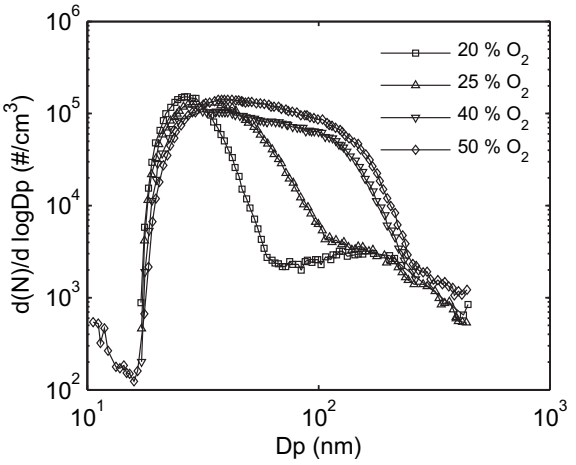


**Fig. 44.** Sub-micrometer particle size distributions for oxy-fuel combustion at different $O_2$ concentrations obtained from combustion of a sub-bituminous coal in a laminar flow reactor with a fixed temperature of 1200 °C. Data taken from [117].

According to Suriyawong et al. [117] this is due to the fact that the nucleation and condensation mechanisms are competing. Below a critical concentration of small particles vaporized species tend to nucleate. Above this limit condensation dominates leading to growth in particle size instead of particle number concentration.

Comparing Figs. 43 and 44 leads to the conclusion that increasing the oxygen concentration in oxy-fuel combustion from 20% to between 25 and 40% will produce a particle size distribution similar to that obtained in air for the small size fraction of ash particles. Experiments reported by Wall et al. [138,128] confirm this observation.

A modelling study by Krishnamoorthy and Veranth [210] investigated the effect of particle size, bulk gas composition, and in-furnace temperature during oxy-fuel combustion on the vaporization of metal sub-oxides from the burning char due to locally reducing conditions within the particles. Fig. 45 shows the ratio between CO and $CO_2$ as a function of radius in a char particle burning in atmospheres of varying $CO_2$ concentrations.

The results indicate that increasing the $CO_2$ level in the bulk gas significantly decreases the $CO/CO_2$ ratio inside the particles even though the absolute concentration of CO increases. Based on equilibrium considerations considering reaction (14) a shift from air-blown to oxy-fuel combustion should thus impose decreased vaporization of refractory oxides from the coal mineral phase during combustion.

### 3.5.3. Ash quality

To the power plants which sell their coal fly ash for cement or concrete production the quality of the ash in this respect is crucial. Especially the sulphur content of the ash is a critical parameter, the limiting value for S is 3 wt% measured as $SO_3$, as described in Section 2.5.1.2. Significantly increased sulphur retention compared to the level which is normal in air-fired operation will make the fly ash useless as a substitute for cement in concrete production. This is due to sulphates reacting with the other components in the concrete matrix after hardening. The result is an expansion of the mineral phase and thus fatal cracks in the structure.

The results published by Farley [72] indicate that the fly ash from oxy-fuel combustion of coal should be "equally acceptable for cement manufacturing as those arising from conventional air-firing". However, the paper provides no reference to the specific restrictions on the fly ash composition applying in the UK by which the above statement cannot be assumed applicable to the regulations and conditions in other countries without further verification.

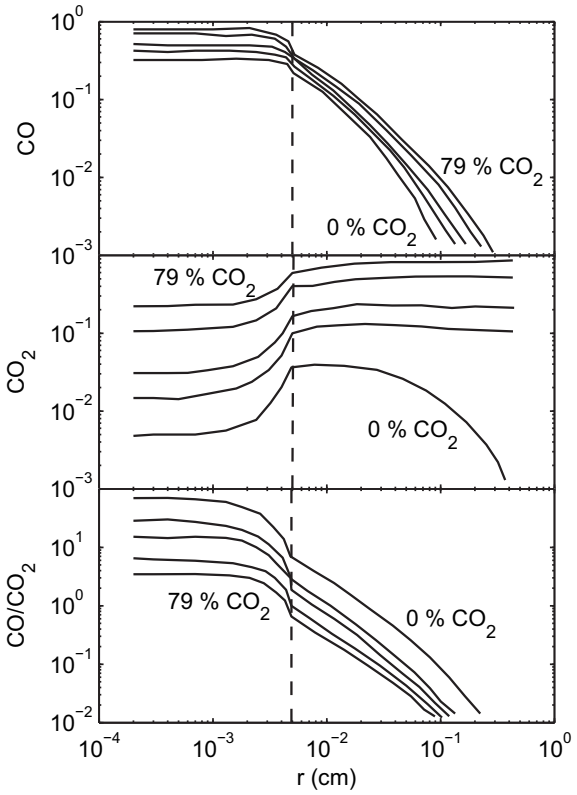


**Fig. 45.** CO and $CO_2$ partial pressures (atm) and the $CO/CO_2$ ratio as a function of radius from the centre of a particle through the boundary layer. Vertical dotted line corresponds to the surface of the particle. The data are for a 100 μm char particle burning in a furnace with walls at 1750 K and 0, 10, 20, 50, and 79 vol% $CO_2$ in the bulk gas. The $O_2$ concentration in the bulk gas is 20 vol% for all simulations. The remainder of the bulk gas consist of 1% $H_2O$ and the difference is $N_2$. Note that the position of the legends in the figure showing the $CO/CO_2$ ratio has been corrected compared to the original figure in [210].

Wall et al. [138] report similar compositions and melting behaviour of both fly and bottom ashes obtained from air and oxy-fuel combustion. The coal with the highest calcium content showed a slightly increased concentration of sulphur. During the experiments emphasis was reported to be on generating the same temperature and heat transfer conditions, i.e. by operating with 27% $O_2$ on a wet basis in the oxidizer. From their experiments Sheng and Li [125] reported a small increase in the content of limestone due to the higher partial pressure of $CO_2$ at oxy-fuel conditions compared to air-firing.

For a flue gas recycle without prior sulphur removal the sulphur level in the boiler could increase with a factor of up to 4–5. This significant increase will induce a risk of enhanced sulphur retention in the fly ash [12,115,128,145]. Lowering the flame temperature in the boiler will also increase the possibility of $SO_2$ retention in ash [12]. Maier et al. [145] state that retention of sulphur in ash does not take place in the radiant section of a boiler due to the temperature being above the 1150 °C where sulphate salts are stable. However, in the convective section the temperature will be lower and the ash will be able to capture sulphur compounds.

Experiments by Croiset et al. [97] on a US eastern bituminous coal have shown that the retention is generally low, i.e. only about 2–3% of the initial S-content in the coal is present in the ash. A later investigation showed that the retention of sulphur in the fly ash is very dependent on the alkaline and alkaline earth content of the ash [122]. For a sub-bituminous coal with a highly alkaline ash they observed that nearly 14% of the initial sulphur content of the coal

was retained in the ash. It is suggested that it is the $SO_3$ in the flue gas that is retained through sulphate salts.

Based on the above, a possible solution could be to restrict the power plants to operate on only low alkaline and/or low sulphur bituminous and sub-bituminous coals and thereby limit the changes in the sulphur content of the fly ash from oxy-fuel combustion. This is however not a desirable restriction for the plant owners as it will reduce the operability of the plants.

The question of ash quality, especially the risk of increased sulphur retention, is still a potential risk for the application of oxy-fuel combustion as a carbon capture technology. The risk is largest for the most frequently proposed process design where flue gas is recycled before the desulphurization plant.

#### 3.5.4. Depositions, slagging, and fouling

Early studies on ash deposition, slagging, and fouling at the ANL 3 $MW_{th}$ pilot scale furnace referred by Payne et al. [86] showed that there were no identifiable differences between air-firing and oxy-fuel combustion. However, Glarborg and Bentzen [172] state that the high CO levels in the near-burner region could promote increased corrosion and slagging. Similarly, Schnurrer et al. [115] saw from their equilibrium calculations that the formation of deposits potentially could occur at furnace wall temperatures 30–60 °C higher than what is seen during conventional combustion in air. This may alter the position of deposits and thus potentially necessitate a relocation of soot blowers, etc. At the same time, they expect oxy-fuel combustion to provide a higher propensity for slagging and fouling caused by increased amounts of molten and solid alkali sulphates.

Experiments conducted by Mitsui Babcock Energy, ltd on a 160 $kW_{th}$ test facility in Renfrew, UK [72], likewise included studies into the impact of oxy-fuel combustion on slagging and fouling. Inserting a deposition probe into the combustion chamber led to the observation of a slightly faster rate of deposition compared to air-firing. The temperature of the probe has not been stated by the author. At the same time the deposition rate was largely independent of the operating parameters such as recycle ratio during oxy-fuel combustion. Also, fouling occurred more rapidly during oxy-fuel than during conventional air combustion. The impact was, however, small and the deposits were easy to remove.

Wall et al. [138,128] collected ash samples from the deposits in the radiative and convective sections of the IHI 1.2 MW test facility. SEM images showed no significant difference between samples from air and oxy-fuel combustion. The furnace deposits, however, contained significantly more sulphur compared to samples collected from air combustion. The deposition rates for the different combustion conditions were different. In the convective section (fouling) the coals tested generally showed increased fouling tendency during oxy-fuel combustion compared to air-firing. The slagging propensity of the different coals tested changed from being higher to less than that in air combustion.

The composition of the deposits from both the radiative and convective sections showed no difference between air and oxy-fuel conditions, except for the $SO_3$ content which was higher (0.65 (oxy) versus 0.2 (air) wt%) during oxy-fuel combustion for the coal with the highest sulphur content (0.88 wt%, dry). This particular coal does, at the same time, have the highest content of alkali and alkali earth metals in the ash prior to combustion. This could be the explanation to the increased sulphur retention, see Section 3.5.3.

A lower conversion of the iron species in the parent coal into oxides can increase the amount of iron melting into glass silicates and thus increase the slagging propensity of the coal. Untransformed FeO-FeS phase with an eutectic temperature of 940 °C will likewise increase the slagging propensity of the ash. This effect of reduced oxidation of iron-bearing species can be seen for relatively low char combustion temperatures and high CO concentrations inside the burning particles. However, no direct comparison between air- and oxy-firing at the same heat transfer rates with respect to slagging has been found. It is thus unknown, whether incompletely oxidized iron will induce a problem in a full-scale boiler.

Deposit sampling tests performed by Mönckert et al. [147] indicate that besides sulphation, carbonization of deposit surfaces occur. The most obvious reason is that the decomposition temperature of carbonates will increase due to the high partial pressure of carbon dioxide [4]. However, the implications of this observation is not clear.

The investigations reported till now indicate that the changes to depositions in an oxy-fuel plant compared to an air-fired unit will not be of essential significance to the plant operation.

### 3.6. Oxy-fuel combustion of biomass

Carbon capture and storage from combustion of biomass has the potential to reduce the $CO_2$ emission to below zero, i.e. to extract $CO_2$ from the atmosphere and possibly limit the anticipated global warming [84,157,180,211–214]. The abbreviation BECS is used to denote the concept of Biomass Energy for Carbon Capture and Sequestration [213–215]. In principle, all CCS technologies suggested for fossil fired power systems can be applied to systems utilizing biomass fuels [216].

This section contains a survey of the very limited amount of literature available on the use of biomass in oxy-fuel combustion. The main type of biomass investigated is wood. This is a natural consequence of its abundance compared to other types of biomass, such as straw and other annual plants, olive residues, or other dedicated energy crops. Additionally, the transport and feeding of wood is easier to perform than for herbaceous energy sources.

When utilizing biomass in oxy-fuel combustion it is important to consider whether there are any special issues regarding biomass compared to coal which could have a significant impact on the combustion process and related phenomena. Of particular importance will be the volatile matter content, the ash composition, i.e. the content of Cl and alkali, and the change in fuel particle size. At the same time, in order to conclude on specific aspects related to the change of combustion atmosphere when co-firing coal and biomass it is necessary to compare the reported results with the behaviour of these types of fuel blends in conventional combustion.

#### 3.6.1. The combustion process

Arias et al. [180] have investigated the ignition behaviour of coal/biomass blends during oxy-fuel combustion and the effect of oxy-fuel conditions on burnout. Their experiments are performed in an electrically heated entrained-flow reactor (EFR) at about 500 °C for ignition tests and 1000 °C for combustion tests. Both fuels are ground and sieved to a particle size of 75–150 μm. Oxy-fuel combustion with 21, 30, and 35 vol% oxygen were compared with results obtained in air, see Fig. 46. As has previously been seen for pure coals, a delay in ignition (higher ignition temperature) is observed as the oxygen concentration in the oxy-fuel oxidizer is reduced. From these experiments the relative effect of oxygen concentration is nearly independent of the type of fuel.

In air there is a reduction in the ignition temperature when the bituminous coal is blended with the biomass, see the three most left-hand-side bars in the figure for each case. The effect is, however, much less pronounced in the case of oxy-fuel combustion regardless of the oxygen concentration. This can be attributed to the fact that even though the biomass has a high reactivity and a high volatile matter content the heating value is lower than for the coal. The heat released from the biomass during ignition is thus

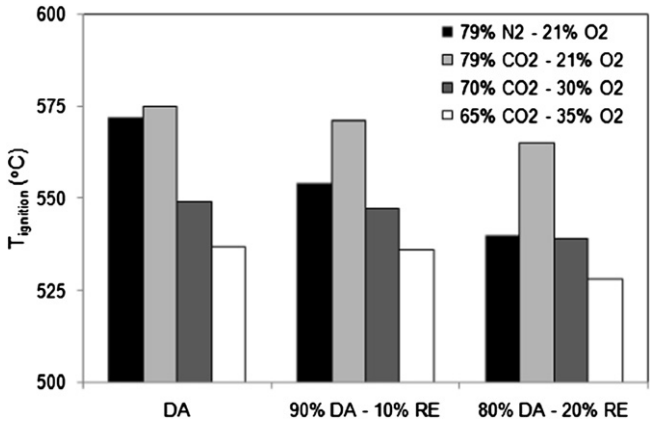


**Fig. 46.** Ignition temperatures of a high-volatile bituminous coal (DA) and blends of the coal and Eucalyptus (RE) in air combustion and oxy-fuel combustion with different $O_2$ concentrations at the inlet. The blending ratio is presumably given on a mass basis. Experiments are performed in an electrically heated entrained-flow reactor. Data taken from [180].

not substantial to enhance the heating of the coal particles and the ignition temperature is thus not increased significantly. As previously described, more heat is needed to increase the temperature of the surrounding gases and hence the coal particles in the case of oxy-fuel combustion than for combustion in air [180].

Results of burnout experiments for the same high-volatile coal and its blends with Eucalyptus are shown in Fig. 47. An obvious difference in burnout degree is seen for all three cases when changing the combustion atmosphere from air to $CO_2$-based. In oxy-fuel combustion with an air-like oxidizer composition the burnout degree decreases below that found in air. For oxygen concentrations of 30 and 35% the burnout increases above that found in air. However, the effect of blending biomass and coal is seen to have only little impact on the burnout, i.e. there is only a minor improvement by an increasing biomass content in the blend.

Because of the significantly higher volatile content in biomass compared to coal an improvement in the burnout degree of the fuel blends could be expected. However, reported data do not confirm this. Arias et al. [180] explain the lack of improvement in burnout for the blends in terms of the changes in oxygen and temperature

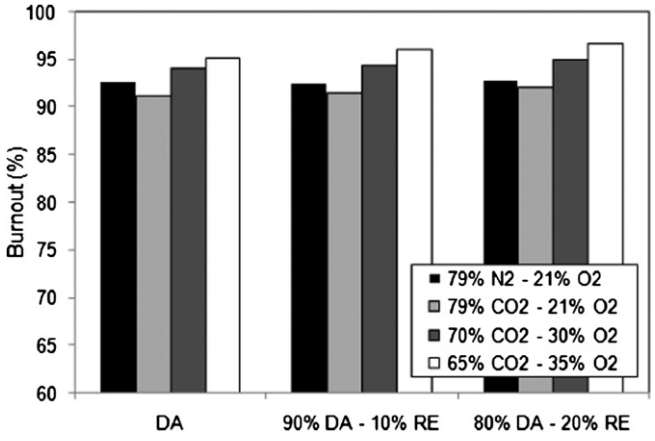


**Fig. 47.** Burnout of a high-volatile bituminous coal (DA) and blends of the coal and Eucalyptus (RE) at a stoichiometric value of 1.25. Experiments are performed in air and oxy-fuel atmospheres with different oxygen concentrations at the inlet of the entrained-flow reactor setup used. The blending ratio is presumably given on a mass basis. Data taken from [180].

profiles in the reactor caused by the introduction of the more reactive biomass fuel.

Characteristics of wood chip, rice husk, and forest residues chars obtained by pyrolysis in air and oxy-fuel atmospheres were investigated by Borrego et al. [217]. They saw that the char characteristics such as pore volume, morphology, optical texture, specific surface area, and reactivity showed no significant difference between air and oxy-fuel combustion. The authors thus concluded that the application of biomass in co-fired oxy-fuel boilers (coal/biomass) should not constitute any specific difficulties regarding the chars.

### 3.6.2. Emissions

In commercial-scale tests co-firing coal and biomass in air, large decreases and moderate increases are occasionally observed for the $NO_x$ yields [218]. Tests by Robinson et al. [218] have shown that these changes most probably are caused by the biomass influencing fluid dynamics as well as temperature and stoichiometry profiles during the combustion. No fundamental synergistic chemical effects could be observed. The coals tested were bituminous whereas the biomass were red oak wood chips and switchgrass.

Fryda et al. [184] have found that the $NO_x$ emission rate during oxy-fuel combustion can be decreased when coal (Russian) and biomass in the form of cocoa residues are co-fired in a lab-scale setup compared to tests with pure coal. Generally, using over-fire air (OFA) reduces the emission rate. The cocoa residues have a higher content of N compared to the pure coal (2.61 versus 0.87 wt%, dry basis) and thus has the fuel blend. The decrease in $NO_x$ emission rate can thus be explained by the increased volatile content and the related, lower amount of fixed carbon in the blend compared to the pure coal.

Emissions of $SO_x$ from oxy-fuel combustion of pure biomass or coal and biomass blends have not been reported in open literature.

### 3.6.3. Ash and corrosion

Robinson et al. [218] have investigated the ash deposition rates from both individual fuels and their blends (wood chips, coal, switchgrass, and wheat straw) during conventional combustion in air. They observed that the particle capture efficiency (the ash deposition rate normalized by the fuel ash content and the size of the deposition probe) was significantly larger for straw than for wood chips and coal in the order: wood chips < coal < switchgrass ≪ wheat straw. The order is closely related to the absolute amount of alkali in the fuels. Blending coal and biomass, especially straw, yield deposition rates which are lower than what would be expected based on the behaviour of the unblended fuels, see the upper part of Fig. 48. Especially in the case of co-firing coal and straw the particle capture efficiency is markedly reduced compared to the predicted value (about 10%). Sulphation of alkali chlorides released from the straw with sulphur from the coal is expected to account for part of the observed effect [218]. The main effect is due to incorporation of mainly potassium from the biomass into alumina-silicates in the coal ash followed by release of HCl, see (15).

$$(Al_2O_3)(SiO_2)_2 + 2KCl + H_2O \rightarrow (K_2O)(Al_2O_3)(SiO_2)_2 + 2HCl \quad (15)$$

This is a recognized method for reducing corrosion in biomass fired boilers.

In the bottom part of Fig. 48 the capture efficiency is calculated based on the amount of available alkali in the blend. It is clearly seen that this is a better measure of the slagging and fouling tendency of the fuel blends.

Studies of deposition and fouling in oxy-fuel combustion performed by Fryda et al. [184] have shown no significant change in

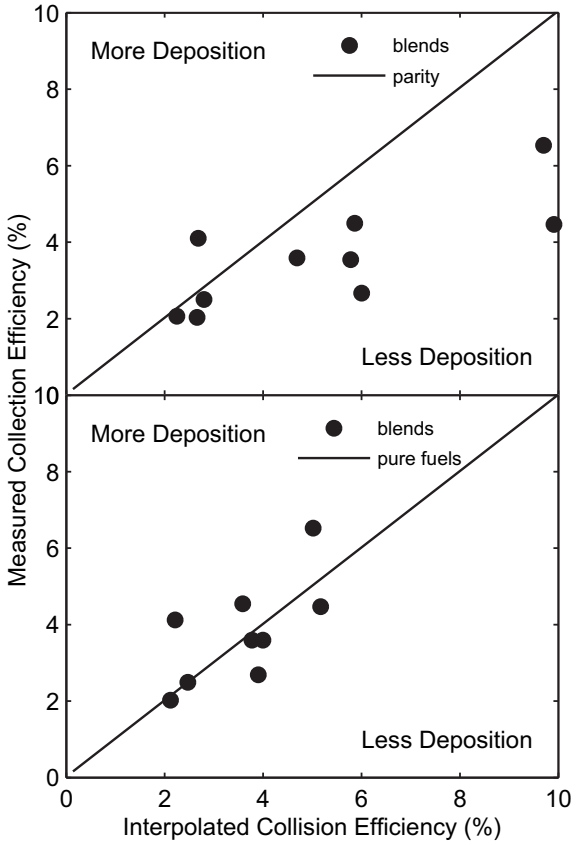


**Fig. 48.** Comparisons of measured and predicted particle capture efficiencies for different blends of coal and biomasses (wood chips, switchgrass, and wheat straw). Experiments are performed in a 30 kW down-fired, turbulent flow facility. Top: The predicted capture efficiencies are based on an interpolation between the two pure fuels and the fraction of the ash content originating from the coal. Bottom: The bias observed in the upper figure is removed by performing the interpolation based on the fuel-available alkali content rather than total ash. Data taken from [218].

deposition rate between pure coal and coal/biomass blends (cocoa residues and wood chips). The coal to biomass ratio in the blends is 80/20 on a mass basis. The coal/wood blends slightly increase the specific fouling factor, whereas blends with cocoa residues slightly decreases the fouling factor. This correlates well with the results obtained by Robinson et al. [218].

In relation to the aspects of corrosion and ash quality during co-combustion of coal and biomass at oxy-fuel conditions the sulphur and alkali contents of the parent fuels could induce both advantages and disadvantages. If the concentration of sulphur in the boiler during oxy-fuel combustion is enhanced there is a larger potential to convert alkali chlorides released from the biomass to sulphates before the flue gas meets the superheater banks and deposition occurs. The corrosion potential could thus be reduced. On the other hand, the higher alkali content in biomass ashes, and especially straw, will potentially increase the sulphur retention in the fly ash when co-firing with coal as described in Section 3.5.3.

### 3.7. Summary

Below is a short summary of the main findings presented in Section 3.

*Research Groups:* 26 research groups with different experimental equipment doing oxy-fuel combustion studies have been identified. The experimental setups range from 4.2 $kW_{th}$ to 30 $MW_{th}$ in size and include units both with and without flue gas recirculation.

*Heat and Mass Transfer:* The differences in thermo-chemical properties between $CO_2$ and $N_2$ cause changes in the heat and mass transfer rates within a boiler if $CO_2$ is substituted directly for $N_2$ in the oxidizer. In order to obtain an adiabatic flame temperature during combustion similar to that seen in air-firing the oxygen concentration in the oxidizer should be increased to 27–35 vol% depending on the type of fuel. Lower rank coals require lower oxygen concentations than higher rank coals.

$CO_2$ and $H_2O$ are radiating gases whereas $N_2$ is not. The radiative heat transfer in oxy-fuel combustion is thus higher than in air combustion for the same flame temperature. In order to match the heat uptake profile in a retrofittet boiler the flame temperature should thus be kept lower than during air operation.

*Combustion Process:* Devolatilization and ignition of coal particles are affected by the change in oxidizer composition from air to oxy-fuel combustion. The rate of devolatilization is primarily determined by the surrounding gas temperature as the difference in thermal conductivity of $N_2$ and $CO_2$ is rather low. Particle ignition, on the other hand, is a strong function of both the transport properties of the gas phase surrounding the particles as well as the combustion heat release rate and the reactivity of the local fuel-oxidizer mixture. Ignition times comparable to those observed during air combustion can be obtained by increasing the oxidizer oxygen concentration to 27–35 vol% and thus the flame temperature. Burnout of volatiles and char are likewise affected by the high $CO_2$ and $H_2O$ concentrations in the flame. Especially the lower diffusivity of both oxygen and small hydrocarbons in $CO_2$ compared to $N_2$ is an important factor. Generally, a slight improvement in char burnout is reported in the literature when the flame temperature matches that of air combustion. This improvement is assumed to be caused primarily by the higher oxygen partial pressure experienced by the burning particles. Gasification reactions and residence time differences are believed to be of minor influence.

Due to the high $CO_2$ concentration in the combustion environment high levels of CO are expected in the near-flame zone. There is thus an increased risk of CO corrosion in this zone. Because of the large oxygen partial pressure the CO is reported to oxidize before leaving the larger of the test furnaces yielding similar CO emission rates as for air combustion.

*Emissions:* $NO_x$ emissions from oxy-fuel combustion is probably the single most investigated area of this technology. Due to the very low levels of molecular nitrogen a potential exists to reduce the emissions rate considerably compared to combustion in air through near-elimination of both thermal and prompt $NO_x$ formation. Reductions by 70–80% have been reported. Different suggestions to the mechanisms responsible for the reduction have been proposed. However, it is generally accepted that reburning reactions play a major role. Experiments indicate that increasing the oxygen concentration and the oxygen excess yield higher emission rates. On the other hand, the use of oxidant staging, recycling of flue gas before drying, increasing the partial pressure of $NO_x$ in the oxidant, increasing the oxygen purity, and limiting the air ingress into the boiler work to decrease the emission rate.

Sulphur oxides is the other major pollutant from coal-fired combustion. The emission of these oxides is not reduced to the same degree as $NO_x$. However, increased retention in ash due to the higher partial pressure of $SO_2$ in the boiler when flue gas is recirculated before the desulphurization unit has been reported. Increased risk of low-temperature corrosion by sulfuric acid and a higher acid dew point are some of the major concerns regarding sulphur in oxy-fuel combustion.

Limited work has been reported on the emission of trace elements from oxy-fuel combustion. The work performed has focused on Hg, Cd, As, and Se with Hg attracting the most attention.

No significant differences between air-firing and oxy-fuel combustion have been reported at this point.

*Ash and Depositions:* The transformations of coal mineral matter during combustion are affected by the temperature and the gas phase composition surrounding the coal particles. At low combustion temperature (for below 30% $O_2$ in $CO_2$) a shift in the size distribution of the sub-mircometer-sized fly ash toward smaller particles can be observed. Increasing the $O_2$ partial pressure provides a size distribution similar to that found in air combustion. The ash quality is crucial to its application in cement and concrete production. Significantly increased sulphur retention could cause problems in this respect.

The propensity for slagging and fouling in oxy-fuel combustion is likewise subject to research. At this point, the reported results suggest that only minor changes compared to air-firing will result from the change in the combustion environment.

*BECS:* Utilization of renewable biomass fuels such as wood, straw, and other energy crops in thermal power plants with carbon capture and storage is attracting increased attention. The combination of $CO_2$ neutral fuels with CCS opens a possibility of extracting $CO_2$ from the atmosphere. Until now, only few experiments on oxy-fuel combustion of biomasses have been reported. It is expected that further work on BECS will reveal comparable changes to the combustion fundamentals as is the case when biomass is introduced during combustion of coal in air.

## 4. Conclusions

The reduction of $CO_2$ emissions from power plants has become an increasing important topic in the discussions of how to prevent global warming arising from antropogenic $CO_2$ emissions. Three CCS (Carbon Capture and Storage) technologies have been suggested for medium term application which will reduce the emissions to near zero; Chemical absorption by amines (post-combustion capture), Integrated gasification combined cycle plants (pre-combustion capture), and oxy-fuel combustion capture. Of these, the post-combustion and oxy-fuel technologies can be applied as retrofit solutions to the existing fleet of pulverized-coal-fired power plants. Compared to post-combustion capture oxy-fuel combustion is less mature and thus requires comprehensive fundamental research as well as pilot and demonstration scale testing before commercial operation of an oxy-fuel power plant seems to be feasible. Currently, no full-scale oxy-fuel plants are in operation. The only announced large demonstration plant (250 $MW_e$) is planned to be put into operation in 2015 by Vattenfall. Commercial operation does thus not seem to be feasible before 2020.

The current literature review describes the available knowledge on the oxy-fuel technology. The focus has been on both the changes induced to an existing, conventional air-fired plant if retrofitted to oxy-fuel combustion and the research performed on the fundamental combustion characteristics including heat transfer effects, ignition and burnout, emissions, ash quality, and deposit build-up. Both coal and the application of $CO_2$ neutral fuels such as wood or other types of biomass are included in the review.

Retrofitting an existing pulverized-coal-fired power plant to oxy-fuel operation requires a number of new process units – an air separation facility to provide the combustion process with almost pure oxygen, ducts and fans for external recirculation of flue gas to the burners in order to control flame temperatures, and a $CO_2$ processing facility producing a near-pure $CO_2$ stream for storage. The retrofit to oxy-fuel operation will reduce the plant electrical efficiency by about 10 percent points depending on the initial efficiency. It is generally accepted that a 95% pure $O_2$ stream constitutes the optimum with respect to minimizing the combined expense for air separation and $CO_2$ cleaning. Leakage of air into the boiler necessitates removal of non-condensable species from the $CO_2$ stream prior to storage. The capture efficiency of an oxy-fuel power plant is thus expected to be around 90%. Two flue gas recycle streams are necessary. The primary stream is used for coal drying and transportation to the burners and should preferably be desulphurized and dry. Most process configuration suggestions avoid addition of $O_2$ to the primary stream. Instead, $O_2$ is added either to the secondary flue gas recycle stream or directly through special lances in the burners. The overall $O_2$ concentration at the inlet to the boiler should be between 27 and 35 vol% in order to yield comparable adiabatic flame temperatures and heat transfer profiles as seen for conventional combustion in air. The exact level depends on the type of coal and the boiler design. Even though $CO_2$ has significantly different thermo-chemical properties compared to $N_2$ increasing the $O_2$ concentration in oxy-fuel combustion yields similar devolatilization and ignition behaviour in the two environments. The burnout is reported to improve in oxy-fuel combustion. The emission rate of CO is reported to be similar in air and oxy-fuel combustion even though significantly increased CO levels are seen within the flame zone in the oxy-fuel environment. $SO_2$ emissions are likewise reported to be of similar magnitude regardless of flue gas composition. The $NO_x$ emission is, however, significantly reduced during oxy-fuel combustion compared to air-firing due to a near-elimination of thermal NO formation and to reburning of $NO_x$ passed through the burners with the recirculated flue gas. Reductions of the emission rate by 70–80% have been reported. Only minor changes to the deposit build-up are expected for oxy-fuel combustion compared to air-firing. However, the oxy-fuel environment is expected to lead to a significant increase in the $SO_3$ concentration within the boiler increasing the risk of both high and low-temperature corrosion as well as increased retention of sulphur in the fly ash.

A significant amount of new information on the oxy-fuel technology has been published since Wall and coworkers released their literature survey in 2005. At that time the following research needs were concluded to require the most attention in order to gain a deeper fundamental understanding of the oxy-fuel technology:

- Match of heat transfer characteristics in retrofitted boilers.
- The cost of electricity and the cost of $CO_2$ avoided.
- Combustion characteristics and emission levels (pilot plant scale).
- Requirements for gas cleaning - especially $SO_2$.

Based on the fact that no full-scale plants are in operation, the required large-scale investigations of heat transfer characteristics still remain. Additional work on both convective and radiative heat transfer in laboratory-scale reactors has however been conducted.

Several techno-economic assessments of the oxy-fuel technology exist and new are continuously being published. However, the estimated costs of electricity and $CO_2$ avoidance costs generally suffer from large uncertainties due to the lack of construction and operation experience from full-scale plants.

Few results regarding combustion characteristics and emission levels in pilot plant scale setups (>1 $MW_{th}$) have been published within the last five years. This area thus needs continued attention.

Suggestions to the purity requirements for $CO_2$ for sequestration and enhanced oil recovery have been published. No standards or legislative requirements have however been found. Clarification of the necessary extent of cleaning is very important to plant configuration and eventually the process economics.

Besides the topics discussed above, this review has revealed that a deeper understanding of the effect of a shift from air-blown combustion to oxy-fuel combustion on the following issues is necessary:

- Optimum oxygen excess and inlet oxygen concentration levels.
- Corrosion at both high and low temperatures.
- Ash quality, especially regarding the risk of enhanced sulphur retention.
- Operability, i.e. start-up and shut-down, dynamics during transients, the need for air-firing capability, etc.
- Models to predict $NO_x$ and $SO_3$ formation.

The oxy-fuel combustion process is still in the developing phase and much research is still required in order to fully clarify the consequences of its implementation in power plants.

## Acknowledgements

The work has been funded by Energinet.dk and The Danish Ministry of Science, Technology and Innovation (VTU) as well as the companies DONG Energy and Vattenfall. The help by Stine Hansen, Department of Chemical Engineering, Technical University of Denmark in producing the figures for this paper is greatly appreciated.

## References

[1] International Energy Agency (IEA). World energy outlook 2007 – China and India insights. IEA Publications; 2007.
[2] International Energy Agency (IEA). World energy outlook 2008. IEA Publications; 2008.
[3] Kavouridis K, Koukouzas N. Coal and sustainable energy supply challenges and barriers. Energy Policy 2008;36(2):693–703.
[4] Buhre BJP, Elliott LK, Sheng CD, Gupta RP, Wall TF. Oxy-fuel combustion technology for coal-fired power generation. Prog Energy Combust Sci 2005;31(4):283–307.
[5] Wall TF. Combustion processes for carbon capture. Proc Combust Inst 2007;31(1):31–47.
[6] Solomon S, Qin D, Manning M, Chen Z, Marquis M, Averyt KB, et al., editors. IPCC, 2007: climate change 2007: the physical science basis. Contribution of working group I to the fourth assessment report of the intergovernmental panel on climate change. Cambridge, United Kingdom and New York, NY, USA: Cambridge University Press; 2007.
[7] Bachu S. $CO_2$ storage in geological media: role, means, status and barriers to deployment. Prog Energy Combust Sci 2008;34(2):254–73.
[8] Davison J. Performance and costs of power plants with capture and storage of $CO_2$. Energy 2007;32(7):1163–76.
[9] Tan Y, Thambimuthu KV, Douglas MA, Mortazavi R. Oxy-fuel combustion research at the CANMET Energy Technology Center. In: Proc 2003 5th Int Symp Coal Combust; 2003. p. 550–54.
[10] Jordal K, Anheden M, Yan J, Strömberg L. Oxyfuel combustion for coal-fired power generation with $CO_2$ capture – opportunities and challenges. In: The 7th International conference on greenhouse gas control technologies (GHGT-7). Vancouver, Canada; September 2004.
[11] Feron PHM, Hendriks CA. $CO_2$ capture process principles and costs. Oil Gas Sci Technol 2005;60(3):451–9.
[12] Tan R, Corragio G, Santos S. Oxy-coal combustion with flue gas recycle for the power generation industry – a literature review. Study report, IFRF Doc. No. G 23/y/1. Velsen Noord, The Netherlands: International Flame Research Foundation (IFRF); September 2005.
[13] Knudsen JN, Vilhelmsen P-J, Jensen JN, Biede O. First year operating experience with a 1 t/h $CO_2$ absorption – pilot plant at Esbjerg coal-fired power plant. VGB PowerTech 2007;87(3):57–61.
[14] Figueroa JD, Fout T, Plasynski S, McIlvried H, Srivastava RD. Advances in $CO_2$ capture technology – the U.S. department of energy's carbon sequestration program. Int J Greenhouse Gas Control 2008;2(1):9–20.
[15] Knauss KG, Johnson JW, Steefel CI, Nitao JJ. Evaluation of the impact of $CO_2$, aqueous fluid, and reservoir rock interactions on the geologic sequestration of $CO_2$, with special emphasis on economic implications. In: 1st national conference on carbon sequestration. NETL Publications; 2001.
[16] Varagani RK, Châtel-Pélage F, Pranda P, Rostam-Abadi M, Lu Y, Bose AC. Performance simulation and cost assessment of oxy-combustion process for $CO_2$ capture from coal-fired power plants. In: The fourth annual conference on carbon sequestration, May 2–5. Alexandria, VA; 2005.
[17] Gozalpour F, Ren SR, Tohidi B. $CO_2$ EOR and storage in oil reservoirs. Oil Gas Sci Technol 2005;60(3):537–46.
[18] Baes Jr CF, Beall SE, Lee DW, Marland G. The collection, disposal, and storage of carbon dioxide. In: Interactions of energy and climate, proceedings of an international workshop; 1980. p. 495–19.
[19] Grimston MC, Karakoussis V, Fouquet R, van der Vorst R, Pearson P, Leach M. The European and global potential of carbon dioxide sequestration in tackling climate change. Clim Policy 2001;1(2):155–71.
[20] Gunter WD, Wong S, Cheel DB, Sjostrom G. Large $CO_2$ Sinks: their role in the mitigation of greenhouse gases from an international, national (Canadian) and provincial (Alberta) perspective. Appl Energy 1998;61(4):209–27.
[21] Metz B, Davidson O, Swart R, Pan J, editors. IPCC, 2001: climate change 2001: mitigation. Contribution of working group III to the third assessment report of the intergovernmental panel on climate change (IPCC). Cambridge, United Kingdom and New York, NY, USA: Cambridge University Press; 2001.
[22] Davison J, Freund P, Smith A. Putting carbon back into the ground. Technology overview, the IEA greenhouse gas R&D programme; February 2001.
[23] Gibbins J, Chalmers H. Carbon capture and storage. Energy Policy 2008a;36(12):4317–22.
[24] Solomon S, Carpenter M, Flach TA. Intermediate storage of carbon dioxide in geological formations: a technical perspective. Int J Greenhouse Gas Control 2008;2(4):502–10.
[25] Bentham M, Kirby G. $CO_2$ storage in saline aquifers. Oil Gas Sci Technol 2005;60(3):559–67.
[26] Cailly B, Le Thiez P, Egermann P, Audibert A, Vidal-Gilbert S, Longaygue X. Geological storage of $CO_2$: a state-of-the-art of injection processes and technologies. Oil Gas Sci Technol 2005;60(3):517–25.
[27] Allam RJ, Spilsbury CG. A study of the extraction of $CO_2$ from the flue gas of a 500 MW pulverised coal fired boiler. Energy Convers Manage 1992;33(5–8):373–8.
[28] Abu-Khader MM. Recent progress in $CO_2$ capture/sequestration. A Review Energy Sources Part A Recovery Utilization Environ Effects 2006;28(14):1261–79.
[29] Fischedick M, Günster W, Fahlenkamp H, Meier H-J, Neumann F, Oeljeklaus G, et al. Separation in power plants – do retrofits make sense in existing plants? VGB PowerTech 2006;4:108–17 [in German].
[30] Pehnt M, Henkel J. Life cycle assessment of carbon dioxide capture and storage from lignite power plants. Int J Greenhouse Gas Control 2009;3(1):49–66.
[31] Sander MT, Mariz CL. The Fluor Daniel econamine FG process: Past experience and present day focus. Energy Convers Manage 1992;33(5–8):341–8.
[32] Reddy S, Scherffius J, Freguia S, Roberts C. Fluor's Econamine FG PlusSM technology – an enhanced amine-based $CO_2$ capture process. In: Proceedings of the second national conference on carbon sequestration. Alexandria, VA, USA: US Department of Energy National Technology Laboratory; May 2003.
[33] Yagi Y, Mimura T, Iijima M, Ishida K, Yoshiyama R, Kamino T. Improvements of carbon dioxide capture technology from flue gas. In: Greenhouse gas control technologies. Proceedings of the seventh international conference on greenhouse gas control technologies, 5–9 September 2004, Vancouver, Canada. Oxford, UK: Elsevier Ltd; 2005.
[34] Wegerich S, Witt A, Huizeling E, Rode H. Untersuchungen zur Nachrüstung einer $CO_2$-Abscheidetechnologie für das neue E.ON Kraftwerk Maasvlakte 3. In: 39. Kraftwerktechnisches Kolloquium. Dresden, Germany; October 11–12, 2007.
[35] Oexmann J, Kather A. Post-combustion $CO_2$-capture from coal-fired power plants – wet chemical absorption processes. VGB PowerTech 2009;89(1/2):92–103 [in German].
[36] Descamps C, Bouallou C, Kanniche M. Efficiency of an integrated gasification combined cycle (IGCC) power plant including $CO_2$ removal. Energy 2008;33(6):874–81.
[37] Kanniche M, Gros-Bonnivard R, Jaud P, Valle-Marcos J, Amann J-M, Bouallou C. Pre-combustion, post-combustion and oxy-combustion in thermal power plant for $CO_2$ capture. Appl Thermal Eng 2010;30(1):53–62.
[38] Okawa M, Kimura N, Kiga T, Takano S, Arai K, Kato M. Trial design for a $CO_2$ recovery power plant by burning pulverized coal in $O_2/CO_2$. Energy Convers Manage 1997;38:123–7.
[39] Altmann H, Stamatelopoulos G-N. Steps towards the minimisation of $CO_2$ emissions from coal-fired power plants. In: Conference and exhibition for the European power generation industry, POWER-GEN Europe 2005. Milan (Italy); June 28–30, 2005.
[40] Singh D, Croiset E, Douglas PL, Douglas MA. Techno-economic study of $CO_2$ capture from an existing coal-fired power plant: MEA scrubbing vs. $O_2/CO_2$ recycle combustion. Energy Convers Manage 2003;44(19):3073–91.
[41] Ewert M. The significance of power stations with $CO_2$ capture in planning future generation portfolio. VGB PowerTech 2005;85(10):36–40 [in German].
[42] Unknown. Chilling news for carbon capture [[carbon dioxide capture process]]. Mod Power Syst 2006;26(12):17–8.
[43] Xu B, Stobbs RA, White V, Wall RA, Gibbins J, Iijima M, et al. Future $CO_2$ capture technology options for the Canadian market. Technical Report Report No. COAL R309 BERR/Pub URN 07/1251. Doosan Babcock Energy Limited; March 2007.
[44] Wheeldon J, Booras G, Holt N. Post-combustion $CO_2$ capture from pulverized coal plants. In: 23rd Annual international Pittsburgh coal conference, PCC – coal-energy, environment and sustainable development; 2006.
[45] Notz R, Asprion N, Clausen I, Hasse H. Selection and pilot plant tests of new absorbents for post-combustion carbon dioxide capture. Chem Eng Res Des 2007;85(A4):510–5.
[46] Lee S, Maken S, Park J-W, Song H-J, Park JJ, Shim J-G, et al. A study on the carbon dioxide recovery from 2 ton-$CO_2$/day pilot plant at LNG based power plant. Fuel 2008;87(8–9):1734–9.
[47] Iea Ghg. Improvement in power generation with post-combustion capture of carbon dioxide. Report PH4/33, IEA greenhouse gas research and development programme; 2004.

[48] Williams TC, Shaddix CR, Schefer RW. Effect of syngas composition and $CO_2$-diluted oxygen on performance of a premixed swirl-stabilized combustor. Combust Sci Technol 2008;180(1):64–88.

[49] Damen K, van Troost M, Faaij A, Turkenburg W. A comparison of electricity and hydrogen production systems with $CO_2$ capture and storage. Part A: review and selection of promising conversion and capture technologies. Prog Energy Combust Sci 2006;32(2):215–46.

[50] Beér JM. High efficiency electric power generation: the environmental role. Prog Energy Combust Sci 2007;33(2):107–34.

[51] McDonald DK, Flynn TJ, DeVault DJ, Varagani R, Levesque S, Castor W. 30 $MW_t$ clean environment development oxy-coal combustion test program. In: The 33rd international technical conference on coal utilization and fuel systems. Clearwater, Florida; 2008.

[52] Minchener AJ. Coal gasification for advanced power generation. Fuel 2005;84 (17):2222–35.

[53] Gericke B, Kuzmanovski P, Nassauer K. Conceptual solutions regarding the influence of the oxy-fuel-process on conventional power plants [Konzeptüberlegungen bezüglich der Auswirkungen des oxy-fuel-prozesses auf konventionelle Kraftwerksanlagen]. VGB PowerTech 2006;86(10):64–72 [in German].

[54] Chen C, Rubin ES. $CO_2$ control technology effects on IGCC plant performance and cost. Energy Policy 2009;37(3):915–24.

[55] Eide LI, Bailey DW. Precombustion decarbonisation processes. Oil Gas Sci Technol 2005;60(3):475–84.

[56] Lambertz J, Ewers J. Clean coal power – the response of power plant engineering to climate protection challenges. VGB PowerTech 2006;86(5):72–7 [in German].

[57] Gibbins J, Chalmers H. Preparing for global rollout: a 'developed country first' demonstration programme for rapid CCS deployment. Energy Policy 2008;36 (2):501–7.

[58] Horn FL, Steinberg M. Control of carbon dioxide emissions from a power plant (and use in enhanced oil recovery). Fuel 1982;61(5):415–22.

[59] Herzog H, Golomb D, Zemba S. Feasibility, modeling and economics of sequestering power plant $CO_2$ emissions in the deep ocean. Environ Prog 1991;10(1):64–74.

[60] Abraham BM, Asbury JG, Lynch EP, Teotia APS. Coal-oxygen process provides $CO_2$ for enhanced recovery. Oil Gas J 1982;80(11):68–70. 75.

[61] Nakayama S, Noguchi Y, Kiga T, Miyamae S, Maeda U, Kawai M, et al. Pulverized coal combustion in $O_2/CO_2$ mixtures on a power plant for $CO_2$ recovery. Energy Convers Manage 1992;33(5–8):379–86.

[62] Simmons M, Miracca I, Gerdes K. Oxyfuel technologies for $CO_2$ capture: a techno-economic overview. In: 7th international conference on greenhouse gas control technologies. Vancouver, Canada; September, 2004.

[63] Châtel-Pélage F, Varagani R, Pranda P, Perrin N, Farzan H, Vecci SJ, et al. Applications of oxygen for $NO_x$ control and $CO_2$ capture in coal-fired power plants. Thermal Sci 2006;10(3):119–42.

[64] Anheden M, Andersson A, Bernstone C, Eriksson S, Yan J, Liljemark S, et-al. $CO_2$ quality requirement for a system with $CO_2$ capture, transport and storage. In: The 7th International Conference on greenhouse gas control technologies (GHGT7). Vancouver, Canada; September 5–9, 2004.

[65] Anheden M, Yan J, De Smedt G. Denitrogenation (or oxy-fuel concepts). Oil Gas Sci Technol 2005;60(3):485–95.

[66] Dillon DJ, Panesar RS, Wall RA, Allam RJ, White V, Gibbins J, et al. Oxy-combustion processes for $CO_2$ capture from advanced supercritical PF and NGCC power plant. In: 7th international conference on greenhouse gas control technologies. Vancouver, Canada; September, 2004.

[67] Dillon DJ, White V, Allam RJ, Wall RA, Gibbins J. Oxy Combustion Processes for $CO_2$ capture from power plant. Engineering Investigation Report, 2005/9, IEA Greenhouse Gas Research and Development Programme; June 2005.

[68] Kather A, Klostermann M, Hermsdorf C, Mieske K, Eggers R, Köpke D. Konzept für ein 600 $MW_{el}$ Steinkohlekraftwerk mit $CO_2$-Abtrennung auf Basis des Oxyfuel-Prozesses. In: Kraftwerksbetrieb unter künftigen Rahmenbedingungen, 38. Kraftwerkstechnisches Kolloquium. Dresden, Germany; October 24–25, 2006.

[69] Rezvani S, Huang Y, McIlveen-Wright D, Hewitt N, Wang Y. Comparative assessment of sub-critical versus advanced super-critical oxyfuel fired pf boilers with $CO_2$ sequestration facilities. Fuel 2007;86(14):2134–43.

[70] Eide LI, Anheden M, Lyngfelt A, Abanades C, Younes M, Clodic D, et al. Novel capture processes. Oil Gas Sci Technol 2005;60(3):497–508.

[71] Hossain MM, de Lasa HI. Chemical-looping combustion (CLC) for inherent $CO_2$ separations–a review. Chem Eng Sci 2008;63(18):4433–51.

[72] Farley M. Developing oxyfuel capture as a retrofit technology. Mod Power Syst 2006;26(4):20–2.

[73] Aspelund A, Jordal K. A study of the interface between $CO_2$ capture and transport. In: The 8th International Conference on Greenhouse Gas Control Technologies (GHGT-8). Trondheim, Norway; 19–22 June, 2006.

[74] Aspelund A, Jordal K. Gas conditioning – the interface between $CO_2$ capture and transport. Int J Greenhouse Gas Control 2007;1(3):343–54.

[75] Sass BM, Farzan H, Prabhakar R, Gerst J, Sminchak J, Bhargava M, et al. Considerations for treating impurities in oxy-combustion flue gas prior to sequestration. Energy Procedia 2009;1(1):535–42.

[76] Anheden M, Rydberg S, Yan J. Consideration for removal of non-$CO_2$ components from $CO_2$ rich flue gas of oxy-fuel combustion. In 3rd workshop of the IEA GHG International oxy-combustion network. Yokohama, Japan; March 5–6, 2008.

[77] Lee CW, Miller CA. Understanding the potential environmental impacts of oxy-fuel combustion. In: 3rd Workshop of the IEA GHG international oxy-combustion network. Yokohama, Japan; March 5–6, 2008.

[78] Fout T. Oxy-COMBUSTION: research, development and systems analysis. In: 3rd Workshop of the IEA GHG international oxy-combustion network. Yokohama, Japan; March 5–6, 2008.

[79] Andersson K, Johnsson F, Strömberg L. Large scale $CO_2$ capture – applying the concept of $O_2/CO_2$ combustion to commercial process data. VGB PowerTech 2003;83(10):1–5.

[80] Andersson K, Johnsson F. Process evaluation of an 865 MWe lignite fired $O_2/CO_2$ power plant. Energy Convers Manage 2006;47(18–19):3487–98.

[81] Kakaras E, Koumanakos A, Doukelis A, Giannakopoulos D, Vorrias I. Simulation of a greenfield oxyfuel lignite-fired power plant. Energy Convers Manage 2007;48(11):2879–87.

[82] Hellfritsch S, Gilli PG, Jentsch N. Concept for a lignite-fired power plant based on the optimised oxyfuel process with $CO_2$ recovery. VGB PowerTech 2004;84(8):76–82.

[83] Zanganeh KE, Shafeen A. A novel process integration, optimization and design approach for large-scale implementation of oxy-fired coal power plants with $CO_2$ capture. Int J Greenhouse Gas Control 2007;1(1):47–54.

[84] Uddin SN, Barreto L. Biomass-fired cogeneration systems with $CO_2$ capture and storage. Renewable Energy 2007;32(6):1006–19.

[85] Li H, Yan J, Yan J, Anheden M. Impurity impacts on the purification process in oxy-fuel combustion based $CO_2$ capture and storage system. Appl Energy 2009;86(2):202–13.

[86] Payne R, Chen SL, Wolsky AM, Richter WF. $CO_2$ recovery via coal combustion in mixtures of oxygen and recycled flue gas. Combust Sci Technol 1989;67(1):1–16.

[87] Kimura N, Omata K, Kiga T, Takano S, Shikisima S. The characteristics of pulverized coal combustion in $O_2/CO_2$ mixtures for $CO_2$ recovery. Energy Convers Manage 1995;36(6–9):805–8.

[88] Woycenko DM, van de Kamp WL, Roberts PA. Combustion of pulverised coal in a mixture of oxygen and recycled flue gas. Summary of the APG research program, IFRF Doc. F98/Y/4. Ijmuiden, The Netherlands: International Flame Research Foundation (IFRF); October 1995.

[89] Tan Y, Douglas MA, Thambimuthu KV. $CO_2$ capture using oxygen enhanced combustion strategies for natural gas power plants. Fuel 2002;81(8): 1007–16.

[90] Andersson K, Normann F, Johnsson F, Leckner B. NO emission during oxy-fuel combustion of lignite. Ind Eng Chem Res 2008a;47(6):1835–45.

[91] Farzan H, McDonald DK, McCauley KJ, Varagani R, Prabhakar R, Periasamy C, et al. Oxy-coal combustion pilot. In: 3rd Workshop of the IEA GHG international oxy-combustion network. Yokohama, Japan; March 5–6, 2008.

[92] Strömberg L, Lindgren G, Jacoby H, Giering R, Anheden M, Burchhardt U, et al. Update on Vattenfall's 30 MWth oxyfuel pilot plant in Schwarze Pumpe. Energy Procedia 2009;1(1):581–9.

[93] Darde A, Prabhakar R, Tranier J-P, Perrin N. Air separation and flue gas compression and purification units for oxy-coal combustion systems. Energy Procedia 2009;1(1):527–34.

[94] Burchhardt U, Radunsky D. Erfahrungen aus der Planung und Genehmigung der Oxyfuel-Forschungsanlage von Vattenfall. In: 39. Kraftwerktechnisches Kolloquium. Dresden, Germany; October 11–12, 2007.

[95] Simpson AP, Simon AJ. Second law comparison of oxy-fuel combustion and post-combustion carbon dioxide separation. Energy Convers Manage 2007;48(11):3034–45.

[96] Hu Y, Naito S, Kobayashi N, Hasatani M. $CO_2$, $NO_x$ and $SO_2$ emissions from the combustion of coal with high oxygen concentration gases. Fuel 2000;79 (15):1925–32.

[97] Croiset E, Thambimuthu KV. $NO_x$ and $SO_2$ emissions from $O_2/CO_2$ recycle coal combustion. Fuel 2001;80(14):2117–21.

[98] White V, Torrente-Murciano L, Sturgeon D, Chadwick D. Purification of oxyfuel-derived $CO_2$. Energy Procedia 2009;1(1):399–406.

[99] Altmann H, Porsche T, Burchhardt U. Erfahrungen aus der Inbetriebnahme und dem Versuchsbetrieb der Oxyfuel-Forschungsanlage von Vattenfall. VGB PowerTech 2009;89(9):96–100.

[100] Smith AR, Klosek J. A review of air separation technologies and their integration with energy conversion processes. Fuel Processing Technol 2001;70 (2):115–34.

[101] Gonschorek S, Hellfritsch S, Weigl S, Gampe U. Entwicklungsstand des Oxyfuel-Prozesses für Braunkohlekraftwerke. In: Kraftwerkstechnisches Kolloquium, Zittau; 26–27 September, 2006.

[102] Vitalis B. Overview of oxy-combustion technology for utility coal-fired boilers. Advances in Materials Technology for Fossil Power Plants. In: Proceedings from the 5th International Conference; 2008. p. 968–81.

[103] Kather A, Klostermann M, Hermsdorf C, Mieske K, Eggers R, Köpke D. Steinkohlekraftwerk mit $CO_2$-Abtrennung auf Basis des Oxyfuel-Prozesses. In: 39. Kraftwerktechnisches Kolloquium. Dresden, Germany; October 11–12, 2007.

[104] European Standard. EN 450–1:2005 Fly ash for concrete. Definition, specifications and conformity criteria; 2005.

[105] Mauder R, Hugot A. Flugaschevermarktung in der Zukunft. VGB PowerTech 2008;88(11):62–6.

[106] Kluger F, Lysk S, Altmann H, Krohmer B, Stamatelopoulos G-N. 30 $MW_{th}$ Oxyfuel-Pilotanlage – Untersuchungsschwerpunkte und Auslegung des Dampferzeugers. In: Kraftwerksbetrieb unter künftigen Rahmenbedingungen, 38. Kraftwerkstechnisches Kolloquium. Dresden, Germany; October 24–25, 2006.

[107] Toporov D, Förster M, Kneer R. How to burn pulverized coal in $CO_2$ atmosphere at low oxygen concentrations. VDI Berichte 1988;55–60:2007.
[108] Toporov D, Bocian P, Heil P, Kellermann A, Stadler H, Tschunko S, et al. Detailed investigation of a pulverized fuel swirl flame in $CO_2/O_2$ atmosphere. Combust Flame 2008;155(4):605–18.
[109] Nikzat H, Pak H, Fuse T, Hu Y, Ogyu K, Kobayashi N, et al. Characteristics of pulverized coal burner using a high-oxygen partial pressure. Chem Eng Res Des 2004;82(1):99–104.
[110] Hellfritsch S, Gonschorek S, Vilhelm R, Löser J, Klemm M, Weigl S, et al. Entwicklungsstand des Oxyfuel-Prozesses für Braunkohlekraftwerke. In Kraftwerksbetrieb unter künftigen Rahmenbedingungen, 38. In: Kraftwerkstechnisches Kolloquium. Dresden, Germany; October 24–25, 2006.
[111] Oryshchyn D, Gerdemann S, Armstrong J, Ochs T, Summers C. Oxy-firing flue-gas character and its effect on FGD – a process study for integrated pollutant removal. In: 23rd Annual international Pittsburgh coal conference, PCC – coal-energy, environment and sustainable development; 2006.
[112] EUROGYPSUM. Association of European gypsum industries. FGD Gypsum – quality criteria and analysis methods, www.eurogypsum.org; April 2005.
[113] Klostermann M. Efficiency Increase of the oxyfuel process by waste heat recovery considering the effects of flue gas treatment. In: 3rd workshop of the IEA GHG international oxy-combustion network. Yokohama, Japan; March 5–6, 2008.
[114] Suriyawong A, Hogan Jr CJ, Jiang J, Biswas P. Charged fraction and electrostatic collection of ultrafine and submicrometer particles formed during $O_2$–$CO_2$ coal combustion. Fuel 2008;87(6):673–82.
[115] Schnurrer S, Elliott L, Wall T, Liu Y. Influence of oxy-fuel environment on sulphur species in ash from pulverized coal combustion. In: Impacts of fuel quality on power production and the environment, September 29–October 3. Banff, Alberta, Canada: The Banff Centre; 2008.
[116] Khare SP, Wall TF, Farida AZ, Liu Y, Moghtaderi B, Gupta RP. Factors influencing the ignition of flames from air-fired swirl pf burners retrofitted to oxy-fuel. Fuel 2008;87(7):1042–9.
[117] Suriyawong A, Gamble M, Lee M-H, Axelbaum R, Biswas P. Submicrometer particle formation and mercury speciation under $O_2$–$CO_2$ coal combustion. Energy Fuels 2006;20(6):2357–63.
[118] Wang CS, Berry GF, Chang KC, Wolsky AM. Combustion of pulverized coal using waste carbon dioxide and oxygen. Combust Flame 1988;72(3):301–10.
[119] Nozaki T, Takano S-i, Kiga T, Omata K, Kimura N. Analysis of the flame formed during oxidation of pulverized coal by an $O_2$–$CO_2$ mixture. Energy 1997;22(2–3):199–205.
[120] Croiset E, Thambimuthu K, Palmer A. Coal combustion in $O_2/CO_2$ mixtures compared with air. Can J Chem Eng 2000;78(2):402–7.
[121] Liu H, Zailani R, Gibbs BM. Comparisons of pulverized coal combustion in air and in mixtures of $O_2/CO_2$. Fuel 2005;84(7–8):833–40.
[122] Tan Y, Croiset E, Douglas MA, Thambimuthu KV. Combustion characteristics of coal in a mixture of oxygen and recycled flue gas. Fuel 2006;85(4):507–12.
[123] Andersson K, Normann F, Johnsson F. Experiments and modeling on oxy-fuel combustion chemistry during lignite-firing. In: The 32nd international technical conference on coal utilization and fuel systems. Clearwater, Florida; 10–15 July2007.
[124] Mackrory AJ, Lokare S, Baxter LL, Tree DR. An investigation of nitrogen evolution in oxy-fuel combustion. In: The 32nd international technical conference on coal utilization and fuel systems, the power of coal. Clearwater, Florida; 10–15 June, 2007.
[125] Sheng C, Li Y. Experimental study of ash formation during pulverized coal combustion in $O_2/CO_2$ mixtures. Fuel 2008;87(7):1297–305.
[126] Molina A, Shaddix CR. Ignition and devolatilization of pulverized bituminous coal particles during oxygen/carbon dioxide coal combustion. Proc Combust Inst 2007;31(2):1905–12.
[127] Liu H, Okazaki K. Simultaneous easy $CO_2$ recovery and drastic reduction of $SO_x$ and $NO_x$ in $O_2/CO_2$ coal combustion with heat recirculation. Fuel 2003;82(11):1427–36.
[128] Wall T, Liu Y, Spero C, Elliott L, Khare S, Rathnam R, et al. An overview on oxyfuel coal combustion–State of the art research and technology development. Chem Eng Res Des 2009;87(8):1003–16.
[129] Bordenet B. Influence of novel cycle concepts on the high-temperature corrosion of power plants. Mater Corros 2008;59(5):361–6.
[130] Bordenet B, Kluger F. Thermodynamic modelling of the corrosive deposits in oxy-fuel fired boilers. Mater Sci Forum 2008;595–598(1):261–9.
[131] Kung SC, Tanzosh JM, Mcdonald DK. Fireside corrosion study using B&W clean environment development facility for oxy-coal combustion systems. Advances in materials technology for fossil power plants. In: Proceedings from the 5th International conference; 2008. p. 982–92.
[132] Abellán JPirón, Olszewski T, Penkalla HJ, Meier GH, Singheiser L, Quadakkers WJ. Scale formation mechanisms of martensitic steels in high $CO_2/H_2O$-containing gases simulating oxyfuel environments. Mater High Temp 2009;26(1):63–72.
[133] Rauscher K. Clean coal in the energy mix from tomorrow. VGB PowerTech 2005;85(9):70–2.
[134] Ritter R, Holling B, Altmann H, Biele M. Konzepte und Ausblick für eine $CO_2$-Anlage eines Oxyfuel-Kraftwerkes am Bespiel Schwarze Pumpe. In: 39. Kraftwerktechnisches Kolloquium. Dresden, Germany; October 11–12, 2007.
[135] McCauley KJ, Farzan H, Alexander KC, McDonald DK, Varagani R, Prabhakar R, et al. Commercialization of oxy-coal combustion: applying results of a large 30 $MW_{th}$ pilot project. Energy Procedia 2009;1(1):439–46.
[136] Kiga T, Takano S, Kimura N, Omata K, Okawa M, Mori T, et al. Characteristics of pulverized-coal combustion in the system of oxygen/recycled flue gas combustion. Energy Convers Manage 1997;38:129–34.
[137] Watanabe S, Endo Y, Kiga T, Kimura N, Okawa M. Analysis of pulverized-coal flames in the system of oxygen/recycled flue gas combustion. Am Soc Mech Engineers, Environ Control Division Publ EC 1997;5:239–46.
[138] Wall TF, Elliott L, Khare S, Liu Y, Yamada T, Tamura M, et al. Ash impacts in oxy-fuel combustion. In: Proceedings: impacts of fuel quality on power production. Utah, USA; 2006.
[139] Wall TF. Performance of PF boilers retrofitted with oxy-coal combustion: understanding burnout, coal reactivity, burner operation, and furnace heat transfer. In: 3rd Workshop of the IEA GHG international oxy-combustion network. Yokohama, Japan; March 5–6, 2008.
[140] Goh B. 1 $MW_{th}$ oxyfuel combustion test facility. "Recent developments in CCS" coal research forum – combustion division meeting 17th April 2007. Imperial College London; 2007.
[141] Goh B. Oxyfuel combustion pilot-scale testing. Oxyfuel combustion: opportunities and challenges–7th of May 2008. University of Leeds; 2008a.
[142] Goh B.E.ON UK's pilot scale oxyfuel combustion experiences: development, testing and modelling. In: 3rd workshop of the IEA GHG international oxy-combustion network. Yokohama, Japan; March 5–6, 2008.
[143] Dhungel B, Mönckert P, Maier J, Scheffknecht G. Investigation of oxy-coal combustion in semi-technical test facilities. In: 3rd international conference on clean coal technology. Italy, 2007.
[144] Maier J, Dhungel B, Mönckert P, Scheffknecht G. Combustion and emission behavior under oxyfuel conditions. In: 39. Kraftwerktechnisches Kolloquium. Dresden, Germany; October 11–12, 2007 [In German].
[145] Maier J, Dhungel B, Mönckert P, Kull R, Scheffknecht G. Impact of recycled gas species ($SO_2$, NO) on emission behaviour and fly ash quality during oxy-coal combustion. In: Proceedings of the 33rd international technical conference on coal utilization and fuel systems. Clearwater, Florida; June 1–5, 2008.
[146] Mönckert P, Reber D, Maier J, Scheffknecht G. Operation of a retrofitted 0.5 $MW_{th}$ PF combustion facility under oxyfuel conditions–an experience report. In: The 32nd international technical conference on coal utilization and fuel systems, the power of coal. Clearwater, Florida; 10–15 June, 2007.
[147] Mönckert P, Dhungel B, Kull R, Maier J. Impact of combustion conditions on emission formation ($SO_2$, $NO_x$) and fly ash. In: 3rd workshop of the IEA GHG international oxy-combustion network. Yokohama, Japan; March 5–6, 2008.
[148] Scheffknecht G, Maier J. Firing issues related to the oxyfuel process. VGB PowerTech 2008;88(11):91–7.
[149] Zheng L, Furimsky E. Assessment of coal combustion in $O_2$ + $CO_2$ by equilibrium calculations. Fuel Processing Technol 2003;81(1):23–34.
[150] Chui EH, Douglas MA, Tan Y. Modeling of oxy-fuel combustion for a western Canadian sub-bituminous coal. Fuel 2003;82(10):1201–10.
[151] Chui EH, Majeski AJ, Douglas MA, Tan Y, Thambimuthu KV. Numerical investigation of oxy-coal combustion to evaluate burner and combustor design concepts. Energy 2004;29(9–10):1285–96.
[152] White V. Purification of oxyfuel-derived $CO_2$. In: 3rd workshop of the IEA GHG international oxy-combustion network. Yokohama, Japan; March 5–6, 2008.
[153] Andersson K, Johnsson F. Flame and radiation characteristics of gas-fired $O_2/CO_2$ combustion. Fuel 2007;86(5–6):656–68.
[154] Leiser S, Schnell U, Scheffknecht G. A kinetic homogeneous reaction model for oxy-fuel combustion. In: 9th conference on energy for a clean environment; 2007.
[155] Andersson K, Johansson R, Johnsson F, Leckner B. Radiation intensity of propane-fired oxy-fuel flames: implications for soot formation. Energy Fuels 2008b;22(3):1535–41.
[156] Normann F, Andersson K, Leckner B, Johnsson F. High-temperature reduction of nitrogen oxides in oxy-fuel combustion. Fuel 2008;87(17):3579–85.
[157] Valero A, Romeo LM, Díez LI, Pérez A. OXY-CO-FIRING: a negative $CO_2$ emission process. In: The 8th international conference on greenhouse gas control technologies (GHGT-8). Trondheim, Norway; 19–22 June, 2006.
[158] Okazaki K, Ando T. $NO_x$ reduction mechanism in coal combustion with recycled $CO_2$. Energy 1997;22(2–3):207–15.
[159] Okazaki K. Technical consideration and challenges of oxy-pulverized coal combustion. In: 3rd workshop of the IEA GHG international oxy-combustion network. Yokohama, Japan; March 5–6, 2008.
[160] Hu YQ, Kobayashi N, Hasatani M. The reduction of recycled-$NO_x$ in coal combustion with $O_2$/recycled flue gas under low recycling ratio. Fuel 2001;80(13):1851–5.
[161] Hu YQ, Kobayashi N, Hasatani M. Effects of coal properties on recycled-$NO_x$ reduction in coal combustion with $O_2$/recycled flue gas. Energy Convers Manage 2003;44(14):2331–40.
[162] Liu H, Zailani R, Gibbs BM. Pulverized coal combustion in air and in $O_2/CO_2$ mixtures with $NO_x$ recycle. Fuel 2005b;84(16):2109–15.
[163] Maier J, Dhungel B, Mönckert P, Scheffknecht G. Coal combustion and emission behaviour under oxy-fuel combustion. In: Proceedings of the 31st international technical conference on coal utilization and fuel systems. Clearwater, Florida; 21–26 May, 2006.
[164] Dhungel B, Maier J, Scheffknecht G. Emission behaviour during oxy-coal combustion in a 20 kW once through furnace. In: 9th conference on energy for a clean environment. Portugal; 2007.
[165] Al-Makhadmeh L, Maier J, Scheffknecht G. Coal pyrolysis and char combustion under oxy-fuel conditions. In: The 34th international technical conference on coal utilization and fuel systems. Clearwater, Florida; May 31–June 4, 2009.

[166] Murphy JJ, Shaddix CR. Combustion kinetics of coal chars in oxygen-enriched environments. Combust Flame 2006;144(4):710–29.
[167] Shaddix CR, Molina A. Effect of $O_2$ and High $CO_2$ concentrations on PC char burning rates during oxy-fuel combustion. In: The 33rd international technical conference on coal utilization and fuel systems, coal for the future. Clearwater, Florida; 1–5 June, 2008.
[168] Shaddix CR, Molina A. Particle imaging of ignition and devolatilization of pulverized coal during oxy-fuel combustion. Proc Combust Inst 2009;32 (2):2091–8.
[169] Shaddix CR, Molina A. Understanding the effects of $O_2$ and $CO_2$ on $NO_x$ formation during oxy-coal combustion. In: 3rd Workshop of the IEA GHG international oxy-combustion network. Yokohama, Japan; March 5–6, 2008.
[170] Becher V, Goanta A, Gleis S, Spliethoff H. Controlled staging with non-stoichiometric burners for oxyfuel processes. In: The 32nd international technical conference on coal utilization and fuel systems, the power of coal. Clearwater, Florida; 10–15 June, 2007.
[171] Goanta A, Becher V, Bohn J-P, Gleis S, Spliethoff H. Controlled staging with non-stoichiometric burners for oxy-fuel processes–numerical validation. In: The 33rd international technical conference on coal utilization and fuel systems, coal for the future. Clearwater, Florida; 1–5 June, 2008.
[172] Glarborg P, Bentzen LLB. Chemical effects of a high $CO_2$ concentration in oxy-fuel combustion of methane. Energy Fuels 2008;22(1):291–6.
[173] Mendiara T, Glarborg P. Reburn chemistry in oxy-fuel combustion of methane. Energy Fuels 2009a;23(7):3565–72.
[174] Mendiara T, Glarborg P. Ammonia chemistry in oxy-fuel combustion of methane. Combust Flame 2009b;156:1937–49.
[175] Mackrory AJ, Tree DR. $NO_x$ Destruction experiments and modeling in oxy-fuel combustion. In: The 33rd international technical conference on coal utilization and fuel systems, coal for the future. Clearwater, Florida; 1–5 June, 2008.
[176] Mackrory AJ, Tree DR. Predictions of $NO_x$ in a laboratory pulverized coal combustor operating under air and oxy-fuel conditions. Combust Sci Technol 2009;181(11):1413–30.
[177] Heil P, Stadler H, Förster M, Kneer R. Flammlose Verbrennung in einer $O_2/CO_2$ Atmosphäre. In: 39. Kraftwerktechnisches Kolloquium. Dresden, Germany, October 11–12, 2007.
[178] Stadler H, Ristic D, Förster M, Schuster A, Kneer R, Scheffknecht G. $NO_x$-emissions from flameless coal combustion in air, $Ar/O_2$ and $CO_2/O_2$. Proc Combust Inst 2009;32(2):3131–8.
[179] Engels S. Developments in oxy-combustion technology for power plants with CCS. 1st Young Researchers Forum Organised by IEA Greenhouse Gas R&D Programme, Hamburg, Germany; December 8, 2006.
[180] Arias B, Pevida C, Rubiera F, Pis JJ. Effect of biomass blending on coal ignition and burnout during oxy-fuel combustion. Fuel 2008;87(12):2753–9.
[181] Bejarano PA, Levendis YA. Single-coal-particle combustion in $O_2/N_2$ and $O_2/CO_2$ environments. Combust Flame 2008;153(1–2):270–87.
[182] Sheng C, Li Y, Liu X, Yao H, Xu M. Ash particle formation during $O_2/CO_2$ combustion of pulverized coals. Fuel Processing Technol 2007a;88(11–12):1021–8.
[183] Sheng C, Lu Y, Gao X, Yao H. Fine ash formation during pulverized coal combustion–a comparison of $O_2/CO_2$ combustion versus air combustion. Energy Fuels 2007b;21(2):435–40.
[184] Fryda L, Cieplik MK, Jacobs JM, van de Kamp WL. Study of oxyfuel combustion of coal and biomass in a lab-scale pulverised fuel combustor. In: 16th European biomass conference and exhibition. Valencia, Spain; June 2–6, 2008.
[185] Spinti JP, Pershing DW. The fate of char-N at pulverized coal conditions. Combust Flame 2003;135(3):299–313.
[186] Zhang J, Eddings EG, Wendt JOL, Smith PJ. Model validation studies for pulverized coal jet ignition in $O_2/CO_2$ environments. In: 3rd workshop of the IEA GHG international oxy-combustion network. Yokohama, Japan; March 5–6, 2008.
[187] Naredi P, Pisupati SV. Comparison of char burnout and CO emissions from oxy-coal combustion with combustion in air: an experimental and numerical study. In: The 33rd international technical conference on coal utilization and fuel systems, coal for the future. Clearwater, Florida; 1–5 June, 2008.
[188] Andersson K, Johansson R, Hjartstam S, Johnsson F, Leckner B. Radiation intensity of lignite-fired oxy-fuel flames. Exp Thermal Fluid Sci 2008c;33(1):67–76.
[189] Huang X, Jiang X, Han X, Wang H. Combustion characteristics of Fine- and micro-pulverized coal in the mixture of $O_2/CO_2$. Energy Fuels 2008;22 (6):3756–62.
[190] Suda T, Masuko K, Sato J, Yamamoto A, Okazaki K. Effect of carbon dioxide on flame propagation of pulverized coal clouds in $CO_2/O_2$ combustion. Fuel 2007;86(12–13):2008–15.
[191] Stanmore BR, Visona SP. The Contribution to char burnout from gasification by $H_2O$ and $CO_2$ during pulverized-coal flame combustion. Combust Flame 1998;113(1–2):274–6.
[192] Varhegyi G, Szabo P, Jakab E, Till F, Richard J-R. Mathematical modeling of char reactivity in $Ar–O_2$ and $CO_2–O_2$ mixtures. Energy Fuels 1996;10(6):1208–14.
[193] Borrego AG, Alvarez D. Comparison of chars obtained under oxy-fuel and conventional pulverized coal combustion atmospheres. Energy Fuels 2007;21(6):3171–9.
[194] Liu F, Guo H, Smallwood GJ. The chemical effect of $CO_2$ replacement of $N_2$ in air on the burning velocity of $CH_4$ and $H_2$ premixed flames. Combust Flame 2003;133(4):495–7.
[195] Liu F, Guo H, Smallwood GJ, Gülder Ö L. The chemical effects of carbon dioxide as an additive in an ethylene diffusion flame: implications for soot and $NO_x$ formation. Combust Flame 2001;125(1–2):778–87.
[196] Masri AR, Dibble RW, Barlow RS. Chemical kinetic effects in nonpremixed flames of $H_2/CO_2$ fuel. Combust Flame 1992;91(3–4):285–309.
[197] Miller JA, Bowman CT. Mechanism and modeling of nitrogen chemistry in combustion. Prog Energy Combust Sci 1989;15:287–338.
[198] Johnsson JE. Formation and reduction of nitrogen oxides in fluidized-bed combustion. Fuel 1994;73:1398–415.
[199] Glarborg P, Jensen AD, Johnsson JE. Fuel nitrogen conversion in solid fuel fired systems. Prog Energy Combust Sci 2003;29(2):89–113.
[200] Turns SR. An introduction to combustion: concepts and applications. International Editions. McGraw-Hill; 2000.
[201] Normann F, Andersson K, Leckner B, Johnsson F. Emission control of nitrogen oxides in the oxy-fuel process. Prog Energy Combust Sci 2009;35 (5):385–97.
[202] Wendt JOL, Sternling CV, Matovich MA. Reduction of sulfur trioxide and nitrogen oxides by secondary fuel injection. Proc Combust Inst 1973;14(1):897–904.
[203] Levy JM, Chan LK, Sarofim AF, Beer JM. NO/char reactions at pulverized coal flame conditions. Proc Combust Inst 1981;18:111–20.
[204] Aarna I, Suuberg EM. A review of the kinetics of the nitric oxide-carbon reaction. Fuel 1997;76(6):475–91.
[205] Aarna I, Suuberg EM. The role of carbon monoxide in the NO-carbon reaction. Energy Fuels 1999;13(6):1145–53.
[206] López D, Calo J. The NO-carbon reaction: the influence of potassium and CO on reactivity and populations of oxygen surface complexes. Energy Fuels 2007;21(4):1872–7.
[207] Park D-C, Day SJ, Nelson PF. Nitrogen release during reaction of coal char with $O_2$, $CO_2$, and $H_2O$. Proc Combust Inst 2005;30(2):2169–75.
[208] Liu H, Katagiri S, Kaneko U, Okazaki K. Sulfation behavior of limestone under high $CO_2$ concentration in $O_2/CO_2$ coal combustion. Fuel 2000;79 (8):945–53.
[209] Liu H, Katagiri S, Okazaki K. Drastic $SO_x$ removal and influences of various factors in $O_2/CO_2$ pulverized coal combustion system. Energy Fuels 2001b;15 (2):403–12.
[210] Krishnamoorthy G, Veranth JM. Computational modeling of $CO/CO_2$ ratio inside single char particles during pulverized coal combustion. Energy Fuels 2003;17(5):1367–71.
[211] Keith DW, Rhodes JS. Bury, burn or both: a two-for-one deal on biomass carbon and energy. Climatic Change 2002;54(3):375–7.
[212] Obersteiner M, Azar C, Kauppi P, Möllersten K, Moreira J, Nilsson S, et al. Managing climate risk. Science 2001;294(5543):786–7.
[213] Kraxner F, Nilsson S, Obersteiner M. Negative emissions from BioEnergy use, carbon capture and sequestration (BECS) – the case of biomass production by sustainable forest management from semi-natural temperate forests. Biomass Bioenergy 2003;24(4–5):285–96.
[214] Azar C, Lindgren K, Larson E, Mollersten K. Carbon capture and storage from fossil fuels and biomass – costs and potential role in stabilizing the atmosphere. Climatic Change 2006;74(1–3):47.
[215] Read P. Bioenergy with carbon storage – strengthening Kyoto through complementary action to address the threat of abrupt climate change. Renewable Energy Dev 2006;19(3):9–11.
[216] Rhodes JS, Keith DW. Biomass with capture: negative emissions within social and environmental constraints: an editorial comment. Climatic Change 2008;87(3–4):321–8.
[217] Borrego AG, Garavaglia L, Kalkreuth WD. Characteristics of high heating rate biomass chars prepared under $N_2$ and $CO_2$ atmospheres. Int J Coal Geol 2009;77(3–4):409–15.
[218] Robinson AL, Junker H, Buckley SG, Sclippa G, Baxter LL. Interactions between coal and biomass when cofiring. Proc Combust Inst 1998;27(1):1351–9.

## Nomenclature

*ASU:* Air Separation Unit
*BECS:* Biomass Energy for Carbon Capture and Sequestration
*CCS:* Carbon Capture and Storage
*EFR:* Entrained-Flow Reactor
*EOR:* Enhanced Oil Recovery
*ESP:* Electrostatic Precipitator
*FGD:* Flue Gas Desulphurization
*IGCC:* Integrated Gasification Combined Cycle
*ITM:* Ion Transport Membrane (for air separation)
*LCV/LHV:* Low Calorific/Heating Value
*RFG:* Recirculated Flue Gas
*SCR:* Selective Catalytic Reduction

## Research groups

*ANL:* Argonne National Laboratory
*BYU:* Brigham Young University (Utah, USA)
*CANMET:* Canada Centre for Mineral and Energy Technology
*DTU:* Technical University of Denmark
*IFRF:* International Flame Research Foundation
*IHI:* Ishikawajima-Harima Heavy Industries
*IVD:* Institute of Process Engineering and Power Plants Technology, University of Stuttgart
*UU:* University of Utah

# Appendix B

# Stoichiometric Calculations

## B.1 Ideal Conditions

Complete combustion of a solid fuel with a molar composition, $C_\alpha H_\beta S_\gamma N_\delta O_\phi \cdot (H_2O)_\mu$, is given by (B.1).

$$\begin{aligned} C_\alpha H_\beta S_\gamma N_\delta O_\phi \cdot (H_2O)_\mu \quad + \quad & \left(\alpha + \frac{\beta}{4} + \gamma + \frac{\delta}{2} - \frac{\phi}{2}\right) O_2 \\ \rightarrow \quad & \alpha\, CO_2 + \left(\frac{\beta}{2} + \mu\right) H_2O + \gamma\, SO_2 + \delta\, NO \end{aligned} \tag{B.1}$$

where the stoichiometric coefficients, $\alpha$, $\beta$, etc., are determined from the ultimate and proximate analysis of the fuel by:

$$\text{coefficient} = \frac{x_i}{M_i} \tag{B.2}$$

$x_i$ is the mass fraction of C, H, S, N, O, or $H_2O$ in the fuel and $M_i$ is the molar mass of that component. The coefficient has units of moles/kg fuel.

The minimum amount of oxidizer needed for complete combustion is given by:

$$N_{OX,\,min} = \frac{N_{O_2,\,min}}{y^{ox}_{O_2}} = \frac{\alpha + \frac{\beta}{4} + \gamma + \frac{\delta}{2} - \frac{\phi}{2}}{y^{ox}_{O_2}} \tag{B.3}$$

where $y^{ox}_{O_2}$ is the molar fraction of $O_2$ in the oxidizer (air or an $O_2/CO_2$ mixture).

The corresponding, minimum amount of flue gas produced is given by:

$$N_{FG,\,min} = N_{OX,\,min} + \frac{\beta}{4} + \mu + \frac{\delta}{2} + \frac{\phi}{2} \tag{B.4}$$

Since the reported experiments have been conducted with different types of oxidizer, the excess ratio, $\lambda$, is defined as the oxygen excess ratio for simplicity:

$$\lambda = \frac{N_{O_2}}{N_{O_2,\,min}} \tag{B.5}$$

It should be noted that the value of $\lambda$ will be equal to *e.g.* the value computed based on the total and minimum air amounts for air experiments.

The amount of flue gas on a wet (total) and dry basis can be determined from:

$$N_{\mathrm{FG}} = N_{\mathrm{FG,\,min}} + (\lambda - 1) N_{\mathrm{OX,\,min}} \tag{B.6}$$

$$N_{\mathrm{FG,\,dry}} = \lambda N_{\mathrm{OX,\,min}} - \frac{\beta}{4} + \frac{\delta}{2} + \frac{\phi}{2} \tag{B.7}$$

For the calculations performed in the present work it is assumed that the pressurized air used as oxidizer is dry, no correction of the oxidant flow is thus necessary. Likewise for the oxyfuel combustion experiments, only dry flue gas recirculation has been simulated.

The molar fractions of the different, major flue gas components in wet and dry flue gas are given by:

$$y_{\mathrm{CO_2}} = \frac{\alpha}{N_{\mathrm{FG}}} \quad ; \quad y^{\mathrm{dry}}_{\mathrm{CO_2}} = \frac{\alpha}{N_{\mathrm{FG,\,dry}}} \tag{B.8}$$

$$y_{\mathrm{O_2}} = \frac{(\lambda - 1)\, N_{\mathrm{OX,\,min}} \cdot y^{\mathrm{ox}}_{\mathrm{O_2}}}{N_{\mathrm{FG}}} \quad ; \quad y^{\mathrm{dry}}_{\mathrm{O_2}} = \frac{(\lambda - 1)\, N_{\mathrm{OX,\,min}} \cdot y^{\mathrm{ox}}_{\mathrm{O_2}}}{N_{\mathrm{FG,\,dry}}} \tag{B.9}$$

$$y_{\mathrm{SO_2}} = \frac{\gamma}{N_{\mathrm{FG}}} \quad ; \quad y^{\mathrm{dry}}_{\mathrm{SO_2}} = \frac{\gamma}{N_{\mathrm{FG,\,dry}}} \tag{B.10}$$

$$y_{\mathrm{NO}} = \frac{\delta}{N_{\mathrm{FG}}} \quad ; \quad y^{\mathrm{dry}}_{\mathrm{NO}} = \frac{\delta}{N_{\mathrm{FG,\,dry}}} \tag{B.11}$$

$$y_{\mathrm{H_2O}} = \frac{\frac{\beta}{2} + \mu}{N_{\mathrm{FG}}} \quad ; \quad y^{\mathrm{dry}}_{\mathrm{H_2O}} = 0 \tag{B.12}$$

## B.2 Incomplete Combustion and False Air Ingress

The expressions in Section B.1 are for the ideal case with complete combustion of the solid fuel and a leak tight reactor system. For the actual experiments, the solid fuel yield incomplete combustion and false air is drawn into the reactor due to the operation at sub-atmospheric pressure.

Including the false air (FA) ingress, for full burnout, leads to:

$$N_{\mathrm{FG,\,FA}} = N_{\mathrm{FG,\,min}} + (\lambda - 1) N_{\mathrm{OX,\,min}} + N_{\mathrm{FA}} \tag{B.13}$$

$$N_{\mathrm{FG,\,dry,\,FA}} = \lambda N_{\mathrm{OX,\,min}} - \frac{\beta}{4} + \frac{\delta}{2} + \frac{\phi}{2} + N_{\mathrm{FA}} \tag{B.14}$$

The concentrations of $CO_2$, $SO_2$, NO, and $H_2O$ are calculated equivalently to equations (B.8), and (B.10)–(B.12). The concentration of $O_2$ in the flue gas will increase compared to the ideal conditions due to the $O_2$ content of the false air. For oxyfuel experiments the $N_2$ content of the flue gas will likewise increase and will be a direct indicator of the level of false air ingress, under the assumption that all Fuel-N is converted to NO, see (B.1), and no thermal NO is formed.

$$y_{O_2}^{FA} = \frac{(\lambda - 1)\, N_{OX,\,min} \cdot y_{O_2}^{ox} + N_{FA} \cdot y_{O_2}^{air}}{N_{FG}} \tag{B.15}$$

$$y_{O_2}^{dry,\,FA} = \frac{(\lambda - 1)\, N_{OX,\,min} \cdot y_{O_2}^{ox} + N_{FA} \cdot y_{O_2}^{air}}{N_{FG,\,dry}} \tag{B.16}$$

$$y_{N_2,\,oxy}^{FA} = \frac{N_{FA} \cdot y_{N_2}^{air}}{N_{FG}} \tag{B.17}$$

$$y_{N_2,\,oxy}^{dry,\,FA} = \frac{N_{FA} \cdot y_{N_2}^{air}}{N_{FG,\,dry}} \tag{B.18}$$

The amount of dry flue gas which is used in the molar balances for C and S can be determined from the measured concentration of $O_2$ (and $N_2$) in the dry flue gas sample. Combining Eqs. (B.14) and (B.16) provides an expression for determining the amount of false air leaking into the reactor, see (B.19). Inserting (B.19) in (B.14) yields a method for calculating the total amount of flue gas from the reactor, see (B.20).

$$N_{FA} = \frac{y_{O_2}^{dry,\,FA} \cdot N_{FG,\,dry} - y_{O_2}^{ox}\,(\lambda - 1)\, N_{OX,\,min}}{\left(y_{O_2}^{air} - y_{O_2}^{dry,\,FA}\right)} \tag{B.19}$$

$$N_{FG,\,dry,\,FA} = \frac{y_{O_2}^{air}\left(\lambda N_{OX,\,min} - \frac{\beta}{4} + \frac{\delta}{2} + \frac{\phi}{2}\right) - y_{O_2}^{ox}\,(\lambda - 1)\, N_{OX,\,min}}{\left(y_{O_2}^{air} - y_{O_2}^{dry,\,FA}\right)} \tag{B.20}$$

For air as oxidant this simplifies to:

$$N_{FG,\,dry,\,FA} = \frac{y_{O_2}^{air}\left(N_{OX,\,min} - \frac{\beta}{4} + \frac{\delta}{2} + \frac{\phi}{2}\right)}{\left(y_{O_2}^{air} - y_{O_2}^{dry,\,FA}\right)} \tag{B.21}$$

With $N_2$ as base:

$$N_{FA} = \frac{y_{N_2,\,oxy}^{dry,\,FA}\left(\lambda N_{OX,\,min} - \frac{\beta}{4} + \frac{\delta}{2} + \frac{\phi}{2}\right)}{\left(y_{N_2}^{air} - y_{N_2,\,oxy}^{dry,\,FA}\right)} \tag{B.22}$$

$$N_{FG,\,dry,\,FA} = \frac{y_{N_2}^{air}}{y_{N_2}^{air} - y_{N_2,\,oxy}^{dry,\,FA}} \tag{B.23}$$

If assuming that the combustible fraction of the fuel left in the fly ash consists solely of C, the amount of flue gas will not change due to incomplete combustion, since C and $O_2$ react in the ratio 1:1. However, the amount of false air determined from the measured oxygen concentration is a function of the fuel burnout. This correction has not been taken into account due to the high degree of burnout observed during the experiments.

# Appendix C

# Mass Balances

The sections below contain the equations used in determining the C and S balances for the individual experiments.

## C.1 Carbon

The incoming carbon originates potentially from both the solid fuel (SF) and the oxidant flow (OX), see (C.1).

$$\begin{aligned} C_{in} &= C_{OX} + C_{SF} \\ C_{in} &= y_{CO_2,OX} \cdot F_{OX} + \alpha \cdot \dot{m}_{SF} \end{aligned} \tag{C.1}$$

where $y_{CO_2,OX}$ is the molar fraction of $CO_2$ in the oxidizer (assumed 0 for air) and $F_{OX}$ is the molar flow rate of oxidizer. $\alpha$ is the fuel carbon content (moles/kg fuel), see Appendix B, and $\dot{m}_{SF}$ is the mass flow rate of solid fuel.

During oxyfuel experiments the amount of $CO_2$ fed with the oxidizer constitute most of the C in the system. However, the C fed with the solid fuel amounts to between 19 and 48 % depending on the fuel, the stoichiometry, and the $O_2$ concentration in the oxidizer. It is thus still relevant to determine the carbon balance.

The equations for the three levels on the "out" term are seen in Eqs. (C.2), (C.3), and (C.5).

**Level 1**

$$C_{out} = (y_{CO} + y_{CO_2}) \cdot F_{FG,dry,FA} \tag{C.2}$$

$y_X$ are the measured concentrations of CO and $CO_2$ in the dry flue gas sample. $F_{FG,dry,FA}$ is the dry flue gas flow. No measurement of the true flue gas flow exist and thus the flue gas flow is determined from the measured oxygen concentration

in the dry flue gas. The determination of $F_{FG,dry,FA}$ takes false air ingress and incomplete combustion into account, see Appendix B, Section B.2.

**Level 2**

$$\begin{aligned} C_{out} &= (y_{CO} + y_{CO_2}) \cdot F_{FG,dry,FA} + \dot{n}_{C\ with\ ash} \\ C_{out} &= (y_{CO} + y_{CO_2}) \cdot F_{FG,dry,FA} + \frac{\dot{m}_{C\ with\ ash}}{M_C} \\ C_{out} &= (y_{CO} + y_{CO_2}) \cdot F_{FG,dry,FA} + \frac{x_{C,ash}}{M_C(1 - x_{C,ash})} \cdot \dot{m}_{ash,SF} \\ C_{out} &= (y_{CO} + y_{CO_2}) \cdot F_{FG,dry,FA} + \frac{x_{C,ash} \cdot x_{ash,SF}}{M_C(1 - x_{C,ash})} \cdot \dot{m}_{SF} \end{aligned} \tag{C.3}$$

$\dot{n}_{C\ with\ ash}$ and $\dot{m}_{C\ with\ ash}$ are the moles and mass of carbon bound in the fly ash, respectively. $M_C$ is the molar mass of carbon. $x_{C,ash}$ is the measured mass fraction of C in the dry fly ash sample. The fraction $x/(1-x)$ is introduced in order to account for the fact that $x_{C,ash}$ is given from Eq. (C.4). $\dot{m}_{ash,SF}$ is the mass flow of ash fed in with the SF. $x_{ash,SF}$ is the mass fraction of ash in the SF (from the proximate analysis), and $\dot{m}_{SF}$ is the mass flow of SF to the burner.

$$x_{C,ash} = \frac{m_{C\ in\ fly\ ash}}{m_{ash\ species\ in\ fly\ ash} + m_{C\ in\ fly\ ash}} \tag{C.4}$$

**Level 3**

$$\begin{aligned} C_{out} &= (y_{CO} + y_{CO_2}) \cdot F_{FG,dry,FA} + \frac{x_{C,ash} \cdot x_{ash,SF}}{M_C(1 - x_{C,ash})} \cdot \dot{m}_{SF} \cdot Y_{ash} \\ C_{out} &= (y_{CO} + y_{CO_2}) \cdot F_{FG,dry,FA} + \frac{x_{C,ash}}{M_C} \frac{m_{fly\ ash}}{\Delta t_{ash}} \frac{F_{FG,dry}}{F_{sampling}} \end{aligned} \tag{C.5}$$

$Y_{ash}$ is the yield of fly ash calculated based on the realized sampling flow through the ash sampling system, see Section 2.3.2.2. $m_{fly\ ash}$ is the total amount of fly ash sampled over the time interval $\Delta t_{ash}$. $F_{FG,dry}$ is the theoretical flue gas flow, disregarding false air ingress and $F_{sampling}$ is the flow rate through the ash sampling system. An average value is used for the latter.

## C.2 Sulphur

Sulphur is introduced with the solid fuel and potentially with the oxidizer. The latter is the case for the oxyfuel experiments with simulated recirculation of $SO_2$ containing flue gas.

$$S_{in} = y_{SO_2,OX} \cdot F_{OX} + \gamma \cdot \dot{m}_{SF} \tag{C.6}$$

where $y_{SO_2,\,OX}$ is the molar fraction of $CO_2$ in the oxidizer (0 for all air experiments) and $F_{OX}$ is the molar flow rate of oxidizer. $\gamma$ is the fuel sulphur content (moles/kg fuel), see Appendix B, and $\dot{m}_{SF}$ is the mass flow rate of solid fuel.

During coal/oxyfuel experiments with $SO_2$ addition to the oxidant the amount of $SO_2$ fed with the oxidizer constitute most of the S in the system. However, the S fed with the coal amounts to between 17 and 57 % depending on the $SO_2$ concentration in the oxidizer. It is thus still relevant to determine the sulphur balance for these experiments.

The equations for the three levels on the "out" term are seen in Eqs. (C.7), (C.8), and (C.9).

**Level 1**

$$S_{out} = y_{SO_2} \cdot F_{FG,\,dry,\,FA} \tag{C.7}$$

$y_{SO_2}$ is the measured concentration of $SO_2$ in the dry flue gas sample. $F_{FG,\,dry,\,FA}$ is the dry flue gas flow. No measurement of the true flue gas flow exist and thus the flue gas flow is determined from the measured oxygen concentration in the dry flue gas. The determination of $F_{FG,\,dry,\,FA}$ takes false air ingress and incomplete combustion into account, see Appendix B, Section B.2.

**Level 2**

$$\begin{aligned}
S_{out} &= y_{SO_2} \cdot F_{FG,\,dry,\,FA} + \dot{n}_{S\ with\ ash} \\
S_{out} &= y_{SO_2} \cdot F_{FG,\,dry,\,FA} + \frac{\dot{m}_{S\ with\ ash}}{M_S} \\
S_{out} &= y_{SO_2} \cdot F_{FG,\,dry,\,FA} + \frac{x_{S,\,ash}}{M_S(1 - x_{C,\,ash})} \cdot \dot{m}_{ash,\,SF} \\
S_{out} &= y_{SO_2} \cdot F_{FG,\,dry,\,FA} + \frac{x_{S,\,ash} \cdot x_{ash,\,SF}}{M_S(1 - x_{C,\,ash})} \cdot \dot{m}_{SF}
\end{aligned} \tag{C.8}$$

$\dot{n}_{S\ with\ ash}$ and $\dot{m}_{S\ with\ ash}$ are the moles and mass of sulphur bound in the fly ash, respectively. $M_S$ is the molar mass of sulphur. $x_{S,\,ash}$ and $x_{C,\,ash}$ are the measured mass fractions of S and C in the dry fly ash sample, respectively. $x_{S,\,ash}$ is assumed to be defined equally to Eq. (C.4). $\dot{m}_{ash,\,SF}$ is the mass flow of ash fed in with the SF. $x_{ash,\,SF}$ is the mass fraction of ash in the SF (from the proximate analysis), and $\dot{m}_{SF}$ is the mass flow of SF to the burner.

**Level 4**

$$
\begin{aligned}
S_{out} &= y_{SO_2} \cdot F_{FG,\,dry,\,FA} + \dot{n}_{S\ in\ fly\ ash} + \dot{n}_{S\ in\ deposits} \\
S_{out} &= y_{SO_2} \cdot F_{FG,\,dry,\,FA} + \frac{x_{S,\,ash}}{M_S} \cdot \dot{m}_{fly\ ash} + \frac{x_{S,\,dep}}{M_S} \cdot \dot{m}_{deposits} \\
S_{out} &= y_{SO_2} \cdot F_{FG,\,dry,\,FA} + \frac{x_{S,\,ash}}{M_S} \cdot \dot{m}_{fly\ ash} + \ldots \\
&\quad \frac{x_{S,\,dep}}{M_S} \cdot (\dot{m}_{ash,\,SF} - \dot{m}_{ash,\,sampled}) \\
S_{out} &= y_{SO_2} \cdot F_{FG,\,dry,\,FA} + \frac{x_{S,\,ash}}{M_S} \cdot \dot{m}_{fly\ ash} + \ldots \\
&\quad \frac{x_{S,\,dep}}{M_S} \cdot (x_{ash,\,SF} \cdot \dot{m}_{SF} \cdot (1 - Y_{ash})) \\
S_{out} &= y_{SO_2} \cdot F_{FG,\,dry,\,FA} + \frac{x_{S,\,ash}}{M_S} \cdot \frac{m_{fly\ ash}}{\Delta t_{ash}} \cdot \frac{F_{FG,\,dry}}{F_{ash\,sampling}} + \ldots \\
&\quad \frac{x_{S,\,dep}}{M_S} \cdot (x_{ash,\,SF} \cdot \dot{m}_{SF} \cdot (1 - Y_{ash}))
\end{aligned}
\tag{C.9}
$$

$\dot{n}_{S\ in\ fly\ ash}$ is the amount of sulphur bound in the sampled fly ash. $\dot{n}_{S\ in\ deposits}$ and $\dot{m}_{S\ in\ deposits}$ are the moles and mass of sulphur in deposits, respectively. $\dot{m}_{fly\ ash}$ is the mass flow rate of the entire fly ash flow, including unburnt carbon. $x_{S,\,dep}$ is the mass fraction of sulphur in deposits. The value used in the calculations is from the upstream part of the sampled deposits as this is assumed to represent the best estimate of the average concentration of sulphur in all deposits in the reactor. $\dot{m}_{deposits}$ is the mass flow rate at which deposits are build up in the reactor and this is assumed to constitute the amount of ash fed to the reactor which does not end up as fly ash, *i.e.*$(1 - Y_{ash})$. $\dot{m}_{ash,\,sampled}$ is the mass flow rate of ash species sampled from the setup. $m_{fly\ ash}$ is the total amount of fly ash sampled over the time interval $\Delta t_{ash}$. $F_{FG,\,dry}$ is the theoretical flue gas flow, disregarding false air ingress and $F_{ash\,sampling}$ is the flow rate through the ash sampling system. An average value is used for the latter.

# Appendix D

# Heating of Large Straw Particles

Heating of large particles ($d_p > 100\ \mu$m) occurs by both radiation and convection. The relative importance of convection decreases with increasing particle size [85].

The energy balance for a particle subject to heating by radiation and convection is seen in (D.1). Regardless of the size of the particle, it has been assumed isothermal.

$$m_p C_{p,p} \frac{dT_p}{dt} = \pi d_p^2 \cdot \left( h \left( T_g - T_p \right) + \epsilon_p \sigma \left( T_w^4 - T_p^4 \right) \right) \tag{D.1}$$

| Parameter | Description | Value |
|---|---|---|
| $m_p$ | particle mass | Eq. (D.2) |
| $C_{p,p}$ | specific heat of the particle | 1000 [J/kg-K] |
| $T_p$ | instantaneous particle temperature | $T_{p,0} = 298$ K |
| $t$ | time | |
| $d_p$ | particle diameter, fixed | 100, 330, and 1000 $\mu$m |
| $h$ | heat transfer coefficient | Eq. (D.3) |
| $T_g$ | flue gas temperature | from T-profile |
| $\epsilon_p$ | particle emissivity | 0.85 (black body) |
| $\sigma$ | Stefan-Boltzmann constant | $5.67051 \cdot 10^{-8}$ [W/m$^2$·K$^4$] |
| $T_w$ | wall temperature | 1000 °C, assumed constant |
| $\rho_p$ | particle density | 500 [kg/m$^3$] |
| Nu | Nusselt number | Eq. (D.4) |
| $\lambda_g$ | thermal conductivity of gas | 0.09 [W/m·K] |
| $m$ | constant | 0.6 (single phase flow) |
| Re | Reynolds number for particle | Eq. (D.5) |
| Pr | Prandtl number | 1 |
| $\rho_g$ | density of flue gas | $f(T_g)$, about 0.3 [kg/m$^3$] |
| $u_t$ | relative velocity of particle to flue gas | Eq. (D.6) or (D.7) |
| $\mu_g$ | viscosity of flue gas | $5 \cdot 10^{-5}$ [kg/m·s] |
| $g$ | gravitational constant | 9.81 [m/s$^2$] |

$$m_p = \frac{\pi}{6}\, d_p^3\, \rho_p \tag{D.2}$$

$$h = \frac{Nu\ \lambda_g}{d_p} \tag{D.3}$$

$$Nu = 2 + m\, Re^{1/2} Pr^{1/3} \tag{D.4}$$

$$Re_p = \frac{\rho_g u_t d_p}{\mu_g} \tag{D.5}$$

$$u_t = \frac{g\, d_p^2\, (\rho_p - \rho_g)}{18\, \mu_g} \quad ;\ Re_p < 2 \tag{D.6}$$

$$u_t = 0.153 \left( \frac{g\, (\rho_p - \rho_g)\, d_p^{1.6}}{\mu_g^{0.6}\ \rho_g^{0.4}} \right)^{0.714} \quad ;\ 2 < Re_p < 400 \tag{D.7}$$

The terminal velocity, relative velocity of particle to flue gas, of the particles are found in an iterative procedure using Equations (D.5) to (D.7).